Aus der Abteilung für Allgemeine Chirurgie, Thorax-, Gefäß- und
Transplantationschirurgie, Klinik und Poliklinik für Chirurgie
Medizinische Fakultät der Universität Rostock
(Abteilungsleiter: Prof. Dr. med. E. Klar)

Charakterisierung molekularer, zellulärer und humoraler Mechanismen der mikrovaskulären Thrombusbildung

Habilitationsschrift

zur

Erlangung des akademischen Grades
doctor medicinae habilitata (Dr. med. habil.)

der Medizinischen Fakultät

der Universität Rostock

urn:nbn:de:gbv:28-diss2008-0033-5

vorgelegt von
Dr. med. Nicole Lindenblatt
geboren am 18.08.1973 in Tönisvorst
aus Rostock

Rostock, 19.06.2007

Inhaltsverzeichnis

Abkürzungsverzeichnis

ADP	Adenosindiphosphat
APC	Aktiviertes Protein C
DNA	Desoxyribonucleic Acid
DPO	Darbepoetin-alpha
ELISA	Enzyme Linked Immuno Sorbent Assay
eNOS	Endothelial Nitric Oxide Synthetase
EPO	Erythropoietin
FITC	Fluorescein Isothiocyanat
GP	Glykoprotein
H_2O_2	Wasserstoffperoxid
HO-1	Hämoxygenase-1
ICAM-1	Intercellular Adhesion Molecule-1
IVM	Intravitalmikroskopie
LAMP-1	Lysosome Associated Membrane Protein-1
LPS	Lipopolysacharid
MAC-1	Macrophage Antigen-1
PAF	Platelet Activating Factor
PAF-R	Platelet Activating Factor Receptor
PAI-1	Plasminogen Activator Inhibitor-1
PGI_2	Prostacyclin (Prostaglandin I_2)
PSGL-1	P-Selectin Glycoprotein Ligand-1
RNA	Ribonucleic Acid
RT-PCR	Reverse Transcriptase Polymerase Chain Reaction
TF	Tissue Factor (Gewebefaktor)
TFPI	Tissue Factor Pathway Inhibitor
TM	Thrombomodulin
tPA	Tissue Plasminogen Activator
TNF-α	Tumor Necrose Factor-alpha
TRAP	Thrombin Receptor Activating Peptide
uPA	Urokinase-type Plasminogen Activator
VCAM-1	Vascular Cell Adhesion Molecule-1
vWF	Von Willebrand Faktor

1 Einleitung

Trotz vieler Fortschritte in Prävention, Diagnostik und Therapie stellen mikro- und makrovaskuläre Thrombosen weiterhin ein klinisch relevantes Problem in der Chirurgie dar. Makrovaskuläre Thrombosen treten als tiefe Venenthrombosen perioperativ, als akute arterielle Verschlüsse der großen extremitätenversorgenden Gefäße, aber auch als Folge von gefäßchirurgischen Eingriffen im Anastomosengebiet auf und resultieren meistens in einer deutlichen klinischen Symptomatik. Mikrovaskuläre Thrombosen finden sich in den kleinsten Gefäßen (Arteriolen, Venolen und Kapillaren) der verschiedenen Gewebe und führen zur Funktionsstörung des jeweiligen Gewebes bis hin zur Nekrose. Dieser Prozess kann einerseits akut auftreten, andererseits kann er sich auch schleichend und zunächst unbemerkt vollziehen. Oftmals ist bei Auftreten eines klinischen Korrelates schon eine deutliche und potentiell nicht reversible Schädigung des Gewebes eingetreten. Weiterhin sind Zirkulationsstörungen durch mikrovaskuläre Thrombosen z.B. im Rahmen der Organtransplantation oder nach Lappenplastiken zur Defektdeckung von Bedeutung. Hauptursache für einen Gewebeverlust nach Lappenplastiken ist neben der Thrombose im zu- und abführenden Gefäßsystem bzw. der Anastomosenregion die Mikrozirkulationsstörung im vaskularisierten Gewebe.

In diesem Zusammenhang sind Möglichkeiten der Prävention von mikrovaskulären Thrombosen, vor allem auch im Rahmen chirurgischer Maßnahmen, von großer Relevanz. Dieses setzt jedoch die genaue Kenntnis der sich im mikrovaskulären Gefäßbett vollziehenden physiologischen und pathologischen Vorgänge voraus.

Studien auf dem Gebiet der Thrombogenese haben im letzten Jahrhundert viele Erkenntnisse bezüglich Blutgerinnungsfaktoren und hereditären Gerinnungsstörungen geliefert. Mit Hilfe von *in vitro* Modellen konnten Proteine isoliert, Aminosäuresequenzen entschlüsselt, Gene identifiziert und in Interaktion mit verschiedenen Komponenten untersucht werden [1]. Die Rolle von unmittelbar an der Thrombusbildung beteiligten Zellen, wie z.B. Thrombozyten, Leukozyten und Endothelzellen wurde *in vitro* und *in vivo* analysiert und hierbei zelluläre Adhäsionsmoleküle charakterisiert [2].

Gegenstand derzeitiger Forschung ist die Identifizierung der an der Thrombogenese beteiligten zellulären und molekularen Mechanismen der Signaltransduktion. Die komplexe Interaktion von Blutkomponenten und Gefäßstrukturen erfordert die direkte und simultane Untersuchung der Entstehung und insbesondere der Beeinflussung der mikrovaskulären Thrombusbildung im lebenden Organismus. Somit ist es von hoher Relevanz, zu charakterisieren, wie die Vorgängige der Thrombusbildung in einem komplexen System *in vivo* tatsächlich ablaufen und vor allem, auf welche Weise eine Beeinflussung möglich ist.

1.1 Humorale, endotheliale und thrombozytäre Faktoren in der Thrombogenese

Die Blutgerinnung beinhaltet drei Grundelemente: Thrombozytenadhäsion, -aktivierung und -aggregation, Fibrinbildung sowie Fibrinolyse. Diese Faktoren interagieren miteinander und mit der Gefäßwand. Unter physiologischen Bedingungen ist der Blutfluss ungestört und eine intravaskuläre Thrombusbildung findet nicht statt [3,4]. Unter pathologischen Umständen, wie z.B. Ischämie-Reperfusion, Inflammation oder Arteriosklerose, wird die Blutgerinnung durch Bedingungen, die als Virchow'sche Trias bezeichnet werden, gefördert, namentlich Gefäßwandschaden, ein verlangsamter Blutfluss und eine veränderte Blutzusammensetzung [5,6].

Prinzipiell sind an der Thrombusbildung drei Komponenten beteiligt: die Gefäßwand (Endothelzellen, glatte Muskelzellen, Matrix- und Bindegewebe), Blutzellen (Thrombozyten, Leukozyten) und das plasmatische Gerinnungssystem [7]. Als zelluläre Strukturen sind demnach Endothelzellen, Thrombozyten und Leukozyten maßgeblich von Bedeutung. Zusätzlich kommt es zu einer Aktivierung der Gerinnungskaskade, welche in ein *intrinsisches* und ein *extrinsisches* System unterteilt wird (Abb. 1). Während beim *intrinsischen System* eine Kontaktaktivierung durch subendothelial exponiertes Kollagen über Faktor XII/XIIa, XI/XIa und IX/IXa zu einer Aktivierung von Thrombin führt, geschieht dieses beim *extrinsischen System* über die Freisetzung von Tissue Factor (TF, Gewebefaktor), welcher als Membranprotein auf den meisten nicht-vaskulären Zellen vorhanden ist [8].

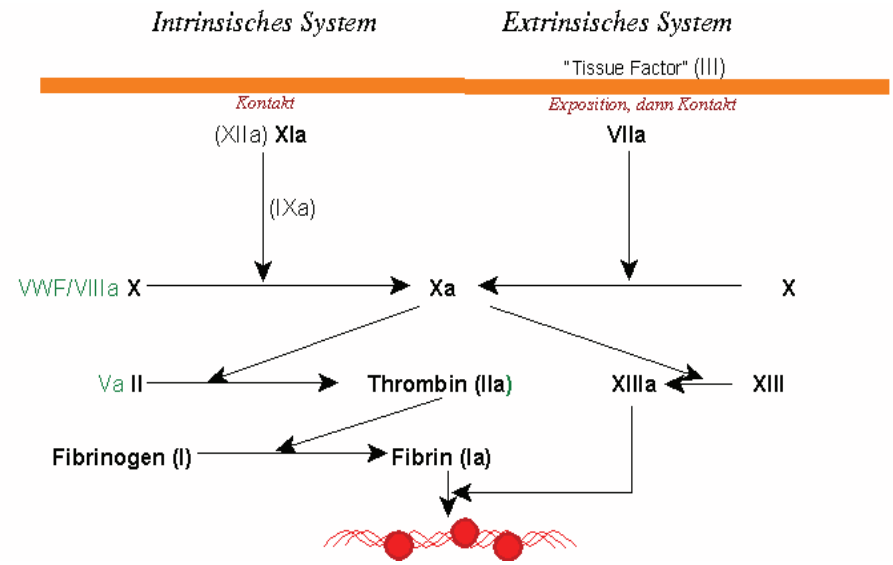

Abb. 1: Gerinnungskaskade (aus: www.biologie.com)

Thrombin katalysiert die Umwandlung von Fibrinogen in Fibrin, welches durch Faktor XIIIa von einem instabilen in ein stabiles Netzwerk überführt wird.

Ein entstandener Thrombus kann durch die Proteinase Plasmin wieder aufgelöst werden, welches als Vorstufe in Form von Plasminogen im Plasma vorliegt und durch andere Proteinasen in die aktive Form überführt wird. Dazu gehören Tissue Plasminogen Activator (t-PA), Streptokinase oder Urokinase (u-PA). Ein potenter Inhibitor des t-PA und somit ein prothrombogener Faktor ist der Plasminogen Aktivator Inhibitor-1 (PAI-1), welcher im Endothel gebildet und ins Blut abgegeben wird [9,10].

In den letzten Jahren wird zunehmend ein ’zellbasiertes’ Modell der Hämostase propagiert, welches folgende Phasen beinhaltet: Initialisierung, Amplifikation und Propagierung [11]. Die Initialisierung umfasst die zelluläre Expression von TF nach einer Endothelläsion durch extravaskuläre Zellen, die Aktivierung von Faktor IX und X durch den Faktor VIIa/TF-Komplex, die Adhärenz von Thrombozyten an Kollagen und andere Matrixkomponenten und die Sekretion von Faktor V aus den α-Granula der Thrombozyten [12,13]. In der Amplifikationsphase wird Thrombin durch TF-tragende Zellen generiert, welches zu einer verstärkten Thrombozytenaktivierung führt [14]. Schlussendlich findet die Phase der Propagierung statt, welche die Aktivierung des Tenasekomplexes (Faktor IXa/VIIIa) und des Prothrombinasekomplexes (Faktor Xa/Va) auf aktivierten Thrombozyten umfasst [12]. Zusätzlich produzieren die gebundenen Thrombozyten große Mengen Thrombin [11].

Das mikrovaskuläre Endothel ist mit einer Reihe von Mediatoren ausgestattet, die einer Thrombusbildung im mikrovaskulären Gefäßsystem vorbeugen. Hierzu gehören Stickstoffmonoxid (NO), Prostacyclin (PGI_2), Adenosin und Nucleotidasen, welche anti-adhäsive, anti-aggregative und vasodilative Eigenschaften besitzen [7,15]. NO und PGI_2 steigern den cAMP-Gehalt in Thrombozyten und vermindern daher deren Aggregationsfähigkeit [16]. Zusätzlich werden im Endothel anti-koagulative Substanzen, wie Thrombomodulin (TM), Tissue Factor Pathway Inhibitor (TFPI) und Heparane gebildet und die Fibrinauflösung durch Plasminogenaktivatoren (tPA, uPA) gefördert (Tab. 1). TM bindet Thrombin und neutralisiert somit seine Wirkung. Weiterhin aktiviert der Thrombin-TM-Komplex Protein C, was zur Initialisierung des Protein C-Pathway mit potenten anti-koagulativen Effekten führt [17]. Aktiviertes Protein C (APC) inaktiviert zwei essentielle Kofaktoren der plasmatischen Blutgerinnung, Faktor VIIIa und Va, und stellt als Protein C/Protein S-Komplex einen der wichtigsten anti-koagulativen Mechanismen dar [18,19].

Dahingegen findet sich bei endothelialer Dysfunktion oder endothelialer Aktivierung ein pro-thrombogener Zustand, welcher durch eine vermehrte Freisetzung von TF, Faktor Va, vWF, Platelet Activating Factor (PAF), P-Selektin und Interleukin-8 gekennzeichnet ist und zu Thrombozytenaktivierung, Fibrinablagerung, Inflammation und Leukozytenaktivierung führt, während die Fibrinolyse durch PAI-1 gehemmt wird [7] (Tab. 2). Die Balance zwischen tPA und PAI-1 kann durch verschiedene Zytokine zugunsten von PAI-1 verschoben werden, was eine Prothrombogenität des Endothels verursacht [20].

Zu den endothelialen Faktoren, die eine Thrombozytenaktivierung verursachen, gehören unter anderem PAF und vWF. PAF ist ein starker Thrombozytenaktivator und fördert die Thrombozytenadhäsion an das Endothel [21]. vWF wird in endothelialen Weibel-Palade-Bodies gespeichert und nach Aktivierung, z.B. durch Thrombin, schnell freigesetzt [22]. Zusätzlich bindet und stabilisiert vWF Faktor VIII und vermittelt die Thrombozytenadhäsion an das Endothel [23]. In Endothelzellen führt Thrombin zur Freisetzung von vWF, P-Selektin und PAF [24].

Anti-thrombogene Faktoren	**Wirkungsprofil**
NO	Inhibition Thrombozytenaktivierung, Vasodilatation
PGI_2	Inhibition Thrombozytenaktivierung
Adenosin	Vasodilatation
TFPI	Inaktivierung Faktor VIIa und Xa
TM	Protein C Aktivierung (als Thrombin-TM-Komplex)
Protein S	Inaktivierung Faktor Va und VIIIa (als Protein C/Protein S-Komplex)
tPA/uPA	Fibrinolyse
Heparansulfat	Kofaktor für Antithrombin

Tab 1: Anti-thrombogene Faktoren des Endothels (modifiziert nach: [7,25])

Pro-thrombogene Faktoren	Wirkungsprofil
vWF	Vermittlung Thrombozytenadhäsion, Trägerprotein Faktor VIII
PAF	Verstärkung der Thrombozytenaktivierung
P-Selektin	Verstärkung der Leukozytenadhäsion
TF	Ko-Faktor Faktor VIIa
FVa	Verstärkung Aktivität Faktor Xa
Phosphatidylserin	Verstärkung der Thrombozytenaktivierung (Annexin V-Ligand)
PAI-1	Inaktivierung tPA

Tab 2: Pro-thrombogene Faktoren des Endothels (modifiziert nach: [7,25])

Während das Endothel unter physiologischen Bedingungen komplett anti-thrombogene und anti-inflammatorische Eigenschaften aufweist, führen endotheliale Aktivierung bzw. Endothelzellschaden, sei es im Rahmen physiologischer Vorgänge, wie einer Gefäßverletzung mit der Notwendigkeit der Blutstillung, oder als pathophysiologischer Zustand, wie z.B. Arteriosklerose, zu einer Verschiebung des Gleichgewichtes hin zum prothrombogenen Zustand. Die Grenzen zwischen „positiver“ Hämostase und „negativer“ verstärkter Thrombusbildung sind teilweise fließend.

Neben einer Vielzahl an Faktoren, welche die Entstehung von Thrombosen beeinflussen, ist das Verhalten der Thrombozyten, v.a. deren Aggregation, Adhäsion und Thrombogenese, von hoher Relevanz in der Pathogenese der Thrombose. Insbesondere prädisponiert eine vermehrte Produktion bzw. ein verminderter Abbau von reaktiven Sauerstoffverbindungen für thrombotische Ereignisse. Der Prozess der Thromboseentstehung beinhaltet u.a. Thrombozyten-Thrombozyten, Thrombozyten-Endothelzell, Thrombozyten-Leukozyten und Leukozyten-Endothelzell-Interaktionen [26,27]. Nach Aktivierung produzieren Thrombozyten reaktive Sauerstoffspezies ihrerseits [28] und stimulieren wiederum die Bildung von reaktiven Sauerstoffverbindungen in Leukozyten.

Die durch Stimulation vermehrte Expression von P-Selektin auf der Thrombozytenoberfläche ermöglicht die Interaktion mit Liganden auf anderen Zellen, insbesondere auf Monozyten. Während P-Selektin keine Thrombozyten-Thrombozyten-Interaktionen vermittelt, stellt P-Selektin auf aktivierten Plättchen einen Bindungsort für

Leukozyten dar und spielt eine entscheidende Rolle bezüglich der Größe und Stabilität eines entstehenden Thrombus [29]. Zusätzlich werden diese Interaktionen über GPIIb-IIIa auf Thrombozyten und MAC-1 (Macrophage antigen-1; CD11b/CD18) auf Leukozyten vermittelt. Weiterhin sind polymorphkernige Granulozyten in der Lage, auf ihrer Oberfläche TF zu exprimieren [30].

Die Bildung von Thrombozyten-Leukozyten Koaggregaten wird daher als inflammatorische Komponente in der Thrombusbildung angesehen [31,32]. Im Rahmen dieser Aktivierung werden vom Endothel Selektine, Vascular Cell Adhesion Molecule-1 (VCAM-1) und Intercellular Cell Adhesion Molecule-1 (ICAM-1) exprimiert und in löslicher Form ins Blut abgegeben, welche die Adhäsion von Monozyten fördern [33]. Im Anschluss migrieren diese Monozyten durch die Endothelzelllücken in die Tunica intima und können dort Endothelzellschäden induzieren [34].

1.2 Phasen der mikrovaskulären Thrombusbildung

Thrombozyten zirkulieren im Blut mit der Aufgabe intaktes von verletztem oder pathologisch verändertem Endothel zu unterscheiden. Tritt ein Endothelschaden auf, führt dieser zum Verlust der Barriere zwischen athrombogener Endothelzellschicht und hoch thrombogener extrazellulärer Matrix [35].

Thrombozytenadhäsion

Nach einer Gefäßläsion kommt es innerhalb von Sekunden zur Ablagerung von Thrombozyten, welche in Abhängigkeit von der Tiefe der Verletzung mit verschiedenen subendothelialen extrazellulären Strukturen in Kontakt kommen. Dazu gehören Kollagen, Proteoglykane, Entactin, Laminin, Fibronektin und Fibulin. Die thrombozytären Membranglykoproteine GPIa-IIa und GPVI interagieren direkt mit Kollagen [36]. Diese Kollagenrezeptoren können bei durch den Blutfluss bedingten hohen Scherkräften von >1000 s^{1} nur dann die Thrombusbildung initiieren und propagieren, wenn sie initial durch die Interaktion von GPIbα und vWF an die Gefäßwand gebunden werden. Diese Bindung von GPIbα an das Endothel vermittelt jedoch keine feste Adhärenz [37]. Thrombozyten exprimieren weiterhin den Lamininrezeptor $\alpha_6\beta_1$ und können über den GP1bα-Rezeptor Fibronektin binden [38].

Thrombozytenaktivierung

Substanzen, die durch die initiale Adhärenz der Thrombozyten freigesetzt werden und im Bereich der Gefäßläsion produziert werden, verstärken innerhalb von Sekunden die prokoagulativen Eigenschaften der Thrombozyten, die in der Nähe des wachsenden Thrombus zirkulieren [37]. Die Aktivierung der Thrombozyten erfolgt durch subendotheliales Kollagen, vWF und durch Thrombin, welches bei der Blutgerinnung entsteht und auf der Membran stimulierter Thrombozyten generiert wird, sowie durch Adenosindiphosphat (ADP), welches ebenfalls von Thrombozyten, aber auch von Endothelzellen produziert wird, und Adrenalin und Thromboxan A_2 aus Thrombozyten.

Die Serinprotease Thrombin aktiviert Thrombozyten über G-Protein gekoppelte Protease Activated Rezeptoren (PAR) [39]. Phänotypische Merkmale der Thrombozytenaktivierung beeinhalten Aktinpolymerisierung, zytoskeletale Reorganisation mit Pseudopodienbildung und Aggregation (Abb. 2).

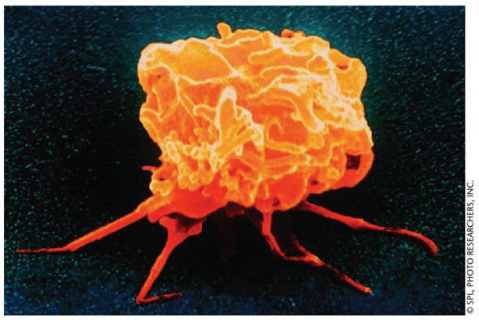

Abb. 2: Aktivierter Thrombozyt (aus: [35])

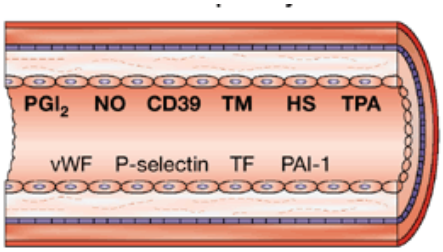

Abb. 3: Endotheliale Faktoren (aus: [35])

Gleichzeitig synthetisiert und exprimiert das vaskuläre Endothel prokoagulative Faktoren, wie vWF, P-Selektin, TF und PAI-1 (Abb. 3) [35]. Diese endotheliale und thrombozytäre Aktivierung wird unter physiologischen Bedingungen durch PGI_2 und NO gehemmt.

Thrombozytenaggregation

Die Aggregation vervielfacht die Zahl der im entstehenden Thrombus akkumulierten Thrombozyten innerhalb von Minuten. Das prinzipielle Resultat stellt die Konformationsänderung des GP IIb-IIIa Rezeptors ($\alpha_{IIb}\beta_3$) dar [40]. Der aktivierte GPIIb-IIIa Rezeptor vermittelt die feste Adhäsion und bindet lösliche Adhäsionsproteine wie Fibrinogen, vWF und Fibronectin. Zusätzlich führt der Endothelzellschaden zur Freisetzung von TF und subsequenter Thrombozytenadhäsion, woraufhin Fibrin in den Thrombus akkumuliert wird [41].

1.3 Wissenschaftliche Fragestellung

Obwohl das Verständnis der pathophysiologischen Prozesse, welche der mikrovaskulären Thrombusbildung zugrunde liegen in den letzten zwei Jahrzehnten stetig zugenommen hat und viele zelluläre und molekulare Faktoren in diesem Zusammenhang isoliert werden konnten, existieren nur wenige Studien, die das Zusammenspiel von endothelialen, thrombozytären und humoralen Faktoren im lebenden Organismus untersucht haben. Ziel der vorliegenden Arbeit war es daher, im *in vivo* Tiermodell die mikrovaskuläre Thrombusbildung zu charakterisieren und die Beeinflussbarkeit durch endogene und exogene Faktoren zu studieren. Ein besonderes Interesse galt dabei der Identifizierung zugrunde liegender Mechanismen auf endothelialer und thrombozytärer Ebene.

Daraus ergaben sich folgende konkrete Fragestellungen:

1. Charakterisierung des Einflusses pathologischer Zustände, wie z.B. Hypothermie und Sepsis, auf mikrovaskuläre Thrombusbildung, Endothelzellfunktion und Thrombozytenfunktion

2. Quantifizierung der mikrovaskulären Thrombogenität nach Induktion endogener Enzymsysteme, wie z.B. Hämoxygenase-1.

3. Beeinflussbarkeit der mikrovaskulären Thrombogenese durch Applikation potentiell protektiver Substanzen, wie z.B. anti-oxidatives Ebselen und C-Peptid, und Identifizierung zugrunde liegender zellulärer und humoraler Mechanismen

4. Beeinflussung der mikrovaskulären Thrombusbildung durch Applikation fraglich pro-thrombogener Substanzen, wie z.B. Darbepoetin-alpha und Nikotin und Identifizierung zugrunde liegender zellulärer und humoraler Mechanismen

1.4 Methoden

Im Folgenden wird ein Überblick über die angewendeten Methoden gegeben:

Tiermodelle

Zur Untersuchung der mikrovaskulären Thrombusbildung verwendeten wir zum einen die Cremastermuskelpräparation an Ratte und Maus, die erstmalig von Baez [42] an der Ratte beschrieben und später von unserer [43] und anderen Arbeitsgruppen [44,45] auf die Maus übertragen wurde. Dabei wird zunächst ein venöser Katheter zur Applikation von Fluoreszenzfarbstoffen in die Vena jugularis gelegt. Danach wird das Skrotum gespalten und der Hoden mit umgebendem Cremastermuskel dargestellt. An der Hodenspitze werden die distalen Gefäße kauterisiert und der Hoden und Nebenhoden mit distalem Anteil des Funiculus spermaticus entnommen. Danach wird die Vorderwand des Muskels unter Schonung der größeren Gefäße eröffnet, so dass der Muskel als axial gestielter Lappen mit dem Körper verbunden bleibt. Nach Präparation des Muskels wird der Samenstrang mit dem Ductus deferens und den Vasa testicularia ligiert und abgetrennt. Der Musculus cremaster wird auf einem Objektträger ausgebreitet, mit Hilfe von Seidenfäden fixiert und mit Kochsalzlösung feucht gehalten (Abb. 4 und 5).

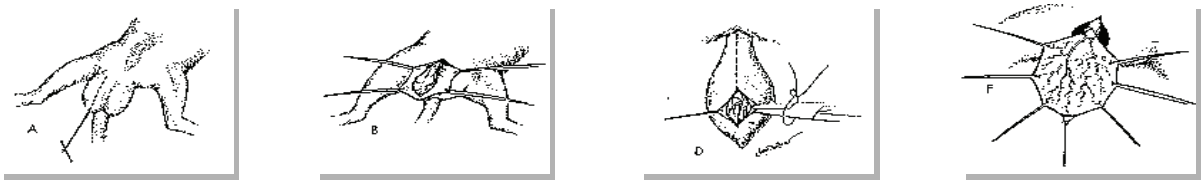

Abb. 4 Cremastermuskelpräparation (aus: [42])

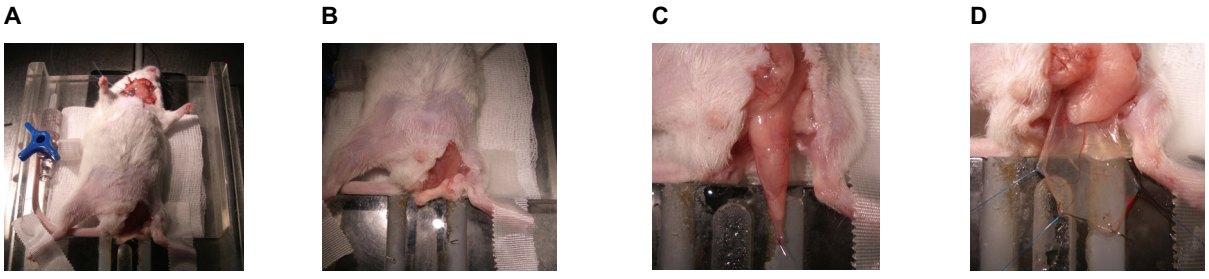

Abb. 5 Katheteranlage und Cremastermuskelpräparation bei der Maus: (A) Venöser Katheter in der Vena jugularis und eröffnete Skrotalhaut, (B) Präparation von Hoden und umgebenden Cremastermuskel, (C) mobilisierter geschlossener Cremastermuskel, (D) eröffneter und ausgespannter Cremastermuskel.

Als weiteres Modell diente die chronische Rückenhautkammer, welche primär für den Hamster [46] im Detail beschrieben und von Lehr et al. auf die Maus übertragen wurde [47] (Abb. 6). Sie ermöglicht eine repetitive intravitalmikroskopische Untersuchung von gestreiftem Skelettmuskel und Subkutangewebe. Dabei wird die Rückenhautfalte angehoben und die sich aus zwei symmetrischen Titaniumrahmen zusammensetzende Rückenhautkammer kaudal der entlang der Schulterbasis verlaufenden Versorgungsgefäßen implantiert. Im kreisrunden Bereich des Beobachtungsfensters der Kammer werden in einem Durchmesser von 15mm die dem Fenster zugewandte Kutis, Subkutis mit Hautmuskel sowie die beiden Schichten des Musculus retractor entfernt und die verbleibenden Gewebeschichten mit einem wiederentfernbaren Deckglas bedeckt und mittels eines Sprengrings im Titanrahmen fixiert, so dass die gegenüberliegende Hautmuskulatur und Subkutis der intravitalmikroskopischen Beobachtung zugänglich sind.

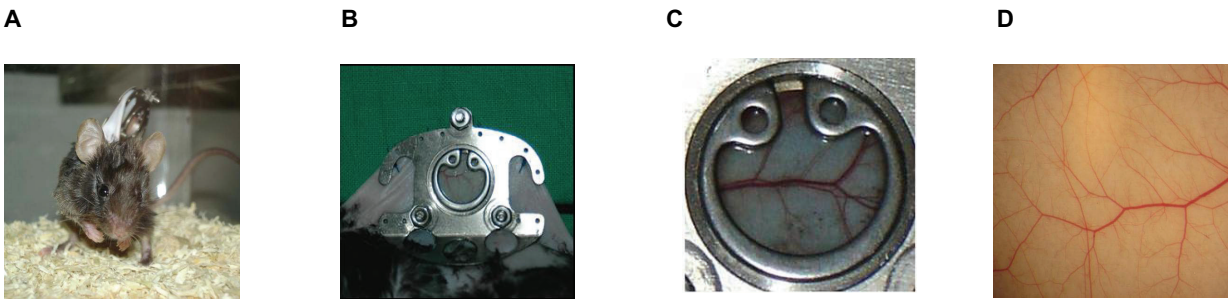

Abb. 6 Chronische Rückenhautkammer der Maus: (A) Maus mit Rückenhautkammer nach der Präparation, (B) Titanrahmen mit Deckglas, (C) Beobachtungsfenster mit Sicht auf (D) die Gefäße der gestreiften Skelettmuskulatur und des Subkutangewebes

In beiden Modellen sind neben der Untersuchung der mikrovaskulären Perfusion eine Analyse von Leukozyten-Endothelzell- und Thrombozyten-Endothelzell-Interaktion sowie eine genaue zeitliche Dokumentation der Thrombusbildung möglich .

Thrombosemodelle

Mikrovaskuläre Thrombosen wurden photochemisch und chemisch induziert. Zur photochemischen Thromboseinduktion wurde das entsprechende mikrovaskuläre Gefäß nach Injektion von Fluorescein Isothiocyanat (FITC)-markiertem Dextran (MW 150000 Da) mit gefiltertem blauen Licht (450-490 nm) einer 100W Quecksilberlampe durch ein x63 Wasserimmersionsobjektiv bestrahlt, wie dies von unserer Arbeitsgruppe zuvor beschrieben wurde [43,48].

Zur chemischen Thrombusinduktion erfolgte die Superfusion des Gewebes mit Eisenchlorid (12,5 mM $FeCl_3$), modifiziert nach Denis [49]. In beiden Modellen kommt es durch Radikalbildung zu einer lokalen Endothelzellschädigung mit subsequenter Initialisierung der Thombusbildung.

Durchflußzytometrie von humanen und murinen Thrombozyten

Die Thrombozytenfunktion wurde entweder *in vitro* nach Zugabe der jeweiligen Substanz oder *ex vivo* nach entsprechender Vorbehandlung der Tiere mittels durchflußzytometrischer Untersuchungen erfasst. Zusätzlich dienten auch humane Thrombozyten freiwilliger Probanden zur spezies-übergreifenden Analyse der Thrombozytenfunktion. Kurz gefasst handelt es sich bei der Durchflußzytometrie um ein Messverfahren zur Beurteilung von Partikeln (Zellen) in wässriger Suspension [50]. Dabei wird die Fluoreszenz der Thrombozyten durch einen Lichtstrahl gemessen, nachdem diese zuvor mit einem gegen spezifische Aktivierungsmarker auf der Thrombozytenoberfläche gerichteten fluoreszierenden Antikörper inkubiert wurden. Die Eigenschaften des auftretenden Streulichts werden von der Zellgröße und der Zellgranulärität bestimmt, während die Intensität der Fluoreszenz von der Anzahl der gebundenen Antikörper und somit von der Expression des jeweiligen Moleküls abhängt [51,52]. Typische thrombozytäre Aktivierungsmarker sind z.B. P-Selektin, GPIIb-IIIa und Lysosome Associated Membrane Protein-1 (LAMP-1). Die Aktivierung von Thrombozyten erfolgt durch die Zugabe von spezifischen Proteinen der Gerinnungskaskade, wie z.B. Thrombin oder Thrombin Receptor Activating Peptide (TRAP), subendothelialen Matrixproteinen (z.B. Kollagen) oder spezifischen, z.B. ADP und Adrenalin, bzw. unspezifischen Mediatoren, z.B. H_2O_2 [52].

Immunhistochemie endothelialer Aktivierungsmarker und Adhäsionsmoleküle

Die Expression endothelialer Aktivierungsmarker und Adhäsionsmoleküle wurde mittels spezifischer Antikörperbindung und nachfolgender Chromogenreaktion in histologischen Schnitten visualisiert und quantitativ analysiert. Zu diesen Molekülen zählen z.B. P-Selektin, ICAM-1, PAI-1 oder PAF-R.

ELISA löslicher endothelialer Aktivierungsmarker

Mit Hilfe von Enzyme Linked Immunosorbent Assays (ELISA) können lösliche Moleküle in einer Probe (Serum, Plasma etc.) durch eine Antikörperreaktion mit anschließender enzymatischer Farbumwandlung nachgewiesen werden. Es erfolgte die Bestimmung löslicher (s=soluble) endothelialer Aktivierungsmarker, wie sP-Selektin, sE-Selektin, sICAM-1, sVCAM-1 und sPAI-Ag, die bei endothelialer Aktivierung exprimiert und im Anschluss ins Blut abgegeben werden (shedding).

Western Blot Proteinanalysen

Ein Western Blot bezeichnet die Übertragung (das Blotten) von Proteinen auf eine Trägermembran, welche anschließend über unterschiedliche Reaktionen nachgewiesen werden können. Vor dem eigentlichen Western Blot wird ein Proteingemisch mit Hilfe einer Gel-Elektrophoresetechnik in einer Trägermatrix entsprechend ihrer Größe, Ladung oder anderer Eigenschaften aufgetrennt. Die Proteinbanden können nun auf der Membran mit Hilfe von spezifischen Antikörpern identifiziert werden. Es wurden sowohl Proteine im Cremastermuskelgewebe (z.B. P-Selektin, HO-1), als auch aus Thrombozytensuspensionen (Tyrosin-spezifische Phosphorylierung) untersucht.

RT-PCR

Die Reverse Transkriptase Polymerase Chain Reaction (RT-PCR) dient dem Nachweis der Transkription eines Gens. Es wird zuerst eine Reverse Transkriptase eingesetzt, eine RNA-abhängige DNA-Polymerase, welche RNA in cDNA umschreibt. Die cDNA kann im Anschluss als Ausgangsprodukt in einer PCR eingesetzt werden, um spezifische Sequenzen aus dieser zu amplifizieren. Die RT-PCR wurde zur Detektion akut hochregulierter Proteine eingesetzt (z.B. eNOS). Die Produkte der RT-PCR lassen sich anschließend elektrophoretisch in einem Agarosegel auftrennen. Verschieden große DNA-Fragmente wandern unterschiedlich schnell im Gel. Durch einen Fluoreszenzfarbstoff (meist Ethidiumbromid) können die Fragmente im UV-Licht sichtbar gemacht und dokumentiert werden.

2 Experimentelle Studien

2.1 Einfluss pathologischer Zustände auf die Thrombogenese

Die intravitalmikroskopischen, durchflußzytometrischen und molekularbiologischen Untersuchungen dienten der Erfassung des Effektes von reversibler systemischer Hypothermie auf die mikrovaskuläre Thrombusbildung und die Thrombozytenfunktion.

2.1.1 Hypothermie

Unter systemisch hypothermen Bedingungen wurden in der Vergangenheit sowohl eine vermehrte Thrombogenität, als auch eine Blutungsneigung beobachtet. Insbesondere wird der Effekt der Hypothermie auf die Thrombozytenfunktion kontrovers diskutiert. Daher wurden in dieser Studie bei Mäusen klinisch auftretende Körperkerntemperaturen von 34°C und 31°C induziert und die Kinetik der mikrovaskulären Thrombusbildung im Cremastermuskel untersucht. Zusätzlich erfolgten die gleichen Versuche nach Hypothermie und Wiedererwärmung auf 37°C. Es zeigte sich eine signifikant schnellere Thrombusbildung bei hypothermen Temperaturen, welche nach Wiedererwärmung komplett aufgehoben war. Die durchflußzytometrischen Untersuchungen ergaben sowohl in ruhenden, als auch in TRAP-stimulierten Thrombozyten, eine signifikant vermehrte Expression der aktiven Konformation des GP IIb-IIIa Rezeptors bei 31°C und 34°C gegenüber Temperaturen von 37°C. Dieses ging einher mit einer ebenfalls signifikant vermehrten thrombozytären Fibrinogenbindung bei diesen Temperaturen. Außerdem war die Tyrosin-spezifische Phosphorylierung unter hypothermen Bedingungen erhöht. Daraus kann geschlussfolgert werden, dass eine moderate, klinisch auftretende Hypothermie einen pro-thrombogenen Effekt besitzt, was wahrscheinlich durch eine verstärkte thrombozytäre GP IIb-IIIa Aktivierung vermittelt ist. Es besteht jedoch keine Prädisposition mit einem erhöhten Risiko für mikrovaskuläre Thrombosen nach Wiedererwärmung auf physiologische Körperkerntemperaturen.

Lindenblatt N, Menger MD, Klar E, Vollmar B

Sustained hypothermia accelerates microvascular thrombus formation in mice

Am J Physiol Heart Circ Physiol 2005; 289: H2680-H2687

Am J Physiol Heart Circ Physiol 289: H2680–H2687, 2005.
First published August 12, 2005; doi:10.1152/ajpheart.00425.2005.

Sustained hypothermia accelerates microvascular thrombus formation in mice

Nicole Lindenblatt,[1,2] Michael D. Menger,[3] Ernst Klar,[2] and Brigitte Vollmar[1]

[1]*Department of Experimental Surgery and* [2]*Department of General Surgery, University of Rostock, Rostock; and* [3]*Department of Clinical and Experimental Surgery, University of Saarland, Homburg-Saar, Germany*

Submitted 28 April 2005; accepted in final form 4 August 2005

Lindenblatt, Nicole, Michael D. Menger, Ernst Klar, and Brigitte Vollmar. Sustained hypothermia accelerates microvascular thrombus formation in mice. *Am J Physiol Heart Circ Physiol* 289: H2680–H2687, 2005. First published August 12, 2005; doi:10.1152/ajpheart.00425.2005.—Cold is supposed to be associated with alterations in blood coagulation and a pronounced risk for thrombosis. We studied the effect of clinically encountered systemic hypothermia on microvascular thrombosis in vivo and in vitro. Ferric chloride-induced microvascular thrombus formation was analyzed in cremaster muscle preparations from hypothermic mice. Additionally, flow cytometry and Western blot analysis was used to evaluate the effect of hypothermia on platelet activation. To test whether preceding hypothermia predisposes for enhanced thrombosis, experiments were repeated after hypothermia and rewarming to 37°C. Control animals revealed complete occlusion of arterioles and venules after 742 ± 150 and 824 ± 172 s, respectively. Systemic hypothermia of 34°C accelerated thrombus formation in arterioles and venules (279 ± 120 and 376 ± 121 s; $P < 0.05$ vs. 37°C). This was further pronounced after cooling to 31°C (163 ± 57 and 281 ± 71 s; $P < 0.05$ vs. 37°C). Magnitude of thrombin receptor activating peptide (TRAP)-induced platelet activation increased with decreasing temperatures, as shown by 1.8- and 3.0-fold increases in mean fluorescence after PAC-1 binding to glycoprotein (GP)IIb-IIIa and 1.6- and 2.9-fold increases of fibrinogen binding on incubation at 34°C and 31°C. Additionally, tyrosine-specific protein phosphorylation in platelets was increased at hypothermic temperatures. In rewarmed animals, kinetics of thrombus formation were comparable to those in normothermic controls. Concomitantly, spontaneous and TRAP-enhanced GPIIb-IIIa activation did not differ between rewarmed platelets and those maintained continuously at 37°C. Moderate systemic hypothermia accelerates microvascular thrombosis, which might be mediated by increased GPIIb-IIIa activation on platelets but does not cause predisposition with increased risk for microvascular thrombus formation after rewarming.

hemodynamics; glycoproteins; microcirculation; platelets

BLEEDING DIATHESIS WITH PROLONGATION of bleeding times has been reported in a variety of clinical settings associated with systemic hypothermia (19, 28, 36). In trauma patients hypothermia has been presumed to adversely affect blood coagulation (7, 31). In line with this, in vitro studies suggested that perioperative hypothermia may aggravate surgical bleeding by impairing platelet P-selectin expression and thromboxane release as well as by reducing activity of coagulation factors (24, 32).

In clear contrast to these reports on hypothermia-related bleeding diathesis, cold-related pathology, such as the seasonal increase in thromboembolic disease in winter, is well recognized (8, 9, 30). Cold is associated with peripheral vasoconstriction and increased cardiac output, blood pressure, and circulating norepinephrine, all of which enhance the risk for cardiac events and coronary heart disease mortality. The fact that in regions without temperature extremes a seasonal variation in myocardial infarction is absent (20) emphasizes the ambient air temperature as an environmental risk factor. Seasonal changes in temperature further influence blood rheology with increase of viscosity of blood and resistance of red blood cells to deform as temperature is lowered, contributing in a major way to impaired circulation in the cold (21, 26). The Caerphilly prospective heart disease study, comprising data on the association of air temperature and risk factors for ischemic heart disease from up to 2,036 men, indicates that the most important effect of a fall in temperature seems to be on the hemostatic system, with an increase of fibrinogen and a decrease in the fibrinolysis-inhibiting α_2-macroglobulin (8). Moreover, platelet count and platelet aggregation have been shown in vitro to increase at hypothermic temperatures (8, 10, 17). Unintentional perioperative hypothermia is associated with postoperative myocardial ischemia, additionally underlining a potential prothrombogenic effect of low body temperature (12).

To further address this issue, we evaluated hypothermia-induced platelet response in vitro using temperatures of 34°C and 31°C, which are likely to be encountered during major surgery, multiple trauma, cold exposure, and the neonatal period. We additionally assessed kinetics of microvascular thrombus formation in an in vivo model of hypothermic mice. To test whether preceding hypothermia predisposes to thrombus formation, in vitro and in vivo experiments were repeated on hypothermia and subsequent rewarming to 37°C.

MATERIALS AND METHODS

Mouse cremaster muscle preparation. On approval by the local government, all experiments were carried out in accordance with German legislation on protection of animals and the National Institutes of Health *Guide for the Care and Use of Laboratory Animals* (Institute of Laboratory Animal Resources, National Research Council). Male C57BL/6J mice with a body weight of 20–25 g were anesthetized by an intraperitoneal injection of ketamine (90 mg/kg body wt) and xylazine (25 mg/kg body wt), and a polyethylene catheter was placed into the right jugular vein for application of fluorescent dyes.

For the study of vascular thrombus formation, we used the opened cremaster muscle preparation, as originally described by Baez (1) in rats and transferred by our group (22, 42) to mice. Before preparation of the cremaster muscle, animals were placed on a heating pad coupled to a rectal probe. A midline incision of the skin and fascia was made over the ventral aspect of the scrotum and extended up to the inguinal fold and to the distal end of the scrotum. The incised tissues

Address for reprint requests and other correspondence: N. Lindenblatt, Dept. of Experimental Surgery and Dept. of General Surgery, Univ. of Rostock, Schillingallee 70, 18055 Rostock, Germany (e-mail: niclindenblatt@hotmail.com).

The costs of publication of this article were defrayed in part by the payment of page charges. The article must therefore be hereby marked "*advertisement*" in accordance with 18 U.S.C. Section 1734 solely to indicate this fact.

0363-6135/05 $8.00 Copyright © 2005 the American Physiological Society

American Journal of Physiology – Heart and Circulatory Physiology

Downloaded from ajpheart.physiology.org on December 20, 2006

American Journal of Physiology – Heart and Circulatory Physiology

were retracted to expose the cremaster muscle sack, which was maintained under gentle traction to carefully separate the remaining connective tissue by blunt dissection from around the cremaster sack. The cremaster muscle was then incised, avoiding cutting of the larger anastomosing vessels. Hemostasis was achieved with 5-0 threads, also serving to spread the tissue. After dissection of the vessel connecting the cremaster and the testis, the epididymis and testis were put to the side of the preparation. The preparation was performed on a transparent pedestal to allow microscopic observation of the cremaster muscle microcirculation by both transillumination and epi-illumination techniques.

After the preparation of the cremaster muscle, the animals were allowed to recover from surgical preparation for 15 min. Thrombus formation was then induced in randomly chosen venules ($n = 1$ or 2 per preparation) and arterioles ($n = 1$ or 2 per preparation).

In vivo thrombosis model. After intravenous injection of 0.1 ml of 5% FITC-labeled dextran (mol wt 150,000; Sigma-Aldrich, Munich, Germany) and subsequent circulation for 30 s, the cremaster muscle microcirculation was visualized by intravital fluorescence microscopy with a Zeiss microscope (Axiotech vario; Zeiss, Jena, Germany). The microscopic procedure was performed at a constant room temperature of 21–23°C. The epi-illumination setup included a 100-W HBO mercury lamp and an illuminator equipped with a blue filter (450- to 490-nm excitation and >520-nm emission wavelengths). Microscopic images were recorded by a charge-coupled device video camera (FK 6990A-IQ; Pieper, Berlin, Germany) and stored on videotapes for offline evaluation (S-VHS Panasonic AG 7350-E; Matsushita, Tokyo, Japan). With a ×20 water immersion objective (Achroplan ×20/0.50 W; Zeiss) blood flow was monitored in individual arterioles (diameter range 30–50 μm) and venules (diameter range 60–80 μm), followed by superfusion with 25 μl of ferric chloride (12.5 mM; Sigma) for induction of microvascular thrombosis (6, 22). Complete vessel occlusion was assumed when blood flow ceased for >60 s because of thrombotic occlusion. Because rapid spreading of ferric chloride solution allowed us to study only 1 or 2 arterioles and venules within each preparation, both left and right cremaster muscles were prepared for analysis of thrombotic vessel occlusion within each animal.

Analysis included the time periods until first standstill of perfusion and sustained cessation of blood flow due to complete vessel occlusion. Additionally, a red blood cell velocity profile was determined to characterize the kinetics of microvascular thrombus formation. Microcirculatory analysis further included the determination of vessel diameter and blood cell velocity before thrombus induction with a calculation of vascular wall shear rates based on the Newtonian definition $\gamma = 8 \times V/D$, with V representing the red blood cell center line velocity divided by 1.6 according to the Baker-Wayland factor (2) and D representing the individual inner vessel diameter.

Experimental design. Immediately after induction of anesthesia, animals were placed on a customized platform comprising a heating pad to facilitate microscopy of the cremaster muscle. Temperature was controlled by a rectal probe and maintained at 37°C ($n = 6$), 34°C ($n = 5$), and 31°C ($n = 5$). Because accurate maintenance of the animals' core body temperature was a prerequisite for this study, the examiner was not blinded to animal temperature.

The assumption that the rectal temperature equaled the core body temperature was confirmed by additional experiments with a LICOX probe (LICOX 1; GMS, Kiel-Mielkendorf, Germany), which was placed via the left jugular vein into the right atrium. Rectal temperature differed no more than ±0.2°C from central temperature and was therefore used subsequently to determine the core body temperature of the animal. Depending on the rectal temperature at the beginning of the experiment and the desired final temperature, heating was started immediately or after the animal cooled down to the required temperature. Artificial cooling was not necessary, because most animals displayed a considerable drop of body temperature after the induction of anesthesia. After the appropriate temperature according to randomization of animals was reached and remained stable for at least 30 min, preparation was started and microvascular thrombus formation was induced as described above. In an additional series of experiments, mice were kept hypothermic at either 34°C ($n = 4$) or 31°C ($n = 4$) for at least 30 min, followed by rewarming to 37°C and subsequent thrombus induction.

Human blood collection and platelet-rich plasma preparation. Written informed consent of all volunteers was obtained for blood drawing. For in vitro tests of platelet function, blood from a total of seven healthy volunteers was drawn from the left cubital vein with a 21-gauge needle into 5-ml S-Monovettes 9NC (Sarstedt, Nümbrecht, Germany) (1:10 citrate vol/vol). Despite differences in size, number, and ultrastructural morphology, human and murine platelets have been shown to exert similar organelle and glycoprotein (GP) subcellular distribution (37). The GPIIb-IIIa receptor in particular exerts comparable functions during platelet activation and aggregation in humans and mice (40). Although species differences cannot be completely excluded, the use of human platelets is justifiable and obvious because of their simple accessibility and ease of handling for flow cytometric studies.

After centrifugation for 15 min at 110 *g* and room temperature (GS-6R Centrifuge; Beckman Coulter, Fullerton, CA), platelet-rich plasma (PRP) was transferred in a separate tube. Platelet count was assessed with a cell counter (Sysmex KX-21; Sysmex, Norderstedt, Germany) and adjusted to 2×10^8/ml by dilution with PBS. In parallel, aliquots of whole blood were processed for the flow cytometric study of thrombin receptor activating peptide (TRAP)/*N*-formylmethionyl-leucyl-phenylalanine (fMLP)-induced platelet-leukocyte aggregates (see below).

Platelet exposure to TRAP and flow cytometric analysis of P-selectin expression, GPIIb-IIIa activation, and fibrinogen binding. After 30 min of resting in a 37°C water bath to eliminate isolation-induced platelet activation, 50 μl of platelet suspensions was incubated for 30 min in water baths at the maintained temperature of 37°C, 34°C, or 31°C, followed by exposure to TRAP (2.5 mM) and incubation with saturating amounts of the appropriate antibody or fluorescence-labeled human fibrinogen. Platelet suspensions were kept for an additional 30 min in the respective water baths in the dark. Platelets were then rapidly cooled on ice and diluted with 1 ml of 4°C 1% paraformaldehyde in PBS (Cell Fix; Becton Dickinson, Heidelberg, Germany). After fixation was completed, platelets were centrifuged at 300 *g* for 4 min at 4°C and washed twice with PBS. The supernatant fraction was decanted, and the pellet was resuspended in PBS for flow cytometry. Expression of P-selectin on platelets was investigated by direct immunofluorescence using a monoclonal anti-human FITC-coupled P-selectin antibody (Santa Cruz Biotechnology, Heidelberg, Germany), diluted 1:50 (vol/vol) with staining medium (0.1% sodium azide and 2% fetal calf serum in PBS). In an additional set of experiments a FITC-coupled PAC-1 antibody (Becton Dickinson Biosciences) directed against the activated conformation of GPIIb-IIIa was used (38, 39). A FITC-coupled IgG_1 isotype-matched control antibody (Santa Cruz) was used to exclude nonspecific binding. To further confirm GPIIb-IIIa activation, Alexa Fluor 488-labeled human fibrinogen (Invitrogen, Karlsruhe, Germany) was added at a concentration of 100 μg/ml. Flow cytometry was performed within the next hour. In an additional set of experiments, platelets were kept at either 34°C or 31°C for 30 min, followed by their transfer into a 37°C water bath for 30 min and subsequent stimulation by TRAP, as described above.

A FACScan flow cytometer (Becton Dickinson) was calibrated with fluorescent standard microbeads (CaliBRITE Beads; Becton Dickinson) for accurate instrument setting. Platelets were identified by their characteristic forward and sideward scatter light and selectively analyzed for their fluorescence properties with the CellQuest program (Becton Dickinson) with assessment of 20,000 events per sample. The relative fluorescence intensity of a given sample was calculated by subtracting the signal obtained when cells were incubated with the

Downloaded from ajpheart.physiology.org on December 20, 2006

American Journal of Physiology – Heart and Circulatory Physiology

Table 1. *Blood flow velocity and wall shear rates in mice cremaster muscle microvessels before ferric chloride-induced thrombus formation*

	Arterioles		Venules	
	Velocity, μm/s	γ, s^{-1}	Velocity, μm/s	γ, s^{-1}
37°C	2,235±55	172±18	1,693±185	107±11
34°C	1,698±159*	181±17	1,243±207	114±18
31°C	1,941±222	223±23	864±190	70±15

Values are means ± SE; n = 7–9 vessels/group. γ, Wall shear rate. *P < 0.05 vs. 37°C.

isotype-specific control antibody from the signal generated by cells incubated with the test antibody.

Whole blood exposure to TRAP/fMLP and flow cytometric analysis of platelet-leukocyte aggregates. Whole blood aliquots of 50 μl were incubated for 25 min with 5 μl of a monoclonal anti-human FITC-coupled CD42b antibody (eBioscience, San Diego, CA) and with 5 μl of a monoclonal anti-human phycoerythrin-coupled CD45 antibody (eBioscience). Aliquots were then incubated at temperatures of 37°C, 34°C, and 31°C in the water bath for 30 min, followed by exposure to TRAP (2.5 mM) and fMLP (10^{-7} M) for an additional 30 min. Subsequently, erythrocytes were lysed in 1.5 ml of lysing solution (Becton Dickinson) for 15 min. The reaction was stopped by diluting the solution with 2 ml of PBS, followed by centrifugation at 300 *g* for 5 min. The aliquots were washed again with PBS, and the pellet was resuspended with 1 ml of Cell Fix. Flow cytometry was performed within the next hour, as described above.

Chemicals. TRAP was purchased from Bachem (Bubendorf, Germany) and dissolved in PBS to yield a 2.5 mM stock solution. fMLP (Sigma-Aldrich, Munich, Germany) was dissolved in PBS and added to the samples to achieve a final concentration of 10^{-7} M.

Western blot analysis of tyrosine-specific phosphorylation of platelet proteins. For whole protein extracts and Western blot analysis of phosphotyrosine (p-Tyr), PRP was prepared as described above. After 30 min of resting in a 37°C water bath, 50 μl of platelet suspensions was incubated for 30 min in water baths maintaining temperature at 37°C, 34°C, or 31°C, followed by exposure to TRAP (2.5 mM) and incubation for an additional 30 min in the respective water baths in the dark. Platelets were then lysed for 30 min on ice (in mM: 10 Tris pH 7.5, 10 NaCl, 0.1 EDTA, and 0.2 PMSF with 0.5% Triton X-100 and 0.02% NaN_3) and centrifuged for 15 min at 10,000 *g*. Before being used, all buffers received a protease inhibitor cocktail (1:100 vol/vol; Sigma). Protein concentrations were determined with the bicinchoninic acid protein assay (Sigma) with bovine serum albumin as standard. Twenty micrograms of protein per lane was separated discontinuously on sodium dodecyl sulfate polyacrylamide gels (10% SDS-PAGE) and transferred to a polyvinyl difluoride membrane (Immobilon-P; Millipore, Eschborn, Germany). After blockade of nonspecific binding sites, membranes were incubated for 2 h at room temperature with a horseradish peroxidase-conjugated mouse monoclonal anti-p-Tyr antibody (PY20) (1:1,000; Santa Cruz Biotechnology). Protein expression was visualized by means of luminol-enhanced chemiluminescence (ECL plus; Amersham Pharmacia Biotech) and exposure of the membrane to a blue light-sensitive autoradiography film (Kodak BioMax Light Film; Kodak-Industrie, Chalon-sur-Saone, France). Signals were densitometrically assessed (Gel-Dokumentationssystem E.A.S.Y. Win32; Herolab, Wiesloch, Germany).

Fibrinogen levels and blood cell count. In a separate set of experiments blood was drawn from the retroorbital venous plexus of mice with 37°C, 34°C, and 31°C body temperature for determination of blood cell count and fibrinogen levels (citrate 1:10 vol/vol). The additional use of separate animals was necessary because fluorescent dyes interfere with chemiluminescence reactions. Platelet and red blood cell count was assessed with a cell counter (Sysmex KX-21; Sysmex). Fibrinogen levels were determined by nephelometry (Image Immunochemistry System; Beckman Coulter, Fullerton, CA) using a polyclonal rabbit anti-human fibrinogen antibody (DAKO Cytomation, Hamburg, Germany).

Statistical analysis. After proving the assumption of normality and equal variance across groups, we assessed differences between groups with one-way ANOVA followed by the appropriate post hoc comparison test. All data were expressed as means ± SE, and overall statistical significance was set at $P < 0.05$. Pearson product moment correlation was performed to evaluate significant correlations between parameters of platelet activation and temperature. Statistics and graphics were performed with the software packages SigmaStat and SigmaPlot (Jandel, San Rafael, CA).

RESULTS

In vivo thrombosis model. The effect of systemic hypothermia was assessed in vivo by superfusion of microvessels with ferric chloride solution, which resulted in complete thrombotic occlusion of the individually exposed vessel.

At baseline, i.e., before thrombus induction, animals of all groups did not significantly differ with respect to velocity and wall shear rates in arterioles and venules, although hypothermic animals tended to exhibit lower blood flow velocities (Table 1). Quantitative analysis of ferric chloride-induced thrombus formation in controls, i.e., animals maintained at a core body temperature of 37°C, revealed complete occlusion of arterioles and venules after 742 ± 150 and 824 ± 172 s, respectively (Fig. 1). Systemic hypothermia of 34°C caused a significant acceleration in microvascular thrombus formation. Arteriolar and venular vessel lumens were found to be clogged at an average time of 279 ± 120 and 376 ± 121 s, respectively ($P < 0.05$ vs. 37°C animals). In both arterioles and venules continuous cooling of the animal to a core body temperature of 31°C led to a further decrease in time until complete vessel occlusion occurred (163 ± 57 and 281 ± 71 s, respectively; $P < 0.05$ vs. 37°C animals).

Within the first 100 and 200 s on ferric chloride superfusion, venular blood cell velocity slowed down by −8% and −20%, respectively, in the control group with 37°C body temperature,

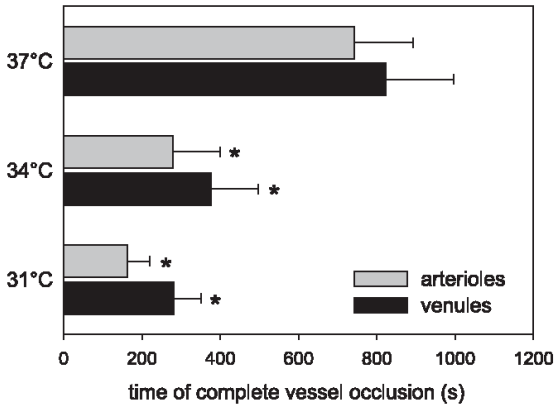

Fig. 1. Occlusion times of arterioles and venules on ferric chloride-induced thrombus formation in animals with normothermia (37°C; n = 6) and systemic hypothermia of 34°C (n = 5) and 31°C (n = 5). Values are means ± SE. *P < 0.05 vs. 37°C.

Downloaded from ajpheart.physiology.org on December 20, 2006

American Journal of Physiology – Heart and Circulatory Physiology

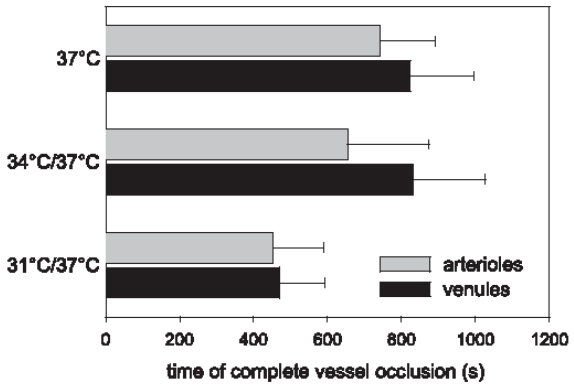

Fig. 2. Occlusion times of arterioles and venules on ferric chloride-induced thrombus formation in animals with normothermia (37°C; $n = 6$) and animals that underwent systemic hypothermia of 34°C ($n = 4$) and 31°C ($n = 4$) for 30 min followed by rewarming up to 37°C. Values are means ± SE.

whereas in animals with systemic hypothermia of 34°C, the decrease in venular blood cell velocity was even more pronounced (−37% and −37%, respectively). The deceleration in venular blood cell velocity was found to be abolished at enforced hypothermia of 31°C (−2% and −25%, respectively). Interestingly, hypothermia of 34°C did not decelerate arteriolar blood cell velocity within the first 100 s (−4%) compared with controls of 37°C (−8%) but even caused a increase of velocities (+14%) when systemic temperature declined to 31°C.

Rewarmed animals exhibited kinetics of thrombus formation comparable to those that were kept continuously at a core temperature of 37°C, although a moderate, but not significant, acceleration in thrombus formation was seen in animals on rewarming from 31°C. Wall shear rates did not differ between the groups. In rewarmed animals, which had been exposed to a 34°C body core temperature for a period of 30 min, arteriolar and venular vessel occlusion occurred at 655 ± 219 and 832 ± 195 s, respectively, and thus was comparable to the kinetics of thrombus formation in animals with a continuous core temperature of 37°C (Fig. 2). In animals that sustained a 30-min cooling period of 31°C, a moderate, but not significant, acceleration in thrombus formation was seen on rewarming to 37°C in both arterioles and venules (453 ± 137 and 469 ± 122 s, respectively).

Flow cytometric analysis of platelet P-selectin expression, GPIIb-IIIa activation, and fibrinogen binding. To closely simulate the clinical situation, we studied moderate degrees of hypothermia and their influences on platelet function in vitro. On incubation at temperatures of 34°C and 31°C, spontaneous expression of P-selectin and the activated conformation of GPIIb-IIIa did not change markedly; however, there was a small but statistically significant increase in PAC-1 binding in unstimulated samples at 31°C, suggestive of spontaneous hypothermia-induced activation (Figs. 3, *A* and *C*, and 4). TRAP exposure caused an increase of PAC-1 binding from 1.4 ±

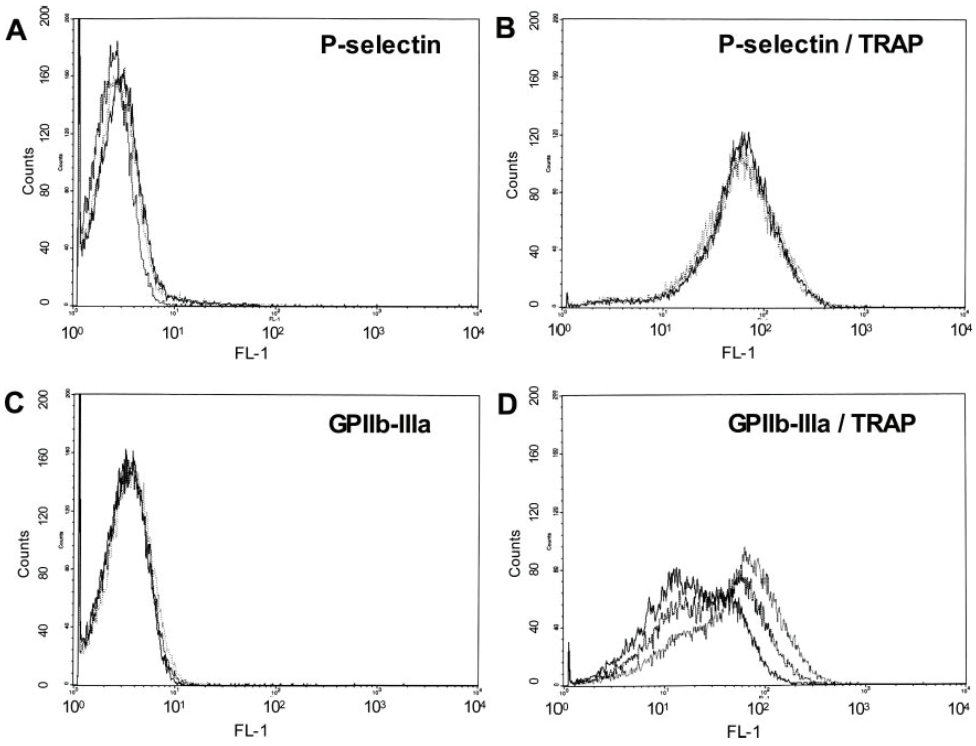

Fig. 3. Flow cytometric analysis of spontaneous (*A* and *C*) and thrombin receptor activating peptide (TRAP)-induced (*B* and *D*) expression of platelet P-selectin (*A* and *B*) and activation of glycoprotein (GP)IIb-IIIa (*C* and *D*) at temperatures of 37°C (solid black line), 34°C (dashed black line), and 31°C (dashed gray line).

Downloaded from ajpheart.physiology.org on December 20, 2006

American Journal of Physiology – Heart and Circulatory Physiology

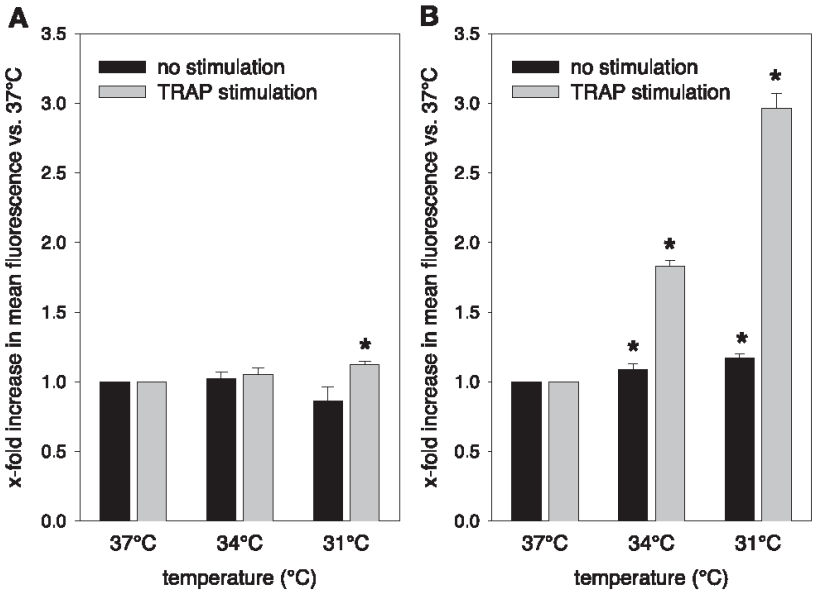

Fig. 4. Spontaneous and TRAP-induced platelet P-selectin expression (FITC-anti-P-selectin antibody; *A*) and GPIIb-IIIa activation (FITC-PAC-1 antibody; *B*) at temperatures of 37°C, 34°C, and 31°C, as assessed by flow cytometry and direct fluorescent antibody binding. Values include a total of 7 independent experiments and are means ± SE. *$P < 0.05$ vs. 37°C.

0.3% to 68 ± 5% of all platelets, showing the conformational change of GPIIb-IIIa (Fig. 3*D*). However, the magnitude of activation in response to TRAP increased with decreasing temperatures, as shown by 1.8-fold and 3-fold shifts in mean fluorescence on binding of PAC-1 (Fig. 4*B*). In line with this, binding of fluorescent-labeled fibrinogen was increased 1.6- and 2.9-fold at 34°C and 31°C after TRAP exposure ($P < 0.05$ vs. 37°C), whereas only small differences of fibrinogen binding were observed in resting platelets (Fig. 5). TRAP was associated with a marked upregulation of P-selectin expression, as shown by 93 ± 1% of positive platelets (Fig. 3*B*). Hypothermia caused a small but significant increase of TRAP-induced P-selectin upregulation at 31°C compared with TRAP-stimulated platelets at 37°C (Fig. 4*A*). Results showed a linear positive correlation between temperature decrease and GPIIb-IIIa activation, i.e., PAC-1 binding ($r = 0.6$; $P < 0.001$), whereas no correlation was found between the temperature decrease and the expression of P-selectin ($r = 0.1$; $P = 0.52$).

Platelets maintained at 34°C or 31°C for 30 min and rewarmed to 37°C exhibited spontaneous PAC-1 binding that was indistinguishable from that of platelets kept steadily at normothermic temperatures (Fig. 6). TRAP exposure caused a marked increase of PAC-1 binding on platelets with intermittent hypothermia and rewarming, which did not differ in magnitude from the response of platelets without hypothermia (Fig. 6). The same results were obtained for spontaneous and TRAP-induced P-selectin expression (data not shown).

Flow cytometric analysis of platelet-leukocyte aggregate formation. Platelet-leukocyte aggregation during hypothermia was determined after stimulation with TRAP/fMLP. Flow cytometric analysis revealed no significant increase after exposure to temperatures of 34°C and 31°C compared with aggregate formation at normothermic temperatures (37°C). After incubation in a 37°C water bath, 14.6 ± 0.9% platelet-leukocyte aggregates were found, represented by the fluorescence intensity of the upper right quadrant in the flow cytometric dot plot. Hypothermia of 34°C and 31°C led to only a marginal, not statistically significant, increase of aggregate formation of 14.7 ± 1.1% and 16.7 ± 1.2%, respectively.

Western blot analysis of tyrosine-specific phosphorylation of platelet proteins. To further underline cold-associated platelet activation, we studied tyrosine-specific protein phosphorylation of platelets at 37°, 34°, and 31°C. As shown in Fig. 7, hypothermia caused enhanced protein phosphorylation at ty-

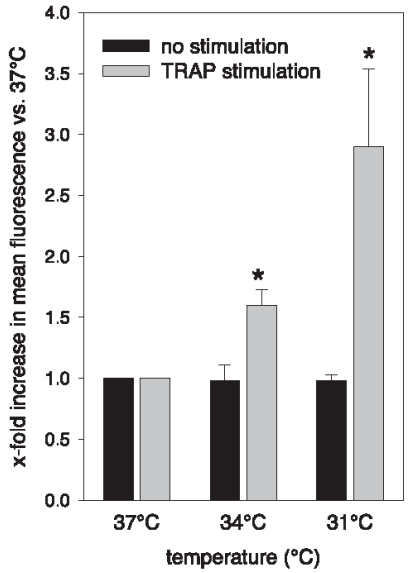

Fig. 5. Spontaneous and TRAP-induced platelet fibrinogen-binding (Alexa Fluor 488-labeled human fibrinogen) at temperatures of 37°C, 34°C, and 31°C, as assessed by flow cytometry. Values include a total of 7 independent experiments and are means ± SE. *$P < 0.05$ vs. 37°C.

Downloaded from ajpheart.physiology.org on December 20, 2006

American Journal of Physiology – Heart and Circulatory Physiology

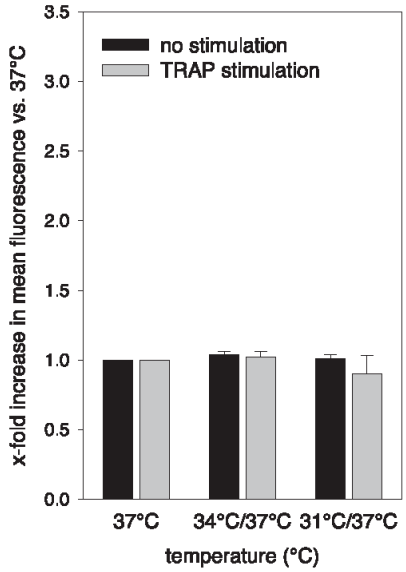

Fig. 6. Spontaneous and TRAP-induced GPIIb-IIIa activation (FITC-PAC-1 antibody) on platelets that were kept steadily at 37°C and on platelets that underwent a 30-min incubation at 34°C and 31°C followed by rewarming up to 37°C, as assessed by flow cytometry and direct fluorescent antibody binding. Values include a total of 7 independent experiments and are means ± SE.

rosine in resting, but in particular in TRAP-activated, platelets. The most prominent protein bands were found migrating with molecular masses of 130, 125, 95, and 84 kDa (Fig. 7).

Fibrinogen levels and blood cell count. Red blood cell and platelet counts ranged between 8.3–8.6 × 10^{12}/l and 900–1,000 × 10^{9}/l without differences among the 37°C, 34°C, and 31°C groups. In contrast, fibrinogen levels were found significantly lower in 34°C and 31°C animals, compared with normothermic controls (0.77 ± 0.07 and 0.78 ± 0.02 vs. 0.92 ± 0.04 g/l; $P < 0.05$), suggesting an augmented consumption of fibrinogen on intravascular coagulation.

DISCUSSION

In this report we communicate the following major findings. Moderate systemic hypothermia causes an acceleration of microvascular thrombus formation both in arterioles and venules. These in vivo findings are underlined by in vitro results demonstrating that hypothermia causes a slight increase of spontaneous platelet activation but a marked rise of agonist-induced responsiveness. Although thrombocytic P-selectin seems to play a minor role in cold-enhanced cell-cell contact, the fibrinogen receptor GPIIb-IIIa is influenced in a major way by temperature changes. The present results provide in vivo evidence for the frequently observed coincidence of increased rates of thrombotic events at reduced core temperatures.

During cold temperatures, impaired rheological properties of the blood, namely, reduced viscosity (21) as well as enhanced stiffness and reduced deformability of cells (3, 26), may compromise tissue perfusion. In addition, a reduction in temperature results in an increase in platelet and red blood cell numbers as well as a reduction in plasma volume (18, 27), further impeding capillary passage and thus nutritive blood flow. These changes together with the winter rise in fibrinogen concentrations (44) have all been used as probable explanations for rapid increases in coronary and cerebral thrombosis in cold weather (18, 30).

In the present study no significant differences in blood cell count were observed at clinically occurring moderate hypothermia of 34°C and 31°C compared with normothermia. However, blood fibrinogen levels were found to be significantly reduced at hypothermic temperatures, most likely because of an increase of consumption on microvascular thrombus formation. Many clinical studies of the past revealed a bleeding diathesis rather than a prothrombotic state in hypothermic individuals (7, 19, 28, 31, 36). Given the fact that a decrease of fibrinogen levels and an increase in microvascular thrombus formation were observed in the present study at core temperatures of 34°C and 31°C, it might be hypothesized that hypothermic temperatures lead to a rise in microvascular thrombus formation via activation of the GPIIb-IIIa receptor and subsequent fibrinogen binding, possibly resulting in coagulopathy later on in the process.

Increased reactivity and adhesiveness of cells may lead to adherence to the vascular lining with partial obturation of vascular cross sections and propagation of complete microvascular blockage. In particular, on exposure of the vessel to a noxious stimulus such as ferric chloride (6, 22), local oxidant stress-induced endothelial injury provides a preferential site for

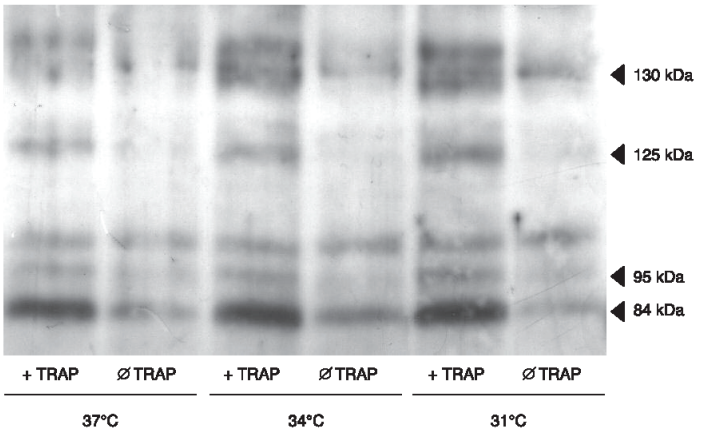

Fig. 7. Representative Western blot of tyrosine-specific protein phosphorylation in platelets at 37°C, 34°C, and 31°C under resting conditions and TRAP stimulation (1 independent experiment per group of a total of 3). Arrowheads denote the most prominent protein bands, migrating with molecular masses of 130, 125, 95, and 84 kDa.

Downloaded from ajpheart.physiology.org on December 20, 2006

American Journal of Physiology – Heart and Circulatory Physiology

cell trapping with thrombus growth. Although the importance of GPIb-IX-V in mediating platelet-endothelial interactions is unequivocal, this ligand seems mandatory for adhesion and thrombus growth at high shear (4). On the contrary, at low shear other adhesion molecules, such as the collagen receptors and GPIIb-IIIa, are mainly involved (4, 25, 33). The vessels monitored in the present study presented with wall shear rates below 300 s^{-1}. Thus we preferentially studied platelets and their cold-related change in activation of the fibrinogen receptor GPIIb-IIIa. It has been shown that unstimulated platelets attach to fibrinogen in a selective, GPIIb-IIIa-dependent process and that the initial attachment is followed by spreading and irreversible adhesion, even in the absence of exogenous agonists or the presence of activation inhibitors (35). In addition, the specific synergy of multiple substrate-receptor interactions with coupling of functions of GPIb with GPIIb-IIIa, allowing the latter to arrest platelets on von Willebrand factor under conditions not permissive for direct binding to fibrinogen, underscores the crucial role of GPIIb-IIIa for thrombogenesis (34). Past studies have shown that thrombin-induced tyrosine phosphorylation of several proteins is dependent on platelet aggregation mediated by fibrinogen binding to GPIIb-IIIa (11, 15). The present results, demonstrating the massive PAC-1 binding of platelets with reduced temperature, indicative of the activated conformation of GPIIb-IIIa (39), underscore the importance of this adhesive receptor in cold-related pathology. Moreover, fibrinogen binding to TRAP-activated platelets and tyrosine-specific phosphorylation of platelet proteins were increased at 34° and 31°C, further substantiating the activating effect of cold on the GPIIb-IIIa receptor.

The present observation that TRAP barely started to increase P-selectin expression at a temperature of 31°C goes along with results of Faraday and Rosenfeld (10), reporting only a modest (1.6 fold) TRAP-induced increase of platelet P-selectin expression at 22°C vs. 37°C compared with an almost 25-fold higher rise in PAC-1 binding. This might imply that P-selectin expression is less temperature sensitive than GPIIb-IIIa, although the effects may in addition greatly depend on the agonists used and the time point of analysis. For example, hypothermia-induced reduction of P-selectin expression, as observed by Michelson et al. (24), was only transient in nature and absent within 10 min after agonist exposure. Because hypothermia failed to influence platelet-leukocyte aggregate formation and because P-selectin is believed to be a key player in this cellular cross talk (14), the present results further emphasize the inferior role of platelet P-selectin expression in mediating hypothermia-associated thrombosis.

Our in vitro data confirm those of others, reporting that hypothermia induces platelet activation in vitro, as indicated by changes in platelet shape and morphology (23, 43), tyrosine-specific protein phosphorylation (11), and fibrinogen receptor exposure and activation as well as platelet aggregation (29). However, we significantly extend current knowledge in that we could prove the relevance of systemic hypothermia in the enhancement of microvascular thrombus formation in vivo. Hypothermic temperatures above 30°C were purposely chosen because they are frequently encountered in a number of clinical settings, such as major surgery, multiple trauma, cold exposure, and the neonatal period (5, 16, 31, 41). It has been shown that unintentional hypothermia is associated with myocardial ischemia, angina, and impaired ventilation and blood oxygenation during the early postoperative period in patients undergoing lower-extremity vascular surgery (12). The impact of temperature is further underscored by the fact that the simple perioperative maintenance of normothermia in patients with cardiac risk factors was associated with a reduced incidence of morbid cardiac events and ventricular tachycardia (13). Thus the enhanced risk for microvascular thrombus formation during cold is best counteracted by an immediate rewarming of the patient, as shown by the complete reversion of platelet hyperresponsiveness on reexposure to 37°C. In line with this, animals subjected to hypothermia followed by rewarming have not been found to be prone to enhanced thrombogenesis.

In summary, moderate systemic hypothermia accelerates microvascular thrombosis, which might be mediated by increased GPIIb-IIIa activation on platelets, but does not cause predisposition with increased risk for microvascular thrombus formation after rewarming. Thus maintaining normothermia or rewarming hypothermic patients represents a common goal in limiting the risk for cold-associated thrombotic events.

ACKNOWLEDGMENTS

The authors kindly thank Berit Blendow, Claudia Vergien, and Maren Nerowski, Department of Experimental Surgery, University of Rostock, and Dr. Christiana Zingler, Institute for Clinical Chemistry and Laboratory Medicine, University of Rostock, for excellent technical assistance.

GRANTS

The study is supported by a grant from the Deutsche Forschungsgemeinschaft, Bonn-Bad Godesberg, Germany (Vo 450/8-1).

REFERENCES

1. **Baez S.** An open cremaster muscle preparation for the study of blood vessels by in vivo microscopy. *Microvasc Res* 5: 384–394, 1973.
2. **Baker M and Wayland H.** On-line volume flow rate and velocity profile measurements for blood in microvessels. *Microvasc Res* 7: 131–143, 1974.
3. **Barbee JH.** The effect of temperature on the relative viscosity of human blood. *Biorheology* 10: 1–5, 1973.
4. **Berndt MC, Shen Y, Dopheide SM, Gardiner EE, and Andrews RK.** The vascular biology of the glycoprotein Ib-IX-V complex. *Thromb Haemost* 86: 178–188, 2001.
5. **Cochrane DA.** Hypothermia: a cold influence on trauma. *Int J Trauma Nurs* 7: 8–13, 2001.
6. **Denis C, Methia N, Frenette PS, Rayburn H, Ullman-Cullere M, Hynes RO, and Wagner DD.** A mouse model of severe von Willebrand disease: defects in hemostasis and thrombosis. *Proc Natl Acad Sci USA* 95: 9524–9529, 1998.
7. **Eddy VA, Morris JA, and Cullinane DC.** Hypothermia, coagulopathy, and acidosis. *Surg Clin North Am* 80: 845–854, 2000.
8. **Eldwood PC, Beswick A, O'Brien JR, Renaud S, Fifield R, Limb ES, and Bainton D.** Temperature and risk factors for ischaemic heart disease in the Caerphilly prospective study. *Br Heart J* 70: 520–523, 1993.
9. **Enquselassie F, Dobson AJ, Alexander HM, and Steele PL.** Seasons, temperature and coronary disease. *Int J Epidemiol* 22: 632–636, 1993.
10. **Faraday N and Rosenfeld BA.** In vitro hypothermia enhances platelet GPIIb-IIIa activation and P-selectin expression. *Anesthesiology* 88: 1579–1585, 1998.
11. **Ferrell JE Jr and Martin GS.** Tyrosine-specific protein phosphorylation is regulated by glycoprotein IIb-IIIa in platelets. *Proc Natl Acad Sci USA* 86: 2234–2238, 1989.
12. **Frank SM, Beattie C, Christopherson R, Norris EJ, Perler BA, Williams GM, and Gottlieb SO.** Unintentional hypothermia is associated with postoperative myocardial ischemia. The Perioperative Ischemia Randomized Anesthesia Trial Study Group. *Anesthesiology* 78: 468–476, 1993.
13. **Frank SM, Fleisher LA, Breslow MJ, Higgins MS, Olson KF, Kelly S, and Beattie C.** Perioperative maintenance of normothermia reduces the

Downloaded from ajpheart.physiology.org on December 20, 2006

American Journal of Physiology – Heart and Circulatory Physiology

incidence of morbid cardiac events. A randomized clinical trial. *JAMA* 277: 1127–1134, 1997.
14. **Furie B, Furie BC, and Flaumenhaft R.** A journey with platelet P-selectin: the molecular basis of granule secretion, signalling and cell adhesion. *Thromb Haemost* 86: 214–221, 2001.
15. **Golden A, Brugge JS, and Shattil SJ.** Role of platelet membrane glycoprotein IIb-IIIa in agonist-induced tyrosine phosphorylation of platelet proteins. *J Cell Biol* 111: 3117–3127, 1990.
16. **Hildebrand F, Giannoudis PV, van Griensven M, Chawda M, and Pape HC.** Pathophysiologic changes and effects of hypothermia on outcome in elective surgery and trauma patients. *Am J Surg* 187: 363–371, 2004.
17. **Kattlove HE and Alexander B.** The effect of cold on platelets. I. Cold-induced platelet aggregation. *Blood* 38: 39–48, 1971.
18. **Keatinge WR, Coleshaw SR, Cotter F, Mattock M, Murphy M, and Chelliah R.** Increases in platelet and red cell counts, blood viscosity, and arterial pressure during mild surface cooling: factors in mortality from coronary and cerebral thrombosis in winter. *Br Med J* 289: 1405–1408, 1984.
19. **Khuri SF, Wolfe JA, Josa M, Axford TC, Szymanski I, Assousa S, Ragno G, Patel M, Silverman A, and Park M.** Hematologic changes during and after cardiopulmonary bypass and their relationship to the bleeding time and nonsurgical blood loss. *J Thorac Cardiovasc Surg* 104: 94–107, 1992.
20. **Ku CS, Yang CY, Lee WJ, Chiang HT, Liu CP, and Lin SL.** Absence of a seasonal variation in myocardial infarction onset in a region without temperature extremes. *Cardiology* 89: 277–282, 1998.
21. **Lecklin T, Egginton S, and Nash GB.** Effect of temperature on the resistance of individual red blood cells to flow through capillary-sized apertures. *Pflügers Arch* 432: 753–759, 1996.
22. **Lindenblatt N, Bordel R, Schareck W, Menger MD, and Vollmar B.** Vascular heme oxygenase-1 induction suppresses microvascular thrombus formation in vivo. *Arterioscler Thromb Vasc Biol* 24: 601–606, 2004.
23. **Maurer-Spurej E, Pfeiler G, Maurer N, Lindner H, Glatter O, and Devine DV.** Room temperature activates human blood platelets. *Lab Invest* 81: 581–592, 2001.
24. **Michelson AD, MacGregor H, Barnard MR, Kestin AS, Rohrer MJ, and Valeri CR.** Reversible inhibition of human platelet activation by hypothermia in vivo and in vitro. *Thromb Haemost* 71: 633–640, 1994.
25. **Moroi M, Jung SM, Shinmyozu K, Tomiyama Y, Ordinas A, and Diaz-Ricart M.** Analysis of platelet adhesion to a collagen-coated surface under flow conditions: the involvement of glycoprotein VI in the platelet adhesion. *Blood* 88: 2081–2092, 1996.
26. **Nash GB, Abbitt KB, Tate K, Jetha KA, and Egginton S.** Changes in the mechanical and adhesive behaviour of human neutrophils on cooling in vitro. *Pflügers Arch* 442: 762–770, 2001.
27. **Neild PJ, Syndercombe-Court D, Keatinge WR, Donaldson GC, Mattock M, and Caunce M.** Cold-induced increases in erythrocyte count, plasma cholesterol and plasma fibrinogen of elderly people without a comparable rise in protein C or factor X. *Clin Sci (Lond)* 86: 43–48, 1994.
28. **Patt A, McCroskey BL, and Moore EE.** Hypothermia-induced coagulopathies in trauma. *Surg Clin North Am* 68: 775–785, 1988.
29. **Peerschke EI and Zucker MB.** Fibrinogen receptor exposure and aggregation of human blood platelets produced by ADP and chilling. *Blood* 57: 663–670, 1981.
30. **Pell JP and Cobbe SM.** Seasonal variations in coronary heart disease. *QJM* 92: 689–696, 1999.
31. **Peng RY and Bongard FS.** Hypothermia in trauma patients. *J Am Coll Surg* 188: 685–696, 1999.
32. **Rohrer M and Natale A.** Effect of hypothermia on the coagulation cascade. *Crit Care Med* 20: 1402–1405, 1992.
33. **Savage B, Almus-Jacobs F, and Ruggeri ZM.** Specific synergy of multiple substrate-receptor interactions in platelet thrombus formation under flow. *Cell* 94: 657–666, 1998.
34. **Savage B, Cattaneo M, and Ruggeri ZM.** Mechanisms of platelet aggregation. *Curr Opin Hematol* 8: 270–276, 2001.
35. **Savage B and Ruggeri ZM.** Selective recognition of adhesive sites in surface-bound fibrinogen by glycoprotein IIb-IIIa on nonactivated platelets. *J Biol Chem* 266: 11227–11233, 1991.
36. **Schmied H, Kurz A, Sessler DI, Kozek S, and Reiter A.** Mild hypothermia increases blood loss and transfusion requirements during total hip arthroplasty. *Lancet* 347: 289–292, 1996.
37. **Schmitt A, Guichard J, Masse JM, Debili N, and Cramer EM.** Of mice and men: comparison of the ultrastructure of megakaryocytes and platelets. *Exp Hematol* 29: 1295–1302, 2001.
38. **Shattil SJ, Cunningham M, and Hoxie JA.** Detection of activated platelets in whole blood using activation-dependent monoclonal antibodies and flow cytometry. *Blood* 70: 307–315, 1987.
39. **Shattil SJ, Hoxie JA, Cunningham M, and Brass LF.** Changes in the platelet membrane glycoprotein IIb.IIIa complex during platelet activation. *J Biol Chem* 260: 11107–11114, 1985.
40. **Smyth SS, Tsakiris DA, Scudder LE, and Coller BS.** Structure and function of murine αIIbβ3 (GPIIb/IIIa): studies using monoclonal antibodies and β3-null mice. *Thromb Haemost* 84: 1103–1108, 2000.
41. **Tunell R.** Prevention of neonatal cold injury in preterm infants. *Acta Paediatr* 93: 308–310, 2004.
42. **Vollmar B, Schmits R, Kunz D, and Menger MD.** Lack of in vivo function of CD31 in vascular thrombosis. *Thromb Haemost* 85: 160–164, 2001.
43. **White JG and Krivit W.** An ultrastructural basis for the shape changes induced in platelets by chilling. *Blood* 30: 625–635, 1967.
44. **Woodhouse PR, Khaw KT, Plummer M, Foley A, and Meade TW.** Seasonal variations of plasma fibrinogen and factor VII activity in the elderly: winter infections and death from cardiovascular disease. *Lancet* 343: 435–439, 1994.

Downloaded from ajpheart.physiology.org on December 20, 2006

2.1.2 Sepsis und Hypothermie

In einem weiterführenden Schritt interessierten wir uns für die Auswirkungen einer Lipopolysacharid (LPS)-induzierten Endotoxinämie, alleine oder in Kombination mit einer systemischen Hypothermie, auf die mikrovaskuläre Thrombogenität, die Endothelzellfunktion und die Thrombozytenfunktion.

Das Auftreten hypothermer Temperaturen während einer Sepsis verschlechtert die Prognose eines Patienten deutlich. Eine schwere Sepsis ist zusätzlich mit einer Aktivierung des Gerinnungssystems und Ausbildung von Mikrothromben mit dem möglichen Resultat eines Multiorganversagens verbunden. Wir stellten uns daher die Frage, inwieweit eine Endotoxinämie per se und eine zusätzliche Hypothermie zur Ausbildung mikrovaskulärer Thrombosen beitragen und wie die endotheliale und thrombozytäre Funktion beeinflusst wird. Es wurden LPS-vorbehandelte Mäuse einer systemischen Hypothermie von 34°C und 31°C ausgesetzt. Die Endotoxinämie beschleunigte die mikrovaskuläre Thrombusformation in 37°C warmen Tieren signifikant. Dieses ging einher mit einem deutlichen Anstieg endothelialer Aktivierungsmarker, Thrombin-induzierter Thrombozytenaktivierung und endothelialer Expression von P-Selektin und PAI-1. Eine zusätzliche Hypothermie führte zu einer Beschleunigung der mikrovaskulären Thrombusbildung, die jedoch nur bei 31°C für Arteriolen gegenüber 37°C warmen endotoxinämischen Tieren signifikant war. Interessanterweise führte die zusätzliche Hypothermie bei endotoxinämischen Tieren zu keiner vermehrten Expression endothelialer Aktivierungsmarker oder verstärkter Thrombozytenaktivierung, verursachte jedoch eine signifikant erhöhte endotheliale PAI-1 Expression und Zirkulation von sPAI-Ag. Demnach wird die Prothrombogenität unter septischen Bedingungen über eine generelle endotheliale und thrombozytäre Aktivierung vermittelt, während eine zusätzliche systemische Hypothermie vielmehr mit einer signifikant verstärkten endothelialen PAI-1 Expression vergesellschaftet ist.

Lindenblatt N, Menger MD, Klar E, Vollmar B
Systemic hypothermia increases PAI-1 expression and accelerates microvascular thrombus formation in endotoxemic mice Crit Care 2006; 10: R148

Available online http://ccforum.com/content/10/5/R148

Research

Open Access

Systemic hypothermia increases PAI-1 expression and accelerates microvascular thrombus formation in endotoxemic mice

Nicole Lindenblatt[1,2], Michael D Menger[3], Ernst Klar[2] and Brigitte Vollmar[1]

[1]Department of Experimental Surgery, University of Rostock, Schillingallee, Rostock 18055, Germany
[2]Department of General Surgery, University of Rostock, Schillingallee, Rostock, 18055, Germany
[3]Institute for Clinical and Experimental Surgery, University of Saarland, Kirrberger Straße, Homburg-Saar, 66424, Germany

Corresponding author: Brigitte Vollmar, brigitte.vollmar@med.uni-rostock.de

Received: 18 Jul 2006 Revisions requested: 26 Jul 2006 Revisions received: 15 Aug 2006 Accepted: 24 Oct 2006 Published: 24 Oct 2006

Critical Care 2006, **10**:R148 (doi:10.1186/cc5074)
This article is online at: http://ccforum.com/content/10/5/R148
© 2006 Lindenblatt *et al.*; licensee BioMed Central Ltd.
This is an open access article distributed under the terms of the Creative Commons Attribution License (http://creativecommons.org/licenses/by/2.0), which permits unrestricted use, distribution, and reproduction in any medium, provided the original work is properly cited.

Abstract

Introduction Hypothermia during sepsis significantly impairs patient outcome in clinical practice. Severe sepsis is closely linked to activation of the coagulation system, resulting in microthrombosis and subsequent organ failure. Herein, we studied whether systemic hypothermia accelerates microvascular thrombus formation during lipopolysacharide (LPS)-induced endotoxemia *in vivo*, and characterized the low temperature-induced endothelial and platelet dysfunctions.

Methods Ferric-chloride induced microvascular thrombus formation was analyzed in cremaster muscles of hypothermic endotoxemic mice. Flow cytometry, ELISA and immunohistochemistry were used to evaluate the effect of hypothermia on endothelial and platelet function.

Results Control animals at 37°C revealed complete occlusion of arterioles and venules after 759 ± 115 s and 744 ± 112 s, respectively. Endotoxemia significantly ($p < 0.05$) accelerated arteriolar and venular occlusion in 37°C animals (255 ± 35 s and 238 ± 58 s, respectively). This was associated with an increase of circulating endothelial activation markers, agonist-induced platelet reactivity, and endothelial P-selectin and plasminogen activator inhibitor (PAI)-1 expression. Systemic hypothermia of 34°C revealed a slight but not significant reduction of arteriolar (224 ± 35 s) and venular (183 ± 35 s) occlusion times. Cooling of the endotoxemic animals to 31°C core body temperature, however, resulted in a further acceleration of microvascular thrombus formation, in particular in arterioles (127 ± 29 s, $p < 0.05$ versus 37°C endotoxemic animals). Of interest, hypothermia did not affect endothelial receptor expression and platelet reactivity, but increased endothelial PAI-1 expression and, in particular, soluble PAI-1 antigen (sPAI-Ag) plasma levels.

Conclusion LPS-induced endotoxemia accelerates microvascular thrombus formation *in vivo*, most probably by generalized endothelial activation and increased platelet reactivity. Systemic hypothermia further enhances microthrombosis in endotoxemia. This effect is associated with increased endothelial PAI-1 expression and sPAI-Ag in the systemic circulation rather than further endothelial activation or modulation of platelet reactivity.

Introduction

Microvascular thrombus formation with subsequent microvessel occlusion and hypoperfusion is a major contributor to organ dysfunction during sepsis [1]. It is well recognized that sepsis involves a complex interaction between the inflammatory and the coagulation system [2]. Bacterial endotoxin (lipopolysacharide (LPS)) induces a variety of metabolic, cellular and regulatory effects that are accompanied by fever in mammals [3]. The pyrogenic effects are exerted by increasing the production of endogenous cytokines such as IL-1, IL-6 and tumor necrosis factor (TNF)-alpha. Severe sepsis is almost invariably associated with activation of the coagulation system, potentially resulting in disseminated intravascular coagulation. Together with other components, the tissue factor-driven generation of thrombin with fibrin accumulation and platelet activation play a pivotal role in this setting [4]. In sepsis, both the

bw = body weight; ELISA = enzyme-linked immunosorbent assay; GP = glycoprotein; ICAM = intercellular adhesion molecule; IL = interleukin; ip = intraperitoneally; LPS = lipopolysacharide; PAI = plasminogen activator inhibitor; PAI-1-Ag = plasminogen activator inhibitor-1 antigen; s = soluble; TNF = tumor necrosis factor; VCAM = vascular cell adhesion molecule.

coagulation and the fibrinolytic system may be affected, as indicated by decreased activation of thrombomodulin and protein C as well as reduction of anti-fibrinolysis and enhancement of plasminogen activator inhibitor (PAI)-1 expression [2]. The production of procoagulant factors, as well as their interaction with platelets and leukocytes in the microvasculature, may lead to intravascular fibrin formation [5].

Septic patients, who develop hypothermia during the course of the illness, have a significantly worse prognosis compared to those who develop fever or maintain body temperature. In addition, in animal models of sepsis it has been observed that hypothermia is associated with immune dysfunction and an unfavorable outcome [6,7]. Presently, it is not clear whether hypothermia during severe sepsis merely serves as a surrogate marker for progression of the disease, representing a general failure of regulatory functions, or whether hypothermia itself negatively influences the course of the disease. Additionally, the reasons for the worse prognosis during sepsis with hypothermia have not been clearly identified.

In previous experiments we were able to show that hypothermia accelerates microvascular thrombus formation and increases platelet reactivity [8]. Based on these studies we hypothesize that hypothermia during severe sepsis aggravates the already existing procoagulant state. This may lead to a further aggravation of microvascular thrombus formation, possibly representing a cause of the worse outcome in septic patients with hypothermia in clinical practice. To address this issue, we analyzed the kinetics of microvascular thrombus formation in a murine *in vivo* LPS model of systemic hypothermia at 34°C and 31°C. The effects of endotoxemia and hypothermia on endothelial function were further determined by assessing plasma levels and tissue expression of endothelial activation markers. We additionally evaluated hypothermia-induced platelet response *in vitro* using temperatures of 34°C and 31°C, which are likely to be encountered during severe hypothermia in the setting of prolonged sepsis.

Materials and methods

Mouse cremaster muscle preparation

Upon approval by the local government, all experiments were carried out in accordance with the German legislation on protection of animals and the National Institutes of Health 'Guide for the Care and Use of Laboratory Animals' (Institute of Laboratory Animal Resources, National Research Council). Male C57BL/6J mice with a body weight (bw) of 20 to 25 g were anesthetized by an intraperitoneal injection of ketamine (90 mg/kg bw) and xylazine (25 mg/kg bw) and a polyethylene catheter was placed into the right jugular vein, serving for application of fluorescent dyes.

For the study of microvascular thrombus formation, we used the cremaster muscle preparation as originally described by Baez in rats [9] and applied by our group in mice [8,10]. Before preparation of the cremaster muscle, animals were placed on a heating pad coupled to a rectal probe. A midline incision of the skin and fascia was made over the ventral aspect of the scrotum and extended up to the inguinal fold and to the distal end of the scrotum. The incised tissues were retracted to expose the cremaster muscle sac, which was maintained under gentle traction to carefully separate the remaining connective tissue by blunt dissection from around the cremaster sac. The cremaster muscle was then incised without damaging larger anastomosing vessels. Hemostasis was achieved with 5–0 threads serving also to spread the tissue. After dissection of the vessel connecting the cremaster and the testis, the epididymus and testis were put to the side of the preparation. The preparation was performed on a transparent pedestal to allow microscopic observation of the cremaster muscle microcirculation by both transillumination and epi-illumination techniques.

After surgical preparation, the animals were allowed to recover for 15 minutes. Thrombus formation was then induced in randomly chosen venules ($n = 1$ to 2 per preparation) and arterioles ($n = 1$ to 2 per preparation).

Experimental design

Mice were pretreated with LPS (*Escherichia coli*, serotype 0128:B12; LOT# 069H4097, Sigma-Aldrich, Munich, Germany) at a dose of 10 mg/kg intraperitoneally (ip) 24 hours before the beginning of the experiments. Following induction of anesthesia, animals were placed on a customized platform with an incorporated heating pad to facilitate microscopy of the cremaster muscle. Temperature was controlled by a rectal probe and maintained at 37°C, 34°C or 31°C. Animals pretreated with physiological saline (10 ml/kg bw, -24 h ip) with a body core temperature of 37°C served as controls. Overall, 10 saline/37°C control cremaster muscles ($n = 5$ animals) and eight cremaster muscles of each of the LPS/37°C, LPS/34°C and LPS/31°C groups ($n = 4$ animals for each group) were studied. Different animals were committed to the analyses at the three different temperatures.

The assumption that the rectal temperature equaled the core body temperature was confirmed by additional experiments using a LICOX probe (LICOX 1, GMS, Kiel-Mielkendorf, Germany) as described before [8]. Depending on the rectal temperature at the beginning of the experiment and the desired final temperature, heating was started immediately or after the animal cooled down to the required temperature. Artificial cooling was not necessary, because most of the animals displayed a considerable drop in body temperature after induction of anesthesia. After the appropriate temperature, according to randomization of animals, was reached and remained stable for at least 30 minutes, the preparation was started and animals were allowed to recover from the surgical trauma for 15 minutes. Thrombus formation was then induced in randomly chosen venules ($n = 1$ to 2 per preparation) and

Available online http://ccforum.com/content/10/5/R148

arterioles ($n = 1$ to 2 per preparation), as described in the next section. Animals were kept under the respective temperature conditions during the whole course of the experiment, including intravital microscopy and microvascular thrombus induction.

In vivo thrombosis model

After intravenous injection of 0.1 ml 5% fluorescein isothiocyanate-labeled dextran (MW 150000, Sigma-Aldrich, Munich, Germany) and subsequent circulation for 30 s, the cremaster muscle microcirculation was visualized by intravital fluorescence microscopy using a Zeiss microscope (Axiotech vario, Zeiss, Jena, Germany). The microscopic procedure was performed at a constant room temperature of 21 to 23°C. The epi-illumination setup included a 100 W HBO mercury lamp and a blue filter (450 to 490 nm/>520 nm excitation/emission wavelength). Microscopic images were recorded by a charge-coupled device video camera (FK 6990A-IQ, Pieper, Schwerte, Germany) and stored on videotapes for off-line evaluation (S-VHS Panasonic AG 7350-E, Matsushita, Tokyo, Japan). Using a ×20 water immersion objective (Achroplan x20/0.50W, Zeiss) baseline blood flow was monitored in individual arterioles (diameter range 30 to 50 μm) and venules (diameter range 60 to 80 μm). Thereafter, microvascular thrombosis was induced by spreading of 25 μl ferric chloride solution (12.5 mmol/l; Sigma) over the cremaster muscle every minute, resulting in a continuous superfusion of the tissue [11,12]. Complete vessel occlusion was assumed to have occurred when blood flow ceased for more than 60 s due to thrombotic occlusion. As rapid spreading of ferric chloride solution allowed the study of only one or two arterioles and venules within each preparation, both left and right cremaster muscles of each animal were prepared for analysis of thrombotic vessel occlusion.

Analysis included the time period until sustained cessation of blood flow due to complete vessel occlusion as well as the determination of vessel diameter and blood cell velocity prior to thrombus induction. Vascular wall shear rates were calculated based on the Newtonian definition $\gamma = 8 \times V/D$, with V representing the red blood cell centerline velocity divided by 1.6 according to the Baker-Wayland factor [13] and D representing the individual inner vessel diameter.

ELISA of circulating endothelial markers

At the end of each experiment, blood was withdrawn from the inferior vena cava by direct puncture into EDTA syringes, followed by centrifugation (GS-6R Centrifuge, Beckman Coulter, Fullerton, CA, USA) at 200 × g and room temperature for 10 minutes with subsequent storage of plasma at -20°C. Plasma concentrations of circulating, that is, soluble (s)P-selectin, sE-selectin, intercellular adhesion molecule (sICAM)-1, vascular cell adhesion molecule (sVCAM)-1 and plasminogen activator inhibitor-1 antigen (sPAI-Ag) were determined using the respective enzyme immunoassay kits (R&D Systems, Minneapolis, MN, USA, and Molecular Innovations Inc., Southfield, MI, USA).

Histology and immunhistochemistry

At the end of each experiment, the cremaster muscle was fixed in 4% phosphate buffered formalin for two to three days and embedded in paraffin. From the paraffin-embedded tissue blocks, 4 μm-sections were cut and stained with hematoxylin and eosin for histological analysis. For immunohistochemical demonstration of P-selectin and PAI-1 expression, sections collected on poly-L-lysine-coated glass slides were treated by microwave for antigen unmasking. Goat anti-human P-selectin and goat anti-human PAI-1 (each 1:100; Santa Cruz Biotechnology, Heidelberg, Germany) were used as primary antibodies and incubated for 90 to 120 minutes at room temperature. This was followed by a horseradish peroxidase-conjugated donkey anti-goat antibody (1:25; Santa Cruz Biotechnology) and development using DAB substrate as chromogen. The sections were counterstained with hematoxylin and examined by light microscopy (Zeiss Axioscop 40, Zeiss).

Preparation of murine platelet rich plasma

For *in vitro* testing of platelet function additional animals were exposed to LPS according to the experimental protocol (10 mg/kg ip; -24 h). Controls received physiological saline (10 ml/kg ip; -24 h). Then 0.5 to 1 ml blood was drawn from the retro-orbital venous plexus with 1.5 cm glass capillaries and collected into a tube containing TRIS buffered saline/heparin (20 U/ml). The sample was centrifuged for five minutes at 500 × g yielding platelet rich plasma that was centrifuged again for eight minutes at 300 × g and 0.5 μM prostacyclin (PGI_2) was added. The platelet pellet was resuspended and apyrase and Tyrode's buffer were added and centrifugation steps were continued as described elsewhere [14]. Aliquots of platelet suspensions were transferred into a 37°C water bath for 30 minutes of resting to eliminate isolation-induced platelet activation.

Platelet suspensions from LPS-treated animals were incubated for 30 minutes in water baths maintaining temperatures at either 37°C, 34°C or 31°C followed by exposure to thrombin (20 U/ml) and incubation with saturating amounts of the appropriate antibody. Platelets from control animals were kept at 37°C continuously. Platelet suspensions were kept for an additional 30 minutes in the respective covered water baths.

Flow cytometric analysis of P-selectin, glycoprotein IIb-IIIa and CD107a expression

For evaluation of receptor expression under resting conditions, 5 μl of specific rat anti-mouse P-selectin, glycoprotein (GP)IIb-IIIa (Emfret Analytics, Eibelstadt, Germany), CD107a (BD Biosciences, Heidelberg, Germany) or negative control antibodies and 25 μl platelet suspension were combined and incubated for 15 minutes at room temperature. The reaction

was stopped by addition of 400 µl phosphate buffered saline. Analysis was performed within the subsequent 30 minutes. In addition, the same set of experiments was carried out following exposure to thrombin for maximal platelet activation (20 U/ml).

A FACScan flowcytometer (Becton Dickinson, Heidelberg, Germany) was calibrated with fluorescent standard microbeads (CaliBRITE Beads, Becton Dickinson) for accurate instrument setting. Platelets were identified by their characteristic forward and sideward light scatter and selectively analyzed for their fluorescence properties using the CellQuest program (Becton Dickinson) with assessment of 20,000 events per sample. The relative fluorescence intensity of a given sample was calculated by subtracting the signal obtained when cells were incubated with the isotype specific control antibody from the signal generated by cells incubated with the test antibody.

Statistical analysis

After proving the assumption of normality and equal variance across groups, differences between groups were assessed using one-way analysis of variance (ANOVA) followed by the appropriate *post hoc* comparison test. All data were expressed as means ± standard error of the mean and overall statistical significance was set at $p < 0.05$. Pearson product moment correlation was performed to evaluate significant correlations between parameters of platelet activation and temperature. Statistics and graphics were performed using the software packages SigmaStat and SigmaPlot (Jandel Corporation, San Rafael, CA, USA).

Results

Intravital microscopic analysis of microvascular thrombosis

In endotoxemic animals, red blood cell velocities were significantly lower when compared with those of the control group at 37°C (Table 1), indicating compromise of microvascular flow conditions at the beginning of the experiments owing to the endotoxemic state. However, wall shear rates did not differ significantly between the experimental groups. After induction of anesthesia the average core temperature for all animals was 36.7 ± 0.5°C. Body temperature decreased within two to five minutes in the anesthetized animals and reached the desired temperatures of 34°C and 31°C without artificial cooling. In control animals this effect was prevented by warming on a heating plate.

In saline controls with a body temperature of 37°C, ferric chloride-mediated thrombus formation induced complete occlusion of arterioles and venules after 759 ± 115 s and 744 ± 112 s, respectively (Figure 1). In contrast, in endotoxemic animals, which were maintained at a core body temperature of 37°C, thrombus formation was markedly accelerated, as indicated by significantly reduced arteriolar and venular occlusion times of 255 ± 35 s and 238 ± 58 s, respectively (Figure 1). Systemic hypothermia at 34°C in endotoxemic animals caused a further but only slight and non-significant acceleration of microvascular thrombus formation. Arteriolar and venular vessel lumen were found clogged at an average time of 224 ± 35 s and 183 ± 35 s, respectively.

In both arterioles and venules, continuous cooling of endotoxemic animals to a core body temperature of 31°C resulted in a further acceleration of thrombus formation, in particular in arterioles. While venular occlusion time was found to be decreased only slightly to 172 ± 18 s, arteriolar occlusion time

Table 1

Red blood cell velocity (µm/s) and wall shear rates (γ; s^{-1}) before thrombus formation

	Arterioles		Venules	
	RBC velocity	γ	RBC velocity	γ
Saline-37°C	2200 ± 79	176 ± 21	1720 ± 245	109 ± 11
LPS-37°C	1175 ± 210*	150 ± 29	815 ± 266[a]	124 ± 52
LPS-34°C	1517 ± 203*	188 ± 31	603 ± 72[a]	72 ± 4
LPS-31°C	1063 ± 177*	157 ± 26	662 ± 172[a]	77 ± 29

Thrombus formation was induced by exposure to ferric chloride. Values are given as means ± standard error of the mean. Saline: 37°C saline controls (10 ml/kg body weight NaCl; -24 h intraperitoneally). LPS: endotoxemic animals (10 mg/kg body weight lipopolysaccharide (LPS); -24 h intraperitoneally); 37°C, systemic normothermia; 34°C, 34°C systemic hypothermia; 31°C, 31°C systemic hypothermia. [a]$p < 0.05$ versus Saline-37°C. RBC, red blood cell.

Figure 1

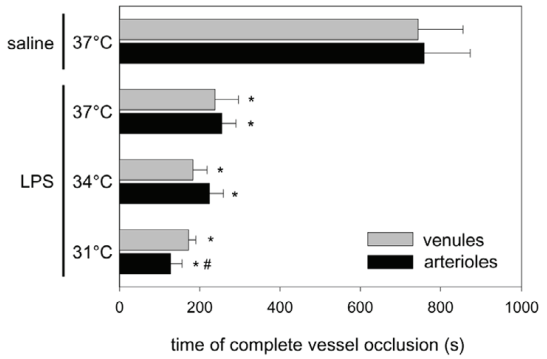

Microvascular thrombus formation *in vivo*. Occlusion times of arterioles and venules upon ferric chloride-induced thrombus formation in 37°C saline controls (10 ml/kg body weight NaCl; -24 h intraperitoneally; N = 10 preparations) and 37°C, 34°C and 31°C endotoxemic animals (10 mg/kg body weight lipopolysacharide (LPS); -24 h intraperitoneally; N = 8 preparations per group). Values are given as means ± standard error of the mean; *$p < 0.05$ versus 37°C saline controls; #$p < 0.05$ versus 37°C endotoxemic animals.

Available online http://ccforum.com/content/10/5/R148

was significantly ($p < 0.05$) reduced (127 ± 29 s) when compared to 37°C endotoxemic controls (Figure 1).

ELISA of circulating endothelial markers

To characterize the effect of endotoxemia and hypothermia on endothelial cell activation, we determined circulating (soluble) endothelial activation molecules. In animals with a core body temperature of 37°C, 24 h endotoxemia caused a drastic increase of sPAI-Ag when compared to 37°C saline controls (Figure 2). Of interest, hypothermia of 34°C and 31°C in endotoxemic animals resulted in a further three- to four-fold increase of sPAI-Ag (Figure 2).

In parallel, endotoxemia in 37°C animals induced a marked increase of sP-selectin, sE-selectin, sICAM-1 and sVCAM-1 when compared to 37°C saline controls (Figure 3). However, apart from sE-selectin, these indicators of endothelial activation were not further increased in endotoxemic animals by systemic hypothermia at 34°C and 31°C (Figure 3).

Flow cytometric analysis of murine platelet P-selectin, glycoprotein IIb-IIIa and CD107a expression

We studied the effect of systemic hypothermia on platelets of LPS-exposed animals. *In vivo* LPS exposure did not significantly affect spontaneous platelet expression of P-selectin, GPIIb-IIIa and CD107a. Also, incubation of platelets from LPS-exposed animals at temperatures of 34°C and 31°C did not result in significant changes in spontaneous P-selectin, GPIIb-IIIa and CD107a expression (data not shown).

Figure 2

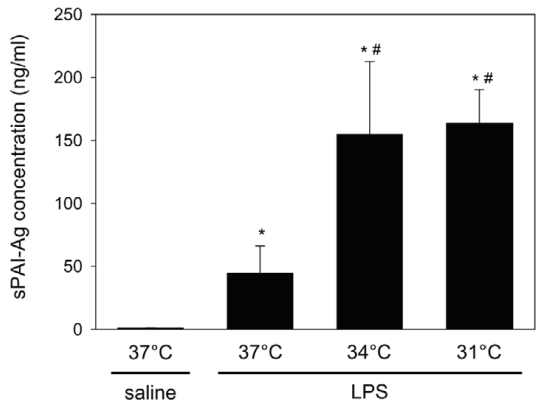

Soluble plasminogen activator inhibitor-1 antigen (sPAI-Ag) concentrations. Plasma concentrations of circulating sPAI-Ag in 37°C saline controls (10 ml/kg body weight NaCl; -24 h intraperitoneally; $n = 5$ animals) and 37°C, 34°C and 31°C endotoxemic animals (10 mg/kg body weight lipopolysacharide (LPS); -24 h intraperitoneally; $n = 4$ animals per group). Values are given as means ± standard error of the mean; $^{*}p < 0.05$ versus 37°C saline controls; $^{\#}p < 0.05$ versus 37°C endotoxemic animals.

In platelets of saline controls (37°C), *in vitro* stimulation with thrombin resulted in elevated expression of P-selectin, GPIIb-IIIa and CD107a. In platelets of endotoxemic 37°C animals, the expression of these markers was slightly, but not significantly, higher compared to saline 37°C warm control animals. However, hypothermic incubation of the LPS-exposed platelets at 34°C and 31°C did not further affect the P-selectin, GPIIb-IIIa and CD107a expression (data not shown).

Immunohistochemical analysis of P-selectin and PAI-1 expression

In general, P-selectin and PAI-1 were expressed within the endothelium of arterioles and venules, while little, if any, immunoreactivity was detected within the surrounding muscle tissue. For determination of immunohistological staining, a cross section of the cremaster muscle was evaluated using ×400 magnification. All vessels within this section were assessed, while the total number of vessels did not markedly vary between tissue specimens (20 to 35 vessels with approximately one-third arterioles and two-third venules within each specimen). Endothelial expression of these molecules was assessed by semiquantitative analysis of staining intensity: 0 corresponds to no staining; 1 to faint staining; 2 to moderate staining; and 3 to intense staining. As there were no notable differences in arteriolar and venular endothelial staining, vessels were not differentially assessed. Endotoxemia resulted in a marked increase in the expression of P-selectin and PAI-1 within the microvascular endothelium. In endotoxemic animals endothelial PAI-1 expression was further pronounced by systemic hypothermia at 31°C when compared to animals at 34°C and 37°C (Figure 4a,b).

Discussion

The major findings of the present study are that LPS-induced endotoxemia is a strong promoter of microvascular thrombosis *in vivo*, most probably due to increased endothelial activation, as indicated by elevated circulating levels of sPAI-Ag, sP-selectin, sE-selectin, sICAM-1 and sVCAM-1. Systemic hypothermia further promotes thrombus formation, particularly in arteriolar vessel structures. Of interest, this hypothermia-induced modulation towards a more procoagulant state is not based on increased expression and release of P-selectin, E-selectin, ICAM-1, VCAM-1 and GPIIb-IIIa because tissue expression and plasma levels of these markers were not affected by the reduction of the core body temperature to 34°C or 31°C. In contrast, the significantly increased sPAI-Ag levels during systemic hypothermia, and the increased endothelial PAI-1 expression in severe hypothermic animals at 31°C may indicate this molecule has a role in aggravation of thrombus formation by low temperatures in endotoxemia.

It is well known that small rodents, mice and rats in particular, initially develop hypothermia after exposure to LPS, which may be followed by a subsequent rise in temperature at later time points [15,16]. The initial hypothermic response seems to be

Figure 3

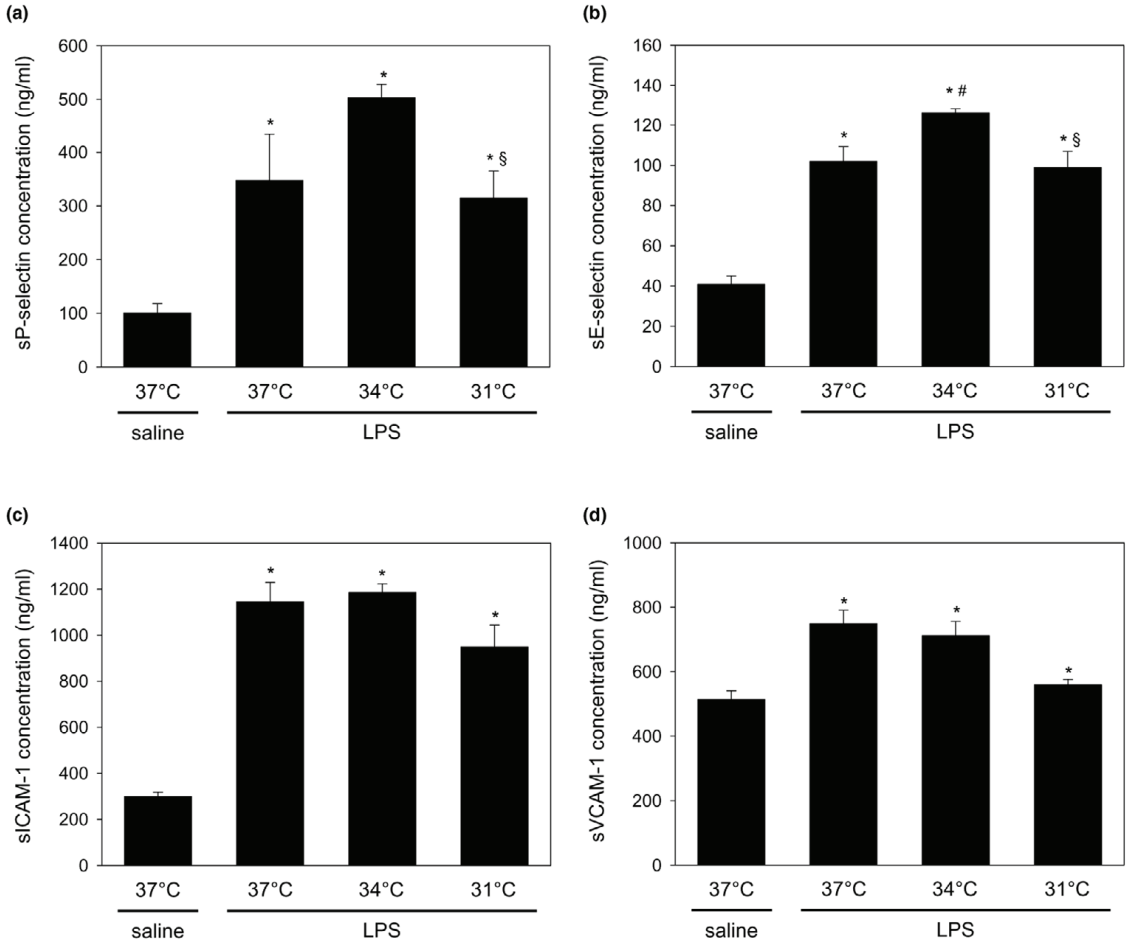

Circulating endothelial activation markers. Plasma concentrations of circulating **(a)** soluble (s)P-selectin, **(b)** sE-selectin, **(c)** intercellular adhesion molecule (sICAM)-1 and **(d)** vascular cell adhesion molecule (sVCAM)-1 in 37°C saline controls (10 ml/kg body weight NaCl; -24 h intraperitoneally; $n = 5$ animals) and 37°C, 34°C and 31°C endotoxemic animals (10 mg/kg body weight lipopolysacharide (LPS); -24 h intraperitoneally; $n = 4$ animals per group). Values are given as means ± standard error of the mean; $^{*}p < 0.05$ versus 37°C saline controls; $^{\#}p < 0.05$ versus 37°C endotoxemic animals; $^{\S}p < 0.05$ versus 34°C endotoxemic animals.

highly dependent on the ambient temperature and the LPS dose [17]. The body temperature usually normalizes after a time period of seven to eight hours, and body rewarming is supposed to be mediated via inducible nitric oxide synthetase [18]. Accordingly, in the present study we observed normothermic temperatures 24 hours after LPS administration.

Previous studies have reported inconsistent data on whether hypothermia affects the expression of surface adhesion molecules on platelets and endothelial cells. *In vitro* hypothermia at 25°C has been shown to inhibit endothelial cell expression of E-selectin [19]. In addition, hypothermic temperatures were found associated with increased P-selectin shedding, although cardiopulmonary bypass patients did not reveal differences in circulating levels of ICAM-1 and VCAM-1 during normothermia and hypothermia [20].

The microvasculature is the critical interface for oxygen and energy delivery to the tissues. Therefore, any obstruction of the microvasculature may have harmful effects on organ function. The generation of pro-inflammatory cytokines during sepsis, including IL-1, IL-6, and IL-8 as well as TNF-alpha activates the endothelial lining cells [21]. The immediate inflammatory response and the stimulation by agonists induce endothelial

Available online http://ccforum.com/content/10/5/R148

Figure 4

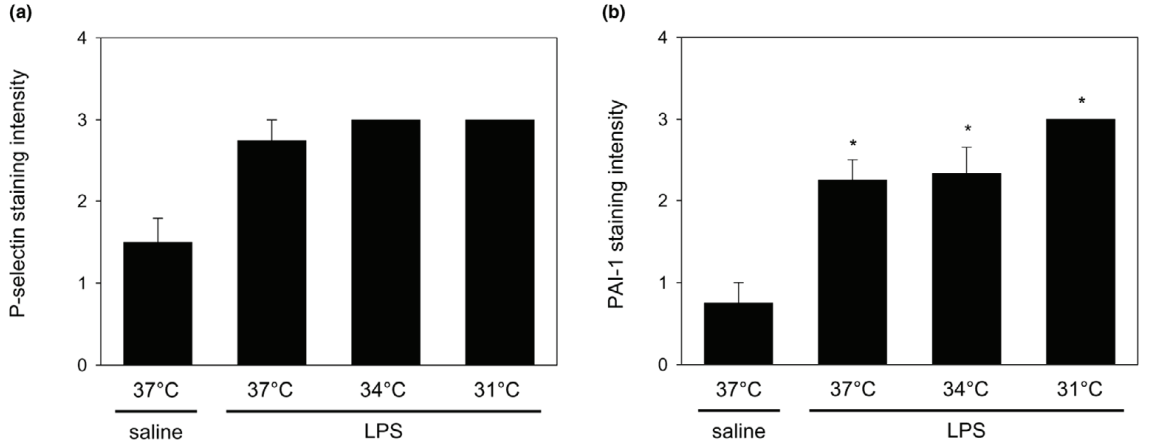

Endothelial P-selectin and plasminogen activator inhibitor (PAI)-1 expression. Analysis of the endothelial expression of **(a)** P-selectin and **(b)** PAI-1 in 37°C saline controls (10 ml/kg body weight NaCl; -24 h intraperitoneally; $n = 10$ tissue specimen) and 37°C, 34°C and 31°C endotoxemic animals (10 mg/kg body weight lipopolysacharide (LPS); -24 h intraperitoneally; $n = 8$ tissue specimens per group). Values are given as means ± standard error of the mean. *$p < 0.05$ versus 37°C saline controls.

cell expression of P-selectin. As a result, the surface of the endothelial cells changes from a non-adhesive and non-thrombogenic character towards a pro-adhesive state. In the delayed endothelial response, E-selectin is expressed on endothelial cells after several hours and reaches its maximum after 12 hours [22]. Our results confirm this, in as much as endotoxemia caused a marked rise in shed circulating endothelial markers. To differentiate whether sP-selectin originated from endothelial cells or platelets, which both have been shown to release a soluble form of P-selectin into the plasma [23], we additionally performed immunohistochemical analyses. By this we could show an increased expression of P-selectin in the microvascular endothelium during exdotoxemia, which may indicate that a significant proportion of the circulating sP-selectin originates from the activated endothelium.

To further elucidate the role of platelets, we tested the effect of endotoxemia and systemic hypothermia at 34°C and 31°C on platelet activation and reactivity *in vitro*. Our results indicate that, in addition to the endothelial activation, enhanced platelet reactivity, as caused by the thrombin activation, may contribute to the acceleration of microvascular thrombus formation in endotoxemic animals. Because P-selectin shed from platelets serves as the main source for circulating P-selectin and platelet activation results in up to 50% secretion of intracellular P-selectin [23], it is reasonable to assume that a major part of the increase in sP-selectin during endotoxemia might also be due to platelet activation. Of interest, 34°C and 31°C hypothermia did not further increase spontaneous platelet activation or platelet responsiveness to agonists when compared to normothermic endotoxemic controls. This is most probably due to the fact that endotoxemia already enhanced platelet responsiveness and agonist-induced reactivity, so that little effect could additionally be induced by hypothermia. This view is supported by our previous study, which demonstrated that platelets from healthy humans are highly responsive upon exposure to hypothermic temperatures [8].

Although the importance of GPIb-IX-V in mediating platelet-endothelial interactions is unequivocal, this ligand is thought to be mandatory for adhesion and thrombus growth at high shear [24]. At low shear other adhesion molecules, such as the collagen receptors and GPIIb-IIIa, are mainly involved in platelet adhesion [25,26]. Because the microvessels analyzed in the present study revealed wall shear rates below 300 s^{-1}, we elucidated the role of the fibrinogen receptor GPIIb-IIIa. Of interest, spontaneous platelet GPIIb-IIIa expression did not increase but even slightly decreased after endotoxin exposure, and thrombin-stimulation of endotoxin-exposed platelets also induced an only slight but not significant elevation of expression. Because concomitant systemic hypothermia also did not affect GPIIb-IIIa expression, our data suggest that platelet expression of this molecule did not substantively contribute to low temperature-induced acceleration of thrombus formation during endotoxemia.

Although increased levels of plasminogen activators such as tissue plasminogen activator (t-PA) have been observed in sepsis [27], their action appears to be counterbalanced by increased PAI-1 levels, resulting in ineffective fibrinolysis and enhanced organ damage [28]. Recently, it has been recognized that endothelial cells play a pivotal role in the pathogen-

esis of sepsis by releasing tissue factor thrombomodulin and PAI-1 [2]. For the first time, we now provide evidence that the expression of PAI-1 is increased in the systemic circulation and thrombus formation in endotoxemia is enhanced by moderate systemic hypothermia. This view is supported by the significant increase in circulating PAI-Ag levels at temperatures of 34°C and 31°C versus 37°C in endotoxemic animals, and the most pronounced endothelial expression of PAI-1 during 31°C hypothermia.

Several studies have suggested that PAI-1 plays a major role in the pathogenesis of atherosclerosis and represents a risk factor for coronary heart disease [29]. PAI-1 is the most important physiological inhibitor of tissue plasminogen activator and, therefore, exerts pro-thrombotic effects. APoE-/-mice with high PAI-1 levels exhibit a prothrombotic phenotype with shortened time to thrombotic vessel occlusion in a model of ferric-chloride induced carotid artery injury [30]. The acceleration of thrombus formation observed in endotoxemic and hypothermic animals may, therefore, at least in part, be due to the increase in endothelial PAI-1 expression and plasma concentration. Because hypothermia in general is known to slow down physiological processes, it is possible that hypothermia causes an increase in endothelial PAI-1 expression, while secretion into systemic blood circulation is decelerated or even impaired. This fact might explain why sPAI-1-Ag levels did not increase from 34°C to 31°C, whereas immunohistological staining revealed a further, though not significant, rise in endothelial PAI-1 expression from 34°C to 31°C.

In the pathogenesis of severe coagulation abnormalities in sepsis, three major mechanisms are supposed to play a role: the tissue-factor driven accumulation of thrombin with subsequent fibrinogen conversion, binding to the platelet surface receptor GPIIb-IIIa, and, finally, platelet activation and clotting; impairment of the anti-thrombin, protein C and tissue factor pathway inhibitor anti-coagulative systems; and inhibition of fibrinolysis by increased PAI-1 production [31]. Generally, the increased mortality of hypothermic and septic patients is ascribed to a diminished host response due to an impaired immune function [6,7] and to an augmentation of the generation of inflammatory cytokines like TNF-alpha and IL-1beta [32]. In addition to this, previous studies have shown that correction of hypothermia during sepsis results in decreased IL-6 levels and a significantly increased survival rate [33]. Based on our results, microvascular thrombus formation with the consequence of deterioration of organ perfusion is dramatically increased during the septic state. Although endotoxemia *per se* had already massively reduced microvessel occlusion time, 31°C hypothermia promoted a further, approximately 50% reduction in arteriolar occlusion time, indicating that microvascular thrombus formation may, indeed, at least in part, contribute to the increased mortality rates during systemic hypothermia observed in septic patients.

Conclusion

Systemic hypothermia superimposed on endotoxemic challenge further increases microvascular thrombus formation *in vivo*. This involves an increase in circulating PAI-1 expression rather than being due to incremental endothelial activation or an elevation of agonist-dependent platelet reactivity.

Key messages

- LPS-induced endotoxemia accelerates microvascular thrombus formation *in vivo* by generalized endothelial activation and increased platelet reactivity
- Systemic hypothermia further enhances microthrombosis in endotoxemia
- Systemic hypothermia in endotoxemia is associated with increased endothelial PAI-1 expression and sPAI-Ag concentrations

Competing interests

The authors declare that they have no competing interests.

Authors' contributions

NL carried out the animal experiments, evaluated the flow cytometric analyses, immunohistological sections and ELISAs, performed the statistics and drafted the manuscript. BV conceived the study, participated in its design and coordination and helped to draft the manuscript. MDM and EK participated in the design and coordination of the study, and in the interpretation of the results. All authors read and approved the final manuscript.

Acknowledgements

The authors kindly thank Berit Blendow, Kathrin Sievert and Doris Butzlaff, Department of Experimental Surgery, University of Rostock, for their excellent technical assistance. This study is supported by a grant from the Deutsche Forschungsgemeinschaft, Bonn-Bad Godesberg, Germany (Vo 450/8-1).

References

1. Zeerleder S, Hack CE, Wuillemin WA: **Disseminated intravascular coagulation in sepsis.** *Chest* 2005, **128**:2864-2875.
2. Vincent JL: **Microvascular endothelial dysfunction: a renewed appreciation of sepsis pathophysiology.** *Crit Care* 2001, **5**:S1-5.
3. Baumann H, Gauldie J: **The acute phase response.** *Immunol Today* 1994, **15**:74-80.
4. Levi M, de Jonge E, van der Poll T: **Rationale for restoration of physiological anticoagulant pathways in patients with sepsis and disseminated intravascular coagulation.** *Crit Care Med* 2001, **29(7 Suppl)**:S90-S94.
5. ten Cate H, Schoenmakers SH, Franco R, Timmerman JJ, Groot AP, Spek CA, Reitsma PH: **Microvascular coagulopathy and disseminated intravascular coagulation.** *Crit Care Med* 2001, **29(7 Suppl)**:S95-S97.
6. Remick DG, Xioa H: **Hypothermia and sepsis.** *Front Biosci* 2006, **11**:1006-1013.
7. Torossian A, Ruehlmann S, Middeke M, Sessler DI, Lorenz W, Wulf HF, Bauhofer A: **Mild preseptic hypothermia is detrimental in rats.** *Crit Care Med* 2004, **32**:1899-1903.

8. Lindenblatt N, Menger MD, Klar E, Vollmar B: **Sustained hypothermia accelerates microvascular thrombus formation in mice.** *Am J Physiol Heart Circ Physiol* 2005, **289**:H2680-H2687.
9. Baez S: **An open cremaster muscle preparation for the study of blood vessels by *in vivo* microscopy.** *Microvasc Res* 1973, 5:384-394.
10. Vollmar B, Schmits R, Kunz D, Menger MD: **Lack of *in vivo* function of CD31 in vascular thrombosis.** *Thromb Haemost* 2001, **85**:160-164.
11. Denis C, Methia N, Frenette PS, Rayburn H, Ullman-Cullere M, Hynes RO, Wagner DD: **A mouse model of severe von Willebrand disease: defects in hemostasis and thrombosis.** *Proc Natl Acad Sci USA* 1998, **95**:9524-9529.
12. Lindenblatt N, Bordel R, Schareck W, Menger MD, Vollmar B: **Vascular heme oxygenase-1 induction suppresses microvascular thrombus formation *in vivo*.** *Arterioscler Thromb Vasc Biol* 2004, **24**:601-606.
13. Baker M, Wayland H: **On-line volume flow rate and velocity profile measurements for blood in microvessels.** *Microvasc Res* 1974, **7**:131-143.
14. Nieswandt B, Schulte V, Bergmeier W: **Flow-cytometric analysis of mouse platelet function.** *Methods Mol Biol* 2004, **272**:255-268.
15. Derijk RH, Van Kampen M, Van Rooijen N, Berkenbosch F: **Hypothermia to endotoxin involves reduced thermogenesis, macrophage-dependent mechanisms, and prostaglandins.** *Am J Physiol* 1994, **266**:R1-R8.
16. Kozak W, Soszynski D, Rudolph K, Leon LR, Conn CA, Kluger MJ: **Soluble tumor necrosis factor alpha receptor prevents decrease of body temperature in mice treated with indomethacin and lipopolysaccharide.** *Ann NY Acad Sci* 1997, **813**:264-271.
17. Rudaya AY, Steiner AA, Robbins JR, Dragic AS, Romanovsky AA: **Thermoregulatory responses to lipopolysaccharide in the mouse: dependence on the dose and ambient temperature.** *Am J Physiol Regul Integr Comp Physiol* 2005, **289**:R1244-R1252.
18. Saia RS, Carnio EC: **Thermoregulatory role of inducible nitric oxide synthase in lipopolysaccharide-induced hypothermia.** *Life Sci* 2006, **79**:1473-1478.
19. Johnson M, Haddix T, Pohlman T, Verrier ED: **Hypothermia reversibly inhibits endothelial cell expression of E-selectin and tissue factor.** *J Card Surg* 1995, **10(4 Suppl)**:428-435.
20. Boldt J, Osmer C, Linke LC, Gorlach G, Hempelmann G: **Hypothermic versus normothermic cardiopulmonary bypass: influence on circulating adhesion molecules.** *J Cardiothorac Vasc Anesth* 1996, **10**:342-347.
21. Cines DB, Pollak ES, Buck CA, Loscalzo J, Zimmerman GA, McEver RP, Pober JS, Wick TM, Konkle BA, Schwartz BS, *et al.*: **Endothelial cells in physiology and in the pathophysiology of vascular disorders.** *Blood* 1998, **91**:3527-3561.
22. Prescott SM, McIntyre TM, Zimmerman GA, Stafforini DM: **Sol Sherry lecture in thrombosis: molecular events in acute inflammation.** *Arterioscler Thromb Vasc Biol* 2002, **22**:727-733.
23. Semenov AV, Romanov YA, Loktionova SA, Tikhomirov OY, Khachikian MV, Vasil'ev SA, Mazurov AV: **Production of soluble P-selectin by platelets and endothelial cells.** *Biochemistry (Mosc)* 1999, **64**:1326-1335.
24. Berndt MC, Shen Y, Dopheide SM, Gardiner EE, Andrews RK: **The vascular biology of the glycoprotein Ib-IX-V complex.** *Thromb Haemost* 2001, **86**:178-188.
25. Moroi M, Jung SM, Shinmyozu K, Tomiyama Y, Ordinas A, Diaz-Ricart M: **Analysis of platelet adhesion to a collagen-coated surface under flow conditions: the involvement of glycoprotein VI in the platelet adhesion.** *Blood* 1996, **88**:2081-2092.
26. Savage B, Almus-Jacobs F, Ruggeri ZM: **Specific synergy of multiple substrate-receptor interactions in platelet thrombus formation under flow.** *Cell* 1998, **94**:657-666.
27. Philippe J, Offner F, Declerck PJ, Leroux-Roels G, Vogelaers D, Baele G, Collen D: **Fibrinolysis and coagulation in patients with infectious disease and sepsis.** *Thromb Haemost* 1991, **65**:291-295.
28. Watanabe R, Wada H, Watanabe Y, Sakakura M, Nakasaki T, Mori Y, Nishikawa M, Gabazza EC, Nobori T, Shiku H: **Activity and antigen levels of thrombin-activatable fibrinolysis inhibitor in plasma of patients with disseminated intravascular coagulation.** *Thromb Res* 2001, **104**:1-6.
29. Alessi MC, Juhan-Vague : **Contribution of PAI-1 in cardiovascular pathology.** *Arch Mal Coeur Vaiss* 2004, **97**:673-678.
30. Schafer K, Muller K, Hecke A, Mounier E, Goebel J, Loskutoff DJ, Konstantinides S: **Enhanced thrombosis in atherosclerosis-prone mice is associated with increased arterial expression of plasminogen activator inhibitor-1.** *Arterioscler Thromb Vasc Biol* 2003, **23**:2097-2103.
31. Levi M, de Jonge E, van der Poll T, ten Cate H: **Novel approaches to the management of disseminated intravascular coagulation.** *Crit Care Med* 2000, **28(9 Suppl)**:S20-S24.
32. Fairchild KD, Singh IS, Patel S, Drysdale BE, Viscardi RM, Hester L, Lazusky HM, Hasday JD: **Hypothermia prolongs activation of NF-kappaB and augments generation of inflammatory cytokines.** *Am J Physiol Cell Physiol* 2004, **287**:C422-C431.
33. Xiao H, Remick DG: **Correction of perioperative hypothermia decreases experimental sepsis mortality by modulating the inflammatory response.** *Crit Care Med* 2005, **33**:161-167.

2.2 Beeinflussung der Thrombogenese durch Induktion endogener Enzyme

Die vorherigen Studien zeigten eine signifikante Beeinflussbarkeit mikrovaskulärer thrombotischer Vorgänge durch Änderung der Körpertemperatur und Induktion einer Endotoxinämie. Es war daher weiterhin von Interesse zu untersuchen, inwieweit die Thrombogenität auch durch Einflussnahme auf ein endogenes Enzymsystem beeinflusst werden kann.

2.2.1 Hämoxygenase-1 (HO-1)

Das mikrovaskuläre Endothel ist mit einer Vielzahl protektiver Mechanismen zur Verhinderung übermäßiger Gerinnungsvorgänge ausgestattet. Dazu gehören die Bildung von anti-adhäsivem und anti-thrombotischem NO und PGI_2. In Analogie zu NO ist Kohlenmonoxid (CO) anti-inflammatorisch wirksam. Zusätzlich haben anti-oxidativ wirkende Moleküle, wie das Bilirubin, anti-thrombotische Eigenschaften. Beide Verbindungen entstehen als Endprodukt bei der Degradierung von Häm durch HO-1. Ziel dieser Studie war es daher, den Effekt der Induktion von HO-1 auf mikrovaskuläre Thrombusbildung zu untersuchen und vor allem die Modulation der Wirkung durch Induktoren oder Inhibitoren der HO-1 zu charakterisieren. *In vivo* konnte bei Mäusen eine signifikante Verlängerung der mikrovaskulären Thrombosezeiten nach Vorbehandlung mit Hämin, einem HO-1 Induktor, beobachtet werden. Dieser Effekt wurde durch Vorbehandlung mit Zinn Protoporphyrin-IX, einem HO-1 Inhibitor, aufgehoben. Die gleichzeitige Gabe des anti-oxidativen Vitamin E Analogons Trolox führte in HO-1 geblockten Tieren wiederum zu verlängerten Thrombosezeiten, was impliziert, dass die anti-thrombogenen Effekte, neben CO, hauptsächlich durch Bilirubin verursacht werden. Western Blot Analysen aus Cremastermuskelgewebe nach HO-1 Induktion konnten einen verminderten Gehalt an P-Selektin als molekulare Basis für die verminderte Thrombogenität nachweisen.

Lindenblatt N, Bordel R, Schareck W, Menger MD, Vollmar B
Vascular heme oxygenase-1 induction suppresses microvascular thrombus formation in vivo *Arterioscler Thromb Vasc Biol* 2004: 24: 601-606.

Vascular Heme Oxygenase-1 Induction Suppresses Microvascular Thrombus Formation In Vivo

N. Lindenblatt, R. Bordel, W. Schareck, M.D. Menger, B. Vollmar

Objective—By heme degradation, heme oxygenase-1 (HO-1) provides endogenous carbon monoxide and bilirubin, both of which play major roles in vascular biology. The current study aimed to examine whether induction of HO-1 and its byproducts modulate the process of microvascular thrombus formation in vivo.

Methods and Results—In individual microvessels of mouse cremaster muscle preparations, ferric chloride-induced thrombus formation was analyzed using intravital fluorescence microscopy. When mice were pretreated with an intraperitoneal injection of hemin, a HO-1 inducer, immunohistochemistry and Western blot protein analysis of cremaster muscle tissue displayed a marked induction of HO-1. In these animals, superfusion with ferric chloride solution induced arteriolar and venular thrombus formation, which, however, was significantly delayed when compared with thrombus formation in animals without HO-1 induction. The delay in thrombus formation in hemin-treated mice was completely blunted by tin protoporphyrin-IX, a HO-1 inhibitor, but not by copper protoporphyrin-IX, which does not inhibit the enzyme. Coadministration of the vitamin E analogue Trolox in HO-1–blocked animals almost completely restored the delay in thrombus formation, implying that, besides CO, the antioxidant HO pathway metabolite bilirubin mainly contributes to the antithrombotic property of HO-1. This was further supported by the fact that bilirubin was found as effective as hemin in delay of ferric chloride-induced thrombus formation. Animals with HO-1 induction revealed reduced P-selectin protein expression in cremaster muscle tissue, which most probably presented the molecular basis for delayed thrombus growth.

Conclusion—Local induction of HO-1 activity may be of preventive and therapeutic value for clinical disorders with increased risk of thrombotic events. (*Arterioscler Thromb Vasc Biol.* 2004;24:601-606.)

Key Words: thrombosis ■ fluorescence microscopy ■ carbon monoxide ■ bilirubin ■ P-selectin

Thromboembolism is still a major problem in almost all fields of clinical medicine, resulting in tissue infarction and ischemic necrosis. Besides specific plasma protein components such as von Willebrand factor and fibrinogen, platelets, leukocytes, and endothelial cells are among the cellular components critical for this process.[1,2] In thrombus formation associated with hemostasis or thrombotic disease, blood platelets first undergo a rapid transition from a circulating to a rolling state, using the GPIb-IX-V complex and PSGL-1 for interaction with the activated endothelium via surface-expressed endothelial P-selectin.[1,3] This causes platelet activation with subsequent firm adhesion leading to shear resistant platelet deposition.[1] The expression of P-selectin on the platelet surface after platelet stimulation and alpha granule secretion allow for interaction and recruitment of leukocytes and monocytes to thrombotic sites with fibrin deposition for thrombus stabilization.[4]

The microvascular endothelium is equipped with a number of mechanisms that prevent thrombus formation in the circulatory system. Among others, it harbors endothelium-derived factors such as nitric oxide and prostacyclin, exerting vasodilatory and anti-adhesive actions.[5] Analogous to nitric oxide, carbon monoxide (CO) has been implicated as a biological second messenger with endothelium-derived relaxing activity and antiinflammatory properties.[6,7] Heme oxygenases are the rate-limiting enzymes in the catabolism of heme into bilirubin, free iron, and CO and exist in different isoforms.[8,9] HO-2 is thought to be constitutive, whereas HO-1 is inducible by various stimuli, such as cytokines and oxidants.[7] Besides CO, the HO byproduct bilirubin additionally exerts antioxidant effects. Further, heme degradation by HO leads to ferritin synthesis with sequestration of iron, thus preventing its participation in subsequent oxidant stress-induced injury.[7] With the view that free radical generation and consequent oxidative stress have a distinctive role in the pathogenesis of thrombotic events,[10] this study aimed to examine whether HO-1 induction could attenuate microvascular thrombus formation in vivo.

Received November 14, 2003; accepted December 9, 2003.

From the Department of Experimental Surgery (N.L., R.B., B.V.) and the Department of General Surgery (N.L., W.S.), University of Rostock, Rostock, Germany; and the Department of Clinical-Experimental Surgery (M.D.M.), University of Saarland, Homburg/Saar, Germany.

Correspondence to Dr Brigitte Vollmar, Department of Experimental Surgery, University of Rostock, Schillingallee 70, 18055 Rostock, Germany. E-mail brigitte.vollmar@med.uni-rostock.de

© 2004 American Heart Association, Inc.

Arterioscler Thromb Vasc Biol. is available at http://www.atvbaha.org DOI: 10.1161/01.ATV.0000118279.74056.8a

Methods

Mice Cremaster Muscle Preparation

On approval by the local government, all experiments were performed in accordance with the German legislation on protection of animals and the National Institutes of Health *Guide for the Care and Use of Laboratory Animals* (Institute of Laboratory Animal Resources, National Research Council). Male C57BL/6J mice with a body weight of 20 to 25 g were anesthetized by an intraperitoneal injection of ketamine (90 mg/kg body weight) and xylazine (25 mg/kg body weight), and a polyethylene catheter was placed into the right jugular vein, serving for application of fluorescent dyes.

For the study of vascular thrombus formation, we used the opened cremaster muscle preparation as originally described by Baez in rats[11] and transferred by our group to mice.[12] A midline incision of the skin and fascia was made over the ventral aspect of the scrotum and extended up to the inguinal fold and to the distal end of the scrotum. The incised tissues were retracted to expose the cremaster muscle sack that was maintained under gentle traction to carefully separate the remaining connective tissue by blunt dissection from around the cremaster sack. Then, the cremaster muscle was incised while avoiding cutting the larger anastomosing vessels. Hemostasis was achieved with 5-0 threads, serving also to spread the tissue. After dissection of the vessel connecting the cremaster and the testis, the epididymis and testis were put to the side of the preparation. The preparation was performed on a transparent pedestal to allow microscopic observation of the cremaster muscle microcirculation by transillumination and epi-illumination techniques.

After the preparation of the cremaster muscle, the animals were allowed to recover from surgical preparation for 15 minutes. Then, induction of thrombus formation was performed in randomly chosen venules (n=1 to 2 per preparation) and arterioles (n=1 to 2 per preparation).

In Vivo Thrombosis Model

After intravenous injection of 0.1 mL 5% fluorescein isothiocyanate-labeled dextran (MW 150000; Sigma, Deisenhofen, Germany) and subsequent circulation for 30 seconds, the cremaster muscle microcirculation was visualized by intravital fluorescence microscopy using a Nikon microscope (E600-FN; Nikon, Tokyo, Japan). The microscopic procedure was performed at a constant room temperature of 21°C to 23°C. The epi-illumination setup included a 100-W HBO mercury lamp and an illuminator equipped with a blue filter (465 to 495 nm/>505 nm excitation/emission wavelengths). Microscopic images were recorded by a charge-coupled device videocamera (FK 6990-IQ-S; Pieper, Schwerte, Germany) and stored on videotapes for off-line evaluation. Using a ×20 water immersion objective (Plan Fluor ×20/0.75; Nikon), resting blood flow was monitored in individual arterioles (diameter range 30 to 50 μm) and venules (diameter range 60 to 80 μm), followed by superfusion with ferric chloride (30 μL of a 25 mmol/L-solution; Sigma) for induction of microvascular thrombosis.[13] Recording of vessels was discontinued after blood flow in the vessel ceased for at least 60 seconds because of complete vessel occlusion. Because rapid spreading of ferric chloride solution allowed us to study only 1 to 2 arterioles and venules within each preparation, left and right cremaster muscles were prepared for analysis of thrombotic vessel occlusion within each animal.

Analysis included the time periods until sustained cessation of blood flow caused by complete vessel occlusion. Microcirculatory analysis further included the determination of vessel diameter and blood cell velocity before thrombus induction with calculation of vascular wall shear rates, based on the Newtonian definition $\gamma = 8 \times V/D$ (V represents the red blood cell centerline velocity divided by 1.6, according to the Baker-Wayland factor,[14] and D represents the individual inner vessel diameter).

Experimental Groups and Protocol

Eighteen hours before the experiment, mice (n=7) were administered hemin (50 μmol/L per kg body weight intraperitoneally) for HO-1 induction. Control animals received equivalent volumes of the vehicle DMSO (n=7). For blockade of HO-1, hemin-treated animals additionally received tin protoporphyrin (SnPP-IX; 50 μmol/L per kg body weight intraperitoneally) 18 hours before the experiment (n=4). Additional hemin-treated animals received the copper protoporphyrin-IX (CuPP-IX; 50 μmol/L per kg body weight) 18 hours before the experiment (n=3). To address the role and impact of CO versus bilirubin, hemin/SnPP-IX–treated animals additionally received Trolox (20 mg/kg intraperitoneally) 15 minutes before induction of thrombus formation (n=4). In an additional series of animals (n=4), cremaster muscle preparations of hemin/SnPP-IX–treated animals were topically exposed to 10 μmol/L bilirubin, followed by superfusion with ferric chloride, as described.

To address the participation of P-selectin in thrombogenesis, P-selectin–deficient mice (Jackson Laboratory; C57BL/6J-*Selp*^{tm1Bay}; n=5) were used for ferric chloride-induced microvascular thrombus formation. Wild-type C57BL/6J mice (n=5) served as controls.

Additional hemin-treated and hemin/SnPP-IX–treated mice (n=3 to 4 each) exclusively served for withdrawal of arterial blood by left ventricular puncture for subsequent analysis of plasma bilirubin (Hitachi 704; Boehringer Mannheim, Mannheim, Germany).

Chemicals

The HO-1 inductor hemin (Fluka, Steinheim, Germany) was dissolved in DMSO to a final concentration of 5 μmol/mL. Tin protoporphyrin-IX (SnPP-IX; Frontier Scientific, Lancashire, UK), a HO-1 inhibitor,[15] and copper protoporphyrin-IX (CuPP-IX; Frontier Scientific, Lancashire, UK), which does not inhibit HO-1,[15] were dissolved in 8.4% sodium-bicarbonate and phosphate-buffered saline to achieve a final concentration of 5 μmol/mL. The solutions were stored at a maximal temperature of 8°C in the dark and used within the next hour. The water-soluble vitamin E analogue Trolox (6-hydroxy-2,5,7,8-tetramethylchroman-2-carbonic acid; Sigma-Aldrich, Steinheim, Germany) was dissolved in phosphate-buffered saline to a final concentration of 20 mg/mL. All solutions were freshly prepared on the day of the experiment according to the manufacturers' directions. Dose and application modes of drugs were chosen in accordance to a previously published work of our group.[16] Bilirubin (Sigma-Aldrich) was dissolved in deionized water (1 mg/mL), adjusted to a pH of 8.4 by addition of 2 N sodium hydroxide, and administered at a final concentration of 10 μmol/L, as described by others.[17]

Western Blot Analysis of HO-1 and P-selectin

For whole protein extracts and Western blot analysis of HO-1 and P-selectin, cremaster muscle tissue was homogenized in lysis buffer (10 mmol/L Tris pH 7.5, 10 mmol/L NaCl, 0.1 mmol/L EDTA, 0.5% Triton-X 100, 0.02% NaN_3, 0.2 mmol/L PMSF), incubated for 30 minutes on ice, and centrifuged for 15 minutes at 10 000g. Before use, all buffers received a protease inhibitor cocktail (1:100 v/v; Sigma). Protein concentrations were determined using the bicinchoninic acid protein assay (Sigma) with bovine serum albumin as standard; 20 μg protein/lane were separated discontinuously on sodium dodecyl sulfate polyacrylamide gels (12%) and transferred to a polyvinyldifluoride membrane (Immobilon-P; Millipore, Eschborn, Germany). After blockade of nonspecific binding sites, membranes were incubated for 2 hours at room temperature with rabbit polyclonal anti-HO-1 (1:2000; StressGen Biotechnologies, Victoria, BC, Canada) and goat polyclonal anti-P-selectin (1:100; Santa Cruz Biotechnology, Heidelberg, Germany) followed by peroxidase-conjugated goat anti-rabbit Ig antibody (1:10000; Cell Signaling Technology, Frankfurt, Germany) or donkey anti-goat Ig antibody (1:40000; Santa Cruz Biotechnology, Heidelberg, Germany) as secondary antibody. Protein expression was visualized by means of luminol-enhanced chemiluminescence (ECL plus; Amersham Pharmacia Biotech) and exposure of the membrane to a blue light-sensitive autoradiography film (Kodak BioMax Light Film; Kodak-Industrie, Chalon-sur-Saone, France). Signals were densitometrically assessed (Gel-Dokumentationssystem E.A.S.Y. Win32; Herolab GmbH, Wiesloch, Germany).

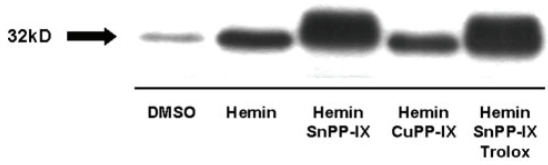

Figure 1. Western blot analysis of HO-1 protein expression in cremaster muscle tissue of DMSO-treated, hemin-treated, hemin/SnPP-IX–treated, hemin/CuPP-IX-treated, and hemin/SnPP-IX/Trolox–treated animals. For detailed information, see Methods. Treatment with hemin induces marked HO-1 protein expression. Note that SnPP-IX, but not CuPP-IX, further upregulates HO-1 protein expression, probably by inhibition of HO-1 enzymatic activity (see reference 15).

Histology and Immunohistochemistry

At the end of each experiment, the cremaster muscle was fixed in 4% phosphate-buffered formalin for 2 to 3 days and embedded in paraffin. From the paraffin-embedded tissue blocks, 4-μm sections were cut and stained with hematoxylin–eosin for histological analysis. For immunohistochemical demonstration of HO-1, sections collected on poly-L-lysine–coated glass slides were treated by microwave for antigen unmasking. Rabbit polyclonal anti-HO-1 (1:200; StressGen Biotechnologies) was used as primary antibody and incubated for 90 to 120 minutes at room temperature, followed by an alkaline–phosphatase conjugated goat anti-rabbit antibody (1:25; Cell Signaling Technology) and development using new fuchsin as chromogen. The sections were counterstained with hematoxylin and examined by light microscopy (Biomed; Leitz, Wetzlar, Germany).

Statistical Analysis

After proving the assumption of normality and equal variance across groups, differences between groups were assessed using 1-way ANOVA followed by the appropriate post-hoc comparison test. All data were expressed as means±SEM and overall statistical significance was set at $P<0.05$. Statistics were performed using the software package SigmaStat (Jandel Corporation, San Rafael, Calif).

Results

Western Blot Analysis and Immunohistochemistry of Cremaster Muscle Tissue

As illustrated by Western blot analysis of mice cremaster muscle tissue, hemin injection induced a marked increase in HO-1 protein expression (Figure 1). Concomitant application of SnPP-IX, but not CuPP-IX, caused a further increase of HO-1 protein expression, presumably caused by the ability of SnPP-IX to act as a potent inhibitor of HO-1 enzymatic activity (Figure 1). Hemin treatment caused some elevation in bilirubin levels (4.7±0.3 μmol/L versus 4.1±0.1μmol/L in DMSO-treated control animals), which in turn was inhibited by coadministration of SnPP-IX (3.8±0.3μmol/L).

Immunohistochemistry of cremaster muscle tissue of DMSO-treated control animals exhibited little, if any, immunoreactivity of HO-1 (Figure 2A). In contrast, cremaster muscle tissue of hemin-treated animals displayed marked immunoreactivity of HO-1 at vascular sites and, although less pronounced, within the muscle tissue (Figure 2B). Vascular smooth muscle cells and, particularly, arteriolar and venular endothelia constituted the major site of prominent HO-1 expression (Figure 2B). Hemin-treated animals further exhibited reduced P-selectin protein expression when compared with DMSO-treated controls (Figure 3).

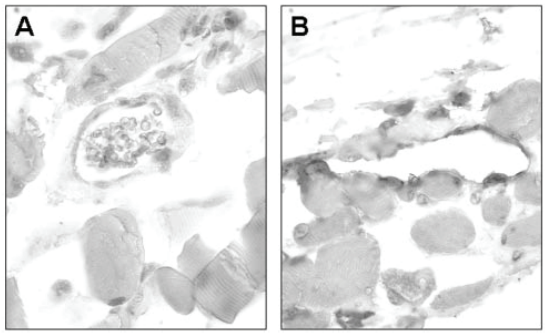

Figure 2. Immunohistochemical staining of HO-1 expression in cremaster muscle tissue after DMSO (A) and hemin (B) treatment. Note the marked induction of HO-1 expression in the hemin-treated animal with preferential localization at the vascular site, whereas there was little, if any, immunostaining for HO-1 in the DMSO-treated control animals. Magnification ×400.

In Vivo Thrombosis Model

The effect of vascular HO-1 expression was assessed in an in vivo thrombosis model. Superfusion of microvessels with ferric chloride solution caused a complete thrombotic occlusion of the individually exposed vessel.

At baseline, ie, before thrombus induction, animals of either of the groups did not differ with respect to velocity and wall shear rates in arterioles and venules (Table). Quantitative analysis of ferric chloride-induced thrombus formation in controls, ie, DMSO-treated animals, revealed a complete occlusion of arterioles and venules after 143±17 seconds and 130±25 seconds, respectively (Figures 4 and 5). Hemin-induced HO-1 expression caused a significant delay in microvascular thrombus formation. Arteriolar and venular vessel lumen were found clogged at an average time of 670±110 seconds and 647±129 seconds (Figures 4 and 5). Accordingly, within the first 100 seconds on ferric chloride superfusion, arteriolar and venular blood cell velocity slowed down by −32% and −47% in the DMSO-treated animals, whereas in animals with hemin-induced HO-1 expression, velocity remained almost unchanged (−9% and −3%). Treatment of HO-1–expressing animals with SnPP-IX, but not CuPP-IX, restored the potential of ferric chloride solution to induce thrombus formation, resulting in vessel occlusion time periods almost equivalent to those observed in the hemin-untreated, DMSO-exposed control animals (Figures 4 and 5).

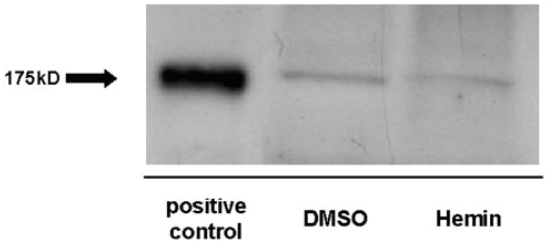

Figure 3. Western blot analysis of P-selectin protein expression in cremaster muscle tissue of DMSO-treated and hemin-treated animals. Protein extract from isolated mouse platelets was used as positive control.

Blood Flow Velocity (μm/s) and Wall Shear Rates (γ; s^{-1}) in Mice Cremaster Muscle Microvessels Before Thrombus Induction by Ferric Chloride Superfusion

	Arterioles		Venules	
	Velocity	Wall Shear Rate	Velocity	Wall Shear Rate
DMSO	950±189	170±32	524±73	72±11
Hemin	1070±158	186±23	534±107	65±11
Hemin/SnPP-IX	1531±338	266±44	640±114	65±14
Hemin/CuPP-IX	888±127	182±41	457±62	49±10
Hemin/SnPP-IX+Trolox	1064±154	197±33	500±90	52±8
Hemin/SnPP-IX+bilirubin	1229±90	227±21	599±72	87±17

Values are given as means±SEM.
Blood flow velocity given in μm/s.
Wall shear rates given as γ and s^{-1}.

In hemin/SnPP-IX–treated animals, the red blood cell velocity profile was found in line with the kinetics of thrombus formation, exhibiting a decrease in blood cell velocity of −24% and −31% in arterioles and venules. In contrast, velocities in hemin/CuPP-IX–treated animals decreased by only −9% (arterioles) and −10% (venules) within the first 100 seconds on ferric chloride superfusion.

To differentiate between the contribution of CO and bilirubin in delay of thrombus formation, animals with hemin-induced HO-1 induction were pretreated with SnPP-IX and Trolox. Interestingly, administration of Trolox in HO-1–blocked animals almost completely restored the delay in kinetics of thrombus growth, as observed in hemin-treated animals (Figures 4 and 5) and partly prevented the initial decrease in arteriolar and venular blood flow velocity (−16% and −7%). In line with this, topical application of cremaster muscle preparations of hemin/SnPP-IX–treated animals with bilirubin exerted antithrombogenic actions similar as observed in hemin-treated animals (Figures 4 and 5), implying that HO-1 exerts its antithrombogenic potential through the metabolite bilirubin rather than CO.

To further evaluate whether reduced P-selectin expression could be a mechanistic basis for the observed antithrombogenic actions of hemin, P-selectin–deficient mice were studied with respect to thrombus formation on ferric chloride superfusion. Thrombotic vessel occlusion was found markedly delayed in mice deficient for P-selectin expression, as given by arteriolar and venular occlusion times of 998±122 seconds and 1152±147 seconds, when compared with P-selectin–competent C57BL/6J wild-type animals (207±55 seconds and 232±63 seconds).

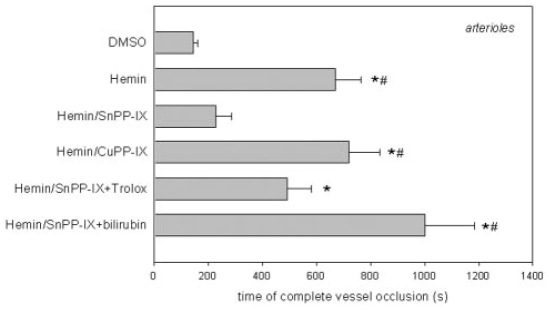

Figure 4. Time of complete occlusion of arterioles on superfusion with ferric chloride solution in animals that were treated with either DMSO, hemin, hemin/SnPP-IX, hemin/CuPP-IX, hemin/SnPP-IX+Trolox, or hemin/SnPP-IX+bilirubin. Means±SEM. *P<0.05 versus DMSO; #P<0.05 versus hemin/SnPP-IX.

Discussion

The vessel wall releases potent platelet-inhibiting substances, such as prostacyclin and nitric oxide, to limit the extent of platelet activation and thrombus formation. Better insight into the role of endogenous anti-thromboembolic substances is of major importance to improve our understanding of clinical disorders in which thromboembolic processes play a role. The current study provides, for the first time to our knowledge, in vivo evidence that microvascular thrombus formation is significantly delayed in microvessels expressing HO-1 and suggests the role of HO-1 pathway metabolites, ie, CO and bilirubin, in this scenario.

Methodological Considerations

The tool we used for induction of HO-1 was the application of hemin. This naturally occurring substrate for HO has been shown to be a potent inducer of HO-1.[7,18] In rat mesentery,

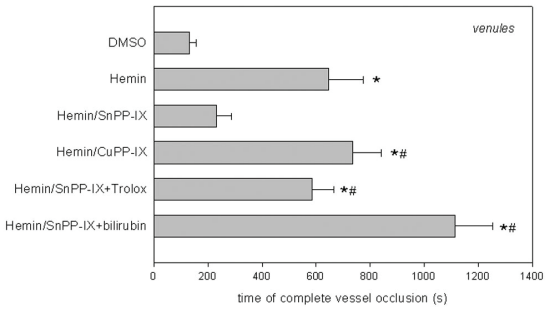

Figure 5. Time of complete occlusion of venules on superfusion with ferric chloride solution in animals that were treated with either DMSO, hemin, hemin/SnPP-IX, hemin/CuPP-IX, hemin/SnPP-IX+Trolox, or hemin/SnPP-IX+bilirubin. Means±SEM. *P<0.05 versus DMSO; #P<0.05 versus hemin/SnPP-IX.

hemin treatment was associated with a transient upregulation and a peak in the increase of HO-1 protein expression at 12 hours, followed by a recovery to the control level at 18 hours,[19] whereas at this time point hemin-treated mice of the present study exhibited marked HO-1 protein expression. Concomitantly, cremaster muscle tissue displayed strong HO-1 immunoreactivity with preferential localization in the microvascular endothelium and vascular smooth muscle cells of supplying arterioles and draining venules.

Local hemodynamics have been shown to be of major influence for blood cell–vessel wall interactions.[20] We, therefore, aimed to choose microvessels of similar diameter/size and vessel order for thrombus induction. Accordingly, calculation of microvascular wall shear rates revealed comparable disperse forces in arterioles and venules of the different groups studied. Thus, it is tenable to exclude local differences in microhemodynamics as cause for the observed differences in kinetics of thrombus formation.

Ferric chloride has originally been used to induce impairment of the blood brain barrier function. Locally released oxygen radicals caused endothelial cell disintegration with increased microvascular permeability.[21] This local endothelial cell injury supports deposition of blood cellular components and represents the ideal site for thrombus formation. In line with this, ferric chloride superfusion represents a common and widely used model, particularly to study molecular and cellular mechanisms underlying thrombosis and impaired hemostasis.[13,22–25]

Role of HO-1 in Microvascular Thrombosis

Numerous studies using HO-1 inducers or gene transfer could demonstrate that tissues expressing high levels of HO-1 are less susceptible to noxious stimuli, such as proinflammatory reagents and oxidant stress.[26–29] In line with this, animals deficient for HO-1 have chronic inflammation and enhanced sensitivity to oxidative stress.[30,31] The increased production of CO and biliverdin/bilirubin has been implicated in the attenuation of the inflammatory response. Scavenging various oxidants, biliverdin, and its reduced product bilirubin exert potent antioxidant and anti-adhesive properties.[19,32] Furthermore CO is known to increase cGMP level, to promote vasodilation, and to reduce microvascular disturbances by c-GMP–dependent and c-GMP–independent mechanisms[33,34] as well as to enhance production of antiinflammatory cytokines,[35] thereby conferring protection against tissue injury.

Among these putative actions of the HO-1 pathway products, the current study now demonstrates that microvessels expressing HO-1 become antithrombogenic and establishes a novel role of HO-1 in thrombogenesis. The observation that the marked delay of thrombus formation in hemin-treated animals is completely inhibited by SnPP-IX, but not by CuPP-IX, underscores the specificity of the HO pathway in maintenance of vessel patency. Considering that blood cell–vessel wall interactions during thrombus formation primarily involve P-selectin on activated endothelial cells, we suggest that the antithrombotic action of HO-1 is mainly related to an inhibitory action on P-selectin in the vasculature, as indicated herein by the reduced P-selectin protein expression in Western blot analysis of hemin-treated animals. This view is further underlined by a study demonstrating by the dual radiolabeled monoclonal antibody technique that pretreatment with hemin attenuated the increased P-selectin expression of endothelial cells normally elicited by lipopolysaccharide.[36] Moreover, using real-time laser confocal video microscopy, Hayashi et al were able to monitor a reduction of H_2O_2-elicited venular P-selectin expression in the hemin-treated versus the hemin-untreated mesentery.[19] Finally, experiments of the present study in P-selectin–deficient mice, demonstrating a marked delay in thrombus formation, additionally underscore the reduced P-selectin expression as a mechanistic basis for the antithrombogenic actions of hemin.

To further distinguish the roles of CO and bilirubin in this model, we studied ferric chloride-mediated thrombus induction by administration of the antioxidant Trolox in HO-1–blocked animals. This regimen significantly prolonged thrombus growth, implying that bilirubin mainly mediates the antithrombotic property of the HO pathway. In line with others,[17] we additionally examined whether direct treatment of cremaster muscle preparations with products of the HO reaction, ie, bilirubin, exerts antithrombogenic action. Interestingly, superfusion of bilirubin at a final concentration of 10 μmol/L was capable to prolong thrombotic vessel occlusion to an extent, similar to that seen in hemin-treated animals. Although it is difficult to finally assess whether direct superfusion with 10 μmol/L bilirubin equals bilirubin release in mice undergoing HO-1 induction by hemin treatment, HO-1 seems to exert its antithrombogenic potential mainly through the metabolite bilirubin.

However, besides bilirubin,[19] CO[37] also has been shown to mimic anti-adhesive properties elicited by hemin-induced HO-1 expression to an extent, which depends on the individual inflammatory stimulus used. Moreover, a recent investigation reported on the paradoxical rescue from ischemic lung injury by inhaled CO, based on its ability to derepress fibrinolysis via modulation of plasminogen activator inhibitor.[38] Thus, it is also reasonable to speculate that reduced expression of plasminogen activator inhibitor and thus limited accrual of microvascular fibrin[38] might, at least in part, account for the observed antithrombotic activity of HO-1.

In summary, vascular HO-1 with release of CO, particularly of bilirubin, attenuates thrombus formation, most probably via modulation of P-selectin expression on endothelial cells. Thus, local induction of HO-1 activity may be of preventive and therapeutic value for clinical disorders with increased risk of thrombotic events.

Acknowledgments

This study is supported by a grant from the University of Rostock (FORUN) and by a grant from the Deutsche Forschungsgemeinschaft (Vo 450/7-1 and 7-2). The authors kindly thank Berith Blendow, Dorothea Frenz, and Maren Nerowski for excellent technical assistance.

References

1. Berndt MC, Shen Y, Dopheide SM, Gardiner EE, Andrews RK. The vascular biology of the glycoprotein Ib-IX-V complex. *Thromb Haemost.* 2001;86:178–188.
2. Furie B, Furie BC. Leukocyte crosstalk at the vascular wall. *Thromb Haemost.* 1997;78:306–309.

3. Yang J, Furie BC, Furie B. The biology of P-selectin glycoprotein ligand-1: its role as a selectin counterreceptor in leukocyte-endothelial and leukocyte-platelet interaction. *Thromb Haemost.* 1999;81:1–7.
4. Palabrica T, Lobb R, Furie BC, Aronovitz M, Benjamin C, Hsu YM, Sajer SA, Furie B. Leukocyte accumulation promoting fibrin deposition is mediated in vivo by P-selectin on adherent platelets. *Nature.* 1992;359: 848–851.
5. van Hinsbergh VW. The endothelium: vascular control of haemostasis. *Eur J Obstet Gynecol Reprod Biol.* 2001;95:198–201.
6. Zakhary R, Gaine SP, Dinerman L, Ruat M, Flavahan NA, Snyder SH. Heme oxygenase-2: endothelial and neuronal localization and role in endothelium-dependent relaxation. *Proc Natl Acad Sci USA.* 1996;93: 795–798.
7. Maines MD. The heme oxygenase system: a regulator of second messenger gases. *Annu Rev Pharmacol Toxicol.* 1997;37:517–554.
8. Maines MD, Trakshel GM, Kutty RK. Characterization of two constitutive forms of rat liver microsomal heme oxygenase. Only one molecular species of the enzyme is inducible. *J Biol Chem.* 1986;261:411–419.
9. Sun Y, Rotenberg MO, Maines MD. Developmental expression of heme oxygenase isozymes in rat brain. Two HO-2 mRNAs are detected. *J Biol Chem.* 1990;265:8212–8217.
10. Ambrosio G, Tritto I, Golino P. Reactive oxygen metabolites and arterial thrombosis. *Cardiovasc Res.* 1997;34:445–452.
11. Baez S. An open cremaster muscle preparation for the study of blood vessels by in vivo microscopy. *Microvasc Res.* 1973;5:384–394.
12. Vollmar B, Schmitz R, Kunz D, Menger MD. Lack of in vivo function of CD31 in vascular thrombosis. *Thromb Haemost.* 2001;85:160–164.
13. Denis C, Methia N, Frenette PS, Rayburn H, Ullman-Cullere M, Hynes RO, Wagner DD. A mouse model of severe von Willebrand disease: defects in hemostasis and thrombosis. *Proc Natl Acad Sci USA.* 1998; 95:9524–9529.
14. Baker M, Wayland H. On-line volume flow rate and velocity profile measurements for blood in microvessels. *Microvasc Res.* 1974;7: 131–143.
15. Smith A, Alam J, Escriba PV, Morgan WT. Regulation of heme oxygenase and metallothionein gene expression by the heme analogs, cobalt-, and tin-protoporphyrin. *J Biol Chem.* 1993;268:7365–7371.
16. Amon M, Menger MD, Vollmar B. Heme oxygenase and nitric oxide synthase mediate cooling-associated protection against TNF-α-induced microcirculatory dysfunction and apoptotic cell death. *FASEB J.* 2003; 17:175–185.
17. Takamiya R, Murakami M, Kajimura M, Goda N, Makino N, Takamiya Y, Yamaguchi T, Ishimura Y, Hozumi N, Suematsu M. Stabilization of mast cells by heme oxygenase-1: an anti-inflammatory role. *Am J Physiol Heart Circ Physiol.* 2002;283:H861–H870.
18. Siow RC, Sato H, Mann GE. Heme oxygenase-carbon monoxide signalling pathway in atherosclerosis: anti-atherogenic actions of bilirubin and carbon monoxide? *Cardiovasc Res.* 1999;41:385–394.
19. Hayashi S, Takamiya R, Yamaguchi T, Matsumoto K, Tojo SJ, Tamatani T, Kitajima M, Makino N, Ishimura Y, Suematsu M. Induction of heme oxygenase-1 suppresses venular leukocyte adhesion elicited by oxidative stress: role of bilirubin generated by the enzyme. *Circ Res.* 1999;85: 663–671.
20. Sato M, Ohshima N. Effect of wall shear rate on thrombogenesis in microvessels of the rat mesentery. *Circ Res.* 1990;66:941–949.
21. Zuccarello M, Anderson DK. Protective effect of a 21-aminosteroid on the blood-brain barrier following subarachnoid hemorrhage in rats. *Stroke.* 1989;20:367–371.
22. HajMohammadi S, Enjyoji K, Princivalle M, Christi P, Lech M, Beeler D, Rayburn H, Schwartz JJ, Barzegar S, de Agostini AI, Post MJ, Rosenberg RD, Shworak NW. Normal levels of anticoagulant heparan sulfate are not essential for normal hemostasis. *J Clin Invest.* 2003;111:989–999.
23. Weiss EJ, Hamilton JR, Lease KE, Coughlin SR. Protection against thrombosis in mice lacking PAR3. *Blood.* 2002;100:3240–3244.
24. Schafer K, Konstantinides S, Riedel C, Thinnes T, Muller K, Dellas C, Hasenfuss G, Loskutoff DJ. Different mechanisms of increased luminal stenosis after arterial injury in mice deficient for urokinase- or tissue-type plasminogen activator. *Circulation.* 2002;106:1847–1852.
25. Andre P, Prasad KS, Denis CV, He M, Papalia JM, Hynes RO, Phillips DR, Wagner DD. CD40L stabilizes arterial thrombi by a β3 integrin-dependent mechanism. *Nat Med.* 2002;8:247–252.
26. Willis D, Moore AR, Frederick R, Willoughby DA. Heme oxygenase: a novel target for the modulation of the inflammatory response. *Nat Med.* 1996;2:87–90.
27. Lee PJ, Alam J, Wiegand GW, Choi AM. Overexpression of heme oxygenase-1 in human pulmonary epithelial cells results in cell growth arrest and increased resistance to hyperoxia. *Proc Natl Acad Sci USA.* 1996;93:10393–10398.
28. Abraham NG, Lavrovsky Y, Schwartzman ML, Stoltz RA, Levere RD, Gerritsen ME, Shibahara S, Kappas A. Transfection of the human heme oxygenase gene into rabbit coronary microvessel endothelial cells: protective effect against heme and hemoglobin toxicity. *Proc Natl Acad Sci USA.* 1995;92:6798–6802.
29. Otterbein LE, Kolls JK, Mantell LL, Cook JL, Alam J, Choi AM. Exogenous administration of heme oxygenase-1 by gene transfer provides protection against hyperoxia-induced lung injury. *J Clin Invest.* 1999; 103:1047–1054.
30. Wiesel P, Patel AP, DiFonzo N, Marria PB, Sim CU, Pellacani A, Maemura K, LeBlanc BW, Marino K, Doerschuk CM, Yet SF, Lee ME, Perrella MA. Endotoxin-induced mortality is related to increased oxidative stress and end-organ dysfunction, not refractory hypotension, in heme oxygenase-1-deficient mice. *Circulation.* 2000;102:3015–3022.
31. Poss KD, Tonegawa S. Heme oxygenase 1 is required for mammalian iron reutilization. *Proc Natl Acad Sci USA.* 1997;94:10919–10924.
32. Stocker R, Yamamoto Y, McDonagh AF, Glazer AN, Ames BN. Bilirubin is an antioxidant of possible physiological importance. *Science.* 1987;235:1043–1046.
33. Suematsu M, Goda N, Sano T, Kashiwagi S, Egawa T, Shinoda Y, Ishimura Y. Carbon monoxide: an endogenous modulator of sinusoidal tone in the perfused rat liver. *J Clin Invest.* 1995;96:2431–2437.
34. Wakabayashi Y, Takamiya R, Mizuki A, Kyokane T, Goda N, Yamaguchi T, Takeoka S, Tsuchida E, Suematsu M, Ishimura Y. Carbon monoxide overproduced by heme oxygenase-1 causes a reduction of vascular resistance in perfused rat liver. *Am J Physiol.* 1999;277: G1088–G1096.
35. Moore BA, Otterbein LE, Turler A, Choi AM, Bauer AJ. Inhaled carbon monoxide suppresses the development of postoperative ileus in the murine small intestine. *Gastroenterology.* 2003;124:377–391.
36. Vachharajani TJ, Work J, Issekutz AC, Granger DN. Heme oxygenase modulates selectin expression in different regional vascular beds. *Am J Physiol Heart Circ Physiol.* 2000;278:H1613–H1617.
37. Morisaki H, Katayama T, Kotake Y, Ito M, Handa M, Ikeda Y, Takeda J, Suematsu M. Carbon monoxide modulates endotoxin-induced microvascular leukocyte adhesion through platelet-dependent mechanisms. *Anesthesiology.* 2002;97:701–709.
38. Fujita T, Toda K, Karimova A, Yan SF, Naka Y, Yet SF, Pinsky DJ. Paradoxical rescue from ischemic lung injury by inhaled carbon monoxide driven by derepression of fibrinolysis. *Nat Med.* 2001;7: 598–604.

2.3 Beeinflussung der Thrombogenese durch Substanzen

Im Kontext einer möglichen therapeutischen Beeinflussung mikrovaskulärer Thrombosen durch die Behandlung mit verschiedenen Substanzen untersuchten wir zwei im Körper vorkommende Moleküle und zwei synthetisch hergestellte Verbindungen auf ihre potentiell protektiven (Ebselen, C-Peptid) bzw. vermuteten negativen (Darbepoetin-alpha, Nikotin) Eigenschaften im Rahmen der mikrovaskulären Thrombusbildung.

2.3.1 Ebselen

Ebselen, eine Selen-haltige organische Substanz mit Glutathionperoxidase-ähnlicher Aktivität, zeigt potente anti-inflammatorische und anti-oxidative Eigenschaften. Da eine diätetische Selen-Defizienz mit einer erhöhten Inzidenz an vaskulären Thrombosen assoziiert zu sein scheint, untersuchten wir die Wirkung von Ebselen auf die Ausbildung mikrovaskulärer Thrombosen in zwei Thrombosemodellen an der Cremaster-muskelpräparation der Ratte. In mit Ebselen vorbehandelten Tieren traten mikrovaskuläre Thrombosen signifikant später, als in den mit Kochsalz behandelten Kontrolltieren auf. Zusätzlich konnte in durchflusszytometrischen Analysen die H_2O_2-vermittelte Hochregulation von thrombozytärem P-Selektin und die Bildung von Thrombozyten-Leukozyten-Aggregaten durch steigende Konzentrationen an Ebselen dosis-abhängig inhibiert werden. Damit kann die von uns erstmals aufgezeigte anti-thrombogene Wirkung von Ebselen auf eine Reduktion der P-Selektin-abhängigen Zell-Zell-, in Sonderheit Thrombozyten-Leukozyten-Interaktion zurückgeführt werden. Angesichts dieses neuen Wirkprofils könnte Ebselen von hohem präventivem und therapeutischem Wert in der Behandlung von Erkrankungen sein, die mit einem erhöhten Thromboserisiko einhergehen.

Lindenblatt N, Schareck W, Belusa L, Nickels RM, Menger MD, Vollmar B
Anti-oxidant ebselen delays microvascular thrombus formation in the rat cremaster muscle by inhibiting platelet P-selectin expression *Thromb Haemost* 2003; 90: 882-892

© 2003 Schattauer GmbH, Stuttgart

Platelets and Blood Cells

Anti-oxidant ebselen delays microvascular thrombus formation in the rat cremaster muscle by inhibiting platelet P-selectin expression

Nicole Lindenblatt[1,2], Wolfgang Schareck[2], Lorenz Belusa[2], Ruth Maria Nickels[3], Michael Dieter Menger[3], Brigitte Vollmar[1]

[1]Department of Experimental Surgery, University of Rostock, Germany
[2]Department of General Surgery, University of Rostock, Germany
[3]Department of Clinical-Experimental Surgery, University of Saarland, Homburg/Saar, Germany

Summary

Ebselen, a seleno-organic compound showing glutathione peroxidase-like activity, has potent anti-inflammatory and anti-oxidant effects. Since selenium deficiency is thought to be associated with an increased incidence of vascular thrombosis, we studied the effect of ebselen on blood cell aggregate formation and vessel occlusion *in vivo*. In individual microvessels of rat cremaster muscle preparations, photochemically induced thrombus formation was analyzed in detail using intravital fluorescence microscopy. In ebselen-pretreated animals (30mg/kg ip), venular thrombus formation was significantly delayed (50% vessel occlusion: 535±34s; initial stasis: 872±82s; complete occlusion: 908±87s) as compared to vehicle-treated controls (416±42; 612±49; 647±51). Moreover, ebselen significantly prolonged the kinetics of arteriolar thrombus formation and even completely prevented blood cell aggregate and thrombus formation in 88.9% of all arterioles studied ($p<0.05$ vs controls: 37.5%). Antithrombotic properties of ebselen could also be observed in a model of ferric chloride-induced microvascular thrombosis, with a low dose (5mg/kg ip) being as effective as a high dose pretreatment (30mg/kg ip). As assessed by flow cytometry of platelet P-selectin immunfluorescence, whole blood isolated from ebselen-treated animals revealed a significantly lower fraction of P-selectin expressing platelets when compared with that of DMSO-treated controls. In addition, oxidant stress-induced upregulation of P-selectin on isolated platelets was found dose-dependently inhibited by increasing concentrations of ebselen (10-100µM). Moreover, ebselen dose-dependently inhibited H_2O_2-induced platelet-leukocyte aggregate formation in whole blood *in vitro*, suggesting that the anti-thrombotic effect of ebselen is achieved by attenuation of P-selectin dependent platelet-leukocyte aggregation. Thus, ebselen represents preventive and therapeutic value for disorders with increased risk for oxidant stress-associated thrombotic events.

Keywords

Thrombosis, platelet, leukocyte, fluorescence microscopy, flow cytometry, oxidant stress

Thromb Haemost 2003; 90: 882–92

Introduction

Despite the advances in medical science, thrombosis is still an exceptionally clinically relevant problem. In the past, a relationship between low serum selenium concentrations and increased risk of death from acute coronary heart disease and from myocardial infarction has been suggested (1-3). In addition, low platelet glutathione peroxidase activity is frequently observed in those cohorts of patients (4, 5). Selenium forms the catalytic site of the enzyme glutathione peroxidase. As a consequence, low glutathione peroxidase activities are usually associated with a low nutritional selenium status (6, 7). Since glutathione perox-

Correspondence to:
Brigitte Vollmar M.D.
Department of Experimental Surgery
University Rostock
Schillingallee 70
18055 Rostock
Germany
Tel.: +49 381 494 6220 or 6221, Fax: +49 381 494 6222
E-mail: brigitte.vollmar@med.uni-rostock.de

Received September 18, 2002
Accepted after revision July 10, 2003

Financial support:
This study is supported by a grant from the University of Rostock (FORUN) and by a grant from the Deutsche Forschungsgemeinschaft (Vo 450/7-1).

DOI: 10.1160/TH02-09-0093

ide enzymes protect cells against peroxidation and control concentrations of intracellular peroxides, selenium deficiency may result in an increased susceptibility to oxidant stress-induced events, such as intravascular thrombus formation.

Among the various factors that affect thrombus formation the behavior of platelets, in particular their aggregation, adhesion and thrombogenesis, are of utmost importance in the pathogenesis of thrombosis. Nonetheless, the fact that glutathione peroxidase activity in platelets is particularly high (8, 9), the maintenance/preservation of this endogenous anti-oxidant capacity might substantially account for the physiological defense against thrombotic cell aggregation. In line with this, *in vitro* studies reported reduced platelet release of proaggregatory thromboxane A_2 with unaffected biosynthesis of prostacyclin upon oral selenium (sodium selenite) administration to normal volunteers and suggested that selenium dietary supplementation should be considered in the prevention of vascular thrombosis (10, 11).

Ebselen (2-phenyl-1,2-benzoisoselenazol-3-(2H)-one) is a non-toxic seleno-organic drug that has been extensively studied during the last decade. A substantial part of the pharmacological profile of ebselen appears to be due to its unique anti-oxidative properties by scavenging organic hydroperoxides, thus, mimicking glutathione peroxidase activities. Ebselen actually inhibits a number of enzymes involved in inflammation such as lipoxygenases, nitric oxide synthases, NADPH oxidase, protein kinase C and H^+/K^+-ATPase (12), and suppresses inflammation in several animal models. Moreover, ebselen has recently been under active investigation as a neuroprotective agent in clinical trials (13, 14). The anti-inflammatory mechanism of ebselen action might further be linked to an inhibitory effect on the inositol (1, 4, 5)-trisphosphate (IP3)-induced calcium release with prevention of cell activation (15). Though this modulation of intracellular calcium homeostasis has been suggested to be responsible for *in vitro* inhibition of platelet aggregation by ebselen (16), little is known about its anti-thrombotic activity *in vivo*. The mechanistic aspect of ebselen as a protective agent in events responsible for vascular thrombosis remains fully elucidated and is the topic of this study. Here we report *in vitro* and *in vivo* observations on the effect of ebselen on platelet function, documenting anti-thrombotic properties in association with a dose-dependent inhibition of P-selectin expression.

Materials and methods

Animal model

Upon approval by the local government, all experiments were performed in accordance with the German legislation on protection of animals and the National Institutes of Health "Guide for the Care and Use of Laboratory Animals" (Institute of Laboratory Animal Resources, National Research Council). Male Sprague-Dawley rats with a body weight (bw) of 200-250 g were anesthetized by an intra-peritoneal injection of pentobarbital (50mg/kg bw) and placed in supine position on a heating pad (36-37°C). Tracheotomy was performed to facilitate spontaneous breathing and to ensure a clear airway. A polyethylene catheter in the right jugular vein served for application of fluorescent dyes.

Rat cremaster muscle preparation

For the study of vascular thrombus formation following ebselen treatment we used the opened cremaster preparation, as originally described by Baez (17). A midline incision of the skin and fascia was made over the ventral aspect of the left scrotum and extended up to the inguinal fold and to the distal end of the scrotum. The incised tissues were retracted to expose the cremaster muscle sack which was maintained under gentle traction to carefully separate the remaining connective tissue by blunt dissection from around the cremaster sack. Then, the cremaster muscle was incised, making sure not to cut the larger anastomosing vessels. Hemostasis was achieved with 5-0 threads serving also to spread the tissue. After dissection of the vessel connecting the cremaster and the testis, the epididymus and testis were put to the side of the preparation. The preparation was performed on a transparent pedestal to allow microscopic observation of the cremaster muscle microcirculation by both transillumination and epi-illumination techniques.

After iv injection of 0.2 ml 5% fluorescein isothiocyanate (FITC)-labelled dextran (MW 150000, Sigma Chemical Co., St. Louis, MO) and subsequent circulation for 30 sec, photochemical thrombus formation was induced by continuous local exposure of filtered light (450-490 nm) from the 100W high pressure mercury lamp and a x63 water immersion objective (Zeiss, numerical aperture 0.9) to the individual microvessels, as described previously (18, 19). Light exposure was discontinued after blood flow in the vessel ceased for at least 60 sec due to complete vessel occlusion. Times necessary for thrombus formation depends on the thickness of the cremaster muscle. Thus, the thinner muscle in mice (19) offers better energy transmission of light and results in faster thrombus formation, when compared with the corresponding times necessary for complete vessel occlusion in rat cremaster muscle.

In an additional series of experiments (n=13), the cremaster muscle preparations were superfused with ferric chloride (250mM; Sigma) for induction of microvascular thrombosis, as described by others (20). This model is not based on thrombus induction by light and, thus, allows the study of anti-thrombotic effects of ebselen regardless its potential light-absorbing property. Using the model of ferric chloride superfusion for induction of microvascular thrombosis, animals received either a high dose (30mg/kg ip; n=5) or low dose of ebselen (5mg/kg ip; n=4).

Intravital fluorescence microscopy

Microcirculatory parameters were analyzed by intravital fluorescence microscopy using the Leitz Orthoplan microscope and the x63 water immersion objective. The microscopic procedure was performed at a constant room temperature of 21-23°C. Contrast enhancement for visualization of the rat cremaster microcirculation was provided by FITC-dextran, while leukocyte flow dynamics and leukocyte-endothelial cell interactions were studied after *in vivo* staining with rhodamine 6G (MW 476, Sigma; 2µmol/kg iv). The epi-illumination setup included a 100 W HBO mercury lamp and a Ploemo-Pak illuminator equipped with an I_2 blue filter (450nm/>515nm excitation/emission wavelengths) and a N_2 green filter (530-560nm/>580nm). Microscopic images were recorded by a charge-coupled device video camera (CF8/1 FMC, Kappa GmbH, Gleichen, Germany) and stored on videotapes for off-line evaluation.

Microcirculation analysis

Kinetics of platelet-leukocyte aggregation with intravascular thrombus formation, i.e. change of inner luminal vessel diameter due to platelet and/or leukocyte adherence to the endothelium of the vessel wall, and microcirculatory parameters were quantified off-line by analysis of the videotaped images using a computer-assisted image analysis system (CapImage, Zeintl Software, Heidelberg, Germany). Analysis included the following parameters: thrombus formation with determination of the time periods until (i) first cell deposition (platelets, leukocytes) was observed along the endothelial lining, (ii) the inner diameter of the microvessel was reduced to 50% by the growing thrombus, (iii) initial occurrence of stasis (at least 5 sec duration) and (iv) sustained cessation of blood flow due to vessel occlusion. The time for thrombus growth was calculated as the difference between the time until flow cessation and the time until first cell deposition. Microcirculatory analysis further included the determination of (i) vessel diameters before and after thrombus induction as well as (ii) vascular wall shear rates, based on the Newtonian definition γ=8xV/D (V represents the red blood cell centerline velocity divided by 1.6 according to the Baker-Wayland factor (21) and D represents the individual inner vessel diameter).

Experimental design

Prior to induction of anesthesia, seven animals were treated with ebselen (30mg/kg bw ip; Sigma), which was dissolved in DMSO at a final concentration of 12mg/ml and kept frozen at -20°C until usage. Control animals (n=7) were treated with equivalent volumes of DMSO ip. At the end of the cremaster muscle preparation, the animals were allowed to recover from surgical preparation for 15 min. Then, photochemical induction of thrombus formation was performed in randomly chosen venules (n=3-8 per animal) and arterioles (n=1-3 per animal). Microcirculatory parameters were measured in identical microvessels prior to thrombus induction (baseline), during thrombus formation, and at the end of vessel occlusion.

Using the model of ferric chloride thrombus formation, four animals received ebselen at a low dose of 5mg/kg and five animals at the high dose of 30mg/kg ip. Control animals were treated with equivalent volumes of DMSO ip (n=4). In these animals left and right cremaster muscles were prepared and superfused with ferric chloride. Rapid spreading of ferric chloride allowed the study of only 1-2 arterioles and venules within each preparation.

Human blood collection and PRP preparation

Blood from healthy volunteers was drawn from the left cubital vein with a 21-gauge needle into 5 ml S-Monovettes 9NC (Sarstedt, Nümbrecht, Germany) (1:10 citrate v/v). After centrifugation for 15 min at 110g and room temperature, platelet rich plasma was transferred in a separate tube. Platelet count was assessed with a Coulter ACT diff Analyzer (Coulter Electronics, Luton, UK) and adjusted to $4x10^8$/ml by dilution with phosphate-buffered saline (PBS). In parallel, aliquots of whole blood were processed for the flow cytometric study of H_2O_2-induced platelet-leukocyte aggregates (see below).

Platelet exposure to hydrogen peroxide and flow cytometric analysis of P-selectin expression

After 30 min of resting in a 37°C water bath, platelets were incubated with increasing amounts of ebselen (10-100µM, dissolved in DMSO) for 5 min followed by exposure to 0.05% H_2O_2 for additional 15 min. Then, platelets were rapidly cooled on ice, diluted with 1 ml 4°C-cold 1% paraformaldehyde in PBS (Cell Fix; Becton Dickinson, Heidelberg, Germany). This was necessary because platelets maintained at room temperature recover from oxidant-induced stimulation. After fixation, platelets were centrifuged at 300g for 4 min at 4°C and washed a second time with PBS. Supernatant fraction was decanted and the platelet pellet was resuspended in PBS for flow cytometry. Platelets, which were incubated with corresponding volumes of DMSO, served as controls and were handled in an identical manner. In an additional set of experiments, catalase (1000U/ml; Sigma) was administered instead of ebselen in order to confirm the oxidant stress induced by H_2O_2.

Expression of P-selectin on platelets was investigated by direct immunofluorescence using a monoclonal anti-human fluorescein-isothiocyanate (FITC)-coupled P-selectin antibody (Ancell Corporation, Bayport, MN, USA), diluted 1:50 (v/v) with staining medium (0.1% sodium azide and 2% fetal calf serum in PBS). A FITC-coupled IgG_1 isotype-matched control antibody (Ancell) was used to exclude unspecific binding. 50µl of fixed platelet suspensions were incubated with saturating amounts (80µl) of diluted FITC-labelled monoclonal anti-human P-selectin antibody or isotype-control antibody for 30

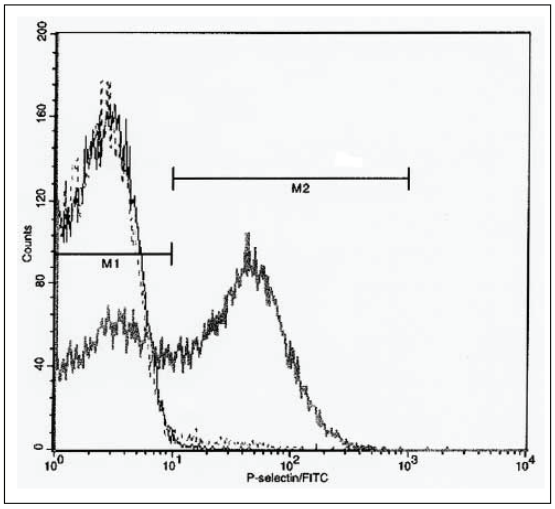

Figure 1: Flow cytometric analysis of P-selectin expression on human platelets, as assessed by FACS analysis of platelet rich plasma (PRP). Histogram plots of FITC-fluorescence signal (FL1) of a negative (*dashed line*; FITC-IgG isotype matched control antibody) and a positive control (*solid thin line*, FITC-labelled anti-P-selectin antibody) of unstimulated/resting platelets as well as of a positive control (*solid thick line*, FITC-labelled anti-P-selectin antibody) of platelets after addition of 0.05% H_2O_2. Fraction of cells within the markers of M2 represent the positive P-selectin expressing platelets (~56%)

min at room temperature in the dark. After incubation, the cells were washed twice with 0.1% sodium in PBS (Cell Wash, Becton Dickinson) to remove excess of antibody. Flow cytometry was performed within the next hour.

FACScan flow cytometer (Becton Dickinson) was calibrated with fluorescent standard microbeads (CaliBRITE Beads, Becton Dickinson) for accurate instrument setting. Platelets were identified by their characteristic forward and sideward scatter light and selectively analysed for their fluorescence properties using the CellQuest data handling program (Becton Dickinson) with assessment of 30,000 events per sample. The relative fluorescence intensity of a given sample was calculated by subtracting the signal obtained when cells were incubated with the isotype specific control antibody from the signal generated by cells incubated with the test antibody (Fig. 1).

Whole blood exposure to hydrogen peroxide and flow cytometric analysis of platelet-leukocyte aggregates

Whole blood aliquots of 50µl were incubated for 25 min with 5µl of a monoclonal anti-human FITC-coupled CD42b antibody (eBioscience, San Diego, CA, USA) and with 5µl of a monoclonal anti-human phycoerythrin (PE)-coupled CD45 antibody (eBioscience). Then, aliquots were incubated with increasing amounts of ebselen (10-200µM, dissolved in DMSO) for 5 min, followed by exposure to 0.025% H2O2 for additional 15 min. Subsequently, erythrocytes were lysed in 1.5 ml of Lysing Solution (Becton Dickinson) for 25 min. The reaction was stopped by diluting the solution with 2 ml of PBS, followed by centrifugation at 400 g for 5 min. The aliquots were washed again with PBS and the pellet was resuspended with 2 ml Cell Fix. Flow cytometry was performed within the next two hours, as described above.

Rat blood collection and platelet isolation for flow cytometric analysis of P-selectin expression

To study whether ebselen modulates platelet P-selectin expression, ebselen (30mg/kg ip)- and DMSO-pretreated control animals were exsanguinated by cardiac puncture (1:10 citrate v/v). After centrifugation for 15 min at 110g and room temperature, platelet rich plasma was transferred in a separate tube and allowed to rest in a 37°C water bath for 30 min. Platelet count was assessed with a Coulter AC.T diff Analyzer (Coulter Electronics, Luton, UK) and adjusted to $4x10^8$/ml by dilution with phosphate-buffered saline (PBS). After fixation for 5 min in 1 ml 4°C-cold 1% paraformaldehyde in PBS, platelets were centrifuged at 300g for 4 min at 4°C, washed again with PBS and the pellet was resuspended in 50 µl PBS. Platelets were incubated for 40 min in the dark with 1.5 µl of a monoclonal FITC-coupled anti-human P-selectin antibody, showing rat cross reactivity (LYP20; Biocytex, Marseille, France). A FITC-coupled IgG1 isotype matched control antibody was used to exclude unspecific binding. Then, platelets were washed twice with PBS, resuspended in 1 ml Cell Fix and measured by flow cytometry within the next two hours, as described above.

Plasma levels of selen

At the end of the *in vivo* experiments, arterial blood samples of ebselen (30mg/kg) or DMSO-treated animals were withdrawn for subsequent analysis of selen using atomic absorption spectrometry.

Statistical analysis

Data are presented as mean±SEM. After testing for normal distribution, ANOVA was followed by appropriate pairwise comparison (Student´s *t*-test) including Bonferroni correction. Chi-square-test was used for statistical analysis of incidence of arteriolar thrombus formation. Dependency between time of light exposure and thrombus growth was analyzed using Pearson product moment correlation. P values less than 0.05 were taken to indicate statistical significance. Statistics were performed using the software package SigmaStat Version 1.0 (Jandel Corporation, San Rafael, CA, USA).

Table 1: Kinetics of thrombus formation, i.e. first plaque formation, half diameter reduction, as well as initial and sustained cessation of blood flow, in arterioles of rat cremaster muscle preparations of either DMSO- (number of animals=7; number of vessels with thrombus growth=5) or ebselen-pretreated animals (number of animals=7; number of vessels with thrombus growth=1). Mean±SEM

	First plaque (sec)	Half diameter (sec)	Initial stasis (sec)	Sustained stasis (sec)
DMSO	326±76	710±104	987±215	1543±231
ebselen	1070	1208	1984	2090

Results

In vivo analysis of kinetics of light-dye induced thrombus formation

Baseline microhemodynamics did not differ between cremaster muscle preparations of ebselen- and DMSO-pretreated controls with physiological values of capillary diameter and functional capillary density as well as blood flow velocities in venules and arterioles (5-7 μm; 150-300 cm/cm^2; 200-500 μm/sec and >800 μm/sec).

Photoactivation of intravascular FITC-dextran with high doses of light induced the formation of platelet thrombi which in most cases grew circumferentially on the entire vessel wall (Fig. 2). Thrombi were confined to the exposed fields. Unless otherwise stated, photoactivation-induced thrombus formation ultimately resulted in vessel occlusion to blood flow. In most cases, flow might resume after a short initial occlusion and then later occlude irreversibly.

In cremaster preparations of DMSO-pretreated control animals, light exposure to venules resulted in first cell deposition at the endothelial lining after a time period of 230±31 sec. Vessel lumen was found reduced to 50% after 416±42 sec due to thrombus growth. Persistent narrowing of inner and outer vessel diameter could not be observed and did not affect the 50% diameter criterium of thrombus formation. Venular blood flow ceased for the first time at 612±49 sec after onset of epi-illumination with sustained occlusion at 647±51 sec (Figs. 2, 3).

In general, thrombus development in arterioles was less rapid in comparison to venules (Fig. 4). In controls, 50% vessel occlusion occurred at 710±104 sec (Table 1). While thrombus growth caused first cessation of blood flow in arterioles after 987±215 sec, complete thrombotic occlusion could be observed after 1543±231 sec (Table 1).

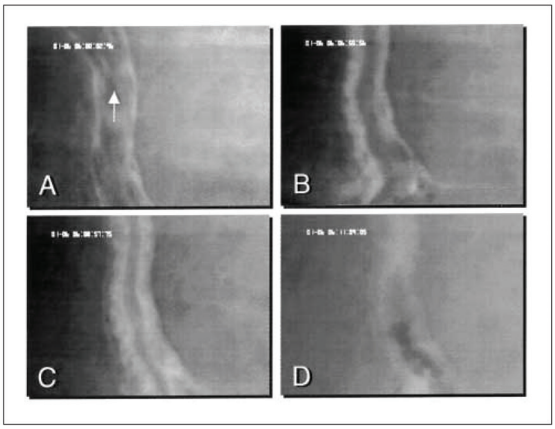

Figure 2: Intravital microscopic images of a postcapillary venule within the rat cremaster muscle preparation of a DMSO-treated control animal before (A) and during photoactivation-induced thrombus formation (B-D). After iv administration of FITC-dextran and blue-light epi-illumination, note the initially patent venule (A, arrow indicates direction of blood flow) as well as the circumferentially located cell deposits with inner luminal diameter reduction to ~50% (B) and ~75% (C), finally resulting in complete vessel occlusion after 669 sec (D). Magnification x350.

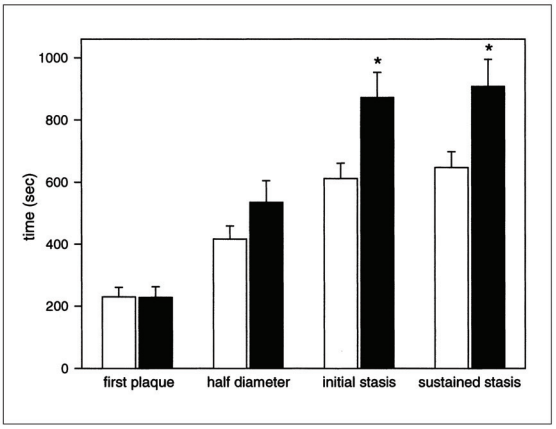

Figure 3: Kinetics of thrombus formation, i.e. first plaque (cell deposit) formation, half diameter reduction as well as initial and sustained cessation of blood flow, in venules of rat cremaster muscle preparations of either DMSO- (open bars; number of animals=7; number of vessels studied=22) or ebselen-treated animals (closed bars; number of animals=7; number of vessels studied=25). Mean±SEM; * $p<0.05$ vs DMSO

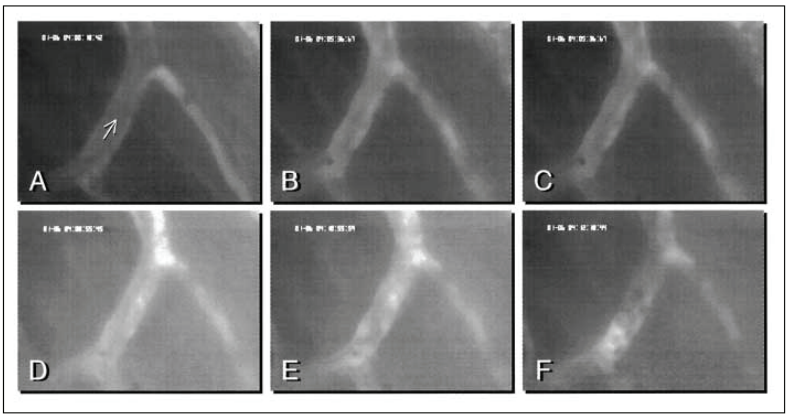

Figure 4: Intravital microscopic images of an arteriole within the cremaster muscle preparation of a DMSO-treated rat before (A) and during photoactivation-induced thrombus formation (B-F). After iv administration of FITC-dextran and blue-light epi-illumination, note the initially patent arteriole (A, arrow indicates direction of blood flow), as well as the steadily increasing adherent cell aggregate (B-E), finally resulting in complete vessel occlusion (F). Magnification x350.

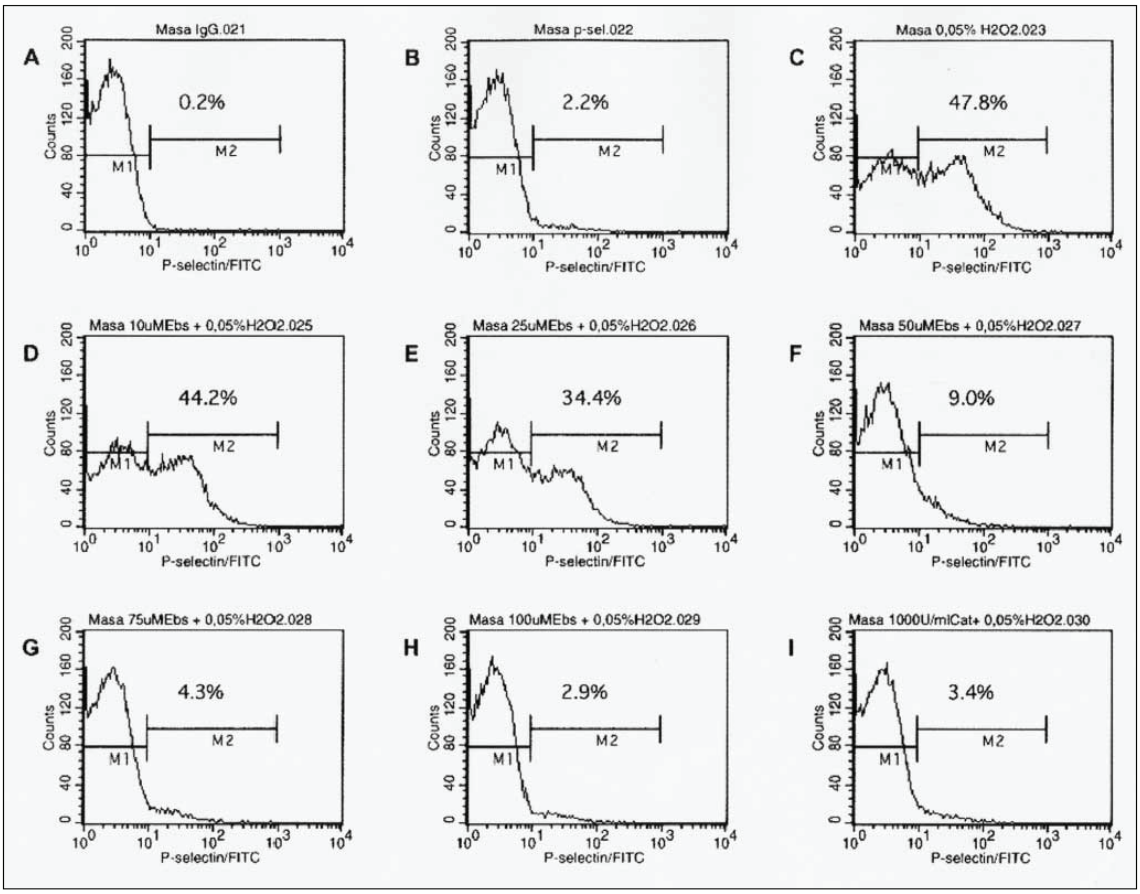

Figure 5: Flow cytometric analysis of P-selectin expression on human platelets exposed to 0.05% H_2O_2 (C) and additionally incubated with increasing amounts of ebselen (10-100µM) (D-H). Note the dose-dependent reduction of platelet P-selectin expression with almost abrogation at 100µM ebselen. Specificity of H_2O_2-induced platelet P-selectin expression was confirmed by its abrogation using catalase (1000U/ml; I). Histogram plots of (A) and (B) represent the negative and positive control of identical platelet preparations without H_2O_2-exposure.

Effect of ebselen on kinetics of light-dye induced thrombus formation

Atomic absorption spectometry for analysis of selen revealed high concentrations of 2.40±0.63mg/l in ebselen-treated animals ($p<0.05$ vs DMSO: 0.31±0.04 mg/l). The effect of ebselen on photoactivation-induced thrombotic occlusion of venules is illustrated in figure 3. While ebselen did not affect the time at which thrombus growth was initiated (228±34 sec vs DMSO: 230±31 sec), ebselen caused a significant prolongation of time necessary to occlude the vessel lumen. Venules in cremaster muscle preparations of ebselen-treated animals required 872±82 sec of continuous photoactivation/epi-illumination for initial occurrence of perfusion standstill ($p<0.05$ vs DMSO; Fig. 3). Sustained venular stasis at 908±87 sec was found significantly longer than in venules of DMSO-pretreated animals ($p<0.05$; Fig. 3).

The antithrombotic effect of ebselen was even more evident in arterioles. The incidence of persistent arteriolar patency upon continuous epi-illumination was found to be significantly ($p<0.05$) higher in ebselen- (88.9%) versus DMSO-pretreated animals (37.5%; Fig. 4). In addition, thrombus growth in the one arteriole, in which cell deposition could be induced, was markedly delayed when compared with the time course of arteriolar thrombus growth of DMSO-pretreated animals and finally occluded the vessel at 2090 sec of photoactivation (Table 1).

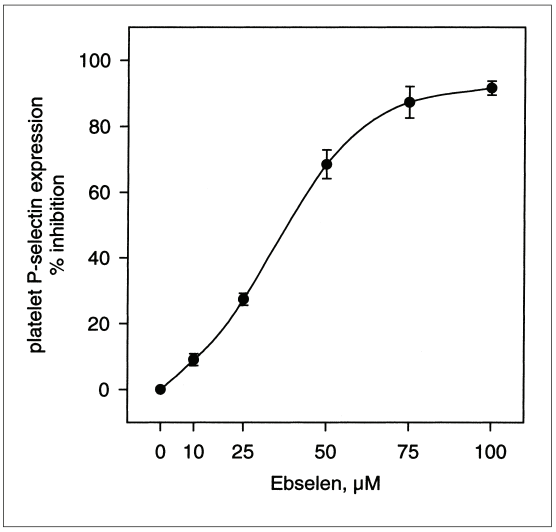

Figure 6: Quantitative analysis of the effect of ebselen on H_2O_2-induced platelet P-selectin expression, as assessed by flow cytometry using a FITC-labelled anti-P-selectin antibody (n=6 independent experiments). Inhibition of P-selectin expression is calculated compared to control values of platelets without ebselen (100%). More detailed information is given in materials and methods.

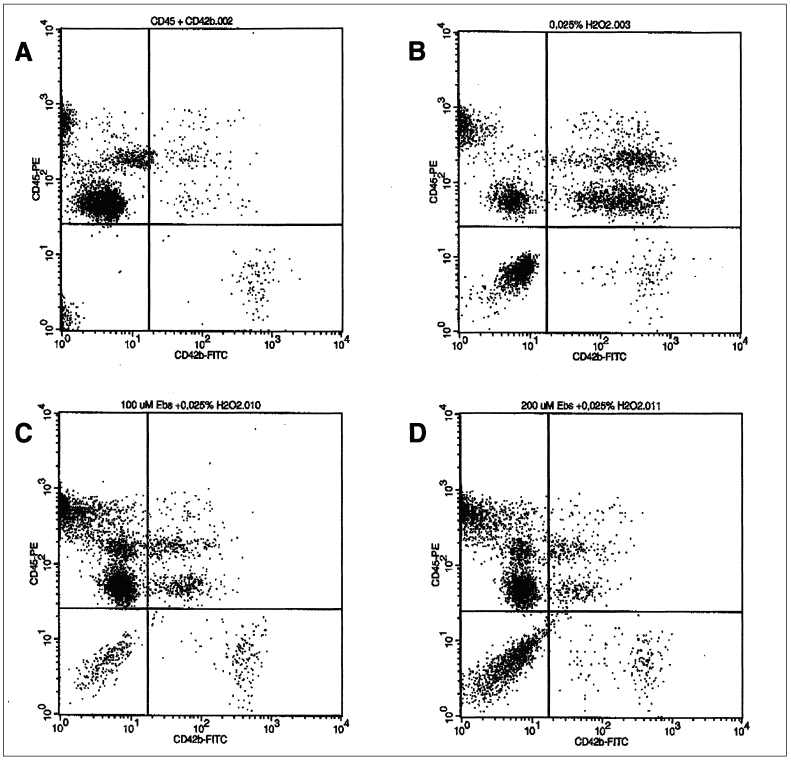

Figure 7: Flow cytometric analysis of platelet-leukocyte aggregate formation (upper right quadrant) in whole human blood without stimulation (A) and upon exposure to 0.025% H_2O_2 (B). Note the increase of platelet-leukocyte aggregate formation upon oxidative stress (B), which was found markedly reduced upon incubation with 100µM (C) and 200µM ebselen (D). Direct immunfluorescence of platelet-leukocyte aggregates was assessed by use of a FITC-coupled CD42b antibody (x-axis of dot blot) and a PE-coupled CD45 antibody (y-axis of dot plot). More detailed information is given in materials and methods

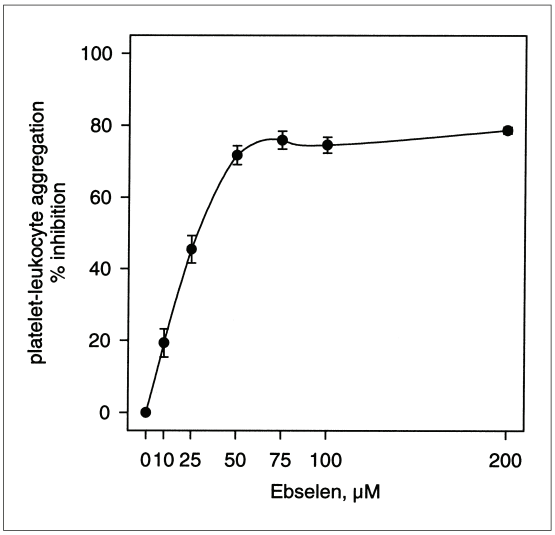

Figure 8: Quantitative analysis of the effect of ebselen on H_2O_2-induced platelet-leukocyte aggregate formation in whole blood, as assessed by flow cytometry using a FITC-coupled CD42b antibody and a PE-coupled CD45 antibody (n=9 independent experiments). Inhibition of platelet-leukocyte aggregate formation is calculated compared to control values of H_2O_2-exposed whole blood without ebselen (100%). More detailed information is given in materials and methods.

Flow cytometric analysis of blood samples from DMSO-pretreated animals revealed a significantly ($p<0.001$) higher fraction of P-selectin expressing platelets (5.24±0.44%) when compared to those of ebselen-pretreated animals (1.98±0.26%), underlining the capability of ebselen to dampen platelet P-selectin expression.

Effect of ebselen on ferric chloride-induced thrombus formation

In DMSO-treated controls, ferric chloride superfusion of cremaster muscle microvessels caused a complete occlusion of venules within 258±45 sec, while thrombotic occlusion of venules was significantly delayed in animals which received ebselen (5mg/kg: 437±81 sec, $p<0.05$ vs DMSO; 30 mg/kg: 511±64 sec, $p<0.01$ vs DMSO). Comparably, occlusion times of arterioles were found significantly longer in ebselen-pretreated animals (5mg/kg: 549±106 sec, $p<0.05$ vs DMSO; 30 mg/kg: 536±100 sec, $p<0.01$ vs DMSO) when compared to those in DMSO-pretreated controls (245±43 sec).

In vitro analysis of platelet P-selectin expression

Exposure of platelets with 0.05% H_2O_2 increased the fraction of P-selectin expressing platelets from 3.2±1.2% at baseline to 50.3±6.7% (Fig. 5). Ebselen treatment of platelets dose-dependently reduced H_2O_2-induced upregulation of P-selectin expression on platelets with 50 µM ebselen causing a downregulation of approximately 70% and 100µM ebselen abrogating platelet P-selectin expression to almost resting (baseline) conditions (Figs. 5, 6). P-selectin expression upon incubation of platelets with H_2O_2 was completely inhibited by 1000U/ml catalase (12.3±3.8% of baseline), indicating that P-selectin expression is caused by H_2O_2-induced oxidant stress. Exposure of unstimulated platelets with increasing amounts of DMSO (vehicle of ebselen) did not affect P-selectin expression and was found in the range as untreated platelets from PRP (<5% P-selectin expressing platelets). Moreover, catalase alone (1000U/ml) had no effect of P-selectin expression with a fraction of 4.1±1.3% P-selectin positive platelets.

In vitro analysis of platelet-leukocyte aggregates

Exposure of whole blood with 0.025% H_2O_2 increased the fraction of platelet-leukocyte aggregates from 5.0±1.0% at baseline to 33.8±2.1% (Fig. 7). Ebselen treatment of whole blood dose-dependently reduced H_2O_2-induced formation of platelet-leukocyte aggregates after addition of increasing concentrations of ebselen (10-200µM; Figs. 7, 8). Differentiation between the leukocyte subpopulations revealed that granulocytes, but in particular monocytes formed aggregates with platelets, while the fraction of lymphocytes within these aggregates was negligible.

Discussion

The major finding of this study is that ebselen provides significant *in vivo* anti-aggregatory and anti-thrombotic potential against thrombotic vessel occlusion in venules and, in particular, in arterioles. Quantitative on-line methods have been used to demonstrate *in vivo* the marked delay in intravascular thrombus growth upon ebselen pre-treatment. This finding is further corroborated by the fact that whole blood from ebselen-pretreated animals revealed a significantly lower fraction of P-selectin expressing platelets when compared to that of DMSO-pretreated controls. In parallel, experiments on isolated platelets and whole blood *in vitro* demonstrated that these anti-thrombotic properties of ebselen reside in a dose-dependent inhibition of oxidant stress-induced P-selectin expression and blockade of P-selectin-dependent platelet-leukocyte aggregate formation.

Methodological remarks

In the present study, thrombus formation was initiated by a photochemical reaction which was induced by transmural blue light exposure and intravenous administration of FITC-dextran. Previous experiments have shown that neither FITC-labeled dyes (22) nor light (23) alone had a discernable effect on microvascular blood flow and microvessel dimensions, thus, imply-

ing that the interaction of light and fluorochrome is necessary for thrombus formation. The phototoxicity of the fluorescently labeled agent is known to cause endothelial injury, as indicated by electron microscopy, demonstrating abundant cytoplasmic vacuolisation, cell membrane damage and interrupted endothelial cell contacts to the basal lamina (18). As a consequence, blood cells adhere to the injured vessel wall, followed by aggregation of platelets and leukocytes and, finally, thrombotic vessel occlusion (18, 24-26).

The fact that ebselen as an antioxidant prevented arteriolar thrombus formation and reduced venular thrombus growth might be related to a reduced damage of the endothelium and, therefore, model specific. To disprove this concern, we applied ebselen in an alternative model of ferric chloride-induced microvascular thrombus formation, which is not primarily based on oxidant stress-induced endothelial damage (20). Ebselen again proved to be efficient to delay thrombus formation, underlining the unique anti-thrombotic property of ebselen.

The seleno-organic compound ebselen exhibits various pharmacological activities. While selenium compounds such as selenite, selenium dioxide, and diselenides exhibit toxicity, the toxicity of ebselen has been shown to be extremely low as metabolism of the compound does not liberate the selenium moiety (12). Thus, safety and tolerability of ebselen are good. The dose of ebselen was chosen in accordance to a report of Haddad et al. in rats (27). Since this dosage is rather high when compared with clinical use of ebselen, i.e. 300mg per 70-kg patient (14), we additionally tested the effect of ebselen at a dosage of 5mg/kg.

Ebselen concentrations *in vitro* (10-100 μM) were chosen as follows: With the assumption of complete absorption of 30mg/kg, ebselen concentration in vivo would be ~0.54μg ebselen per one million circulating platelets. In parallel, 75μM ebselen in vitro equals ~0.51μg ebselen per one million platelets *in vitro*. Thus, the concentration range of 10-100 μM of ebselen *in vitro* ideally covers the estimated concentrations of ebselen *in vivo*.

Effect of ebselen on kinetics of thrombus formation

To determine the potential of a glutathione peroxidase mimick in the prevention of microvascular thrombosis, we investigated the effect of ebselen pretreatment on photochemically induced thrombus formation. While ebselen did not affect the first cell deposition in venules, it tended to delay the time necessary for 50% vessel occlusion and significantly prolonged the development of both initial and sustained stasis of venular blood flow. Most strikingly, ebselen effectively inhibited the entire process of thrombus formation in arterioles with an enormous high fraction of vessels remaining patent despite the continuous light/dye exposure.

In thrombus formation associated with hemostasis or thrombotic disease, blood platelets first undergo a rapid transition from a circulating to an adherent state, followed by activation and aggregation. This process potentially involves platelet-platelet, platelet-endothelium, platelet-subendothelial matrix and platelet-leukocyte interactions, a variety of mediators and specific adhesion molecules (28-30). Among the latter, the expression of P-selectin on the platelet surface following platelet stimulation and alpha granule secretion allows for interaction of P-selectin with ligands on other cells, particularly leukocytes and monocytes. It has been shown in an *ex vivo* baboon model that leukocyte accumulation within a thrombus growing on a Dacron graft is mediated by P-selectin on adherent platelets (31). These results underscore that leukocytes are bound via specific adhesion molecules rather than mechanically trapped within the fibrin clot. The prothrombotic role of P-selectin is further given by the fact that P-selectin induces synthesis of tissue factor in monocytes (32) and tissue factor is critical for the activation of blood coagulation. Moreover, the observation of prolonged bleeding times in P-selectin deficient mice matches the view that P-selectin is essentially involved in the process of thrombogenesis (33).

While P-selectin does not mediate platelet-platelet interaction, P-selectin provides an anchoring source for leukocytes on activated platelets and, may thus play a very important role in determining the size and stability of the platelet aggregates in the developing thrombus (34). When activated by agonists, platelets are known to produce oxidant species including H_2O_2 by themselves (35) and to stimulate generation of oxidant species in neutrophils and monocytes by a mechanism that requires mutual cell-cell-contact and the presence of P-selectin on the platelet surface. Reactive oxidant species in turn rapidly inactivate nitric oxide, an endothelial product which inhibits platelet activation and aggregation (36). Thus, increased production and/or impaired metabolism of oxidant species predisposes to thrombotic disorders.

Our present observation on the dose-dependent reduction of H_2O_2-induced P-selectin expression on isolated platelets by ebselen *in vitro* is in line with its anti-thrombotic activity *in vivo*. It is conceivable to suggest that by exerting antioxidant capacity as glutathione peroxidase mimick ebselen limits oxidative stress and its sequelae, i.e. vascular injury, cell activation with adhesion molecule expression and cell-cell contact (10). Beside the scavenging function, the inhibition of the IP_3-induced calcium release by ebselen (16) may account for the herein reported action of ebselen in reducing platelet P-selectin expression, since secretion of granules with outward translocation of the P-selectin residues requires activation of protein kinase C and elevation of intracellular Ca^{2+} (37). Thus, platelets with limited or even absent P-selectin expression may not represent an ideal nidus where leukocytes accumulate within the developing thrombus (38). This view is supported by the

present finding that increasing amounts of ebselen significantly reduced the H_2O_2-induced platelet-leukocyte aggregate formation. Reduced tissue factor synthesis due to limited P-selectin expression (32) might further contribute to the delay of thrombotic vessel occlusion, as observed in ebselen-pretreated animals.

The finding that ebselen exerted a more pronounced antithrombotic effect in arterioles than in venules can be attributed to different reactions of arterioles and venules to light/dye exposure, as indicated by Sato and Oshima (39) or to different antiaggregatory and pro-aggregatory substances released by arteriolar as opposed to venular endothelium (40). Ebselen has been demonstrated to inhibit biosynthesis of thromboxane A_2 and lipoxygenase products, but not of prostacyclin in both endothelial cells and platelets (10). Because endogenous nitric oxide and prostaglandins synergistically counteract ongoing thromboembolism in arterioles, but not in venules (40), ebselen-associated modulation of the cyclooxygenase pathway might be particularly effective in arterioles. In addition, one may speculate that ebselen-induced inhibition of platelet P-selectin may play a greater role in arterial thrombosis due to the increased presence of platelets known to exist histologically in arterial thrombi (41).

In conclusion, the antagonism of H_2O_2-induced platelet P-selectin expression seems to be a potential mechanism of the anti-thrombotic action of ebselen. With the recognition of the importance of P-selectin in developing thrombi, pharmacological approaches such as ebselen, which target the P-selectin dependent platelet-leukocyte interaction and the promotion of fibrin deposition, may represent a safe and effective therapeutic strategy against thrombotic disorders in humans.

References

1. Salonen JT, Alfthan G, Huttunen JK, et al.. Association between cardiovascular death and myocardial infarction and serum selenium in a matched-paired longitudinal study. Lancet 1982; 2: 175-9.
2. Moore JA, Noiva R, Wells IC. Selenium concentrations in plasma of patients with arteriographicallly defined coronary atherosclerosis. Clin Chem 1984; 30: 1171-3.
3. Jackson ML. Selenium: geochemical distribution and associations with human heart and cancer death rates and longevity in China and the United States. Biol Trace Elem Res 1988; 15: 13-21.
4. Wang YX, Bocker K, Reuter H, et al.. Selenium and myocardial infarction: glutathione peroxidase in platelets. Klin Wochenschr 1981; 59: 817-818.
5. Guidi GC, Schiavon R, Sheiban I, et al.. Platelet glutathione peroxidase activity is impaired in patients with coronary heart disease. Scand J Clin Lab Invest 1986; 46: 549-51.
6. Perona G, Guidi GC, Piga A, et al.. In vivo and in vitro variations of human erythrocyte glutathione peroxidase activity as result of cells aging, selenium availability and peroxide activation. Br J Haematol 1978; 39: 399-408.
7. Levander OA, Alfthan G, Arvilommi H, et al.. Bioavailability of selenium to Finnish men as assessed by platelet glutathione peroxidase activity and other blood parameters. J Clin Nutr 1983; 37: 887-897.
8. Kasperek K, Iyengar GV, Kiem J, et al.. Elemental composition of platelets. Part III. Determination of Ag, Au, Cd, Co, Cr, Cs, Mo, Rb, Sb, and Se in normal human platelets by neutron activation analysis. Clin Chem 1979; 25: 711-5.
9. Guidi GC, Schiavon R, Biasioli A, et al.. The enzyme glutathione peroxidase in arachidonic acid metabolism of human platelets. J Lab Clin Med 1984; 104: 574-582.
10. Perona G, Schiavon R, Guidi GC, et al.. Selenium dependent glutathione peroxidase: a physiogical regulatory system for platelet function. Thromb Haemost 1990; 64: 312-8.
11. Ricetti MM, Guidi GC, Tecchio C, et al.. Effects of sodium selenite on in vitro interactions between platelets and endothelial cells. Int J Clin Lab Res 1999; 29: 80-4.
12. Parnham M, Sies H. Ebselen: prospective therapy for cerebral ischemia. Expert Opin Investig Drugs 2000; 9: 607-19.
13. Yamaguchi T, Sano K, Takakura K, et al.. for the Ebselen study group. Ebselen in acute ischemic stroke. A placebo-controlled, double-blind clinical trial. Stroke 1998; 29: 12-7.
14. Ogawa A, Yoshimoto T, Kikuchi H, et al.. for the Ebselen study group. Ebselen in acute middle cerebral artery occlusion: a placebo-controlled, double-blind clinical trial. Cerebrovasc Dis 1999; 9: 112-8.
15. Dimmeler S, Brüne B, Ullrich V. Ebselen prevents inositol (1,4,5)-triphosphate binding to its receptor. Biochem Pharmacol 1991; 42: 1151-3.
16. Brüne B, Diewald B, Ullrich V. Ebselen affects calcium homeostasis in human platelets. Biochem Pharmacol 1991; 41: 1805-1.
17. Baez S. An open cremaster muscle preparation for the study of blood vessels by in vivo microscopy. Microvasc Res 1973; 5: 384-94.
18. Roesken F, Ruecker M, Vollmar B, et al.. A new model for quantitative in vivo microscopic analysis of thrombus formation and vascular recanalisation: the ear of the hairless (hr/hr) mouse. Thromb Haemost 1997; 78: 1408-4.
19. Vollmar B, Schmitz R, Kunz D, et al.. Lack of in vivo function of CD31 in vascular thrombosis. Thromb Haemost 2001; 85: 160-4.
20. Denis C, Methia N, Frenette PS, et al.. A mouse model of severe von Willebrand disease: defects in hemostasis and thrombosis. Proc Natl Acad Sci USA 1998; 95: 9524-9
21. Baker M, Wayland H. On-line volume flow rate and velocity profile measurements for blood in microvessels. Microvasc Res 1974; 7: 131-43.
22. Miller FN, Sims DE, Schuschke DA, et al.. Differentiation of light-dye effects in the microcirculation. Microvasc Res 1992; 44: 166-84.
23. Lindberg RA, Slaaf DW, Lentsch AB, et al.. Involvement of nitric oxide and cyclooxygenase products in photoactivation-induced microvascular occlusion. Microvasc Res 1994; 47: 203-21.
24. Saniabadi AR, Umemura K, Matsumoto N, et al.. Vessel wall injury and arterial thrombosis induced by a photochemical reaction. Thromb Haemost 1995; 73: 868-72.
25. Herrmann KS. Platelet aggregation induced in the hamster cheek pouch by a photochemical process with excited fluorescein isothiocyanate-dextran. Microvasc Res 1983; 26: 238-49.
26. Watson BD, Dietrich WD, Busto R, et al.. Induction of reproducible brain infarction by photochemically initiated thrombosis. Ann Neurol 1985; 17: 497-504.
27. Haddad el-B, McCluskie K, Birrell MA, et al.. Differential effects of ebselen on neutrophil recruitment, chemokine, and inflammatory mediator expression in a rat model of lipopolysaccharide-induced pulmonary inflammation. J Immunol 2002; 169: 974-82.
28. Furie B, Furie BC, Flaumenhaft R. A journey with platelet P-selectin: the molecular basis of granule secretion, signalling and cell adhesion. Thromb Haemost 2001; 86: 214-21.
29. Yang J, Furie BC, Furie B. The biology of P-selectin glycoprotein ligand-1: its role as a selectin counterreceptor in leukocyte-endothe-

lial and leukocyte-platelet interaction. Thromb Haemost 1999; 81: 1-7.
30. Shebuski RJ, Kilgore KS. Role of inflammatory mediators in thrombogenesis. J Pharmacol Exp Ther 2002; 300: 729-35.
31. Palabrica T, Lobb R, Furie BC, et al.. Leukocyte accumulation promoting fibrin deposition is mediated in vivo by P-selectin on adherent platelets. Nature 1992; 359: 848-51.
32. Celi A, Pellegrini G, Lorenzet R, et al.. P-selectin induces the expression of tissue factor on monocytes. Proc Natl Acad Sci USA 1994; 91: 8767-71.
33. Subramaniam M, Frenette PS, Saffaripour S, et al.. Defects in hemostasis in P-selectin-deficient mice. Blood 1996; 87: 1238-42.
34. Merten M, Thiagarajan P. P-selectin expression on platelets determines size and stability of platelet aggregates. Circulation 2000; 102: 1931-6.
35. Del Principe DD, Menichelli A, De Matteis W, et al.. Hydrogen peroxide is an intermediate in the platelet activation cascade triggered by collagen, but not by thrombin. Thromb Res 1991; 62: 365-75.
36. Loscalzo J. Nitric oxide insufficiency, platelet activation, and arterial thrombosis. Circ Res 2001; 88: 756-62.
37. Walker TR, Watson SP. Synergy between Ca2+ and protein kinase C is the major factor in determining the level of secretion from human platelets. Biochem J 1993; 289: 277-82.
38. Furie B, Furie BC. Leukocyte crosstalk at the vascular wall. Thromb Haemost 1997; 78: 306-9.
39. Sato M, Ohshima N. Effect of wall shear rate on thrombogenesis in microvessels of the rat mesentery. Circ Res 1990; 66: 941-9.
40. Broeders MA, Tangelder GJ, Slaaf DW, et al.. Endogenous nitric oxide and prostaglandins synergistically counteract thromboembolism in arterioles but not in venules. Arterioscler Thromb Vasc Biol 2001; 21: 163-9.
41. Hashimoto I, Nakanishi H, Shono Y, et al.. The effects of desferrioxamine on thrombus formation in injured microvessels of the rabbit ear. J Med Invest 1999; 46: 200-4.

2.3.2 C-Peptid

Makro- und Mikroangiopathien mit der Konsequenz einer vielfach erhöhten kardiovaskulären Morbidität und Mortalität stellen ein wesentliches Problem für den diabetischen Patienten dar. Gabe des Proinsulin-Spaltproduktes C-Peptid führte bei diabetischen Patienten zur Verbesserung der Mikrozirkulation von Haut und Muskel und zur verminderten endothelialen Aktivierung. Ziel der vorliegenden Studie an normalen und diabetischen Mäusen war es daher zu untersuchen, inwieweit C-Peptid eine anti-thrombogene Wirkung hat und ob diese Wirkung durch die zusätzliche -und klinisch notwendige- Applikation von Insulin beeinflusst wird. Es wurde erneut das Cremastermodell der Maus verwendet und ein besonderes Augenmerk auf die endotheliale PAI-1 Expression als pro-thrombogener Faktor gerichtet.

C-Peptid in hoher, nicht aber niedriger Dosierung führte gegenüber inaktiviertem C-Peptid zu einer signifikanten Verzögerung der Thrombusbildung bei diabetischen Tieren und bei nicht-diabetischen Tieren. Dieser Effekt wurde durch Superfusion mit Insulin aufgehoben. Die endotheliale PAI-1 Expression war in den C-Peptid-behandelten diabetischen wie nicht-diabetischen Tieren gegenüber Kontrolltieren deutlich reduziert. C-Peptid führte zur leichten, aber signifikanten Reduktion der Expression von GPIIb/IIIa und P-Selektin ruhender Thrombozyten, während bei gleichzeitiger Maximalstimulierung der Plättchen mit TRAP C-Peptid diesen Effekt verlor.

Die vorliegenden Untersuchungsergebnisse weisen auf eine anti-thrombogene Wirkung von C-Peptid *in vivo* hin. Eine kausale Rolle von PAI-1 in diesem Zusammenhang kann vermutet werden. Dennoch stellt C-Peptid aufgrund der Tatsache, dass es durch gleichzeitige Insulinapplikation in seiner Wirkung abgeschwächt wird, keine brauchbare Alternative in der Behandlung diabetischer Angiopathien dar.

Lindenblatt N, Braun B, Menger MD, Klar E, Vollmar B

C-peptide exerts antithrombotic effects that are repressed by insulin in normal and diabetic mice *Diabetologia* 2006; 49: 792-800

Diabetologia (2006) 49: 792 800
DOI 10.1007/s00125-006-0152-4

ARTICLE

N. Lindenblatt · B. Braun · M. D. Menger ·
E. Klar · B. Vollmar

C-peptide exerts antithrombotic effects that are repressed by insulin in normal and diabetic mice

Received: 4 September 2005 / Accepted: 24 November 2005 / Published online: 23 February 2006
© Springer-Verlag 2006

Abstract *Aims/hypothesis:* Diabetic macro- and microangiopathy are associated with a high risk of vascular complications. The diabetic patient exhibits a pathological coagulation state, with an increased synthesis of coagulation factors and plasminogen activator inhibitor 1 (PAI-1) as well as an enhanced aggregation of platelets. Previous studies have shown that C-peptide can reduce leucocyte-endothelial cell interaction and improve microvascular blood flow in patients with type 1 diabetes. In the present study, we examined in vivo whether C-peptide is able to reduce platelet activation and through that microvascular thrombus formation. *Materials and methods:* In the microvessels of cremaster muscle preparations taken from normal and diabetic mice, ferric chloride-induced thrombus formation was analysed using intravital fluorescence microscopy. *Results:* I.V. administration of C-peptide in high dose (70 nmol/kg), but not in low dose (7 nmol/kg), caused a significant delay in arteriolar and venular thrombus growth in normal and diabetic mice. This effect was repressed by cremaster muscle superfusion with insulin (100 μU/ml) in diabetic animals, but particularly in normal animals. In parallel, immunohistochemistry demonstrated a higher number of PAI-1-expressing vessels in cremaster muscle tissue from control animals and from animals treated with C-peptide and insulin compared with tissue from animals with C-peptide treatment application alone. *Conclusions/interpretation:* We conclude that C-peptide possesses antithrombotic actions in vivo. A causal role of PAI-1 in this scenario needs to be further addressed. However, the reversal of C-peptide action by insulin may invalidate the use of this peptide as a treatment option to improve rheology and microcirculation in diabetic patients.

Keywords C-peptide · Diabetes · Insulin · In vivo microscopy · Microvascular thrombosis · Platelets · Streptozotocin

Abbreviations FITC: fluorescein isothiocyanate · GPIIb/IIIa: glycoprotein IIb/IIIa · Na^+-K^+-ATPase: sodium potassium ATPase · NO: nitric oxide · PAI-1: plasminogen activator inhibitor 1 · RBC: red blood cell · TRAP: thrombin-receptor-activating peptide

N. Lindenblatt · B. Braun · B. Vollmar (✉)
Department of Experimental Surgery, University of Rostock,
Schillingallee 70,
18055 Rostock, Germany
e-mail: brigitte.vollmar@med.uni-rostock.de
Tel.: +49-381-4946220
Fax: +49-381-4946222

N. Lindenblatt · E. Klar
Department of General Surgery, University of Rostock,
Rostock, Germany

M. D. Menger
Department of Clinical and Experimental Surgery,
University of Saarland,
Homburg-Saar, Germany

Introduction

The excess mortality and high morbidity of diabetic patients are predominantly determined by vascular dysfunctions. Diabetic microangiopathy not only manifests as nephropathy, retinopathy and delayed wound healing, but also predisposes the patient to the development of coronary artery, cerebrovascular and peripheral artery disease [1, 2]. The pathophysiology of diabetic vasculopathy involves the dysfunction of the endothelium, which is caused by increased production of reactive oxygen species as a consequence of hyperglycaemia, which in turn inactivates the vasodilator nitric oxide (NO). As a consequence, nuclear factor κB is upregulated and the formation of vasoconstrictive prostanoids and endothelins is increased [3, 4]. Plasminogen activator inhibitor 1 (PAI-1) levels have also been found to be elevated in diabetic patients, resulting in defective fibrinolysis and an increased risk for intravascular thrombosis [5, 6].

In addition to these endothelium-confined factors, platelet dysfunction [7–9] and an imbalance of plasmatic coagulation factors further contribute to a prothrombotic state in the diabetic patient. In particular, augmented

synthesis of factor VII, thrombin, tissue factor and PAI-1 is detected in the diabetic patient, while anticoagulative substances, such as thrombomodulin and protein C, are diminished [10–12].

Administration of C-peptide, the cleavage product from proinsulin, has been shown to improve skin microcirculation in patients with type 1 diabetes [13]. C-peptide further induces endothelial NO-synthetase and, thus, NO production [14]. In addition, it may reduce leucocyte–endothelium interaction through a diminution of endothelial P-selectin and intracellular adhesion molecule type 1 expression [15]. Based on this, insulin deficiency, and thus lack of anti-adhesive C-peptide action, could be a causal factor in the development of procoagulative status in diabetic patients. We therefore used intravital fluorescence microscopy to investigate the effect of systemic C-peptide administration on microvascular thrombus formation in vivo in normal and diabetic mice. We additionally performed flow cytometric and immunohistological studies to characterise further the potential underlying cellular and molecular mechanisms. Since exogenous insulin application is essential for type 1 diabetic patients, we also tested the effect on microvascular thrombus formation of additional insulin application.

Materials and methods

Mouse cremaster muscle preparation

Upon approval by the local government, all experiments were carried out in accordance with the German legislation on protection of animals and the National Institutes of Health 'Guide for the Care and Use of Laboratory Animals' (Institute of Laboratory Animal Resources, National Research Council). Male C57BL/6 mice (Charles River, Sulzfeld, Germany) with a body weight of 20–25 g were anaesthetised with an i.p. injection of ketamine (90 mg/kg body weight) and xylazine (25 mg/kg body weight) and a polyethylene catheter was placed into the right jugular vein to allow for administration of C-peptide and fluorescent dyes.

For the study of vascular thrombus formation, we used the opened cremaster muscle preparation, as described originally by Baez [16] and applied as a model of microvascular thrombus formation in previous studies [17–20]. After the preparation of the cremaster muscle, the animals were allowed to recover from surgery for 15 min before induction of thrombus formation.

In vivo thrombosis model

The cremaster muscle microcirculation was visualised by intravital fluorescence microscopy as described previously by our group [20]. Using a ×20 water immersion objective (Achroplan ×20/0.50 W; Zeiss, Jena, Germany) and 5% fluorescein isothiocyanate (FITC)-labelled dextran for contrast enhancement, blood flow was monitored in individual arterioles (diameter range 30–60 μm) and venules (diameter range 40–80 μm), followed by superfusion with 25 μl ferric chloride (12.5 mmol/l; Sigma, Steinheim, Germany) for induction of microvascular thrombosis. Recording of vessels was discontinued after blood flow in the vessel had ceased for at least 60 s. As the rapid spreading of ferric chloride solution allowed only one or two arterioles and venules to be studied within each preparation, both left and right cremaster muscles were prepared for analysis of thrombotic vessel occlusion within each animal.

Analysis included the time periods until first standstill of perfusion and sustained cessation of blood flow as a result of complete vessel occlusion. To characterise the kinetics of microvascular thrombus formation, a red blood cell (RBC) velocity profile was determined using the line-shift method (CapImage; Zeintl, Heidelberg, Germany). Microcirculatory analysis also included the determination of vessel diameter and RBC velocity before thrombus induction with calculation of vascular wall shear rates, based on the Newtonian definition $\gamma = 8 \times V/D$, where V represents the RBC-velocity divided by 1.6 according to the Baker–Wayland factor [21] and D represents the individual inner vessel diameter. The wall shear rate calculated might differ from values given in studies using different methods, such as the dual-slit photodiode technique and Doppler flowmetry [22, 23]; however, it will fit well with values found in studies using the line-shift method or comparable systems [20, 24, 25].

Experimental groups and protocol

Experiments were performed in normal and diabetic mice. Diabetes was induced by application of streptozotocin (40 mg/kg i.p.) on five consecutive days. Animals were kept in their accustomed environment and monitored for polyuria for the following 35–40 days. Starting on day 42 the diabetic metabolic state was confirmed by repeated positive testing for hyperglycaemia and glucosuria. Glucosuria was tested with test strips (Medi-test, Combi 3A; Macherey-Nagel, Düren, Germany) and was considered positive if the glucosuria was >56 mmol/l on five consecutive days. Hyperglycaemia was confirmed by blood glucose testing with a digital glucometer (elite 2000; Beyer Diagnostics GmbH, Munich, Germany). Mice were considered diabetic if their blood glucose levels were >11.1 mmol/l for three consecutive days.

Human C-peptide was administered to mice via the right jugular vein in a low dose of 7 nmol/kg (n=6) and a high dose of 70 nmol/kg (n=6) 15 min before the experiment. Control animals received equivalent volumes of heat-inactivated C-peptide (30 min at 95°C) (n=14). The C-peptide concentrations were chosen because previous experiments had shown that injection of 130 nmol/kg human C-peptide into rats increased the physiological C-peptide plasma levels ten-fold 3 h after injection [26]. Therefore, the higher dose of 70 nmol/kg used in this study is likely to induce an approximately five-fold increase in C-peptide plasma level, which has

been shown to correct vascular permeability and neuronal dysfunction in diabetic rats [26]. Additionally, Scalia et al. demonstrated that this concentration of C-peptide inhibited leucocyte–endothelial interaction during acute endothelial dysfunction [15]. To examine the role of insulin in C-peptide function, the cremaster muscles of animals treated with C-peptide at either low (7 nmol/kg; n=4) or high (70 nmol/kg; n=4) dose were superfused with insulin solution at a concentration of 100 μU/ml before thrombus induction. This concentration was applied because postprandial insulin levels in humans typically reach 60–80 μU/ml. Insulin was applied topically because systemic application of insulin might have resulted in uncontrollable lowering of blood glucose levels and thus unstable metabolic conditions. Identical sets of experiments were performed in diabetic mice with systemic C-peptide administration at low (n=5) and high (n=4) doses, using heat-inactivated C-peptide (n=11) as well as with additional insulin superfusion at low (n=4) and high (n=4) doses of C-peptide.

To rule out a difference in the effect of C-peptide and insulin between systemic and topical application and to further clarify the effect of insulin application alone, additional in vivo experiments were performed superfusing the cremaster muscle with insulin (100 μU/ml) alone in normal (n=4) and diabetic (n=4) mice. In addition, cremaster muscle preparations were superfused with insulin (100 μU/ml) and C-peptide (7 nmol/l) in normal (n=4) and diabetic (n=5) animals.

Human blood collection and preparation of platelet-rich plasma

Following acquisition of informed consent, blood was drawn from the left cubital vein of healthy volunteers using a 21-gauge needle into 5-ml S-Monovettes 9NC (Sarstedt, Nümbrecht, Germany) (1:10 citrate, v/v). After centrifugation for 15 min at 110 g and room temperature (GS-6R Centrifuge; Beckman Coulter, Fullerton, CA, USA), platelet-rich plasma was transferred to a separate tube. Platelet count was assessed with a Cell Counter (Sysmex KX-21; Sysmex, Norderstedt, Germany) and adjusted to 2×10^8/ml by dilution with PBS. Aliquots of platelet-rich plasma were transferred into a 37°C water–bath to rest for 30 min to eliminate isolation-induced platelet activation.

Flow cytometric analysis of P-selectin and glycoprotein IIb/IIIa expression

For evaluation of receptor expression under resting conditions, 50 μl of platelet suspensions were incubated for 30 min with the isotype-specific control antibody, the P-selectin antibody or the glycoprotein IIb/IIIa (GPIIb/IIIa) antibody in the presence of C-peptide at concentrations of either 0.3 or 1 nmol/l. Platelet suspensions without C-peptide served as controls. A similar set of experiments was carried out following exposure to thrombin-receptor-activating peptide (TRAP) for maximal platelet activation (2.5 mmol/l).

C-peptide concentrations of 0.3 and 1.0 nmol/l were chosen because the physiological concentration of C-peptide in human blood ranges between 0.5 and 1.5 nmol/l. In addition, reports studying a potential C-peptide receptor on renal tubular cells showed a half-saturation at a C-peptide concentration of 0.3 nmol/l and a full saturation at 0.9 nmol/l C-peptide [27]. An additional set of experiments was carried out, adding insulin at final concentrations of 10 and 100 μU/ml (which cover fasting [6–25 μU/ml] and postprandial [60–100 μU/ml, maximum 200 μU/ml] insulin levels in humans [28]) alone and in combination with C-peptide concentrations of 0.3 and 1.0 nmol/l. Then, platelets were rapidly cooled on ice and diluted with 1 ml 4°C 1% paraformaldehyde in PBS (Cell Fix; Becton Dickinson, Heidelberg, Germany). After fixation, platelets were centrifuged at 300 g for 4 min at 4°C and washed twice with PBS. The supernatant was decanted and the pellet was resuspended in PBS for flow cytometry.

Expression of P-selectin on platelets was investigated by direct immunofluorescence using a monoclonal anti-human FITC-coupled P-selectin antibody (Santa Cruz Biotechnology, Heidelberg, Germany), diluted 1:50 (v/v) with staining medium (0.1% sodium azide and 2% FCS in PBS). In an additional set of experiments a FITC-coupled PAC-1 antibody (Becton Dickinson Biosciences, Heidelberg, Germany) directed against the activated conformation of GPIIb/IIIa was employed [29]. A FITC-coupled IgG1 isotype-matched control antibody (Santa Cruz Biotechnology) was used to exclude unspecific binding. Flow cytometry was performed within the next hour.

The FACScan flow cytometer (Becton Dickinson) was calibrated with fluorescent standard microbeads (Cali-BRITE Beads; Becton Dickinson) for accurate instrument setting. Platelets were identified by their characteristic forward and sideward scatter light and were selectively analysed for their fluorescence properties using the CellQuest program (Becton Dickinson) with assessment of 20,000 events per sample. The relative fluorescence intensity of a given sample was calculated by subtracting the signal obtained when cells were incubated with the isotype-specific control antibody from the signal generated by cells incubated with the test antibody.

Histology and immunohistochemistry

At the end of each experiment, the cremaster muscle was fixed in 4% phosphate-buffered formalin for 2–3 days and embedded in paraffin. From the paraffin-embedded tissue blocks, 4-μm sections were cut and stained with haematoxylin and eosin for histological analysis. For immunohistochemical demonstration of PAI-1, sections collected on poly-L-lysine-coated glass slides were treated by microwave for antigen unmasking. Goat polyclonal anti-PAI-1 (1:200; Santa Cruz Biotechnology) was used as primary antibody and incubated for 90–120 min at room

temperature, followed by a horseradish peroxidase-conjugated donkey anti-goat antibody (1:25; Santa Cruz Biotechnology) and development using DAB substrate as chromogen. The sections were counterstained with haematoxylin and examined by light microscopy (Zeiss Axioscop 40; Zeiss).

Chemicals and drugs

Human 31-residue C-peptide (Sigma) was dissolved in 0.5 mol/l acetic acid with further dilutions being made with 0.9% saline, as previously described [15]. Human C-peptide was applied because of its simple availability and similar structure compared with rat or mouse C-peptides. Human C-peptide has been used in several small animal models and has been shown to induce positive effects on vascular and neuronal dysfunction as well as on leucocyte–endothelial cell dysfunction [15, 26]. Streptozotozin (Sigma) was dissolved in citrate buffer (pH 4.5, 0.1 mol/l) and used directly following preparation. Porcine insulin was also purchased from Sigma and dissolved in PBS to final concentrations of 10 and 100 μU/ml. As insulin from different species interacts with porcine insulin sera to a similar degree [30], porcine insulin was chosen because it is more easily available and is cheaper. TRAP was purchased from Bachem (Bubendorf, Germany) and dissolved in PBS to yield a 2.5 mmol/l stock solution. All solutions were stored in the dark at a maximum temperature of −20°C.

Statistical analysis

After proving the assumption of normality and equal variance across groups, differences between groups were assessed using one-way ANOVA followed by the appropriate post hoc comparison test. All data were expressed as means ± SEM and overall statistical significance was set at $p<0.05$. Linear regression analysis was performed to evaluate significant correlations between kinetics of thrombus formation and PAI-1 expression. Statistics and graphics were performed using the software packages SigmaStat and SigmaPlot (Jandel Corporation, San Rafael, CA, USA).

Results

In vivo thrombosis model

The effect of systemic application of C-peptide in low (7 nmol/kg) and high (70 nmol/kg) doses was assessed in vivo by superfusion of microvessels with ferric chloride solution, which resulted in complete thrombotic occlusion of the individually exposed vessel.

At baseline, i.e. before thrombus induction, animals did not significantly differ between the groups with regard to the diameter and wall shear rates in arterioles and venules (Table 1). Thus, the distinct times until complete vessel occlusion are only barely attributable to differences in microhaemodynamics.

Effect of low-dose C-peptide on microvascular thrombosis

Quantitative analysis of ferric chloride-induced thrombus formation in normal controls, i.e. animals that received heat-inactivated C-peptide, revealed complete occlusion of venules and arterioles at 449±55 s and 411±76 s, respectively (Fig. 1a). C-peptide neither alone nor in

Table 1 Vessel diameters (μm) and wall shear rates (γ; s^{-1}) in mice cremaster muscle microvessels prior to ferric chloride-induced thrombus formation

	Arterioles		Venules	
	Diameter	γ	Diameter	γ
Normal				
Control	45±4	116±9	51±6	73±12
C-peptide 7 nmol/kg	52±7	133±32	72±10	56±9
C-peptide 7 nmol/kg+insulin	55±4	134±9	61±4	99±12
Control	37±4	129±18	46±4	63±18
C-peptide 70 nmol/kg	45±4	150±25	50±4	98±16
C-peptide 70 nmol/kg+insulin	54±5	127±13	58±5	94±4
Diabetic				
Control	48±3	134±12	53±5	96±8
C-peptide 7 nmol/kg	55±5	140±9	66±6	141±46
C-peptide 7 nmol/kg+insulin	41±6	198±40	56±7	73±6
Control	56±6	128±9	56±6	120±14
C-peptide 70 nmol/kg	38±4	136±32	50±4	140±25
C-peptide 70 nmol/kg+insulin	48±7	173±37	61±5	75±9

Values are given as means ± SEM; for further information, see Materials and methods

combination with insulin had a major influence on these microvascular occlusion times in normal animals (Fig. 1a). Moreover, microvascular thrombus formation in diabetic mice did not differ between control animals and those that received low-dose C-peptide alone or in combination with insulin (Fig. 1b), ranging between 375 and 510 s for arterioles and 400 and 570 s for venules.

Effect of high-dose C-peptide on microvascular thrombosis

In contrast, the application of a high dose of C-peptide caused a significant delay in arteriolar and venular thrombus growth and in occlusion time in both normal (Fig. 2a) and diabetic animals (Fig. 2b). Notably, this prolongation in microvascular thrombus formation with high-dose C-peptide exposure was abolished by superfusion of the cremaster muscle with insulin in normal mice and resulted in complete occlusion of arterioles and venules within the time periods, as observed in controls (Fig. 2a). As in normal mice, insulin superfusion repressed the C-peptide-induced delay in thrombotic vessel occlusion in diabetic mice towards the values found in controls (Fig. 2b). This effect was also seen when the cremaster muscle was superfused with insulin and C-peptide, as indicated by the comparable arteriolar and venular occlusion times in normal and diabetic animals. Insulin superfusion alone resulted in even shorter times until complete vessel occlusion compared with combined insulin and C-peptide treatment in normal mice, but in particular in diabetic animals (Table 2).

Flow cytometric analysis of platelet P-selectin and GPIIb/IIIa expression

Upon incubation with C-peptide alone or in combination with insulin, spontaneous expression of P-selectin and GPIIb/IIIa did not show a marked change and was below 10%. Moreover, both C-peptide alone and C-peptide combined with insulin failed to affect maximal P-selectin and GPIIb/IIIa expression, as induced by TRAP exposure of platelets (data not shown).

PAI-1 immunohistochemistry

PAI-1 was expressed within the endothelium of arterioles and venules, while little, if any, immunoreactivity was detected within the surrounding muscle tissue (Fig. 3a,b). Immunohistochemistry of cremaster muscle tissue with low-dose C-peptide exposure in both normal and diabetic animals exhibited a slight reduction in the fraction of PAI-expressing vessels when compared to their corresponding normal and diabetic controls (Fig. 4a,b). Interestingly, in animals with additional insulin superfusion, the fraction of PAI-expressing vessels was found to be higher than that in animals that received C-peptide alone and even exceeded that found in controls (Fig. 4b).

In normal and diabetic animals that received C-peptide at the high dose of 70 nmol/kg, PAI-1 expression was markedly reduced, with only 1.5–2% of all vessels displaying specific immunoreactivity (Fig. 5a,b). Notably, insulin superfusion in diabetic animals reversed the C-peptide-induced repression of PAI-expression towards the values found in controls (~10%), while in normal animals the fraction of PAI-expressing vessels averaged almost 30% upon C-peptide and insulin superfusion (Fig. 5a,b). Superfusion of the cremaster muscle with both C-peptide (7 nmol/l) and insulin caused a slight, but not significant, increase in vascular PAI-1 expression in relation to systemic C-peptide application plus superfusion with insulin. Insulin superfusion alone resulted in a marked and significant increase in endothelial PAI-1 expression within the cremaster muscle compared with additional C-peptide treatment (Table 2).

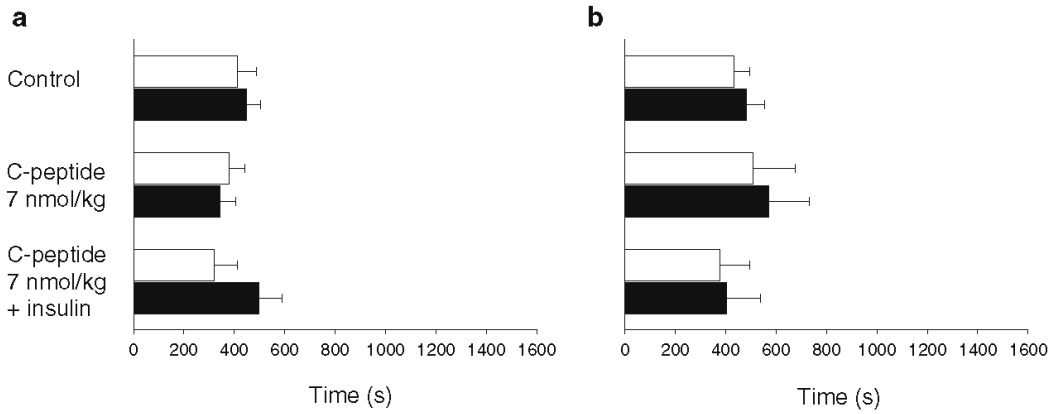

Fig. 1 Occlusion times of arterioles (*open bars*) and venules (*filled bars*) upon ferric chloride-induced thrombus formation in normal (**a**) and diabetic (**b**) mice following treatment with heat-inactivated C-peptide (control), C-peptide at low dose (7 nmol/kg) and C-peptide at low dose (7 nmol/kg) with additional superfusion of insulin (100 μU/ml). Values are given as means ± SEM

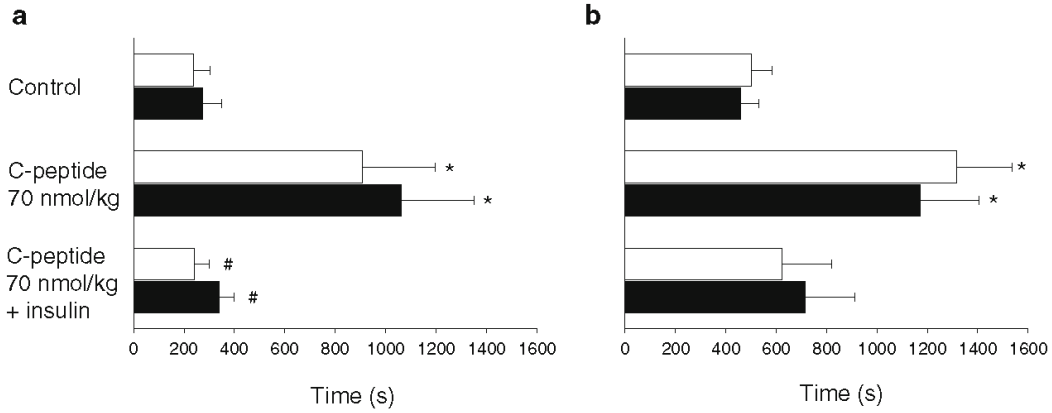

Fig. 2 Occlusion times of arterioles (*open bars*) and venules (*filled bars*) upon ferric chloride-induced thrombus formation in normal (**a**) and diabetic (**b**) mice following treatment with heat-inactivated C-peptide (control), C-peptide at high dose (70 nmol/kg), C-peptide at high dose (70 nmol/kg) with additional superfusion of insulin (100 μU/ml). Values are given as means ± SEM; *$p<0.05$ vs control; #$p<0.05$ vs C-peptide high dose (70 nmol/kg)

Discussion

The main reason for morbidity and mortality in diabetic patients is cardiovascular complications. However, the link between diabetes and macro- and microangiopathic impairment is still not fully understood. Moreover, sufficient treatment options have not been established, despite improved glycaemic control of diabetes. To find novel therapeutic strategies and, in particular, to counteract the procoagulative status in diabetic patients, we studied the effect of proinsulin C-peptide administration on microvascular thrombus formation in vivo.

Our results demonstrate that administration of i.v. C-peptide at 70 nmol/kg leads to a significant deceleration of microvascular thrombus formation not only in diabetic but also in normal mice. This provides evidence for a substantial antithrombotic effect of proinsulin C-peptide. These in vivo results are further underlined by immunohistological findings, demonstrating that C-peptide administration prompts a decrease in vascular PAI-1 expression. Of interest, insulin application completely blunted the anticoagulative effect of C-peptide in normal and diabetic mice. This is supported by the fact that the percentage of PAI-1-expressing vessels within the cremaster muscle tissue was increased in animals which underwent C-peptide treatment and consecutive insulin superfusion compared with animals treated with C-peptide alone. The effect of C-peptide and insulin treatment was similar regardless of whether a local or systemic mode of C-peptide application was chosen. Insulin superfusion alone caused even faster vascular occlusion times, once more underlining the prothrombotic effect of insulin.

FACScan analysis of human platelets did not reveal major changes upon C-peptide and C-peptide + insulin exposure. Despite differences in size, number and ultrastructural morphology human and murine platelets have been shown to exert similar organelle and glycoprotein subcellular distributions [31]. The GPIIb/IIIa receptor in particular exerts comparable functions during platelet activation and aggregation in humans and mice [32]. However, we are aware that species differences cannot be completely excluded.

Since the discovery of insulin biosynthesis and the subsequent identification of proinsulin and C-peptide, numerous studies have been undertaken to characterise a distinct role for C-peptide apart from being merely a

Table 2 Vessel occlusion times and percentage of PAI-1-expressing vessels in mice cremaster muscle upon ferric chloride-induced thrombus formation

	Arteriolar occlusion time (s)	Venular occlusion time (s)	PAI-1-expressing vessels (%)
Normal			
Superfusion of C-peptide (7 nmol/l)+insulin	319±101	370±101	34.6±2.4
Superfusion of insulin	278±68	279±76	56.7±8.8
Diabetic			
Superfusion of C-peptide (7 nmol/l)+insulin	510±70	672±77	17.6±2.8
Superfusion of insulin	182±84	238±84	63.4±1.4

Values are given as means ± SEM; for further information, see Materials and methods and Results

798

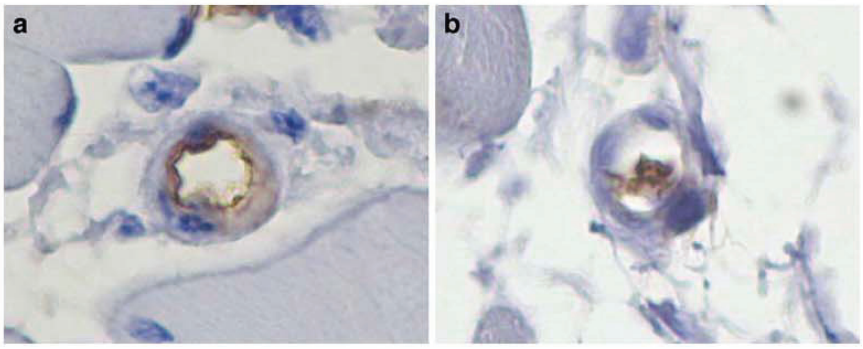

Fig. 3 Immunohistochemical staining of PAI-1 expression in cremaster muscle tissue after treatment with (**a**) heat-inactivated C-peptide (control) and (**b**) C-peptide at the high dose (70 nmol/kg). Note the marked expression of PAI-1 in the control animal with preferential localisation at the vascular site, while there was little immunostaining for PAI-1 in the C-peptide-treated animal. Magnification ×400

'connecting' peptide [33]. Despite some effects reported on glucagon release in the rat pancreas [34], it became common opinion that C-peptide had no biological activity on its own. However, evidence for multiple beneficial effects of C-peptide administration in diabetic patients has been rising over the past decade.

Forst et al. reported positive effects of C-peptide administration on skin microcirculation in patients with type 1 diabetes [13]. Moreover, C-peptide has been demonstrated to cause a dilatation of skeletal muscle arterioles that was probably based on increased NO production and could only be observed in the presence of insulin [35]. This NO-releasing effect of C-peptide was confirmed in a study on leucocyte–endothelium interaction after C-peptide administration in the mesentery of normal rats [15] and in vitro in bovine aortic endothelial cells, which showed a time- and concentration-dependent release of NO [14]. It has further been demonstrated that C-peptide elicits a concentration-dependent stimulation of Na^+-K^+-ATPase activity in renal tubular cells [36]. Consistent with this, the activity of Na^+-K^+-ATPase was reduced in membranes of erythrocytes of diabetic patients, which led to a reduced erythrocyte deformability and an increased blood viscosity. C-peptide infusion restored RBC deformability and microvascular blood flow concomitant with Na^+-K^+-ATPase activity [37, 38]. As a consequence it has been assumed that beneficial effects of C-peptide on microvascular blood flow and haemorrheology are exerted largely via stimulation of endothelial NO-synthetase (with subsequent NO-release) and Na^+-K^+-ATPase of erythrocytes [39].

Several studies have suggested that PAI-1 plays a major role in the pathogenesis of atherosclerosis and represents a risk factor for coronary heart disease [1, 40]. PAI-1 is the most important physiological inhibitor of tissue plasminogen activator, which activates plasminogen to plasmin and therefore exerts prothrombotic effects. Its role in the insulin-resistance syndrome has been defined in the past [41]. ApoE $^{-/-}$ mice with high PAI-1 levels exhibited a prothrombotic phenotype with shortened time to thrombotic vessel occlusion in a model of ferric-chloride-induced carotid artery injury [42]. In this study, we provide evidence that C-peptide possesses antithrombotic effects that could eventually be related to the biology of PAI-1. We show that cremaster muscle tissue of control animals and animals treated with C-peptide and insulin present with a higher number of PAI-1-expressing vessels compared

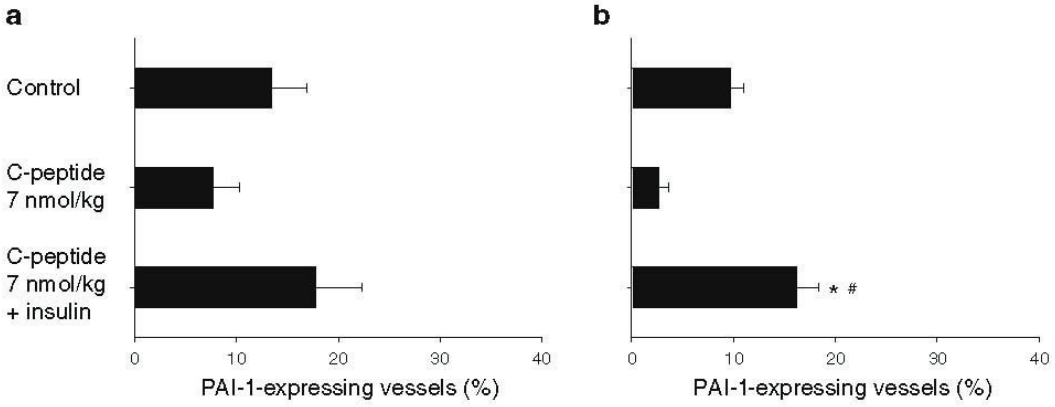

Fig. 4 Immunohistological analysis of vascular PAI-1 expression represented by percentage of positively stained vessels within the cremaster muscle for normal (**a**) and diabetic (**b**) mice after pretreatment with inactivated C-peptide (control), C-peptide at low dose (7 nmol/kg) and C-peptide at low dose with additional superfusion of insulin (100 μU/ml). Values are given as means ± SEM; *p<0.05 vs control; #p<0.05 vs C-peptide low dose (7 nmol/kg)

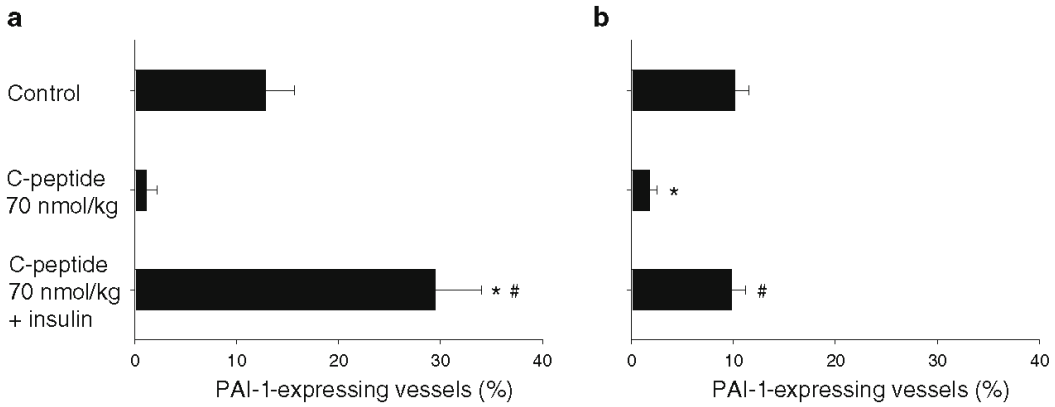

Fig. 5 Immunohistological analysis of vascular PAI-1 expression represented by percentage of positively stained vessels within the cremaster muscle for normal (**a**) and diabetic (**b**) mice after pre-treatment with inactivated C-peptide (control), C-peptide at high dose (70 nmol/kg), C-peptide at high dose with additional superfusion of insulin (100 μU/ml). Values are given as means ± SEM; *$p<0.05$ vs control; #$p<0.05$ vs C-peptide high dose (70 nmol/kg)

with animals given only C-peptide, implying a link between reduced PAI-1 expression and the antithrombotic effect of C-peptide. However, postulation of a direct causal relationship between C-peptide and PAI-1 requires further mechanistic investigation.

The effects of insulin on vascular biology have been controversially discussed in the past. Insulin has been found to mediate NO-induced vasodilatation [43], to inhibit platelet aggregation by inducing the synthesis of prostacyclin in endothelial cells, to upregulate prostacyclin receptors and downregulate α_2-adrenergic receptors on platelets, and to release tissue plasminogen activator from the platelet membrane [44]. On the other hand, insulin caused an two-fold upregulation of PAI-1 gene expression within 3 h in rabbits, is found to be elevated in hyperinsulinaemic type 2 diabetic patients [6, 45] and results in overexpression of endothelin in vascular smooth muscle cells [46]. Moreover, insulin but not C-peptide enhanced platelet fibrinogen binding in vitro in platelets from type 1 diabetic patients and healthy subjects [47] and enhanced platelet aggregability and leucocyte CD11b expression in whole blood from healthy patients [48]. In line with this, we now show that insulin reverses the antithrombotic effects of C-peptide in normal and diabetic mice.

It has repeatedly been stated that positive effects of C-peptide cannot be detected in healthy humans or animals but only in diabetic patients or animals that exhibit very low or missing C-peptide plasma levels [49, 50]. This was explained by the binding characteristics of a presumed G-protein-coupled membrane receptor [27] with saturation already at very low C-peptide concentrations. Thus, in healthy subjects with saturating physiological C-peptide levels there will be no additional effects upon exogenous C-peptide application. In contrast to that, we did not observe a difference in antithrombotic action of C-peptide between normal and diabetic animals. However, as it has been reported that C-peptide-induced prevention of vascular dysfunction is mediated by non-chiral interactions instead of stereospecific receptors or binding sites, we propose that the antithrombotic property of C-peptide and subsequently the effect of C-peptide on PAI-1 expression is more likely to be based on non-receptor actions.

Acknowledgements The authors would like to thank B. Blendow, D. Frenz and C. Vergien, Department of Experimental Surgery, University of Rostock, and Dr C. Zingler, Institute for Clinical Chemistry and Laboratory Medicine, University of Rostock, for their excellent technical assistance.

References

1. Calles-Escandon J, Cipolla M (2001) Diabetes and endothelial dysfunction: a clinical perspective. Endocr Rev 22:36 52
2. Creager MA, Luscher TF, Cosentino F, Beckman JA (2003) Diabetes and vascular disease: pathophysiology, clinical consequences, and medical therapy: Part I. Circulation 108:1527 1532
3. De Vriese AS, Verbeuren TJ, Van de Voorde J, Lameire NH, Vanhoutte PM (2000) Endothelial dysfunction in diabetes. Br J Pharmacol 130:963 974
4. Luft FC (2002) Proinflammatory effects of angiotensin II and endothelin: targets for progression of cardiovascular and renal diseases. Curr Opin Nephrol Hypertens 11:59 66
5. Auwerx J, Bouillon R, Collen D, Geboers J (1988) Tissue-type plasminogen activator antigen and plasminogen activator inhibitor in diabetes mellitus. Arteriosclerosis 8:68 72
6. Jokl R, Laimins M, Klein RL, Lyons TJ, Lopes-Virella MF, Colwell JA (1994) Platelet plasminogen activator inhibitor 1 in patients with type II diabetes. Diabetes Care 17:818 823
7. Vericel E, Januel C, Carreras M, Moulin P, Lagarde M (2004) Diabetic patients without vascular complication display enhanced basal platelet activation and decreased antioxidant status. Diabetes 53:1046 1051
8. Vinik AI, Erbas T, Park TS, Nolan R, Pittenger GL (2001) Platelet dysfunction in type 2 diabetes. Diabetes Care 24:1476 1485
9. Li Y, Woo V, Bose R (2001) Platelet hyperactivity and abnormal Ca^{2+} homeostasis in diabetes mellitus. Am J Physiol Heart Circ Physiol 280:H1480 H1489

10. Ceriello A, Giacomello R, Stel G et al (1995) Hyperglycemia-induced thrombin formation in diabetes. The possible role of oxidative stress. Diabetes 44:924 928
11. Pandolfi A, Cetrullo D, Polishuck R et al (2001) Plasminogen activator inhibitor type 1 is increased in the arterial wall of type II diabetic subjects. Arterioscler Thromb Vasc Biol 21:1378 1382
12. Hafer-Macko CE, Ivey FM, Gyure KA, Sorkin JD, Macko RF (2002) Thrombomodulin deficiency in human diabetic nerve microvasculature. Diabetes 51:1957 1963
13. Forst T, Kunt T, Pohlmann T et al (1998) Biological activity of C-peptide on the skin microcirculation in patients with insulin-dependent diabetes mellitus. J Clin Invest 101: 2036 2041
14. Wallerath T, Kunt T, Forst T et al (2003) Stimulation of endothelial nitric oxide synthetase by proinsulin C-peptide. Nitric Oxide 9:95 102
15. Scalia R, Coyle KM, Levine BJ, Booth G, Lefer AM (2000) C-peptide inhibits leukocyte endothelium interaction in the microcirculation during acute endothelial dysfunction. FASEB J 14:2357 2364
16. Baez S (1973) An open cremaster muscle preparation for the study of blood vessels by in vivo microscopy. Microvasc Res 5:384 394
17. Pierangeli SS, Colden-Stanfield M, Liu X, Barker JH, Anderson GL, Harris EN (1999) Antiphospholipid antibodies from antiphospholipid syndrome patients activate endothelial cells in vitro and in vivo. Circulation 99:1997 2002
18. Thorlacius H, Vollmar B, Seyfert UT, Vestweber D, Menger MD (2000) The polysaccharide fucoidan inhibits microvascular thrombus formation independently from P- and L-selectin function in vivo. Eur J Clin Invest 30:804 810
19. Vollmar B, Schmitz R, Kunz D, Menger MD (2001) Lack of in vivo function of CD31 in vascular thrombosis. Thromb Haemost 85:160 164
20. Lindenblatt N, Bordel R, Schareck W, Menger MD, Vollmar B (2004) Vascular heme oxygenase-1 induction suppresses microvascular thrombus formation in vivo. Arterioscler Thromb Vasc Biol 24:601 606
21. Baker M, Wayland H (1974) On-line volume flow rate and velocity profile measurements for blood in microvessels. Microvasc Res 7:131 143
22. Dunne JL, Ballantyne CM, Beaudet AL, Ley K (2002) Control of leukocyte rolling velocity in TNF-alpha-induced inflammation by LFA-1 and Mac-1. Blood 99:336 341
23. Kaul DK, Fabry ME, Costantini F, Rubin EM, Nagel RL (1995) In vivo demonstration of red cell endothelial interaction, sickling and altered microvascular response to oxygen in the sickle transgenic mouse. J Clin Invest 96:2845 2853
24. Lindenblatt N, Schareck W, Belusa L, Nickels RM, Menger MD, Vollmar B (2003) Anti-oxidant ebselen delays microvascular thrombus formation in the rat cremaster muscle by inhibiting platelet P-selectin expression. Thromb Haemost 90:882 892
25. Kim MB, Sarelius IH (2004) Regulation of leucocyte recruitment by local wall shear rate and leucocyte delivery. Microcirculation 11:55 67
26. Ido Y, Vindigni A, Chang K et al (1997) Prevention of vascular and neural dysfunction in diabetic rats by C-peptide. Science 277:563 566
27. Rigler R, Pramanik A, Jonasson P et al (1999) Specific binding of proinsulin C-peptide to human cell membranes. Proc Natl Acad Sci USA 96:13318 13323
28. Horwitz DL, Starr JI, Mako ME, Blackard WG, Rubenstein AH (1975) Proinsulin, insulin, and C-peptide concentrations in human portal and peripheral blood. J Clin Invest 55:1278 1283
29. Shattil SJ, Cunningham M, Hoxie JA (1987) Detection of activated platelets in whole blood using activation-dependent monoclonal antibodies and flow cytometry. Blood 70:307 315
30. Kitabchi AE (1977) Proinsulin and C-peptide: a review. Metabolism 26:547 587
31. Schmitt A, Guichard J, Masse JM, Debili N, Cramer EM (2001) Of mice and men: comparison of the ultrastructure of megakaryocytes and platelets. Exp Hematol 29:1295 1302
32. Smyth SS, Tsakiris DA, Scudder LE, Coller BS (2000) Structure and function of murine alphaIIbbeta3 (GPIIb/IIIa): studies using monoclonal antibodies and beta3-null mice. Thromb Haemost 84:1103 1108
33. Wahren J (2004) C-peptide: new findings and therapeutic implications in diabetes. Clin Physiol Funct Imaging 24:180 189
34. Wojcikowski C, Fussgänger R, Pfeiffer E (1977) Inhibition of insulin and glucagon secretion of the isolated rat pancreas by synthetic human and rat C-peptide. In: Beyer J, Krause U, Naegele W (eds) C-peptide. Schnetzor, Konstanz, pp 75 88
35. Jensen ME, Messina EJ (1999) C-peptide induces a concentration-dependent dilatation of skeletal muscle arterioles only in presence of insulin. Am J Physiol Heart Circ Physiol 45: H1223 H1228
36. Ohtomo Y, Aperia A, Sahlgren B, Johansson BL, Wahren J (1996) C-peptide stimulates rat renal tubular Na^+, $K^{(+)}$-ATPase activity in synergism with neuropeptide Y. Diabetologia 39:199 205
37. Kunt T, Schneider S, Pfutzner A et al (1999) The effect of human proinsulin C-peptide on erythrocyte deformability in patients with type I diabetes mellitus. Diabetologia 42:465 471
38. Vague P, Coste TC, Jannot MF, Raccah D, Tsimaratos M (2004) C-peptide, Na^+,$K^{(+)}$-ATPase, and diabetes. Exp Diabesity Res 5:37 50
39. Forst T, Kunt T (2004) Effects of C-peptide on microvascular blood flow and blood hemorheology. Exp Diabesity Res 5:51 64
40. Alessi MC, Juhan-Vague I (2004) Contribution of PAI-1 in cardiovascular pathology. Arch Mal Coeur Vaiss 97:673 678
41. Juhan-Vague I, Morange PE, Alessi MC (2002) The insulin resistance syndrome: implications for thrombosis and cardiovascular disease. Pathophysiol Haemost Thromb 32:269 273
42. Schafer K, Muller K, Hecke A et al (2003) Enhanced thrombosis in atherosclerosis-prone mice is associated with increased arterial expression of plasminogen activator inhibitor-1. Arterioscler Thromb Vasc Biol 23:2097 2103
43. Steinberg HO, Brechtel G, Johnson A, Fineberg N, Baron AD (1994) Insulin-mediated skeletal muscle vasodilation is nitric oxide dependent. A novel action of insulin to increase nitric oxide release. J Clin Invest 94:1172 1179
44. Chakraborty K, Sinha AK (2004) The role of insulin as an antithrombotic humoral factor. Bioessays 26:91 98
45. Nordt TK, Sawa H, Fujii S, Sobel BE (1995) Induction of plasminogen activator inhibitor type-1 (PAI-1) by proinsulin and insulin in vivo. Circulation 91:764 770
46. Trovati M, Anfossi G (2002) Influence of insulin and of insulin resistance on platelet and vascular smooth muscle cell function. J Diabetes Complications 16:35 40
47. Hu H, Li N, Ekberg K, Johansson BL, Hjemdahl P (2002) Insulin, but not proinsulin C-peptide, enhances platelet fibrinogen binding in vitro in type 1 diabetes mellitus patients and healthy subjects. Thromb Res 106:91 95
48. Hu H, Hjemdahl P, Li N (2002) Effects of insulin on platelet and leukocyte activity in whole blood. Thromb Res 107:209 215
49. Johansson BL, Borg K, Fernqvist-Forbes E, Kernell A, Odergren T, Wahren J (2000) Beneficial effects of C-peptide on incipient nephropathy and neuropathy in patients with type 1 diabetes mellitus. Diabet Med 17:181 189
50. Johansson BL, Borg K, Fernqvist-Forbes E, Odergren T, Remahl S, Wahren J (1996) C-peptide improves autonomic nerve function in IDDM patients. Diabetologia 39:687 695

2.3.3 Darbepoetin-alpha (DPO)

Die Therapie mit Erythropoietin (EPO) wird aufgrund des in Folge erhöhten Hämatokritwertes generell mit prothrombogenen Effekten assoziiert. Die Aussagen verschiedenster Studien der letzten Jahre sind diesbezüglich jedoch sehr widersprüchlich, teilweise wird von einer Blutungsneigung nach Gabe von EPO oder seinen Derivaten berichtet. Ziel der vorliegenden Studie war es daher, den Einfluss von DPO, einem 3-fach länger wirksamen EPO-Derivat, auf mikrovaskuläre Thrombusbildung sowie endotheliale und thrombozytäre Funktion zu charakterisieren.

Die Vorbehandlung mit DPO (10 µg/kg) über 4 Wochen resultierte in einer signifikanten Erhöhung von Hämatokrit, Hämogobinkonzentration und Retikulozytenanteil. Die mikrovaskuläreThrombusformation wurde jedoch nicht signifikant durch DPO beeinflusst. In Übereinstimmung damit zeigten sich eine verminderte Thrombozytenaktivierbarkeit und eine reduzierte endotheliale Aktivierung. Immunhistochemisch und mittels RT-PCR konnte eine signifikante Hochregulation von eNOS im mikrovaskulären Endothel nachgewiesen werden.

In einem zweiten Versuchsschritt wurden daher eNOS -/- Mäuse in gleicher Weise mit DPO behandelt. Bei unbehandelten eNOS -/- Tieren zeigte sich bereits eine geringfügig beschleunigte mikrovaskuläre Thrombusbildung gegenüber unbehandelten Wildtyp-Tieren. Die zusätzliche Vorbehandlung der eNOS -/- Tiere mit DPO führte zu einer signifikanten Beschleunigung der Ausbildung mikrovaskulärer Thrombosen im Vergleich zu DPO behandelten eNOS Wildtyp-Tieren.

Somit führt die chronische Gabe von DPO zur Reduktion der Aktivierung von Thrombozyten und Endothelzellen. Diese Reduktion wird wohl über Hochregulation von eNOS vermittelt, was als kompensatorischer Mechanismus gegenüber der durch Erythropoese und Hämatokriterhöhung bedingten Prothrombogenität von DPO bzw. EPO interpretiert werden kann. Damit ist gezeigt, dass mit chronischer Gabe von EPO bzw. DPO nicht notwendigerweise ein erhöhtes thromboembolisches Risiko gegeben ist, solange eine adäquate eNOS Gegenregulation des Endothels im Sinne von Anti-Thrombogenität gewährleistet ist.

Lindenblatt N, Menger MD, Klar E, Vollmar B

Darbepoetin does not promote microvascular thrombus formation in mice – role of eNOS-dependent protection through platelet and endothelial cell deactivation *Arterioscler Thromb Vasc Biol* 2007; 27: 1191-1198.

Darbepoetin-Alpha Does Not Promote Microvascular Thrombus Formation in Mice

Role of eNOS-Dependent Protection Through Platelet and Endothelial Cell Deactivation

Nicole Lindenblatt, Michael D. Menger, Ernst Klar, Brigitte Vollmar

Objective—Erythropoietin (EPO) treatment has become the standard treatment of renal anemia. Though a link between hematopoiesis-stimulating drugs and thrombosis has not been proven, it is generally assumed that systemic application of EPO and its analogues increases the risk for thrombotic events.

Methods and Results—Here we show in C57BL/6J mice that 4-week treatment with the long-lasting EPO analogue darbepoetin-alpha (DPO) at a dose of 10 μg/kg/week induces a reduction of platelet reactivity using flow cytometry and Western blot analysis of tyrosine-specific platelet phosphorylation. Additionally, immunohistochemistry of endothelial adhesion molecule expression and ELISA of circulating endothelial activation markers demonstrated a reduced endothelial activation. Immunohistochemistry and RT-PCR analysis revealed a significant ($P<0.05$) increase of eNOS expression. Further, DPO did not exert prothrombogenic effects in a murine intravital microscopic thrombosis model of the cremaster muscle. The role of eNOS in prevention of DPO-mediated microvascular thrombosis is further underlined by a significantly accelerated thrombus formation on DPO treatment in eNOS (−/−) mice.

Conclusion—Thus, DPO-related erythropoiesis with a raised hematocrit is not associated with an increased risk for thrombosis as long as endothelial NO production serves as compensatory mechanism. (***Arterioscler Thromb Vasc Biol.* 2007;27:1191-1198.**)

Key Words: endothelium ■ intravital microscopy ■ nitric oxide ■ platelets ■ thrombosis

The glycoprotein hormone EPO is mainly of renal origin and acts by binding to the transmembrane EPO receptor on erythroid progenitors in the bone marrow.[1,2] It increases the number of circulating red blood cells not only by promoting proliferation and differentiation, but mainly by decreasing the rate of apoptotic cell death.[3] The EPO-induced increase of red blood cell mass also increases the oxygen supply to the muscles and aerobic performance, which is the reason why rhuEPO is increasingly exploited in competitive sports.[4] The use of EPO, however, may also be associated with distinct side effects. Although not clearly demonstrated, a relationship between an increased red blood cell count and thrombus formation is generally admitted.

Apart from the increase in hematocrit, EPO has additionally been shown to stimulate endothelial cells, as indicated by activation of signaling pathways, thrombogenic properties and tissue factor production in vitro,[5] and release of plasminogen activator-inhibitor (PAI)-1 in vivo.[6] Besides, experimental and clinical studies have demonstrated that EPO enhances platelet production and reactivity.[7–9] EPO further increases thrombin–antithrombin III complexes[10] and platelet adherence to thrombotic surfaces in vivo.[11] On the other hand, elevated hematocrits are not necessarily associated with increased thrombus formation,[12] and overexpression of EPO has been shown to reduce blood viscosity[13] and to diminish clot formation in in vitro thrombelastography.[14] Additionally, EPO and its analogues seem to exert protective effects in studies of stroke and cerebral ischemia.[15]

Thus, there is no clear evidence whether or not EPO and the EPO-associated erythrocytosis increase the risk of thrombus formation.

Methods

Animals and Materials

Animals

Male C57BL/6J mice and eNOS (−/−) mice (B6.129P2/Nos3, bred on C57BL/6J background) were purchased from Charles River Laboratories, Sulzfeld, Germany.

Chemicals

Darbepoetin-alpha (DPO) was purchased from Amgen (Amgen Inc) and dissolved in physiological saline solution. Thrombin was purchased from Sigma (Sigma-Aldrich) and dissolved in PBS to yield a

Original received December 21, 2006; final version accepted February 22, 2007.

From the Institute for Experimental Surgery (N.L., B.V.) and the Department of General Surgery (N.L., E.K.), University of Rostock, and the Institute for Clinical & Experimental Surgery (M.D.M.), University of Saarland, Germany.

Correspondence to Brigitte Vollmar, MD, Institute for Experimental Surgery, University of Rostock, Schillingallee 69a, 18055 Rostock, Germany. E-mail brigitte.vollmar@med.uni-rostock.de

© 2007 American Heart Association, Inc.

Arterioscler Thromb Vasc Biol. is available at http://www.atvbaha.org DOI: 10.1161/ATVBAHA.107.141580

Downloaded from atvb.ahajournals.org at Bibliothèque Faculte Medecine Geneve on May 28, 2007

20 U/mL stock solution. All solutions were stored at a maximal temperature of −20°C in the dark.

Experimental Groups

For determination of the dose with the maximum erythropoietic effect, animals were pretreated with DPO at a dose of 1 μg/kg bw once per week sc for 4 weeks (DPO1), 10 μg/kg bw once per week sc for 4 weeks (DPO10), and 25 μg/kg bw once per week sc for 4 weeks (DPO25). In addition, acute DPO application was carried out at a dose of 25 μg/kg bw iv 5 minutes before the experiment (aDPO25). Controls received saline (10 mL/kg bw NaCl 1×/week sc for 4 weeks). As a consequence of the maximum effect at a dose of 10 μg/kg bw DPO, the following in vitro and in vivo experiments were studied in saline controls and after chronic DPO10 treatment. Induction of microvascular thrombosis in eNOS (−/−) mice was performed in saline controls (eNOS (−/−): 10 mL/kg bw NaCl once per week sc for 4 weeks) and after chronic DPO10 treatment (eNOS (−/−) + DPO10: 10 μg/kg bw once per week sc for 4 weeks).

Analytical Experiments

Blood Analysis

To determine hematocrit, hemoglobin concentration and fraction of reticulocytes blood was drawn from the retroorbital venous plexus of DPO-treated animals and controls. Hematocrit and hemoglobin concentration were assessed with a Cell Counter (Sysmex KX-21, Sysmex). Reticulocytes were counted (Sysmex XE-2100-SP100) and expressed as percentage of total red blood cell number (%).

Histology and Immunohistochemistry

At the end of each experiment, the cremaster muscle was fixed in 4% phosphate buffered formalin for 2 to 3 days and embedded in paraffin. From the paraffin-embedded tissue blocks, 4-μm sections were cut and stained with hematoxylin-eosin (HE) for histological analysis. For immunohistochemical demonstration of intercellular adhesion molecule-1 (ICAM-1), P-selectin, and eNOS, tissue sections collected on poly-L-lysine-coated glass slides were treated by microwave for antigen unmasking. Goat anti–ICAM-1 (1:200) and anti–P-selectin (1:100) (each Santa Cruz Biotechnology, Heidelberg, Germany) as well as rabbit anti-eNOS (1:50; CalBiochem, San Diego, Calif) were used as primary antibodies and incubated overnight at 4°C, followed by a horseradish peroxidase (HRP)- or alkali phosphatase (AP)-conjugated donkey anti-goat (1:200; Santa Cruz Biotechnology) or AP-conjugated goat anti-rabbit/mouse antibody (1:200; DAKO, Hamburg, Germany) and development using ACE or fuchsin substrate as chromogen. The sections were counterstained with hematoxylin and examined by light microscopy (Zeiss Axioscop 40, Jena, Germany).

ELISA of Circulating Endothelial Markers

Plasma concentrations of circulating, ie, soluble (s) sICAM-1, sVCAM-1, sP-selectin, and sE-selectin were determined using the respective enzyme immunoassay kits (R&D Systems). Blood samples were prepared by centrifugation for 10 minutes at 2000*g* and room temperature (GS-6R Centrifuge, Beckman Coulter).

Preparation of Murine Platelet Rich Plasma

For in vitro testing of platelet function, animals were pretreated either with saline or DPO10 according to the experimental protocol. Then 0.5 to 1 mL blood was drawn from the retroorbital venous plexus of DPO-treated and control mice with 1.5 cm glas capillaries and collected into a tube containing 300 μL Tyrode buffer solution (TBS) and heparin (20 U/mL). The sample was centrifuged for 5 minutes at 750*g*, followed by recentrifugation of the supernatant for 6 minutes at 150*g*, yielding platelet rich plasma (PRP). PRP was centrifuged again for 5 minutes at 1825*g* and the cell pellet was resuspended in 1 mL TBS with 1 μmol/L prostacyclin and 10 U/mL heparin for subsequent incubation at 37°C for 10 minutes. Centrifugation (5 minutes at 1825*g*) and resuspension was repeated twice. Finally, the platelet pellet was resuspended in 450 μL TBS with 2 μL apyrase.[16] Platelet suspensions were transferred into a 37°C water bath for 30 minutes of resting in order to eliminate isolation-induced platelet activation.

Flowcytometric Analysis of P-Selectin Expression

For evaluation of receptor expression under resting conditions, 5 μL of specific rat anti-mouse P-selectin (Emfret Analytics) or negative control antibody were incubated with 25 μL platelet suspension for 15 minutes at room temperature. The reaction was stopped by addition of 400 μL PBS and analyzed within 30 minutes. For evaluation of receptor expression on stimulation, the same set of experiments was carried out after exposure to thrombin for maximal platelet activation (20 U/mL).

FACScan flowcytometer (Becton Dickinson) was calibrated with fluorescent standard microbeads (CaliBRITE Beads, Becton Dickinson) for accurate instrument setting. Platelets were identified by their characteristic forward and sideward scatter light and selectively analyzed for their fluorescence properties using the CellQuest program (Becton Dickinson) with assessment of 20 000 events per sample. The relative fluorescence intensity of a given sample was calculated by subtracting the signal obtained when cells were incubated with the isotype specific control antibody from the signal generated by cells incubated with the test antibody.

Western Blot Analysis of Tyrosine-Specific Phosphorylation of Platelet Proteins

For whole protein extracts and Western blot analysis of phosphotyrosine (p-Tyr) PRP was prepared as described above. After 30 minutes of resting in a 37°C water bath 50 μL of platelet suspensions from DPO-treated and control animals were analyzed in resting state and at 30 minutes after exposure to thrombin (20 U/mL). The platelets were lysed for 30 minutes on ice (extraction buffer: 50 mmol/L HEPES pH 7.4, 1% Triton-100, 0.15 mol/L NaCl, 10% glycerol, 1.5 mmol/L $MgCl_2$, 1 mmol/L EDTA, 1 mmol/L Na_3NO_4, 10 mmol/L $Na_4P_2O_7$, 1 mmol/L AEBSF, 10 mmol/L NaF, 10 mg/L aprotinin, 10 mg/L leupeptin) and centrifuged for 15 minutes at 10 000*g*. Before use, all buffers received a protease inhibitor cocktail (1:100 v/v; Sigma). Protein concentrations were determined using the bicinchoninic acid (BCA) protein assay (Sigma) with bovine serum albumin as standard. 20 μg protein/lane were separated discontinuously on sodium dodecyl sulfate polyacrylamide gels (10% SDS-PAGE) and transferred to a polyvinyldifluoride membrane (Immobilon-P, Millipore). After blockade of nonspecific binding sites, membranes were incubated for 1 hour at room temperature with a HRP-conjugated mouse monoclonal anti–p-Tyr antibody (PY20) (1:1000; Santa Cruz Biotechnology). Protein expression was visualized by means of luminol enhanced chemiluminescence (ECL plus; Amersham Pharmacia Biotech) and exposure of the membrane to a blue light sensitive autoradiography film (Kodak BioMax Light Film, Kodak-Industrie). Signals were densitometrically assessed (Quantity One, Gel Doc XR, Bio-Rad Laboraties GmbH).

RT-PCR of eNOS in Cremaster Muscle Tissue

Total RNA from cremaster muscles was isolated using the RNeasy Mini Kit (Quiagen) according to the manufacturer's instructions. RNA concentration was determined spectrophotometrically. cDNA was prepared by reverse transcription of 1 μg of total RNA using oligo $(dT)_{18}$ primer (Biolabs) and Superscript II RNaseH-Reverse Transcriptase (Invitrogen). Mouse endothelial nitric oxide synthetase (eNOS; 292 bp) was amplified by 35 cycles of PCR using *Taq*DNA polymerase (Amersham Bioscience) and the following intron-spanning primers: 5′-AAG ACA AGG CAG CGG TGG AA-3′ and 5′-GCA GGG GAC AGG AAA TAG TT-3′. In a comparable assay, the RNA integrity and cDNA synthesis was tested using mouse GAPDH as a house keeping gene and the following primers: 5′-AAC GAC CCC TTC ATT GAC-3′ and 5′-TCC ACG ACA TAC trichloroacetic acid (TCA) GCA C- 3′. In parallel, controls with H_2O instead of DNA were carried out for every PCR reaction. PCR products were separated by electrophoresis on 2.0% agarose gels. Ethidium-bromide stained bands were visualized by UV-illumination and densitometrically quantified (Quantity One).

Downloaded from atvb.ahajournals.org at Bibliotheque Faculte Medecine Geneve on May 28, 2007

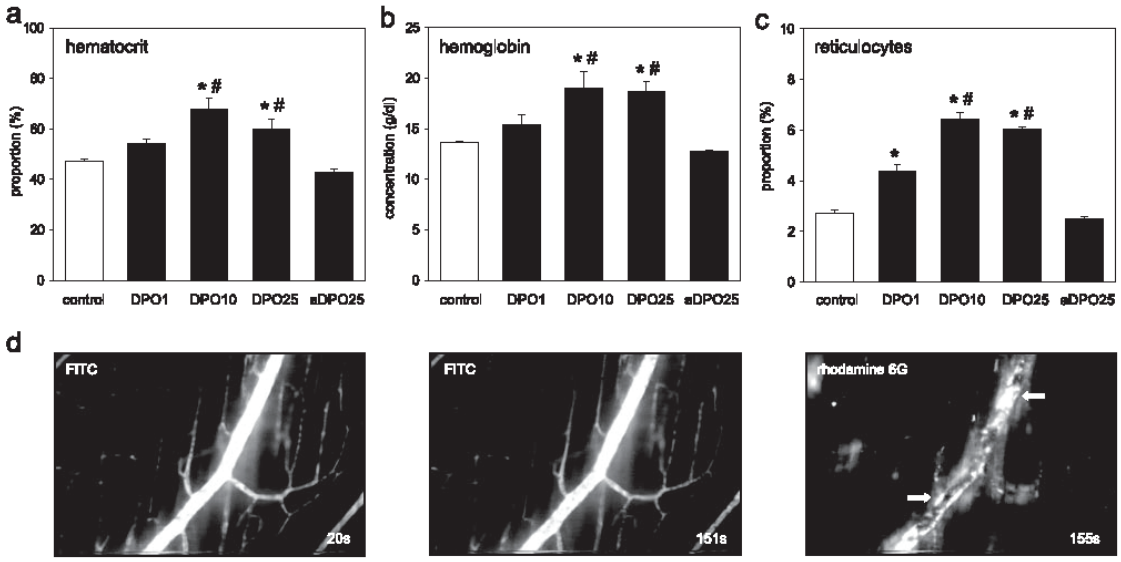

Figure 1. Hematocrit (a), hemoglobin concentration (b), and fraction of reticulocytes (c) of saline controls and on chronic and acute DPO treatment. d, Intravital fluorescence microscopy of cremaster muscle microcirculation showing a growing venular thrombus (arrows; ×200 magnification). Chronic DPO application at a dose of 10 μg/kg bw resulted in a maximal increase of hematocrit, hemoglobin concentration, and reticulocyte fraction and therefore was chosen as treatment dose for subsequent experiments. Values are given as means±SEM; *$P<0.05$ vs control; #$P<0.05$ vs DPO1.

In Vivo Experiments

Mouse Cremaster Muscle Preparation

For the study of vascular thrombus formation in vivo, we used the opened cremaster muscle preparation, as originally described by Baez in rats[17] and used as a model of microvascular thrombus formation in previous studies.[18] On approval by the local government, all experiments were carried out in accordance with the German legislation on protection of animals and the National Institutes of Health *Guide for the Care and Use of Laboratory Animals* (Institute of Laboratory Animal Resources, National Research Council). Male C57BL/6J mice with a body weight (bw) of 20 to 25 g were anesthetized by an intraperitoneal injection of ketamine (90 mg/kg bw) and xylazine (25 mg/kg bw). We intended to study the effects of chronic administration of DPO on endothelial and platelet functions in hemostasis. For chronic exposure mice were injected with DPO10. The DPO dose was chosen based on the dose-finding experiments and on prior reports in animal studies.[15] Control mice received saline sc corresponding to the fluid amount applied in the verum experiments.

Before the preparation of the cremaster muscle animals were placed on a heating pad coupled to a rectal temperature probe. A midline incision of the skin and fascia was made over the ventral aspect of the scrotum and extended up to the inguinal fold and to the distal end of the scrotum. The incised tissues were retracted to expose the cremaster muscle sack that was maintained under gentle traction to carefully separate the remaining connective tissue by blunt dissection from around the cremaster sack. Then, the cremaster muscle was incised avoiding to cut the larger anastomosing vessels. Hemostasis was achieved with 5–0 threads serving also to spread the tissue. After dissection of the vessel connecting the cremaster and the testis, the epididymis and testis were put to the side of the preparation. The preparation was performed on a transparent pedestal to allow microscopic observation of the cremaster muscle microcirculation by both transillumination and epi-illumination techniques.

After the preparation of the cremaster muscle, the animals were allowed to recover from surgical preparation for 15 minutes. Fluorescent dyes were injected via the retroorbital venous plexus. Then, thrombus formation was induced in randomly chosen venules (n=1 to 2 per preparation) and arterioles (n=1 to 2 per preparation).

Thrombosis Model

After iv injection of 0.1 mL 2% fluorescein isothiocyanate (FITC)-labeled dextran (MW 150000, Sigma-Aldrich) and 0.05 mL 0.2% rhodamine 6G (MW 476, Sigma) and subsequent circulation for 30 seconds, the cremaster muscle microcirculation was visualized by intravital fluorescence microscopy using a Zeiss microscope (Zeiss Axiotech Vario; Figure 1d). The microscopic procedure was performed at a constant room temperature of 22°C. The epi-illumination setup included a 100 W HBO mercury lamp and an illuminator equipped with a blue filter (450 to 490 nm/>520 nm excitation/emission wavelengths). Microscopic images were recorded by a charge-coupled device (CCD) video camera (FK 6990A-IQ, Pieper) and stored on videotapes for off-line evaluation (S-VHS Panasonic AG 7350-E, Matsushita). Using a ×20 water immersion objective (Achroplan ×20/0.50 W, Zeiss) blood flow was monitored in individual arterioles (diameter range 30 to 50 μm) and venules (diameter range 60 to 80 μm), followed by superfusion with 25 μL ferric chloride (12.5 mmol/L; Sigma) for induction of microvascular thrombosis.[18,19] Blood flow velocities were about 1700 to 1900 μm/s for arterioles and 600 to 700 μm/s for venules with no significant differences between the groups studied. Wall shear rates were 160 to 200 s^{-1} for arterioles and 50 to 60 s^{-1} for venules, respectively. Recording of vessels was discontinued after blood flow in the vessel ceased for at least 60 seconds because of complete vessel occlusion. As rapid spreading of ferric chloride solution allowed studying only 1 to 2 arterioles and venules within each preparation, both left and right cremaster muscles were prepared for analysis of thrombotic vessel occlusion within each animal.

Analysis included the time periods until first standstill of perfusion and sustained cessation of blood flow because of complete vessel occlusion. Microcirculatory analysis further included the determination of vessel diameter and red blood cell (RBC) velocity before thrombus induction with calculation of vascular wall shear rates, based on the Newtonian definition $\gamma=8\times V/D$, with V representing the red blood cell centerline velocity divided by 1.6, according to the

Downloaded from atvb.ahajournals.org at Bibliotheque Faculte Medecine Geneve on May 28, 2007

TABLE 1. Red Blood Cell (RBC) Velocity (μm/s), Vessel Diameter (μm), and Wall Shear Rates (γ; s^{-1}) in Arterioles and Venules of the Cremaster Muscle Before Induction of Thrombus Formation and Complete Occlusion Times (s) of Arterioles and Venules Upon Ferric Chloride–Induced Thrombus Formation in Saline Controls and DPO10-Treated Animals

	Arterioles			Venules		
	Control	DPO10	*P*	Control	DPO10	*P*
RBC velocity	1842±360	1700±342	0.53	637±89	633±73	0.92
Vessel diameter	48±5	44±4	0.78	60±5	60±3	0.97
Wall shear rate	200±44	205±49	0.94	56±9	54±7	0.92
Complete occlusion time	627±148	1044±146	0.07	573±146	861±145	0.19

Values are given as means±SEM.

Baker–Wayland factor[20] and D representing the individual inner vessel diameter.

Subaquatic Tail Bleeding Time

Subaquatic bleeding time was measured after standardized dissection of the tail tip. The tail was cut at a diameter of 0.15 mm and placed in 37°C 0.9% saline solution. Time until cessation of blood flow was determined.

Statistical Analysis

After proving the assumption of normality and equal variance across groups, differences between groups were assessed using 1-way ANOVA followed by the appropriate post-hoc comparison test. All data revealed normal distribution and were expressed as means±SEM and overall statistical significance was set at $P<0.05$. Statistics and graphics were performed using the software packages SigmaStat and SigmaPlot (Jandel Corporation).

Results and Discussion

To study the role of EPO in microvascular thrombosis in vivo we performed intravital fluorescence microscopic studies of the cremaster muscle preparation in male C57BL/6J mice. Microvascular thrombus formation was induced in arterioles and venules by ferric-chloride superfusion. Before the experiments, mice were injected with DPO1 (n=4 animals), DPO10 (n=4 animals), and DPO25 (n=3 animals) chronically and with aDPO25 (n=3 animals) 5 minutes before the experiment to define the dosage with the maximal hematopoetic effect in this model. Control mice received injections of physiological saline. As a consequence of DPO pretreatment hematocrit (Figure 1a), hemoglobin concentrations (Figure 1b) and fraction of reticulocytes (Figure 1c) increased with a maximum effect at a dose of 10 μg/kg bw (DPO 10). Thus, the hematopoetic response of mice to DPO application can be considered as saturable in C57BL/6J mice. Of note, the hemoglobin concentration of animals treated with DPO10 was comparable to that seen in humans after EPO treatment and above the cut-off values of 16 g/dL (females) and 17 g/dL (males) accepted by the International Ski Federation (FIS).[21] Based on these facts, the dose DPO10 was chosen for the subsequent experiments. Surprisingly, times until complete vessel occlusion after ferric chloride superfusion in these animals (n=7 preparations) were not reduced in cremaster muscle arterioles and venules when compared with controls (n=7 preparations), but rather tended to be prolonged (Table 1). This result is in line with studies of the past, describing no effect of EPO treatment on coagulation and fibrinolysis in elective hip surgery[22] and no prothrombogenic effects of uremic media on endothelial cells in the presence of EPO.[23] Moreover, an in vitro study investigating the effect of hematocrits between 20 and 55% on hemostasis as well as platelet and fibrin accumulation into a collagen-coated tube under different flow conditions showed no dependence of thrombus growth on hematocrit under high shear stress and even a reduced thrombus formation at high hematocrits under low flow conditions.[12] On the other hand, data concerning therapeutic hemodilution indicate beneficial effects of a reduced hematocrit on microcirculation in general[24] and in particular on thrombotic microvessel occlusion per se[25] and after microsurgery.[26,27] However, a study investigating the effect of the hematocrit during deep hypothermic bypass on cerebral microcirculation in piglets revealed a significantly higher functional capillary density and number of rolling leukocytes at a hematocrit of 30% versus 10%.[28] Our results indicate that microvascular thrombus formation is not increased at high hematocrits exceeding 60% after DPO treatment. Moreover, despite a significantly raised hematocrit in the DPO10 group (Figure 1a), rheological parameters (RBC velocity, vessel diameter, wall shear rate) were comparable to controls implying the absence of detrimental effects of the DPO-related raised hematocrit on the microcirculation (Table 1). Thus, the lack of susceptibility for thrombosis and the unchanged rheological parameters despite a significantly raised hematocrit following DPO application may probably be attributable to protective intrinsic properties of DPO.

To further elucidate the effects of DPO on thrombus formation in vivo we studied the subaquatic tail bleeding time as parameter for platelet-associated hemostasis. With bleeding times of 188±20 seconds in controls and 190±17 seconds in DPO10-treated animals, we confirmed that the coagulative status is not increased on DPO.

Because the vascular endothelial function plays a major role in thrombogenesis, we further were interested in the mechanisms of modulation of endothelial function attributable to chronic DPO treatment. Stohlawetz et al reported substantial activation of endothelial cells as a consequence of treatment with rhuEPO in humans[9] and Quaschning et al observed a significant activation of the endothelin system.[29] On the other hand, EPO might have potential beneficial effects on the endothelium including antiapoptotic, mitogenic, and angiogenic activities, which may enhance overall cardiac function.[30] To further address this issue, we determined the circulation of soluble endothelial activation mark-

Downloaded from atvb.ahajournals.org at Bibliotheque Faculte Medecine Geneve on May 28, 2007

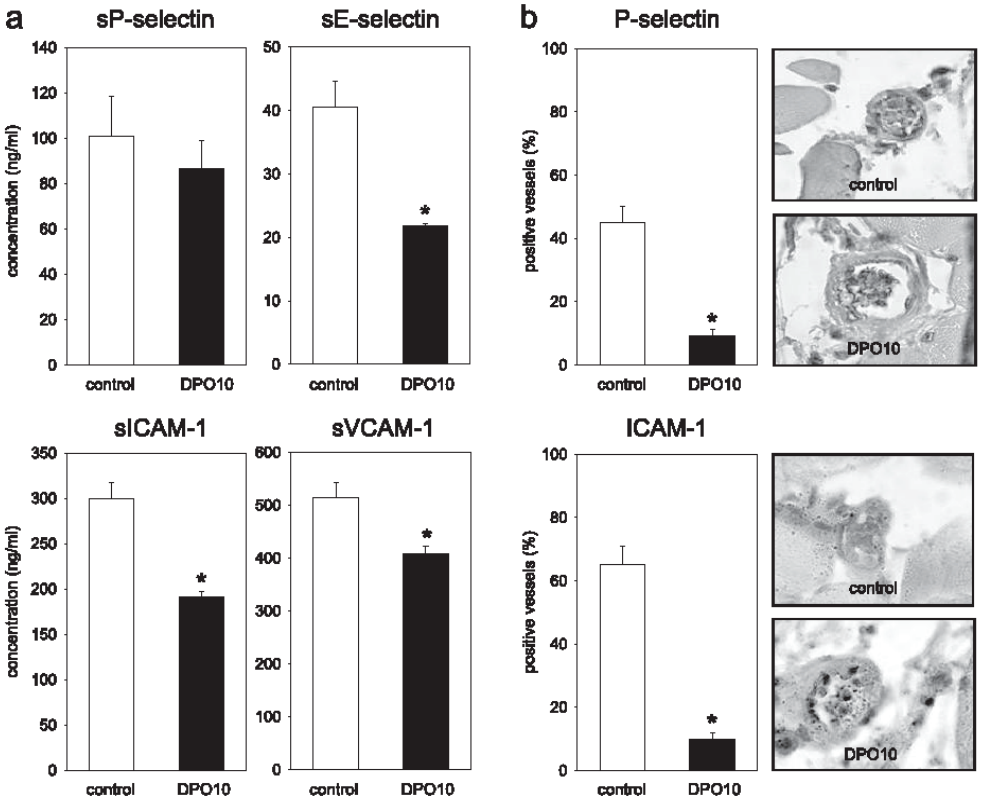

Figure 2. a, Plasma concentrations of circulating sP-selectin, sE-selectin, sICAM-1, and sVCAM-1 in saline controls and DPO10-treated animals. We found a significant reduction of sE-selectin, sICAM-1, and sVCAM-1 after chronic DPO treatment, when compared with controls. b, Analysis of the endothelial expression of P-selectin and ICAM-1 in saline controls and DPO10-treated animals. Quantitative analysis of immunohistochemistry was carried out and expressed as percentage of positively stained vessels within the cremaster muscle tissue, revealing a significant reduction of P-selectin and ICAM-1 expression after chronic application of DPO. Values are given as means±SEM. *$P<0.05$ vs control.

ers in plasma samples of DPO10-treated (n=4 animals each) and control (n=6 animals each) mice. In general, DPO pretreatment lead to a reduction of endothelial activation, represented by a moderate decrease of sP-selectin and a significant decline of sE-selectin, sICAM-1, and sVCAM-1 in murine plasma (Figure 2a). Immunohistochemical staining of cremaster muscle sections confirmed a significant downregulation of P-selectin and ICAM-1 on the vascular endothelium after DPO10 application (n=6 specimens per group) when compared with controls (n=6 specimens per group; Figure 2b). Thus, DPO10 treatment for 4 weeks appears to reduce endothelial activation, which correlates with the prolongation in time until complete thrombotic vessel occlusion in vivo.

Next to the endothelial dysfunction, platelet activation and subsequent aggregation is an important factor in microvascular perfusion failure and thrombus formation. Wolf at al suggested that hyperreactive platelets are responsible for a prothrombotic effect of EPO in an arteriovenous shunt model in dogs.[11] Also, a study investigating the effect of EPO infusion in healthy human volunteers could demonstrate a 10% to 20% increased platelet count and a 2- to 3-fold increased expression of P-selectin during EPO treatment.[9] On the other hand, thrombocytopenia has been reported after EPO treatment, suggesting a reduced tendency for clot formation.[8] Thus, we further studied the effect of DPO on platelet count and platelet reactivity. Platelet numbers in the peripheral blood did not increase after DPO10 treatment when compared with controls (561±69 versus 558±17×10^9/L). In addition, there were no marked differences in spontaneous platelet activation. However, on thrombin stimulation flow cytometric analyses revealed a reduced expression of P-selectin on platelets from DPO10-treated mice when compared with platelets of controls (Figure 3a). Further, tyrosine-specific phosphorylation in platelets of DPO10-treated animals was found reduced, indicating a dampening effect of DPO on platelet reactivity (Figure 3b). Thus, reduced agonist-induced platelet reactivity might further contribute to the fact that DPO treatment does not boost microvascular thrombus formation in our study. However, in light of the fact that previous studies in humans and dogs showed discrepant findings, species-related differences of platelet response to EPO and its derivatives might exist.

In a next step we intended to define the mechanisms for this unexpected finding. Several studies in EPO-overexpressing

Downloaded from atvb.ahajournals.org at Bibliotheque Faculte Medecine Geneve on May 28, 2007

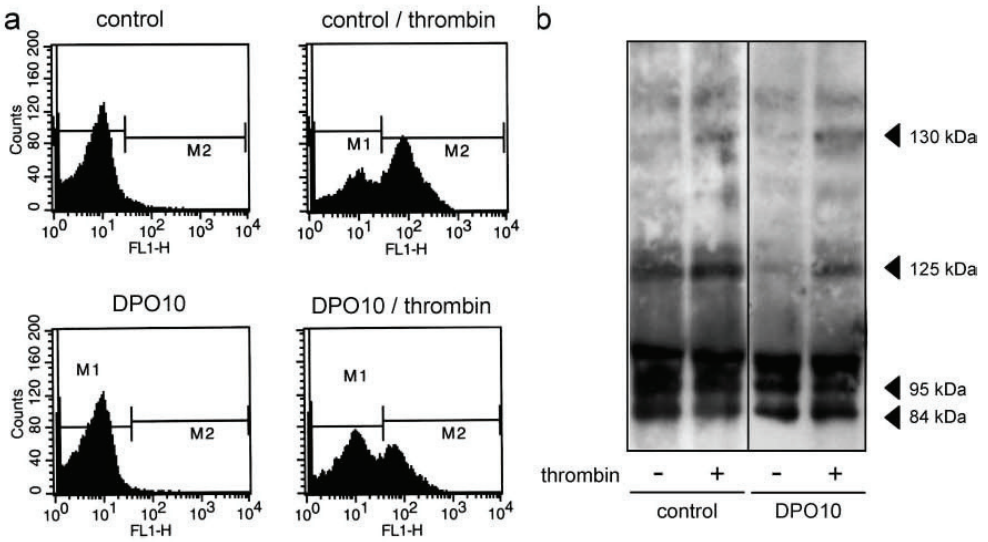

Figure 3. a, Flow cytometric analysis (representative histograms) of platelet P-selectin expression after pretreatment with saline and DPO10. Note the reduced expression of P-selectin on the platelet surface as a result of chronic DPO application under resting conditions, but in particular on stimulation by thrombin (20 U/mL). b, Representative Western blot of tyrosine-specific protein phosphorylation in platelets. The arrowheads denote the most prominent protein bands, migrating with a molecular mass of 84 kDa, 95 kDa, 125 kDa, and 130 kDa. Protein phosphorylation was found to be markedly reduced in platelets of DPO-treated animals.

transgenic mice with a hematocrit of about 80% revealed new aspects of EPO-associated alterations of physiological functions. Simply the fact that these mice were viable already contradicted the assumption that such a high hematocrit invariably results in thromboembolic complications. However, immunohistological studies of the brain revealed increased infarct volumes in these polyglobulic mice after permanent occlusion of the middle cerebral artery.[31] In contrast to these findings, subsequent studies showed a reduced plasmatic coagulation activity in vitro, increased bleeding times, and no evidence of microthrombosis in several organs of these transgenic mice.[14] Finally, it was demonstrated that eNOS levels, NO-mediated endothelial-dependent relaxation, as well as circulating and vascular tissue NO were significantly increased, which was regarded as a protective mechanism, counteracting a potentially increased risk of thrombosis.[32] Therefore, we studied whether exogenous application of DPO might also increase eNOS expression in our model. EPO has been shown to stimulate eNOS expression with the consequence of raised NO production in vitro,[33] but in vivo studies linking this effect to a reduced thrombus formation are missing. To verify, whether DPO influences endothelial expression of NOS, we performed immunohistology of the cremaster muscle. eNOS expression in the vascular endothelium was significantly increased after chronic DPO10 treatment (n=6 specimens per group) when compared with controls (Figure 4a). These results could be confirmed by RT-PCR (Figure 4b). We hypothesized that chronic DPO application itself, or the DPO-associated rise of hematocrit leads to an increase of eNOS production with the consequence of antiadhesive and antithrombogenic effects, resulting in a decrease of endothelial and platelet activation. To further delineate the potential protective effects of eNOS in this setting, we performed additional in vivo experiments in B6 background B6.129P2/Nos3 knock out mice (eNOS −/−), which were also pretreated with DPO10 (eNOS (−/−)+ DPO10; n=6 preparations). Control animals received saline (eNOS (−/−); n=6 preparations) as described above. Interestingly, eNOS (−/−) mice responded to the chronic DPO treatment only with a mild increase of hematopoetic parameters when compared with saline-treated eNOS (−/−) controls (Table 2). The preferential mechanism by which EPO maintains and increases erythropoiesis is the prevention of apoptosis of erythropoietic progenitor cells.[3] Because the physiological continuous production of NO by eNOS has been identified as an antiapoptotic factor in the past,[34–37] the weak effect of exogenous DPO application in eNOS (−/−) on erythropoiesis may be explained by a generally proapoptotic state. Therefore it might be assumed that a lack of eNOS activity leads to a reduction of erythrocyte progenitor cell proliferation and differentiation capacity. Platelet count in eNOS (−/−) mice tended to be higher than in wild-type mice, and additional DPO treatment resulted in a small, but not significant, increase.

In vivo, saline-treated eNOS (−/−) animals revealed slightly accelerated thrombosis times in arterioles and venules (574±124 seconds and 384±166 seconds) when compared with wild-type control mice (627±148 seconds; $P=0.78$ and 573±146 seconds; $P=0.42$). Moreover in eNOS (−/−) mice, thrombotic vessel occlusion in venules tended to occur faster than in arterioles (384±166 seconds versus 574±124 seconds; $P=0.37$). This seems to be in line with previous observations of Broeders and coworkers that the role of endogenous NO in inhibiting thromboembolic processes is more important in venules than in arterioles.[38] In a later study by this group, it was shown that NO and prostaglandins in turn synergistically counteract thromboembolism in arterioles, but not in venules, and that the combination of

Downloaded from atvb.ahajournals.org at Bibliotheque Faculte Medecine Geneve on May 28, 2007

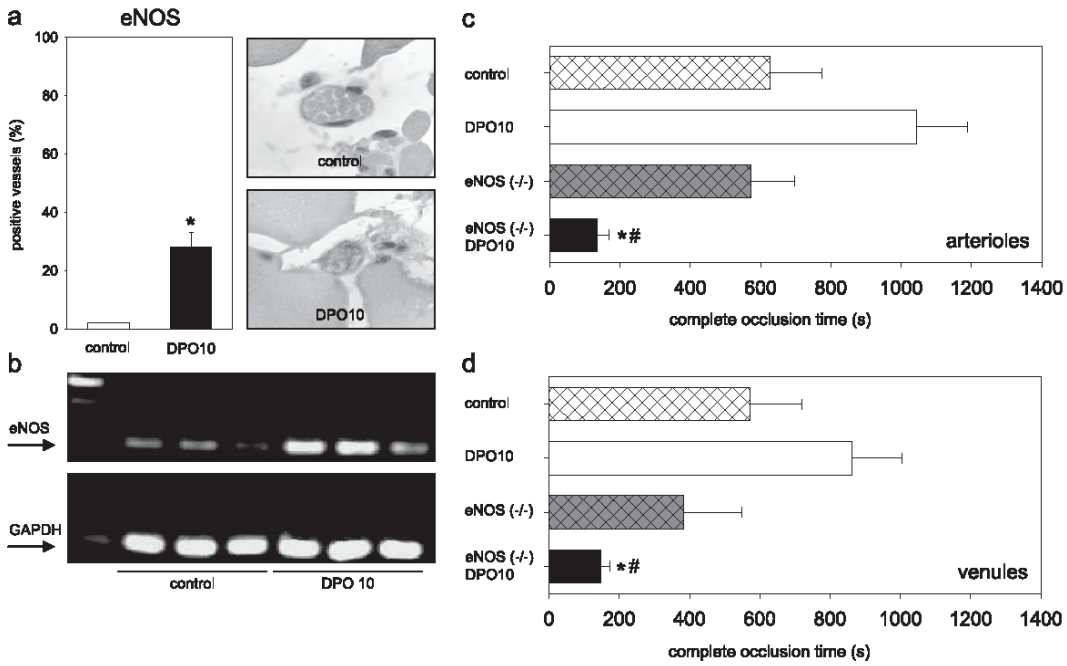

Figure 4. a, Immunohistochemical analysis of eNOS expression in controls and DPO10-treated animals. eNOS expression in the vascular endothelium was significantly increased after chronic DPO treatment. b, RT-PCR of eNOS in cremaster muscle tissue of saline- and DPO10-treated animals. Chronic treatment with DPO induced a marked increase of eNOS mRNA transcripts (292 bp, upper panel) in comparison to controls. Mouse GAPDH was coamplified as internal control (191 bp, lower panel). c and d, Occlusion times of arterioles and venules in wild-type and eNOS (−/−) mice on ferric chloride–induced thrombus formation in saline controls and after chronic DPO10 treatment. Values are given as means±SEM. *$P<0.05$ vs eNOS (−/−), #$P<0.05$ vs DPO10. While eNOS (−/−) control mice already revealed slightly accelerated thrombosis times when compared with wild-type controls, we found a significant prothrombogenic effect of additional chronic DPO treatment in eNOS (−/−) mice.

endogenous NO and prostaglandins appears to protect against enhancement of arteriolar thromboembolism by wall shear.[39] Thus, next to faster thrombotic occlusion attributable to a generally lower RBC velocity in venules, a synergistic effect of NO and prostaglandins in arterioles may also be responsible for differences in arteriolar and venular occlusion times in eNOS (−/−) mice.

Interestingly, additional DPO treatment for 4 weeks significantly decreased the time until complete vessel occlusion in both arterioles (135±34 seconds; $P=0.004$ versus eNOS (−/−)) and venules (148±25 seconds; $P=0.04$ versus eNOS (−/−)) identifying the eNOS-dependent NO production as the crucial compensatory mechanism preventing thrombosis during DPO treatment (Figure 4c and d).

We conclude from these data that DPO-associated eNOS production with platelet and endothelial cell deactivation counteracts prothrombotic actions during DPO treatment.

TABLE 2. Hematocrit (%), Hemoglobin Concentration (g/dL), Reticulocyte Fraction (%), and Platelet Count (×10⁹/L) in Saline-Treated eNOS (−/−) Mice (control) and eNOS (−/−) Mice, That Were Pretreated With DPO Chronically at a Dose of 10 μg/kg bw (eNOS (−/−) + DPO 10)

	eNOS (−/−) control	eNOS (−/−) + DPO10	*P*
Hematocrit	45±1	47±2	0.16
Hemoglobin concentration	12.7±0.4	14.1±0.6	0.13
Reticulocyte fraction	2.4±0.1	2.4±0.2	0.99
Platelet count	760±247	932±208	0.63

Values are given as means±SEM.

Acknowledgments

The authors kindly thank Berit Blendow, Doris Butzlaff, Dorothea Frenz, Maren Nerowski, and Kathrin Sievert from the Institute for Experimental Surgery, University of Rostock, for their excellent technical assistance.

Sources of Funding

This study is supported by a grant from the Deutsche Forschungsgemeinschaft, Bonn-Bad Godesberg, Germany (VO 450/10-1).

Disclosures

None.

References

1. Krantz SB. Erythropoietin. *Blood.* 1991;77:419–434.
2. Jelkmann W. Molecular biology of erythropoietin. *Intern Med.* 2004;43:649–659.
3. Fisher JW. Erythropoietin: Physiology and pharmacology update. *Exp Biol Med.* 2003;228:1–14.
4. Bham B. Unhealthy competition. *EMBO Reports.* 2003;4:927–929.
5. Fuste B, Serradell M, Escolar G, Cases A, Mazzara R, Castillo R, Ordinas A, Diaz-Ricart M. Erythropoietin triggers a signaling pathway in endo-

Downloaded from atvb.ahajournals.org at Bibliotheque Faculte Medecine Geneve on May 28, 2007

thelial cells and increases the thrombogenicity of their extracellular matrices in vitro. *Thromb Haemost*. 2002;88:678–685.
6. Borawski J, Mysliwiec M. Effects of recombinant erythropoietin therapy on circulating endothelial markers in hemodialysis patients. *Clin Appl Thromb Hemost*. 2002;8:77–84.
7. Wolf RF, Peng J, Friese P, Gilmore LS, Burstein SA, Dale GL. Erythropoietin administration increases production and reactivity of platelets in dogs. *Thromb Haemost*. 1997;78:1505–1509.
8. Beguin Y. Erythropoietin and platelet production. *Haematologica*. 1999; 84:541–547.
9. Stohlawetz PJ, Dzirlo L, Hergovich N, Lackner E, Mensik C, Eichler HG, Kabrna E, Geissler K, Jilma B. Effects of erythropoietin on platelet reactivity and thrombopoiesis in humans. *Blood*. 2000;95:2983–2989.
10. Taylor JE, McLaren M, Henderson IS, Belch JJ, Stewart WK. Prothrombotic effect of erythropoietin in dialysis patients. *Nephrol Dial Transplant*. 1992;7:235–239.
11. Wolf RF, Gilmore LS, Friese P, Downs T, Burstein SA, Dale GL. Erythropoietin potentiates thrombus development in a canine arteriovenous shunt model. *Thromb Haemost*. 1997;77:1020–1024.
12. Cadroy Y, Hanson SR. Effects of red blood cell concentration on hemostasis and thrombus formation in a primate model. *Blood*. 1990;75: 2185–2193.
13. Vogel J, Kiessling I, Heinicke K, Stallmach T, Ossent P, Vogel O, Aulmann M, Frietsch T, Schmid-Schonbein H, Kuschinsky W, Gassmann M. Transgenic mice overexpressing erythropoietin adapt to excessive erythrocytosis by regulating blood viscosity. *Blood*. 2003;102: 2278–2284.
14. Shibata J, Hasegawa J, Siemens HJ, Wolber E, Dibbelt L, Li D, Katschinski DM, Fandrey J, Jelkmann W, Gassmann M, Wenger RH, Wagner KF. Hemostasis and coagulation at a hematocrit level of 0.85: functional consequences of erythrocytosis. *Blood*. 2003;101:4416–4422.
15. Belayev L, Khoutorova L, Zhao W, Vigdorchik A, Belayev A, Busto R, Magal E, Ginsberg MD. Neuroprotective effect of darbepoetin alfa, a novel recombinant erythropoietic protein, in focal cerebral ischemia in rats. *Stroke*. 2005;36:1071–1076.
16. Nieswandt B, Schulte V, Bergmeier W. Flow-cytometric analysis of mouse platelet function. *Methods Mol Biol*. 2004;272:255–268.
17. Baez S. An open cremaster muscle preparation for the study of blood vessels by in vivo microscopy. *Microvasc Res*. 1973;5:384–394.
18. Lindenblatt N, Bordel R, Schareck W, Menger MD, Vollmar B. Vascular heme oxygenase-1 induction suppresses microvascular thrombus formation in vivo. *Arterioscler Thromb Vasc Biol*. 2004;24:601–606.
19. Denis C, Methia N, Frenette PS, Rayburn H, Ullman-Cullere M, Hynes RO, Wagner DD. A mouse model of severe von Willebrand disease: defects in hemostasis and thrombosis. *Proc Natl Acad Sci U S A*. 1998; 95:9524–9529.
20. Baker M, Wayland H. On-line volume flow rate and velocity profile measurement for blood in microvessels. *Microvasc Res*. 1974;7:131–143.
21. Rentzsch R Bad Blood. News@Nature (20.02.06).
22. Hasegawa Y, Takamatsu J, Iwase T, Iwasada S, Kitamura S, Iwata H. Effects of recombinant human erythropoietin on thrombosis and fibrinolysis in autologous transfusion for hip surgery. *Arch Orthop Trauma Surg*. 1999;119:384–387.
23. Fuste B, Diaz-Ricart M, Cases A, Lopez-Pedret J, Ordinas A, Escolar G. Erythropoietin does not modify the prothrombotic effect induced by uremic media on endothelial cells. *Haematologica*. 2002;87:1006–1008.
24. Klar E, Herfarth C, Messmer K. Therapeutic effect of isovolemic hemodilution with dextran 60 on the impairment of pancreatic microcirculation in acute biliary pancreatitis. *Ann Surg*. 1990;211:346–353.
25. Frost-Arner L, Bergqvist D. Effect of isovolemic hemodilution with dextran and albumin on thrombus formation in artificial vessel grafts inserted into the abdominal aorta of the rabbit. *Microsurgery*. 1995;16: 357–361.
26. Farina JA Jr., Piccinato CE, Campos AD, Rossi MA. Comparative study of isovolemic hemodilution with 3% albumin, dextran-40, and prophylactic enoxaparin (LMWH) on thrombus formation at venous microanastomosis in rats. *Microsurgery*. 2006;26:456–464.
27. Atchabahian A, Masquelet AC. Experimental prevention of free flap thrombosis. II: Normovolemic hemodilution for thrombosis prevention. *Microsurgery*. 1996;17:714–716.
28. Duebener LF, Sakamoto T, Hatsuoka S, Stamm C, Zurakowski D, Vollmar B, Menger MD, Schafers HJ, Jonas RA. Effects of hematocrit on cerebral microcirculation and tissue oxygenation during deep hypothermic bypass. *Circulation*. 2001;104(12 Suppl 1):I260–264.
29. Quaschning T, Ruschitzka F, Stallmach T, Shaw S, Morawietz H, Goettsch W, Hermann M, Slowinski T, Theuring F, Hocher B, Luscher TF, Gassmann M. Erythropoietin-induced excessive erythrocytosis activates the tissue endothelin system in mice. *FASEB J*. 2003;17:259–261.
30. Smith KJ, Bleyer AJ, Little WC, Sane DC. The cardiovascular effects of erythropoietin. *Cardiovasc Res*. 2003;59:538–548.
31. Wiessner C, Allegrini PR, Ekatodramis D, Jewell UR, Stallmach T, Gassmann M. Increased cerebral infarct volumes in polyglobulic mice overexpressing erythropoietin. *J Cereb Blood Flow Metab*. 2001;21: 857–864.
32. Ruschitzka FT, Wenger RH, Stallmach T, Quaschning T, de Wit C, Wagner K, Labugger R, Kelm M, Noll G, Rulicke. T, Shaw S, Lindberg RL, Rodenwaldt B, Lutz H, Bauer C, Luscher TF, Gassmann M. Nitric oxide prevents cardiovascular disease and determines survival in polyglobulic mice overexpressing erythropoietin. *Proc Natl Acad Sci U S A*. 2000;97:11609–11613.
33. Beleslin-Cokic BB, Cokic VP, Yu X, Weksler BB, Schechter AN, Noguchi CT. Erythropoietin and hypoxia stimulate erythropoietin receptor and nitric oxide production by endothelial cells. *Blood*. 2004; 104:2073–2080.
34. Dimmeler S, Zeiher AM. Nitric oxide and apoptosis: another paradigm for the double-edged role of nitric oxide. *Nitric Oxide*. 1997;1:275–281.
35. Mannick JB, Asano K, Izumi K, Kieff E, Stamler JS. Nitric oxide produced by human B lymphocytes inhibits apoptosis and Epstein-Barr virus reactivation. *Cell*. 1994;79:1137–1146.
36. Mannick JB, Miao XQ, Stamler JS. Nitric oxide inhibits Fas-induced apoptosis. *J Biol Chem*. 1997;272:24125–24128.
37. Rossig L, Fichtlscherer B, Breitschopf K, Haendeler J, Zeiher AM, Mulsch A, Dimmeler S. Nitric oxide inhibits caspase-3 by S-nitrosation in vivo. *J Biol Chem*. 1999;274:6823–6826.
38. Broeders MA, Tangelder GJ, Slaaf DW, Reneman RS, oude Egbrink MG. Endogenous nitric oxide protects against thromboembolism in venules but not in arterioles. *Arterioscler Thromb Vasc Biol*. 1998;18:139–145.
39. Broeders MA, Tangelder GJ, Slaaf DW, Reneman RS, Egbrink MG. Endogenous nitric oxide and prostaglandins synergistically counteract thromboembolism in arterioles but not in venules. *Arterioscler Thromb Vasc Biol*. 2001;21:163–169.

Downloaded from atvb.ahajournals.org at Bibliotheque Faculte Medecine Geneve on May 28, 2007

2.3.4 Nikotin

Das Rauchen von Tabak ist mit einer Erhöhung des Risikos für myokardiale Erkrankungen assoziiert. Gleichzeitig wird bei weiblichen Rauchern die Einnahme von Östrogenpräparaten mit einem erhöhten Thromboserisiko in Verbindung gebracht. In Gegensatz dazu führt eine transdermale Nikotinapplikation in klinischen Studien zu keinen negativen Effekten. Ein Zusammenhang zwischen Nikotinexposition und Thrombogenität ist somit bis dato nicht eindeutig gesichert. Ziel dieser Studie war es daher, den Einfluss von Nikotin auf die mikrovaskuläre Thrombogenität geschlechtsabhängig zu untersuchen und eventuell zugrunde liegende Mechanismen genauer zu charakterisieren. Es wurde daher das Modell der chronischen Rückenhautkammer gewählt und mikrovaskuläre Thrombosen mittels Licht induziert sowie die Thrombozyten- und Endothelzellfunktion analysiert.

Bei Tieren beiden Geschlechts war die Bildung mikrovaskulärer Thromben gegenüber den Kontrolltieren nicht beschleunigt Die durchflußzytometrischen Analysen ergaben keinen wesentlichen Effekt von Nikotin auf die Thrombozytenfunktion. Allein in männlichen Tieren resultierte die chronische Nikotingabe in einer signifikant verminderten endothelialen Aktivierung. Im Gegensatz dazu resultierte die akute hochdosierte Gabe von Nikotin in einer signifikant schnelleren vaskulären Okklusion in weiblichen Tieren.

Zusammenfassend lässt sich also sagen, dass eine chronische Nikotingabe keine prothrombogene Wirkung bei Tieren beiden Geschlechts verursacht. Dahingegen wirkt die akute Applikation bei weiblichen Tieren thrombogen. Es ist somit eine geschlechtsabhängige Wirkung von Nikotin *in vivo* zu vermuten.

Lindenblatt N, Platz U, Hameister J, Klar E, Menger MD, Vollmar B
Distinct effects of acute and chronic nicotine application on microvascular thrombus formation and endothelial function in male and female mice
Langenbecks Arch Surg 2007; 392: 285-295.

Langenbecks Arch Surg
DOI 10.1007/s00423-007-0173-6

ORIGINAL ARTICLE

Distinct effects of acute and chronic nicotine application on microvascular thrombus formation and endothelial function in male and female mice

Nicole Lindenblatt · Uwe Platz · Jörn Hameister · Ernst Klar · Michael D. Menger · Brigitte Vollmar

Received: 4 January 2007 / Accepted: 6 February 2007
© Springer-Verlag 2007

Abstract
Background and aims Cigarette smoking is linked to thromboembolic events; however, a relationship between nicotine exposition and thrombosis has not been established. Thus, we intended to study the effect of acute and chronic nicotine application in an in vivo mouse model.
Materials and methods In microvessels of the dorsal skin fold chamber, light-dye-induced thrombus formation was analyzed using intravital fluorescence microscopy. Male and female C57BL/6J mice received nicotine chronically via the drinking water (100 μg/ml) for 8 weeks. An additional series of experiments was performed with acute iv nicotine treatment (3 mg/kg body weight).
Results No significant differences in microvascular thrombus formation were detected after chronic nicotine application in male and female animals when compared with controls. Accordingly, flow cytometric analysis did not show significant effects on platelet activity. Chronic nicotine treatment resulted in a significantly reduced endothelial activation in male, but not in female mice. In contrast, acute iv application of nicotine revealed significantly shorter thrombosis times in arterioles of female mice and a significantly increased endothelial P-selectin expression in mice of both genders.
Conclusion Chronic nicotine application does not promote microvascular thrombus formation in mice of either gender, whereas acute high-dose iv administration caused a significant increase of arteriolar thrombosis in female animals *probably via a synergistic effect of increased endothelial P-selectin expression and female hormone levels*. A gender-dependency of acute nicotine action can be presumed.

Keywords Nicotine · Microvascular thrombosis · Dorsal skinfold chamber · Endothelium · Platelet

Best abstracts — Surgical Forum 2007

N. Lindenblatt · U. Platz · B. Vollmar
Institute for Experimental Surgery, University of Rostock,
Schillingallee 70,
18055 Rostock, Germany

N. Lindenblatt (✉) · E. Klar
Department of General Surgery, University of Rostock,
Schillingallee 35,
18055 Rostock, Germany
e-mail: niclindenblatt@hotmail.com

J. Hameister
Institute for Toxicology, University of Rostock,
Schillingallee 70,
18055 Rostock, Germany

M. D. Menger
Institute for Clinical and Experimental Surgery,
University of Saarland,
Kirrberger Strasse,
66424 Homburg-Saar, Germany

Introduction

Cigarette smoking is the leading cause of preventable premature death in the developed world [1]. It promotes atherosclerosis and is associated with an increased risk of cardiac death, myocardial infarction, angina pectoris, peripheral vascular disease, and stroke [2]. This predisposition for atherosclerotic diseases is based on the damaging effects of cigarette smoke on the endothelium [3], increased platelet activation [4, 5], increased fibrinogen and thrombin levels, and an activation of plasmatic coagulation [6, 7]. Nicotine is the addiction-causing agent in cigarette fume and has been suspected to contribute to some of the negative effects of smoking. For example, acute local exposure to nicotine was associated with an impaired

response to endothelium-derived nitric oxide in human veins [8]. However, a causal role of nicotine for these cardiovascular disorders has not been proven [9, 10]. In fact, nicotine, at concentrations seen in smokers, has been shown to exert an inhibitory effect on platelet activation in vitro [11]. Furthermore, nicotine substitution therapy is considered as a safe aid to smoking cessation and did not increase adverse cardiac events in a randomized, double-blind placebo-controlled trial in patients with transdermal nicotine replacement and cardiac disease [12].

To further address this ambiguous issue, we studied the effect of chronic nicotine treatment on microvascular thrombus formation in an in vivo mouse model applying intravital fluorescence microcopy of the dorsal skinfold chamber. Concomitantly, in vitro experiments were conducted to investigate the influence of nicotine on endothelial cell function and platelet reactivity. All experiments were performed in animals of either sex to address the gender differences in the prognosis after ischemic coronary events [13]. Smoking appears to be the crucial factor for the increased prothrombotic risk in the context of oral contraceptive use, underlining a potential coherence with female sex hormone levels [14, 15]. Finally, we did not only study the effects of chronic nicotine exposure but also chose high-dose intravenous nicotine exposition to address the immediate toxicity of nicotine.

Materials and methods

Mouse dorsal skinfold chamber Upon approval by the local government, all experiments were carried out in accordance with the German legislation on protection of animals and the National Institutes of Health 'Guide for the Care and Use of Laboratory Animals' (Institute of Laboratory Animal Resources, National Research Council). C57BL/6J mice with a body weight (bw) of 23 27 g were anesthetized by an intraperitoneal injection of ketamine (90 mg/kg bw) and xylazine (25 mg/kg bw).

For the study of microvascular thrombus formation, we used the dorsal skinfold chamber, as originally described by Lehr et al. [16] in mice. Before the preparation, animals were placed on a heating pad coupled to a rectal probe. Briefly, a double skin layer on the back on the animal was implanted between two symmetric titanium frames. One skin layer was then completely removed in a circular area of 15 mm in diameter, and the remaining layers (consisting of striated skin muscle, subcutaneous tissue, and skin) were covered with a glass coverslip incorporated into one of the titanium frames (Fig. 1a c). Animals tolerated the chamber well and showed no signs of discomfort or changes of sleeping and feeding habits. Before intravital microscopy, animals were allowed a recovery period of 3 days.

In vivo thrombosis model On day 4, after the skinfold chamber preparation, thrombus formation was induced in randomly chosen venules (n=3 4 per preparation) and arterioles (n=1 2 per preparation). After injection of 0.1 ml fluorescein isothiocyanate (FITC)-labeled dextran (2%; MW 150000, Sigma-Aldrich, Munich, Germany) into the retro-orbital venous plexus and subsequent circulation for 30 s, microcirculation of the striated muscle tissue was visualized by intravital fluorescence microscopy using a Zeiss microscope (Axiotech vario, Zeiss, Jena, Germany). The microscopic procedure was performed at a constant room temperature of 21 23°C. The epi-illumination setup included a 100-W HBO mercury lamp and a blue filter (450 490/>520 nm excitation/emission wavelength). Mi-

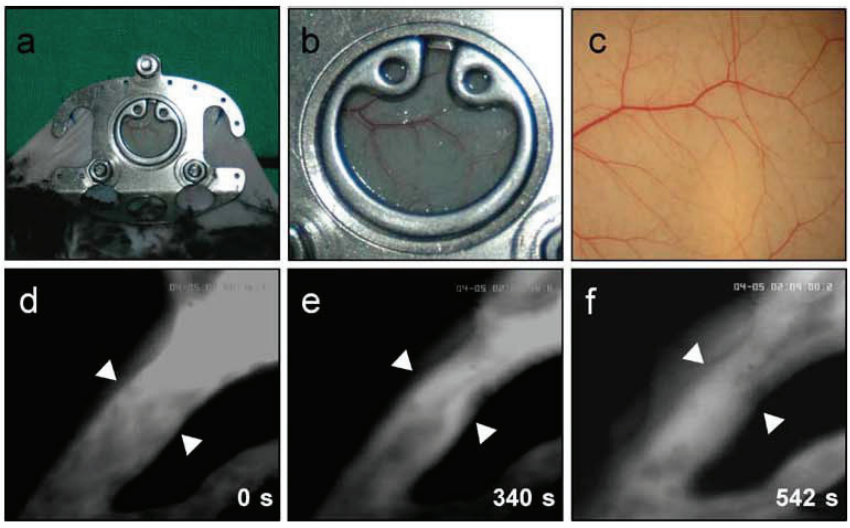

Fig. 1 **a** Dorsal skinfold chamber preparation with **b** the observation window, allowing the **c** direct visualization of the striated muscle microcirculation. **d–f** Developing venular microvascular thrombus (*arrow heads*) at three different time points after light-dye-induced endothelial damage (magnification ×630)

croscopic images were recorded by a charge-coupled device video camera (FK 6990A-IQ, Pieper, Schwerte, Germany) and stored on videotapes for off-line evaluation (S-VHS Panasonic AG 7350-E, Matsushita, Tokyo, Japan). Using a ×20 water immersion objective (Achroplan ×20/0.50 W, Zeiss), baseline blood flow was monitored in individual arterioles (diameter range 15–30 μm) and venules (diameter range 20–40 μm). Subsequently, photochemical thrombus formation was induced by continuous local exposure of filtered light (450–490/>520 nm excitation/emission wavelength) and a ×63 water immersion objective (Achroplan ×63/0.95 W, Zeiss) to the individual microvessels (Fig. 1d–f), as described previously [17–19]. The light/dye thrombosis model used is based on endothelial injury by phototoxicity induced by exposure of FITC to excitation light. The phenomenon is mediated by reactive oxygen species, in particular singlet oxygen, generated by excitation of the fluorochrom. Microvascular thrombosis in this model involves endothelial injury, although not widespread denudation. Thrombi are primarily composed of platelets and a smaller number of leukocytes [20]. Light exposure was discontinued after blood flow in the vessel ceased for at least 60 s due to complete vessel occlusion.

Microcirculation analysis Intravascular thrombus formation, i.e., change of inner luminal vessel diameter due to platelet and/or leukocyte adherence to the endothelium of the vessel wall, and microcirculatory parameters (blood flow velocity, vessel diameter) were quantified off-line by analysis of the videotaped images using a computer-assisted image analysis system (CapImage, Zeintl Software, Heidelberg, Germany). Analysis included the following parameters: thrombus formation with determination of the time periods until (1) first cell deposition (platelets, leukocytes) was observed along the endothelial lining, (2) the inner diameter of the microvessel was reduced to 50% by the growing thrombus, (3) initial occurrence of stasis (at least 5-s duration), and (4) sustained cessation of blood flow due to vessel occlusion. Microcirculatory analysis further included the determination of vascular wall shear rates based on the Newtonian definition $\gamma = 8 \times V/D$ (V represents the red blood cell centerline velocity divided by 1.6 according to the Baker–Wayland factor [21], and D represents the individual inner vessel diameter).

Experimental design To closely resemble the usual way of nicotine uptake, male and female C57BL/6J mice received nicotine chronically via the drinking water (100 μg/ml) for 8 weeks. Oral intake of nicotine at this dosage has been shown to induce cotinine levels, the stable major metabolite of nicotine, similar to those seen in chronic smokers in previous studies in mice [22, 23]. Additionally, plasma levels of cotinine were determined to ensure appropriate levels in this particular study. Control animals of both genders received normal drinking water. As nicotine content of the drinking water with possible alterations in taste and smell might theoretically deter mice from consuming this water, drinking bottles were weighted for both treatment groups to demonstrate an equal amount of fluid intake over a representative time period of 7 days. To study the effects of acute nicotine application on microvascular thrombus formation, additional male and female mice were injected with nicotine (3 mg/kg iv) 5 min before the beginning of the experiments.

Determination of cotinine levels by gas chromatography Two hundred microliter serum was filled in tubes spiked with 1 μl of internal standards solution for cotinine-d3 (2 μg/ml). Then, samples were vortexed, allowed to equilibrate for 5 min, and alkalinized with 100 μl 2.0 M potassium carbonate. One hundred microliter of a mixture of trichlormethane, acetonitrile, and ethyl acetate (4:3:2) were added. Samples were capped and mixed for 5 min on the vortex mixer and then centrifuged. The organic phase was used for injection into the GC-MS (Hewlett Packard GC 6890 Series II with 5971 MSD, Column 12 m Ultra 1, Hewlett Packard, Boblingen, Germany). For quantification of cotinine, 98/101 m/z was used. The analyte concentrations in the samples were determined using five-point calibration lines with cotinine concentrations ranging from 0 to 100 ng/ml. Linearity of the calibration lines was good, with typical r^2 values of 0.997. The limit of quantification was 4.9 ng/ml.

Preparation of murine platelet rich plasma For in vitro testing of platelet function, 0.5–1 ml blood was drawn from the retro-orbital venous plexus of untreated mice with 1.5-cm glass capillaries and collected into a tube containing 300 μl Tyrode buffer solution (TBS) and heparin (20 U/ml). The sample was centrifuged for 5 min at 750×*g*, followed by recentrifugation of the supernatant for 6 min at 150×*g*, yielding platelet rich plasma (PRP). PRP was centrifuged again for 5 min at 1,825×*g*, and the cell pellet was resuspended in 1 ml TBS with 1 μM prostacyclin and 10 U/ml heparin for subsequent incubation at 37°C for 10 min. Centrifugation (5 min at 1,825×*g*) and resuspension were repeated twice. Finally, the platelet pellet was resuspended in 450 μl TBS with 2 μl apyrase [24]. Platelet suspensions were transferred into a 37°C water bath for 30 min of resting to eliminate isolation-induced platelet activation. Then, platelets were incubated with nicotine (50 nM) for additional 30 min in water followed by exposure to thrombin (20 U/ml) and incubation with saturating amounts of the appropriate antibody. The nicotine concentration of 50 nM nicotine is comparable to levels in chronic smokers [11]. Platelets from control

animals were kept continuously at 37°C without addition of nicotine.

Flow cytometric analysis of P-selectin and CD107a expression For evaluation of receptor expression under resting conditions, 5 μl of specific rat anti-mouse P-selectin (Emfret Analytics, Eibelstadt, Germany) and CD107a (BD Biosciences, Heidelberg, Germany) or negative control antibodies and 25 μl platelet suspension were combined and incubated for 15 min at room temperature. The reaction was stopped by addition of 400 μl PBS. Analysis was performed within the subsequent 30 min. In addition, the same set of experiments was carried out after exposure to thrombin for maximal platelet activation (20 U/ml).

FACScan flowcytometer (Becton Dickinson) was calibrated with fluorescent standard microbeads (CaliBRITE Beads, Becton Dickinson) for accurate instrument setting. Platelets were identified by their characteristic forward and sideward light scatter and selectively analyzed for their fluorescence properties using the CellQuest program (Becton Dickinson) with assessment of 20.000 events per sample. The relative fluorescence intensity of a given sample was calculated by subtracting the signal obtained when cells were incubated with the isotype specific control antibody from the signal generated by cells incubated with the test antibody.

Enzyme-linked immunosorbent assay of circulating endothelial markers Plasma concentrations of circulating, i.e., soluble (s) sP-selectin, sE-selectin, intercellular adhesion molecule-1 (sICAM-1), and vascular cell adhesion molecule-1 (sVCAM-1), were determined using the respective enzyme immunoassay kits (R&D Systems, Minneapolis, MN, USA). Blood samples were prepared by centrifugation for 10 min at 2,000×*g* and room temperature (GS-6R Centrifuge, Beckman Coulter, Fullerton, CA, USA).

Histology and immunohistochemistry At the end of each experiment, a cross-section tissue block of the dorsal skinfold chamber was fixed in 4% phosphate buffered formalin for 2–3 days and embedded in paraffin. From the paraffin-embedded tissue blocks, 4-μm sections were cut and stained with hematoxylin and eosin (HE) for histological analysis. For immunohistochemical demonstration of P-selectin, ICAM-1, and PAF-R expression, sections collected on poly-L-lysine-coated glass slides were treated by microwave for antigen unmasking. For evaluation of PAI-1 expression, sections were treated by proteinase K. Goat anti-P-selectin (1:100), anti-PAF-R (1:400), anti-ICAM-1 (1:200), and anti-PAI-1 (1:100, all Santa Cruz Biotechnology, Heidelberg, Germany) were used as primary antibodies and incubated for 90–120 min at room temperature. This was followed by a horseradish peroxidase-conjugated donkey anti-goat antibody (1:25; Santa Cruz Biotechnology) and development using DAB (P-selectin) and ACE (PAF-R, ICAM-1, PAI-1) substrate as chromogen. The sections were counterstained with hematoxylin and examined by light microscopy (Zeiss Axioscop 40, Zeiss, Jena, Germany).

Statistical analysis After proving the assumption of normality and equal variance across groups, differences between groups were assessed using one-way analysis of variance followed by the appropriate post-hoc comparison test. All data were expressed as means±SEM, and overall statistical significance was set at $p<0.05$. Statistics and graphics were performed using the software packages SigmaStat and SigmaPlot (Jandel Corporation, San Rafael, CA, USA).

Results

Influence of nicotine content on intake of drinking water and cotinine plasma levels Consumption of drinking water over a time period of 7 days was −9.2±0.5% of the initial bottle weight for nicotinated water and −9.1±0.4% for unaltered water (p = not significant), implying an equal amount of fluid intake irrespective of nicotine content. Nicotine intake calculated from the animals' body weights and usage of drinking water averaged ~15 mg kg ^{1} day ^{1}. Cotinine plasma levels amounted to >100 ng/ml in nicotine-treated mice and <10 ng/ml in control mice. These data are very similar to those obtained by other groups, and the model appears to be suitable for exposing experimental animals to nicotine for several weeks [25].

Chronic nicotine treatment does not influence microvascular thrombus formation in vivo Red blood cell (RBC) velocities and wall shear rates did not differ significantly between chronic nicotine treatment and controls in mice of either gender (Table 1). In male controls, light-dye mediated thrombus formation induced complete occlusion of arterioles and venules after 577±78 and 520±89 s, respectively. After chronic nicotine treatment, complete occlusion of arterioles and venules did not differ significantly from these values (arterioles, 640±96 s; venules, 427±51 s; Fig. 2a and b). In parallel, thrombus formation in female mice was not significantly influenced by chronic nicotine treatment. Arteriolar and venular vessels were found clogged at an average time of 866±24 and 459±61 s in female controls and at 715±130 and 493±79 s in nicotine-treated females (Fig. 2a and b). In addition to this, we did not observe differences in thrombus formation between males and females either with or without nicotine treatment.

Table 1 RBC velocity (μm/s) and wall shear rates (γ, s^{-1}) in striated muscle arterioles and venules of the dorsal skinfold chamber before induction of thrombus formation

Values are given as means± SEM. p = not significant

	Arterioles		Venules	
	RBC velocity	γ	RBC velocity	γ
M-con	1431±102	274±42	413±86	65±9
M-nic	1196±199	310±72	313±87	53±14
F-con	1162±61	222±28	566±85	84±9
F-nic	1306±181	233±31	621±96	91±12

Nicotine exposition does not effect murine platelet P-selectin and CD107a expression We studied the effect of nicotine application at a concentration of 50 nM on murine platelet activation. Thrombin-stimulation resulted in a marked increase of the expression of P-selectin and a slight increase of CD107a on the platelet surface of normal and nicotine-exposed platelets indicated by an increase in mean fluorescence. In vitro nicotine exposure did not significantly affect spontaneous platelet P-selectin and CD107a expression when compared to controls. In line with this, thrombin-induced expression of these two platelet activation markers also was not significantly influenced by nicotine neither in male nor in female mice (data not shown).

Chronic nicotine application reduces circulation of endothelial activation markers in male, but not in female mice To characterize the effect of chronic nicotine exposure on endothelial cell activation, we determined circulating (soluble) endothelial activation markers. In male mice, nicotine exposure for 8 weeks resulted in a significant reduction of sP-selectin and sE-selectin when compared to controls (Fig. 3a and b). This effect was not seen in female mice, although a tendency towards a reduction could be observed. sICAM-1 was significantly elevated in female control mice when compared to male control mice, but nicotine treatment did not affect sICAM-1 circulation in mice of either sex (Fig. 3c). There were no substantial differences concerning sVCAM-1 (Fig. 3d). However, although chronic nicotine exposition did not significantly reduce the circulation of endothelial activation markers in female mice, it did, at least, not elicit an increase of these markers.

Chronic nicotine application dampens endothelial activation predominantly in male mice In general, adhesion molecules were found expressed within the endothelium of arterioles and venules, whereas little, if any, immunoreactivity was detected within the surrounding subcutaneous and muscle tissue of the dorsal skinfold chamber. Endothelial expression of these molecules was assessed as percentage of positively stained vessels. Interestingly, chronic nicotine treatment caused a significant reduction of the endothelial expression of P-selectin, PAF-R, and PAI-1 in male mice when compared to controls (Fig. 4a,b and d). In contrast to this, a significant reduction in female mice was merely seen for PAI-1 after nicotine treatment when compared to female controls (Fig. 4d). Once again, the expression of ICAM-1 was not influenced by nicotine in mice of both genders (Fig. 4c). Of note, the expression of PAF-R was significantly higher in female mice compared to male mice after nicotine treatment (Fig. 4b).

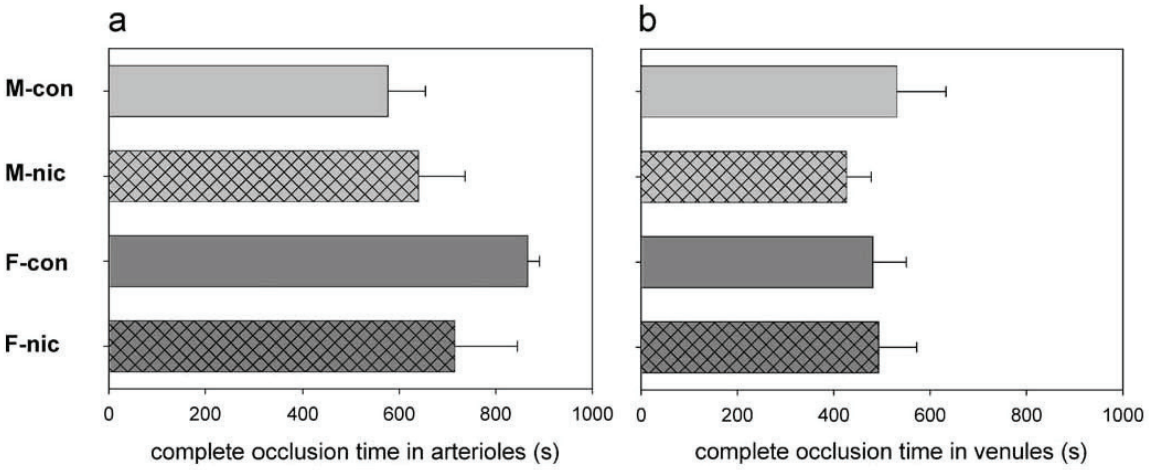

Fig. 2 Occlusion times of arterioles (**a**) and venules (**b**) upon light-dye-induced thrombus formation in male (*M-con*; n=8) and female (*F-con*; n=6) controls (normal drinking water) and after chronic nicotine treatment of male (*M-nic*; n=7) and female (*F-nic*; n=6) mice [nicotine via drinking water for 8 weeks (100 μg/ml)]. Values are given as means±SEM; p=not significant

Acute application of high-dose nicotine acts prothrombotic in arterioles of female mice To test the direct effect of nicotine on the endothelium and on thrombogenicity in vivo, we injected nicotine at a dose of 3 mg/kg iv 5 min before thrombus induction. Of note, the average dose during chronic oral nicotine application amounted to ~15 mg kg^{-1} day^{-1} or approximately 0.01 mg kg^{-1} min^{-1}. In males, light-dye mediated thrombus formation induced complete occlusion of arterioles and venules after 419±90 and 334±31 s, respectively (Fig. 5a and b). Thrombosis times did not differ significantly from control mice. In contrast to this, arteriolar occlusion in female mice occurred significantly faster after acute nicotine application than in controls (arterioles, 302±63 s; $p<0.05$ vs controls, 832± 39 s), whereas acute nicotine exposure did not affect venular thrombus formation in female mice (Fig. 5b).

Acute application of high-dose nicotine boosts endothelial activation According to the primary study design, we determined circulating (soluble) endothelial activation molecules after acute nicotine application. Briefly, we did not observe a reduction of the circulation of these four markers, but rather an increase of sP-selectin (Fig. 6a), sE-selectin (Fig. 6b), and sVCAM-1 (Fig. 6d) in both male and female mice. sICAM-1 was markedly reduced in both sexes (Fig. 6c). Immunohistochemistry confirmed this proneness for endothelial activation as a result of acute nicotine exposition, in particular for endothelial P-selectin expression (Fig. 7a) and, to a lesser extent, for PAF-R (Fig. 7b) and ICAM-1 (Fig. 7c). However, PAI-1 expression was found to be reduced in these mice (Fig. 7d). In summary, acute high-dose nicotine exposition in general exerted activating effects on the vascular endothelium.

Discussion

The major findings of the present study are that chronic oral nicotine exposition in a comparable extent as seen in

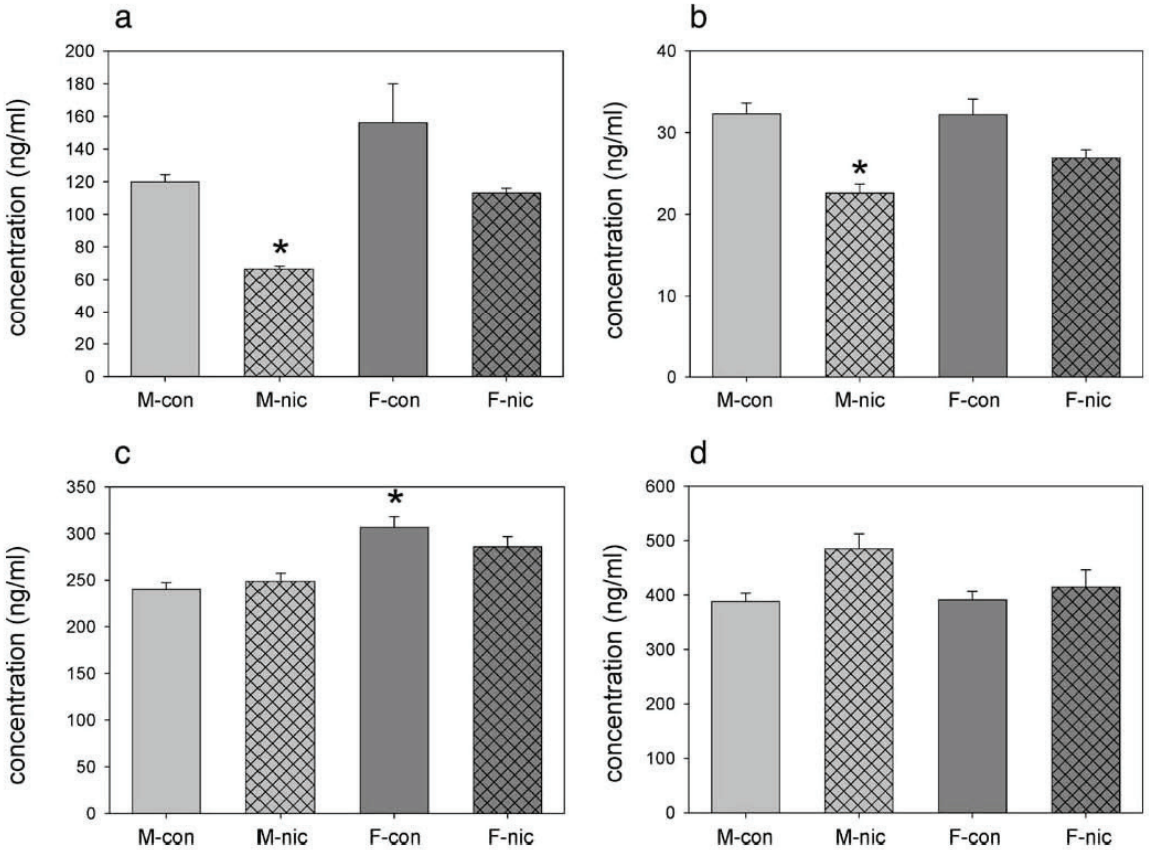

Fig. 3 Plasma concentrations of circulating sP-selectin (**a**) and sE-selectin (**b**), sICAM-1 (**c**), and sVCAM-1 (**d**) in male (*M-con*) and female (*F-con*) controls (normal drinking water) and after chronic nicotine treatment of male (*M-nic*) and female (*F-nic*) mice [nicotine via drinking water for 8 weeks (100 μg/ml)]. n=6–8 animals per group. Values are given as means±SEM; *$p<0.05$ vs M-con

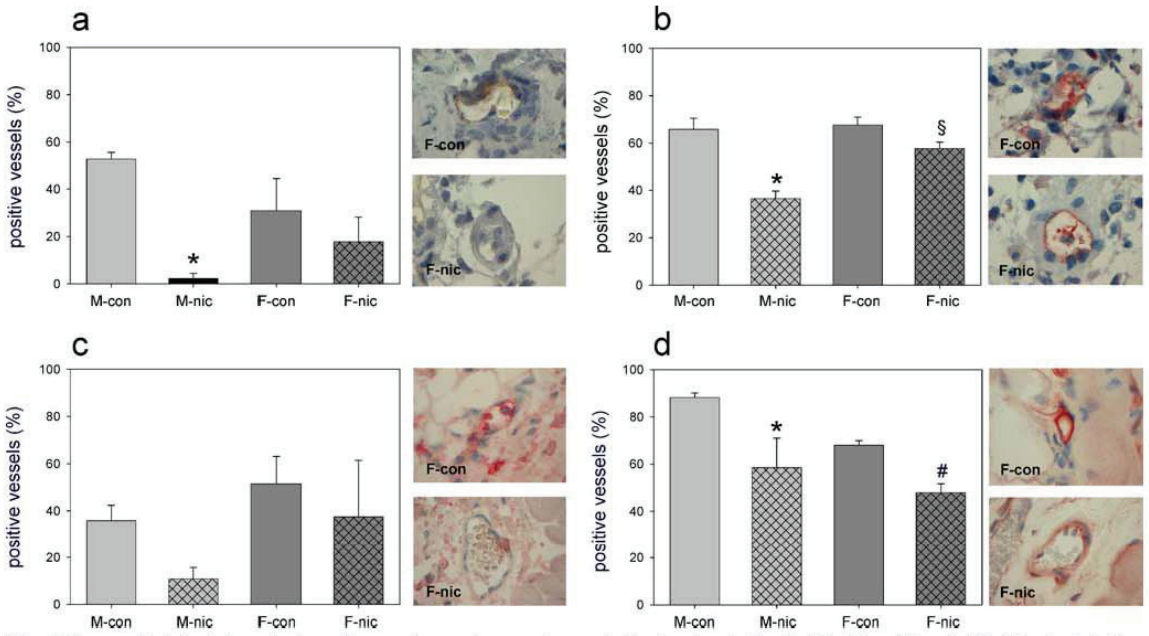

Fig. 4 Immunohistological analysis and exemplary microscopic images of female mice of the endothelial expression of P-selectin (**a**), PAF-R (**b**), ICAM-1 (**c**), and PAI-1 (**d**) in male (*M-con*) and female (*F-con*) controls (normal drinking water) and after chronic nicotine treatment of male (*M-nic*) and female (*F-nic*) mice [nicotine via drinking water for 8 weeks (100 μg/ml)]. n=6–8 animals per group. Values are given as means±SEM. $^{*}p<0.05$ vs M-con, $^{\#}p<0.05$ vs F-con, $^{\S}p<0.05$ vs M-nic

smokers does not promote microvascular thrombus formation in vivo in animals of either gender. This might, at least in part, be due to the fact that nicotine did not cause an increase of spontaneous or thrombin-induced platelet activation in vitro. Furthermore, endothelial activation, as represented by endothelial expression and blood circulation of endothelial activation markers, was largely found to be abridged after 8 weeks of chronic nicotine uptake. This effect predominantly occurred in male mice, except for the expression of PAI-1 which was significantly reduced in both male and female animals. In contrast to this, we found a significantly increased thrombus formation in arterioles of female mice after acute high-dose exposure of nicotine, which was associated with a tendency towards enhanced

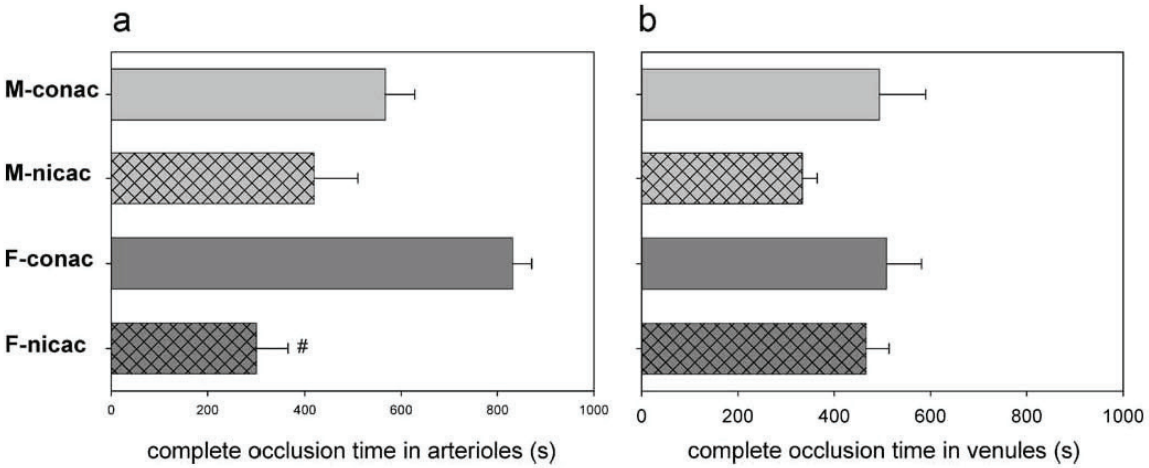

Fig. 5 Occlusion times of arterioles (**a**) and venules (**b**) upon light-dye-induced thrombus formation in male (*M-conac*; n=8) and female (*F-conac*; n=8) controls (saline exposure) and after acute nicotine treatment of male (*M-nicac*; n=4) and female (*F-nicac*; n=6) mice (nicotine 3 mg/kg iv at 5 min). Values are given as means±SEM; $^{\#}p<0.05$ vs F-conac

expression of PAF-R and ICAM-1 and a significant increase in endothelial P-selectin expression. Male mice did not exhibit accelerated thrombosis times after iv application of nicotine despite similar effects on endothelial activation. Based on these data, acute nicotine application at a high concentration has prothrombotic properties predominantly in females, implying a gender-dependency of acute nicotine action.

Cigarette smoking continues to be one of the world's most serious public health problems, being the major risk factor of ischemic heart disease and thrombo embolic events [26]. Being aware that the smoke of a cigarette contains more than 4,000 potential noxious substances, numerous studies have been conducted attempting to identify the harmful agent in cigarette smoke. Nicotine exerts sympathomimetic effects and leads to vasoconstriction and hypertension [9]. On the other hand, other components of the cigarette smoke, among them tar, carbon monoxide, polycyclic aromatic hydrocarbons, cyanide, and cadmium, might have detrimental effects, as these have been shown to increase platelet activation, fibrinogen levels, and leukocyte adhesion [5, 12, 27]. Thus, it has to be differentiated between the possible effects of cigarette smoke and nicotine itself. Cigarette smoking has, in most cases, been shown to elicit negative effects on platelet and endothelial function. A clinical study in smokers showed an impairment of endothelial nitric oxide production with the possible consequence of increased thrombogenicity [28]. Cigarette smoke caused leukocyte adhesion to the vascular endothelium and increase of xanthine oxidase activity in hamsters, which could be attenuated by pretreatment with superoxide dismutase [29]. Platelets from chronic smokers express significantly more P-selectin in a resting state and bind more fibrinogen via the GP IIb IIIa receptor after activation when compared to platelets from non-smokers [5]. Additionally, platelet-dependent thrombin generation is

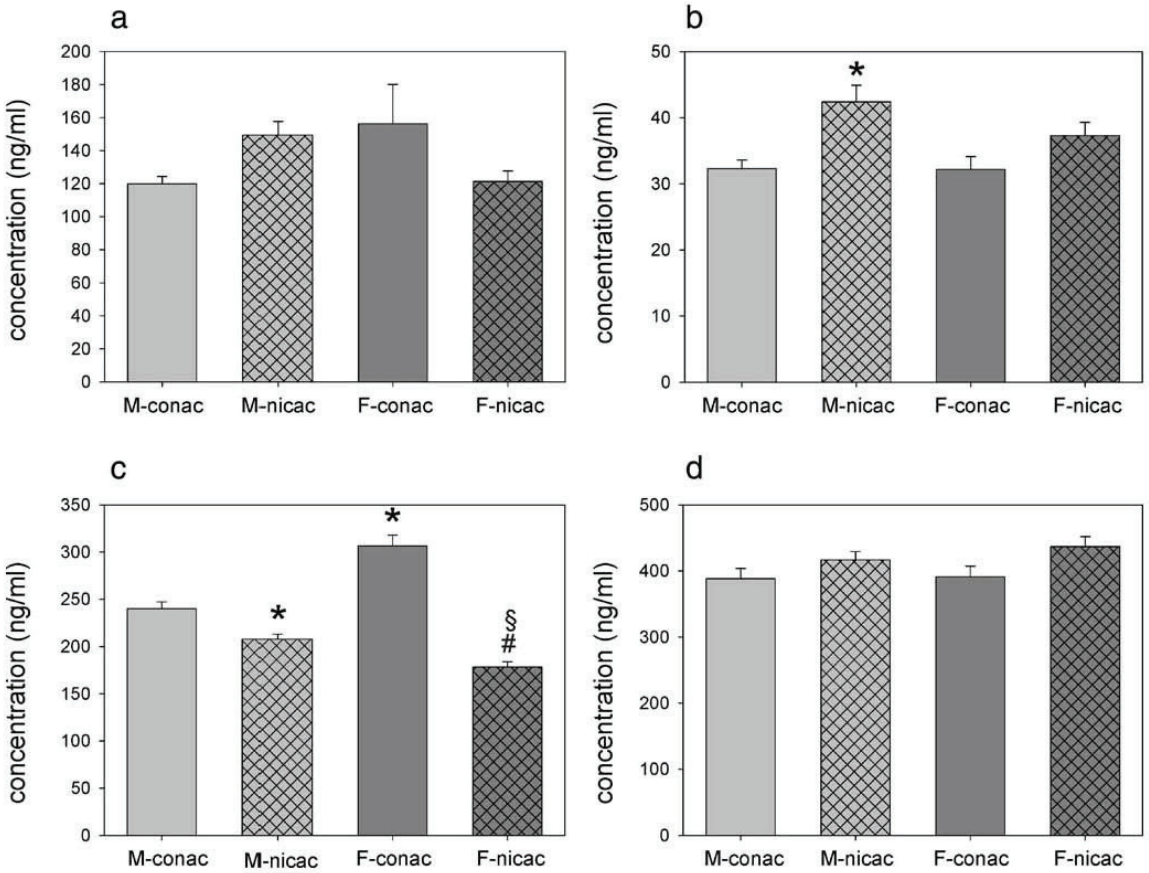

Fig. 6 Plasma concentrations of circulating sP-selectin (**a**) and sE-selectin (**b**), sICAM-1 (**c**), and sVCAM-1 (**d**) in male (*M-conac*) and female (*F-conac*) controls (saline exposure) and after acute nicotine treatment of male (*M-nicac*) and female (*F-nicac*) mice (nicotine 3 mg/kg iv at 5 min). n=6–8 animals per group. Values are given as means±SEM; $^{*}p<0.05$ vs M-conac; $^{\#}p<0.05$ vs F-conac, $^{\S}p<0.05$ vs M-nicac

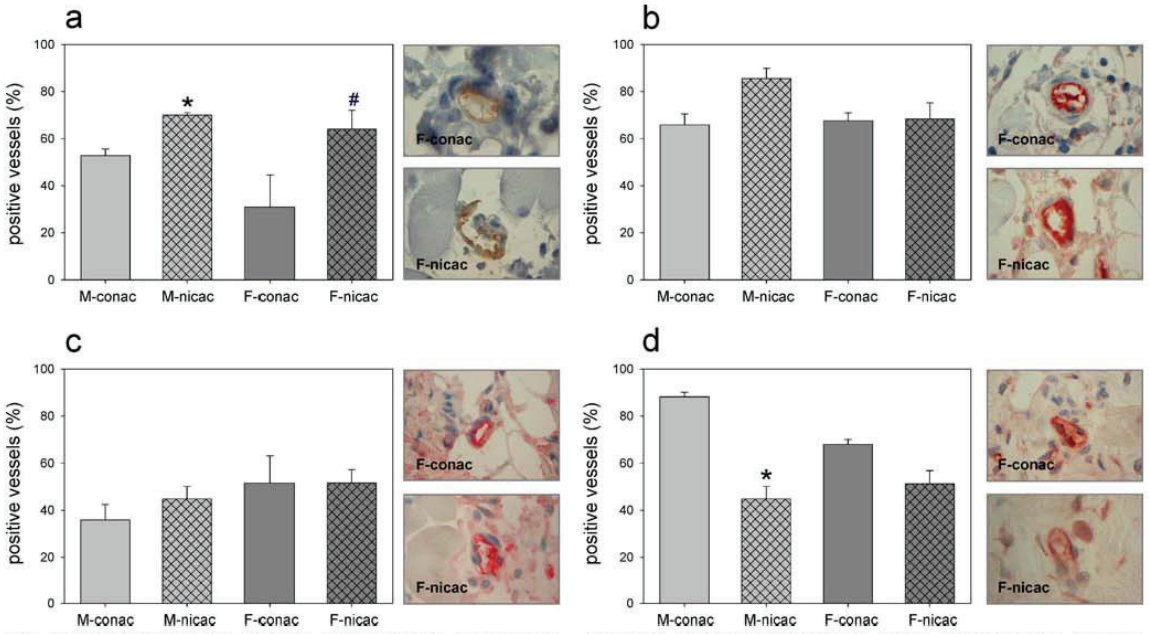

Fig. 7 Immunohistological analysis and exemplary microscopic images of female mice of the endothelial expression of P-selectin (**a**), PAF-R (**b**), ICAM-1 (**c**), and PAI-1 (**d**) in male (*M-conac*) and female (*F-conac*) controls (saline exposure) and after acute nicotine treatment of male (*M-nicac*) and female (*F-nicac*) mice (nicotine 3 mg/kg iv at 5 min). n=6–8 animals per group. n=6–8 animals per group. Values are given as means±SEM. $^{*}p<0.05$ vs M-conac, $^{\#}p<0.05$ vs F-conac

enhanced in smokers [7]. However, concerning the intrinsic effects of nicotine as the addiction-causing substance itself on endothelial and platelet activation and thrombus formation, in vitro data are controversial, and in vivo studies are scarce.

It has become common assumption that nicotine substitution to quit smoking is safe. In a placebo-controlled double-blind study using nicotine nasal spray in a smoking cessation program, cardiovascular risk factor could be significantly reduced without negative effects caused by nicotine substitution [30]. This is in line with a study showing a rapid decrease of the circulation of the endothelial adhesion molecules sICAM-1, sCD44v5, and sCD44v6 during chronic nicotine replacement therapy after smoking cessation [31]. In contrast to this, chronic nicotine application enhanced focal ischemic brain injury and reduced tissue plasminogen activator (t-PA) in a middle cerebral artery occlusion model in rats [32] and increased the production of PAI-1 by human brain endothelial cells in cell cultures [33]. In line with the effects caused by cigarette smoke in previous studies [29], acute nicotine application enhanced selectin-dependent rolling of leukocytes on nicotine-exposed microvessels of lung allografts [34]. Nicotine impaired endothelium-dependent dilatation in human veins in vivo, implying a defective endothelial function [8]. However, studies dealing with the effects of nicotine on platelet function revealed a reduced susceptibility of platelets to shear stress after nicotine exposition [35] and a 75% decline of the shear-dependent platelet activation [11]. Thus, a rather protective effect of nicotine on platelet reactivity has been proposed.

The results of this study now indicate that chronic nicotine consumption does not convey prothrombogenic effects in vivo. Concordantly, negative side effects are not observed with long-term transdermal nicotine substitution in the clinical setting. This might partly be due to the fact that endothelial activation was found to be reduced and that there was no significant impact on platelet function in both genders.

In a second step, we questioned whether acute intravenous nicotine application with a rapid rise in plasma nicotine levels might have different effects on microvascular thrombus formation and endothelial activation than constant uptake of nicotine. A steep increase of plasma nicotine concentration has been associated with adverse cardiac events due to its sympathomimetic properties [12]. In fact, cigarette smoking with deep inhalation of fume results in a rapid absorption of nicotine over the lungs occurring at a rate similar to that after iv administration [36]. The acute application of nicotine on HUVECS in in vitro studies resulted in an increased expression of ICAM-1 and VCAM-1 via a second messenger pathway involving

PKC and p38 MAPK-mediated activation of NF-kappaB and AP-1 [37]. Moreover, acute nicotine exposure induced MAPK-mediated P-selectin and E-selectin-dependent leukocyte adhesion in allograft lung microvessels in vivo [34].

Based on our results, it can be presumed that a rapid increase in nicotine levels leads to an increase of endothelial activation. Therefore, it is possible that not the mere presence of nicotine in the blood, but rather speed and dose of nicotine exposure is crucial for its prothrombotic effects. Although the prothrombogenic effect of acute nicotine administration was seen in mice of both genders in this study, microvascular thrombus formation was solely increased in female mice. An in vitro study investigating platelet adhesion in patients prone to arterial and venous thrombosis in dependence to gender and smoking revealed that higher platelet activation occurs in men, ex-smokers and current smokers [38]. However, this study did not show an increased platelet reactivity in females. On the other side, numerous clinical and experimental studies link female hormone treatment to a generally increased risk for thrombotic and ischemic events [39, 40]. These adverse effects in particular occurred in smoking women [41]. We now show that gender differences exist in the context of acute nicotine application and would like to propose an increased, possibly MAPK-mediated, expression of endothelial P-selectin in combination with female hormone levels as underlying mechanism for the prothrombogenic effect of nicotine in arterioles of female mice. While P-selectin does not mediate platelet–platelet interaction, P-selectin provides an anchoring source for leukocytes on activated platelets and, thus, may play a very important role in determining the size and stability of the platelet aggregates in the developing thrombus [42]. In light of the fact that increased microvascular thrombosis was observed only in female, but not in male, mice despite a comparable rise in endothelial P-selectin expression after acute nicotine application, a relevant impact of female hormones can be assumed.

In general, unharmful effects of nicotine, independent of acute or chronic application, were mostly seen in male mice, whereas microvascular thrombus formation was only found to be accelerated in female mice.

Conclusion

Chronic continuous nicotine application does not promote microvascular thrombus formation on mice of either gender, which is supported by the fact that a general reduction of endothelial activation and a lack of impact on platelet activation were observed. In contrast to this, acute high-dose iv administration of nicotine caused a significant increase of arteriolar thrombus formation in female, but not in male animals, and boosted endothelial P-selectin expression in mice of both genders. Based on these data, acute nicotine application at a high concentration acts prothrombogenic particularly in females, probably implying a synergistic effect between increased endothelial P-selectin-expression and the presence of female hormones.

Acknowledgments The authors kindly thank Berit Blendow, Doris Butzlaff, Dorothea Frenz, Maren Nerowski, and Kathrin Sievert, Institute for Experimental Surgery, University of Rostock for their excellent technical assistance. This study is supported by a grant from the Deutsche Forschungsgemeinschaft, Bonn-Bad Godesberg, Germany (Vo 450/8-1).

References

1. US Department of Health and Human Services (1990) The health benefits of smoking cessation. US Department of Health and Human Services, Public Health Service, Centers for Disease Control, Center for Chronic Disease Prevention and Health Promotion, Office on Smoking and Health, Washington, DC. DHHS Publication No. (CDC) 90–8416
2. US Department of Health and Human Services (1983) The health consequences of smoking: cardiovascular disease: a report of the surgeon general. US Department of Health and Human Services, Public Health Service, Centers for Disease Control, Center for Chronic Disease Prevention and Health Promotion, Office on Smoking and Health, Washington, DC. DHHS Publication No: (PHS) 84–50204
3. Zeiher AM, Schachinger V, Minners J (1995) Long-term cigarette smoking impairs endothelium-dependent coronary arterial vasodilator function. Circulation 92:1094–1100
4. Fuster V, Chesebro JH, Frye RL, Elveback LR (1981) Platelet survival and the development of coronary artery disease in the young adult: effects of cigarette smoking, strong family history and medical therapy. Circulation 63:546–551
5. Nair S, Kulkarni S, Camoens HM, Ghosh K, Mohanty D (2001) Changes in platelet glycoprotein receptors after smoking—a flow cytometric study. Platelets 12:20–26
6. Fitzgerald GA, Oates JA, Nowak J (1988) Cigarette smoking and hemostatic function. Am Heart J 115:267–271
7. Hioki H, Aoki N, Kawano K, Homori M, Hasumura Y, Yasumura T, Maki A, Yoshino H, Yanagisawa A, Ishikawa K (2001) Acute effects of cigarette smoking on platelet-dependent thrombin generation. Eur Heart J 22:56–61
8. Chalon S, Moreno H Jr, Benowitz NL, Hoffman BB, Blaschke TF (2000) Nicotine impairs endothelium-dependent dilatation in human veins in vivo. Clin Pharmacol Ther 67:391–397
9. Benowitz NL (1988) Pharmacologic aspects of cigarette smoking and nicotine addition. N Engl J Med 319:1318–1330
10. Benowitz NL (1997) Systemic absorption and effects of nicotine from smokeless tobacco. Adv Dent Res 11:336–341
11. Ramachandran J, Rubenstein D, Bluestein D, Jesty J (2004) Activation of platelets exposed to shear stress in the presence of smoke extracts of low-nicotine and zero-nicotine cigarettes: the protective effect of nicotine. Nicotine Tob Res 6:835–841
12. Joseph AM, Norman SM, Ferry LH, Prochazka AV, Westman EC, Steele BG, Sherman SE, Cleveland M, Antonnucio DO, Hartman N, McGovern PG (1996) The safety of transdermal nicotine as an aid to smoking cessation in patients with cardiac disease. N Engl J Med 335:1792–1798

13. Vaccarino V, Parsons L, Every NR, Barron HV, Krumholz HM (1999) Sex-based differences in early mortality after myocardial infarction. National registry of myocardial infarction 2 participants. N Engl J Med 341:217–225
14. Roy S (1999) Effects of smoking on prostacyclin formation and platelet aggregation in users of oral contraceptives. Am J Obstet Gynecol 180:S364–368
15. Holschermann H, Terhalle HM, Zakel U, Maus U, Parviz B, Tillmanns H, Haberbosch W (1999) Monocyte tissue factor expression is enhanced in women who smoke and use oral contraceptives. Thromb Haemost 82:1614–1620
16. Lehr HA, Leunig M, Menger MD, Nolte D, Messmer K (1993) Dorsal skinfold chamber technique for intravital microscopy in nude mice. Am J Pathol 143:1055–1062
17. Thorlacius H, Vollmar B, Seyfert UT, Vestweber D, Menger MD (2000) The polysaccharide fucoidan inhibits microvascular thrombus formation independently from P-and L-selectin function in vivo. Eur J Clin Investig 30:804–810
18. Vollmar B, Schmits R, Kunz D, Menger MD (2001) Lack of in vivo function of CD31 in vascular thrombosis. Thromb Haemost 85:160–164
19. Roesken F, Ruecker M, Vollmar B, Boeckel N, Morgenstern E, Menger MD (1997) A new model for quantitative in vivo microscopic analysis of thrombus formation and vascular recanalisation: the ear of the hairless (hr/hr) mouse. Thromb Haemost 78:1408–1414
20. Rumbaut RE, Randhawa JK, Smith CW, Burns AR (2004) Mouse cremaster venules are predisposed to light/dye-induced thrombosis independent of wall shear rate, CD18, ICAM-1, or P-selectin. Microcirculation 11:239–247
21. Baker M, Wayland H (1974) On-line volume flow rate and velocity profile measurements for blood in microvessels. Microvasc Res 7:131–143
22. Suner IJ, Espinosa-Heidmann DG, Marin-Castano ME, Hernandez EP, Pereira-Simon S, Cousins SW (2004) Nicotine increases size and severity of experimental choroidal neovascularization. Investig Ophthalmol Vis Sci 45:311–317
23. Heeschen C, Jang JJ, Weis M, Pathak A, Kaji S, Hu RS, Tsao PS, Johnson FL (2001) Nicotine stimulates angiogenesis and promotes tumor growth and atherosclerosis. Nat Med 7:833–839
24. Nieswandt B, Schulte V, Bergmeier W (2004) Flow-cytometric analysis of mouse platelet function. Methods Mol Biol 272:255–268
25. Rowell PP, Hurst HE, Marlowe C, Bennett BD (1983) Oral administration of nicotine: its uptake and distribution after chronic administration to mice. J Pharmacol Methods 9:249–261
26. McBride PE (1992) The health consequences of smoking. Cardiovascular diseases. Med Clin North Am 76:333–353
27. Howard G, Wagenknecht LE, Burke GL, Diez-Roux A, Evans GW, McGovern P, Nieto FJ, Tell GS (1998) Cigarette smoking and progression of atherosclerosis: The Atherosclerosis Risk in Communities (ARIC) Study. JAMA 279:119–124
28. Barua RS, Ambrose JA, Eales-Reynolds LJ, DeVoe MC, Zervas JG, Saha DC (2001) Dysfunctional endothelial nitric oxide biosynthesis in healthy smokers with impaired endothelium-dependent vasodilatation. Circulation 104:1905–1910
29. Lehr HA, Kress E, Menger MD, Friedl HP, Hubner C, Arfors KE, Messmer K (1993) Cigarette smoke elicits leukocyte adhesion to endothelium in hamsters: inhibition by CuZn-SOD. Free Radic Biol Med 14:573–581
30. Ludviksdottir D, Blondal T, Franzon M, Gudmundsson TV, Sawe UJ (1999) Effects of nicotine nasal spray on atherogenic and thrombogenic factors during smoking cessation. J Intern Med 246:61–66
31. Palmer RM, Stapleton JA, Sutherland G, Coward PY, Wilson RF, Scott DA (2002) Effect of nicotine replacement and quitting smoking on circulating adhesion molecule profiles (sICAM-1, sCD44v5, sCD44v6). Eur J Clin Investig 32:852–857
32. Wang L, Kittaka M, Sun N, Schreiber SS, Zlokovic BV (1997) Chronic nicotine treatment enhances focal ischemic brain injury and depletes free pool of brain microvascular tissue plasminogen activator in rats. J Cereb Blood Flow Metab 17:136–146
33. Zidovetzki R, Chen P, Fisher M, Hofman FM, Faraci FM (1999) Nicotine increases plasminogen activator inhibitor-1 production by human brain endothelial cells via protein kinase C-associated pathway. Stroke 30:651–655
34. Sikora L, Rao SP, Sriramarao P (2003) Selectin-dependent rolling and adhesion of leukocytes in nicotine-exposed microvessels of lung allografts. Am J Physiol Lung Cell Mol Physiol 285:L654–L663
35. Rubenstein D, Jesty J, Bluestein D (2004) Differences between mainstream and sidestream cigarette smoke extracts and nicotine in the activation of platelets under static and flow conditions. Circulation 109:78–83
36. Tutka P, Mosiewicz J, Wielosz M (2005) Pharmacokinetics and metabolism of nicotine. Pharmacol Rep 57:143–153
37. Ueno H, Pradhan S, Schlessel D, Hirasawa H, Sumpio BE (2006) Nicotine enhances human vascular endothelial cell expression of ICAM-1 and VCAM-1 via protein kinase C, p38 mitogen-activated protein kinase, NF-kappaB, and AP-1. Cardiovasc Toxicol 6:39–50
38. Lilienberg G, Venge P (1998) Platelet adhesion in patients prone to arterial and venous thrombosis: the impact of gender, smoking and heredity. Scand J Clin Lab Invest 58:279–286
39. Helmerhorst FM, Bloemenkamp KW, Rosendaal FR, Vandenbroucke JP (1997) Oral contraceptives and thrombotic disease: risk of venous thromboembolism. Thromb Haemost 78:327–333
40. Tanis BC, Rosendaal FR (2003) Venous and arterial thrombosis during oral contraceptive use: risks and risk factors. Semin Vasc Med 3:69–84
41. Chasan-Taber L, Stampfer MJ (1998) Epidemiology of oral contraceptives and cardiovascular disease. Ann Intern Med 128:467–477
42. Merten M, Thiagarajan P (2000) P-selectin expression on platelets determines size and stability of platelet aggregates. Circulation 102:1931–1936

3 Zusammenfassende Diskussion

Die mikrovaskuläre Thrombusbildung mit der Konsequenz einer Zirkulationsstörung des Gewebes stellt in der Chirurgie ein Problem von hoher klinischer Relevanz dar. Eine durch Thrombosen der kleinsten Gefäße sich ausbildende Mikrozirkulationsstörung kann im ungünstigsten Fall zur Gewebsnekrose mit für den Patienten potentiell schwerwiegenden Komplikationen führen. In der klinischen Praxis sind mikrovaskuläre Perfusionsstörungen vor allem in der Wiederherstellungschirurgie nach freien und gestielten Lappenplastiken gefürchtet [53,54]. Die Rate an primären und postprimären Komplikationen kann je nach Grunderkrankung bis zu 15% betragen. Mikrozirkulationsstörungen spielen aber auch eine wichtige Rolle in der Transplantationschirurgie und sind prinzipiell eine Gefährdung für die Wund- und Gewebeheilung nach allen Operationen [55-58]. Weiterhin kommt es bei der im freien Gewebetransfer unweigerlich auftretenden Ischämie/Reperfusion zur Bildung von freien Sauerstoffradikalen und Interaktionen von Leukozyten mit dem Endothel, welche die kapillare Perfusion zusätzlich beeinträchtigen [59].

Trotz dieses großen Einflusses mikrovaskulärer Perfusionstörungen auf den Erfolg von operativen Maßnahmen bestehen zum jetzigen Zeitpunkt vergleichsweise wenig präventive und therapeutische Möglichkeiten.

Das heutzutage vorrangig praktizierte Prinzip zur Prävention und Therapie mikrovaskulärer Durchblutungsstörungen in der Chirurgie ist die therapeutische Hämodilution mit kolloiden Lösungen, wie z.B. Dextran oder Hydroxyethylstärke [60,61]. Die normovolämische Hämodilution konnte eine Verbesserung des mikrovaskulären Blutflusses im Myokard [62], Gehirn [63], Pankreas [64] und in ischämischen Lappenplastiken [65,66] zeigen. Weiterhin zeigten auch künstliche Sauerstoffträger oder die gleichzeitige Applikation von liposomalen Hämoglobin zusätzlich zur Hämodilution in experimentellen Studien einen positiven Effekt [67,68].

Verschiedenste Studien untersuchen die Effekte einer Reihe von möglicherweise rheologieverbessernden Substanzen, wie tPA [69], Aspirin [70], unfraktionertes Heparin [71], niedermolekulares Heparin [72], Pentoxyphyllin [73], PGI_2 [74] oder Antithrombin [75]. Es waren positive Effekte im Bezug auf die mikrovaskuläre Perfusion nachweisbar, die jedoch teilweise mit einem erhöhten Blutungsrisiko einhergingen. Zusätzlich wurde häufig die mikrovaskuläre Perfusion im Allgemeinen und nicht das Entstehen, Wachsen oder die Beeinflussung mikrovaskulärer Thromben direkt untersucht.

Ein weiterer Ort für die Entstehung einer Thrombose ist die mikrovaskuläre Anastomose, was unter Umständen die Revisionsoperation mit dem Versuch der Thrombektomie notwendig macht [76]. Die Anlage einer Anastomose birgt die Gefahr einer Endothelverletzung mit Entstehung eines prothrombogenem Fokus und es konnte gezeigt werden, dass vermehrt vasokonstriktives Endothelin-1 dabei freigesetzt wird [77].

Ziel der vorliegenden Untersuchungen war zunächst die Untersuchung der Entstehung mikrovaskulärer Thrombosen in einem komplexen Tiermodell, um Einsicht in die pathophysiologisch ablaufenden Vorgänge im Rahmen der mikrovaskulären Thrombogenese zu erarbeiten. Ein spezielles Augenmerk lag zusätzlich in der Charakterisierung der Rolle von Endothelzelle, Thrombozyt und Leukozyt in der mikrovaskulären Thrombusbildung. Im Anschluss daran sollten verschiedene physiologische oder pathologische Bedingungen bezüglich eines prothrombogenen Milieus evaluiert werden, um letztendlich Möglichkeiten zur Einflussnahme durch applizierbare Substanzen zu entwickeln.

3.1 Einfluss pathologischer Zustände auf die Thrombogenese

In dieser Versuchsreihe sollte der Effekt einer reversiblen, klinisch relevanten, systemischen Hypothermie auf die mikrovaskuläre Thrombusbildung evaluiert werden. Es wurde die Hypothermie als physiologisch vorkommender Zustand gewählt, da hier wesentliche Kontroversen hinsichtlich des Effektes auf die Thrombogenität existieren.

Studien der Vergangenheit zeigten auf der einen Seite eine vermehrte Neigung zu thrombotischen Ereignissen, wie eine erhöhte Herzinfarktrate im Winter [78,79]. Gleichzeitig besteht bei Hypothermie nach Polytrauma oder auch intraoperativ häufig eine Blutungsneigung [80,81]. In unserer Untersuchung war bei Körperkerntemperaturen von 34°C und 31°C *in vivo* eine deutlich prothrombogene Wirkung nachweisbar, die durch eine verstärkte Thrombozytenaktivierung mit Konformationsänderung des Fibrinogen-Rezeptors GP IIb-IIIa erklärt werden kann. Dieser Effekt war nach Wiedererwärmung der Tiere bzw. der Thrombozyten komplett reversibel. In Übereinstimmung damit weisen die zusätzlich erniedrigten Fibrinogenspiegel bei hypothermen Temperaturen auf einen Verbrauch von Gerinnungsfaktoren im Rahmen der Thrombogenese hin.

Ein Problem vieler vorheriger Studien ist, dass die Thrombozytenfunktion oftmals stark hypotherme Temperaturen von weniger als 25°C *in vitro* untersucht wurden. Wir wählten hypotherme Temperaturen von mehr als 30°C, um die klinische Relevanz zu wahren und die Anwendung in einem Tiermodell zu ermöglichen.

Weiterhin gelang es den Einfluss hypothermer Temperaturen von 34°C und 31°C auf die Thrombozytenaggregation klarer herauszustellen. Es kam zu einer, mit mehreren Methoden nachweisbaren, temperaturabhängigen Thrombozytenaktivierung, wie zuvor von anderen Autoren berichtet wurde [82,83]. Eine zusätzliche Erkenntnis war, dass die P-Selektin Expression kaum beeinflusst wurde, während es zu einer Konformationsänderung des GP IIb-IIIa Rezeptors kam. Dieses ist in Übereinstimmung mit der Tatsache, dass die Thrombozyten-Leukozyten-Aggregatbildung nicht signifikant beeinflusst wurde, da dieses wesentlich durch die Interaktion von thrombozytärem P-Selektin und leukozytärem P-Selektin Glykoprotein Ligand-1 (PSGL-1) bestimmt wird [84].

Somit konnte mit Hilfe dieser Untersuchung erstmalig *in vivo* gezeigt werde, dass sich eine systemische Hypothermie in der Summe im lebenden Organismus in einer verstärkten Neigung zur mikrovaskulären Thrombusbildung äußert und die klinisch bestehende Blutungsneigung wahrscheinlich durch einen erhöhten Verbrauch an Gerinnungsfaktoren bedingt ist. Die Ergebnisse dieser Studie bestätigen den positiven Effekt einer schnellen Wiedererwärmung in der Klinik (z.B. polytraumatisierte Patienten) zur Verbesserung der mikrovaskulären Zirkulation.

Es ist aus früheren Studien bekannt, dass hypotherme Temperaturen im Verlauf einer Sepsis die Prognose signifikant verschlechtern [85]. Des Weiteren trägt das Auftreten vom Mikrothrombosen mit anschließender Hypoperfusion zur Ausbildung eines Multiorganversagens im Rahmen der Sepsis bei [86]. Zusätzlich ist eine Sepsis durch eine komplexe Interaktion von Entzündung und Gerinnungssystem charakterisiert [87]. Es ist daher nach wie vor nicht geklärt, ob eine Hypothermie während einer Sepsis lediglich eine Verschlechterung des Gesamtzustandes repräsentiert, oder ob die Hypothermie selbst direkt einen negativen Einfluss, wie z.B. eine verschlechterte Organperfusion aufgrund von Mikrothromben, ausübt. Daher war es für uns von Interesse, die Kombination von Hypothermie und Endotoxinämie hinsichtlich mikrovaskulärer Thrombogenität zu untersuchen. Erneut lag eine zusätzliche Betonung auf der Evaluierung der thrombozytären und endothelialen Funktion.

Die LPS-induzierte Endotoxinämie beschleunigte die Ausbildung der thrombotischen Gefäßokklusion bei 37°C Körpertemperatur signifikant, welches mit einer generell erhöhten endothelialen und Thrombin-vermittelten thrombozytären Aktivierung einherging. Dieses ist ,in Übereinstimmung mit den Angaben mehrerer anderer Autoren, in Anbetracht des in der Sepsis aktivierten Gerinnungssystem auch zu erwarten [86-90]. Eine zusätzliche Hypothermie von 31°C führte zu einer signifikant schnellen Thrombusbildung in Arteriolen.

Interessanterweise ging die zusätzliche Hypothermie lediglich mit einer vermehrten PAI-1 Expression und einem erhöhten sPAI-Ag Spiegel, jedoch nicht mit einer weiteren generellen endothelialen Aktivierung einher, so dass für PAI-1 eine spezifische Rolle unter hypothermen Bedingungen vermutet werden kann.

Während einer Sepsis werden pro-inflammatorische Zytokine, wie Interleukin-1, Interleukin-6 und Tumor Nekrose Faktor-alpha (TNF-α) gebildet, welche das Endothel aktivieren [91]. Die entzündliche Antwort des Endothels umfasst die Hochregulation von P-Selektin, ICAM-1, VCAM-1. E-Selektin wird verzögert mobilisiert. Alle Moleküle werden ins Blut abgegeben und sind dort in löslicher Form detektierbar [92]. Neue Studien konnten zeigen, dass Endothelzellen eine entscheidende Rolle in der Pathogenese der Sepsis spielen, indem sie PAI-1 und TF freisetzen [87]. In der vorliegenden Studie konnte erstmalig Anhalt dafür gegeben werden, dass die durch Endotoxinämie verursachte PAI-1 Expression durch eine zusätzliche Hypothermie noch verstärkt wird und somit ein Faktor in der Prognoseverschlechterung bei Hypothermie sein könnte. Als Konsequenz für die Klinik ergibt sich, dass bei einer Sepsis angestrebt werden sollte, die Körpertemperatur konstant zu halten und insbesondere Hypothermiephasen zu vermeiden.

3.2 Beeinflussung der Thrombogenese durch Induktion endogener Enzyme

In einem weiterführenden Projekt zur Untersuchung der mikrovaskulären Thrombusbildung am Cremastermuskel der Maus wurde das Enzym HO-1, welches den letzten Schritt des Abbaus von Häm mit Freisetzung äquimolarer Mengen an Eisen, Biliverdin/Bilirubin und CO katalysiert, untersucht. Verschiedene Studien zu HO-1 Induktoren konnten zeigen, dass Gewebe, die viel HO-1 exprimieren, weniger anfällig für oxidativen Stress oder proinflammatorische Zustände sind [93,94]. Da die freie Radikalbildung mit der Folge von oxidativem Stress auch eine wichtige Rolle in der Pathogenese thrombotischer Ereignisse spielt, war es Ziel der Studie zu klären, ob die Induktion von HO-1 die Bildung mikrovaskulärer Thromben moduliert und damit die Athrombogenität des Endothels erhöht werden kann. Auf diese Weise sollte untersucht werden, in wieweit der Organismus selbst in der Lage ist, protektive Mechanismen, wie die vermehrte Bildung von anti-adhäsivem CO und anti-oxidativem Bilirubin, durch einen externen Stimulus hochzuregulieren.

Hämoxygenasen existieren in verschiedenen Isoformen, wobei HO-2 konstitutiv exprimiert wird und HO-1 induzierbar ist [95,96]. Nach Vorbehandlung mit Hämin, einem HO-1-Induktor, zeigten Western Blot Analysen eine deutliche Induktion von HO-1 Protein im Cremastermuskel, welche mittels Immunhistochemie vor allem im Bereich des vaskulären Endothels von Arteriolen und Venolen lokalisiert werden konnte. Bei diesen Tieren war die Bildung arteriolärer und venulärer Thromben signifikant gegenüber der Kontrollgruppe

verzögert. Diese verminderte Thrombogenität wurde durch die Gabe des HO-1 Inhibitors Zinn-Protoporphyrin-IX komplett aufgehoben. HO-1 exprimierende Tiere zeigten mittels Western Blot Analyse im Vergleich zu Kontrolltieren eine reduzierte Expression von P-Selektin Protein im Cremastermuskel. Die Rolle von P-Selektin in der Thrombogenese wurde durch eine Versuchsreihe mit P-Selektin-Knock-out-Mäusen bestätigt, wobei die Thrombusformation bei den P-Selektin-defizienten Tieren signifikant verzögert war. Somit konnten wir den protektiven Effekt einer HO-1 Induktion letztendlich auf eine Reduktion der endothelialen P-Selektin Expression zurückführen. Diese Annahme wird durch eine Studie unterstützt, in der die LPS-vermittelte P-Selektin Hochregulation durch Behandlung mit Hämin verhindert werden konnte [97].

Zusätzliche Experimente mit Bilirubinsuperfusion des Cremastermuskels ergaben eine deutliche Verzögerung der Thrombusbildung, so dass davon auszugehen ist, dass der protektive Effekt von HO-1 neben den Effekten des CO vor allem über das freigesetzte, anti-oxidative Bilirubin vermittelt ist. Dieses ist in Übereinstimmung mit Studien der Vergangenheit, welche potente anti-oxidative und anti-adhäsive Eigenschaften des Biliverdins bzw. in reduzierter Form des Bilirubins nachweisen konnten [98,99]. Dennoch sind auch die anti-koagulativen Eigenschaften von CO zunehmend Gegenstand der Diskussion. So konnte eine verminderte PAI-1 Expression mit verbesserter Fibrinolyse nach Inhalation von CO im Lungengewebe nach Ischämie gezeigt werden [100].

Es konnte in diesem Projekt erstmalig eine anti-thrombotische Wirkung durch Induktion der Hämoxygenase-1 charakterisiert werden. Dieser Ansatz könnte die Grundlage für eine vektorbasierte Therapie in der Klinik sein, um das vaskuläre Endothel in einen weniger thrombogenen Zustand im Rahmen von Risikooperationen zu versetzen.

3.3 Beeinflussbarkeit der Thrombogenese durch Substanzen

Die vorherigen Studien untersuchten den Einfluss körpereigener Zustände oder Mechanismen auf die mikrovaskuläre Thrombogenese. Im Weiteren war es jetzt unser Ziel, die Thrombusfomation durch verschiedene exogen applizierte Substanzen zu modulieren. Dabei wurden zum einen prinzipiell als protektiv angesehene Moleküle, wie das anti-oxidative Ebselen und C-Peptid, angewendet, zum anderen erfolgte die Applikation von fraglich pro-thrombogenen Verbindungen, wie Darbepoetin-alpha und Nikotin.

Ebselen

Verschiedene Untersuchungen der Vergangenheit vermuteten einen Zusammenhang zwischen einem Mangel des Spurenelementes Selen und dem Risiko für akute koronare

Ereignisse [101,102]. Selen ist Bestandteil des Enzyms Glutathionperoxidase, welches Zellen gegen oxidativen Stress schützt. Niedrige Selenspiegel sind in der Regel mit einer niedrigen Aktivität der Glutathionperoxidase und somit mit einem erhöhten Niveau an freien Radikalen assoziiert [103].

In einer Untersuchung am Cremastermuskel der Ratte konnten wir jetzt erstmals *in vivo* eine anti-thrombotische Wirksamkeit der selenhaltigen Substanz Ebselen nachweisen. Weiterhin zeigten sich nach Gabe von Ebselen eine signifikant verminderte thrombozytäre P-Selektin-Expression nach Stimulation mit H_2O_2 und eine Reduktion der Thrombozyten-Leukozyten-Aggregatbildung. Es konnte in einer früheren Studie gezeigt werden, dass die Akkumulation von Leukozyten in einen wachsenden Thrombus über thrombozytäres P-Selektin vermittelt wird [104]. Außerdem wirkt P-Selektin prothrombogen, indem es die Synthese von TF in Monozyten induziert [105].

Die dosisabhängige Reduktion der H_2O_2-induzierten Thrombozytenaktivierung *in vitro* durch Ebselen legt die Vermutung nahe, dass dessen anti-oxidative Eigenschaften die Folgeerscheinungen des oxidativen Stresses wie Gefäßwandschaden, Thrombozytenaktivierung und Zell-Zell-Interaktion vermindern.

Damit konnte die von uns erstmals aufgezeigte anti-thrombogene Wirkung von Ebselen auf eine Reduktion der P-Selektin-abhängigen Zell-Zell-, in Sonderheit Thrombozyten-Leukozyten-Interaktion zurückgeführt werden. Angesichts dieses neuen Wirkprofils könnte Ebselen von hohem präventiven und therapeutischen Wert in der Behandlung von thrombotischen Erkrankungen sein.

C-Peptid

Die hohe Morbidität und Mortalität diabetischer Patienten wird hauptsächlich durch vaskuläre Komplikationen bestimmt. Die Pathophysiologie der diabetischen Vaskulopathie beinhaltet die endotheliale Dysfunktion mit vermehrter Produktion von PAI-1, reaktiven Sauerstoffverbindungen und verminderter Produktion von NO sowie eine Thrombozytendysfunktion und ein Ungleichgewicht plasmatischer Gerinnungsfaktoren [106-111]. Das Insulinspaltprodukt C-Peptid wurde in der Vergangenheit als biologisch inaktiv angesehen. Neuere Studien zeigten jedoch molekulare und physiologische Effekte, welche auf eine Bioaktivität des Peptids hinweisen [112]. Von verschiedenen Autoren wurde ein vasodilativer Effekt von C-Peptid auf Skelettmuskelarteriolen beobachtet und eine NO-Freisetzung als Ursache nachgewiesen [113,114]. Ziel unserer Studie war daher, den Einfluss einer C-Peptid Applikation hinsichtlich mikrovaskulärer Thrombusbildung und thrombozytärer und endothelialer Funktion in gesunden und diabetischen Tieren zu untersuchen.

Die Gabe von C-Peptid in hoher Dosierung von 70 nmol/kg führte zu einer signifikanten Verzögerung der mikrovaskulären Thrombusbildung in gesunden und diabetischen Tieren. Dieser Effekt wurde durch die gleichzeitige Gabe von Insulin jedoch unterdrückt. Als ursächlich ist eine verminderte PAI-1 Expression auf dem vaskulären Endothel anzusehen. Die Thrombozytenfunktion wurde durch C-Peptid nicht beeinflusst.

In früheren Studien konnte durch C-Peptid eine Verbesserung der Skelettmuskeldurchblutung [115,116], der glomerulären Filtration [117,118] und der Nervenfunktion [119] gezeigt werden. Mit der vorliegenden Arbeit ist gezeigt, dass C-Peptid zusätzlich einen Einfluss auf die mikrovaskuläre Thrombusbildung ausübt. PAI-1 wurde bereits in der Vergangenheit als prothrombogener Faktor identifiziert [120,121]. Aufgrund der Ergebnisse der vorliegenden Untersuchung ist eine Rolle von PAI-1 in der anti-thrombogenen Wirkung von C-Peptid wahrscheinlich. Ebenso ist bekannt, dass Insulin die PAI-1 Expression verstärkt und zu einer erhöhten Endothelinproduktion führt, was mit der vermehrten Thrombogenität nach Insulinsuperfusion in dieser Studie vereinbar ist [122,123]. Es wurde mehrfach beschrieben, dass die positiven Effekte von C-Peptid nur in Typ 1-diabetischen Individuen nachweisbar sind [119,124]. Dieses wurde mit der Sättigungskinetik des C-Peptid Rezeptors unter physiologischen Bedingungen erklärt [125]. Da in dieser Studie die anti-thrombogenen Effekte von C-Peptid sowohl in diabetischen, als auch in gesunden Tieren beobachtet wurden, ist von einer nicht-rezeptorvermittelten Wirkung auszugehen. Dennoch erscheint die Gabe von C-Peptid beim diabetischen Patienten zur Therapie der Vaskulopathie nicht von Vorteil, da Typ-1 Diabetiker auf Insulingaben angewiesen sind. Eine therapeutische Gabe beim Nicht-Diabetiker zur Verminderung mikrovaskulärer Thrombusbildung wäre jedoch denkbar.

Darbepoetin-alpha

Das Hormon Erythropoietin, kurz EPO, wird in der Medizin zur Therapie der renalen Anämie eingesetzt und ist in den letzten Jahren zunehmend durch Doping im Leistungssport in der Öffentlichkeit bekannt geworden [126]. Es erhöht die Zahl der roten Vorläuferzellen im Knochenmark durch anti-apoptotische Effekte [127]. Der Einfluss auf die Thrombogenität des Blutes unter der Therapie mit EPO wird zunehmend kontrovers diskutiert. Zum einen wurde von einer vermehrten endothelialen Aktivierung, erhöhter Produktion von TF, vermehrter PAI-1 Expression und erhöhter Thrombozytenaggregation berichtet [128-130]. Zum anderen wurde in EPO-überexprimierenden Mäusen eine geringere Blutviskosität und verminderte Gerinnselfestigkeit beobachtet [131,132]. Die Klärung dieser Frage ist von großer Relevanz, da insbesondere im Leistungssport auch Fälle aufgetreten sind, bei denen „Schutzsperren“ allein aufgrund eines höheren Hämatokritwertes verhängt wurden, ohne dass EPO-Doping

nachgewiesen werden konnte. Dieses Vorgehen wurde mit einer Gefährdung der Athleten durch eine erhöhte Thrombosegefahr begründet.

Wir untersuchten daher das EPO-Derivat DPO im Tiermodell. Es zeigte sich, dass die 4-wöchige Behandlung mit DPO in Hämatokrit-erhöhenden Dosen zu keiner signifikanten Steigerung der mikrovaskulären Thrombogenität führte, solange eNOS als kompensatorischer Mechanismus zur Verfügung stand. So hatten eNOS knock-out Tiere eine signifikant verstärke Thromboseneigung unter DPO-Behandlung. Die durch eNOS Hochregulation erhöhte Produktion von NO führte zu einer endothelialen und thrombozytären Deaktivierung. Interessanterweise zeigten sich auch keine negativen Effekte auf Blutflussgeschwindigkeit und Scherstress durch den erhöhten Hämatokrit. Dieses wurde bereits zuvor in einer *in vivo* Studie beschrieben, in der bei Hämatokritwerten von 20 bis 55% unter verschiedenen Flussbedingungen keine erhöhte Thrombusbildung beobachtet wurde [133].

Eine vermehrte Expression von eNOS war bereits in transgenen EPO-Mäusen beschrieben worden und als Schutzmechanismus gegen die endogen erhöhten hohen Hämatokritwerte von ca. 80% gewertet worden [134]. Wir konnten erstmals *in vivo* zeigen, dass die eNOS Produktion auch durch die exogene Gabe von DPO stimuliert werden kann.

Somit führt die Behandlung mit DPO nicht zu anti-thrombogenen Effekten, sie ist aber auch nicht prothrombogen, solange die Gegenregulation durch eNOS funktioniert. Dieses könnte auch erklären, warum erhöhte Hämatokritwerte, wie z.B. nach Doping im Leistungssport, nur in einzelnen Fällen zu fatalen Komplikationen führen.

Nikotin

Schlussendlich sollte der Einfluss von Nikotin auf die mikrovaskuläre Thrombogenese im geschlechtsspezifischen Tiermodell untersucht werden. Das Rauchen stellt die Hauptursache für vermeidbare Todesfälle in der industrialisierten Welt dar [135]. In Studien der Vergangenheit wurde vermutet, dass Nikotin ein das kardiale Risiko negativ beeinflussender Faktor ist. Zusätzlich ist die Einnahme von oralen Kontrazeptiva mit einem 2- bis 4-fach erhöhten Risiko für eine tiefe Venenthrombose (TVT) assoziiert und somit eine geschlechtsspezifische hormonabhängige Prädisposition Thrombosen zu entwickeln, wahrscheinlich [136]. Trotzdem wird ein direkter kausaler Zusammenhang bis dato kontrovers diskutiert [137,138].

Wir untersuchten daher männliche und weibliche Mäuse in Bezug auf mikrovaskuläre Thrombogenität durch Nikotin. Die chronische Vorbehandlung mit Nikotin induzierte bei beiden Geschlechtern keine vermehrte mikrovaskuläre Thrombusbildung. Bei männlichen, jedoch nicht bei weiblichen Tieren, war dieses mit einer endothelialen Deaktivierung

verbunden. Im Gegensatz dazu resultierte eine akute hochdosierte Nikotingabe in einer signifikant schnelleren Thrombusbildung in Arteriolen weiblicher Tiere, was unter anderem mit einer erhöhten endothelialen P-Selektin Expression vergesellschaftet war. Es konnte in Studien gezeigt werden, dass Nikotin zu einer Störung der NO-vermittelten Vasodilatation in Arteriolen und Venolen führt [139]. Des Weiteren war nach Nikotinexposition ein Anstieg von Plasminogen-Aktivator-Inhibitor-1 (PAI-1) in Endothelzellen nachzuweisen [140]. Auf der anderen Seite wurde unter Substitution von Nikotin-Nasenspray, Nikotin-Kaugummi oder Nikotin-Pflaster nach Einstellung des Rauchens eine deutliche Verbesserung des Cholesterinspiegels und kein Einfluss auf Blutdruck, Thrombozytenzahl, Blutviskosität oder AT III-Spiegel beobachtet [140,141]. In der vorliegenden Arbeit konnte gezeigt werden, dass eine akute Hochdosisapplikation, nicht aber eine chronische Nikotinexposition mit niedrigen Dosen, thrombogen *in vivo* wirkt, wobei dieser prothrombogene Effekt nur in weiblichen Tieren zu beobachten war. Die negativen Effekte des Rauchens, die auch bei männlichen Individuen beobachtet werden, sind demnach weniger auf das Nikotin an sich, als vielmehr auf einen der vielen anderen schädlichen Substanzen im Zigarettenrauch zurückzuführen. Nikotin selbst hingegen wirkt bei schneller Anflutung in hoher Dosierung prothrombogen in weiblichen Tieren. Diese unterstützt die These einer geschlechtspezifischen Wirkung von Nikotin.

4 Zusammenfassung

Die mikrovaskuläre Thrombusbildung und deren zugrunde liegenden molekularen, zellulären und humoralen Mechanismen wurden bislang selten in komplexen *in vivo* Modellen untersucht. Eine suffiziente mikrovaskuläre Perfusion ist die Vorraussetzung für das Gelingen sämtlicher chirurgischer Eingriffe, insbesondere aber für das Überleben von Lappenplastiken, und bestimmt wesentlich das Outcome des Patienten. In der Klinik würde ein verbessertes Verständnis der während der mikrovaskulären Thrombogenese ablaufenden pathophysiologischen Vorgänge von großem Vorteil sein und potentiell neue Therapiemöglichkeiten nach sich ziehen. Bezüglich der Identifizierung neuer anti-thrombogener Substanzen hat es in den letzten Jahren kaum Forschritte in der Forschung gegeben, so dass weiterhin auf alt bekannte Therapie- und Präventionsstrategien zurückgegriffen wird. Diese sind teilweise jedoch auch mit negativen Effekten, wie z.B. einem vermehrten Blutungsrisiko, verbunden.

Ziel der vorliegenden Studien war es daher, primär die Mechanismen der mikrovaskulären Thrombusbildung im komplexen Tiermodell zu charakterisieren und endotheliale und thrombozytäre Funktion durch zusätzliche *in vitro* Methoden zu identifizieren. Danach sollten verschiedene Faktoren, die in diesem Zusammenhang potentiell einen Einfluss ausüben könnten, wie z.B. eine pathologisch auftretende reversible Hypothermie, eine pathologische Endotoxinämie oder die Induktion eines Enzymsystems, wie Hämoxygenase-1, evaluiert werden. Schlussendlich sollten dann verschiedene Substanzen hinsichtlich ihres Einflusses auf die mikrovaskuläre Thrombogenität untersucht werden, um klinisch einsetzbare Präventions- und Therapiemöglichkeiten daraus zu entwickeln.

Die Untersuchung der mikrovaskulären Thrombogenität unter hypothermen Bedingungen ergab einen prothrombogenen Effekt bei Körperkerntemperaturen unter 34°C, welcher nach Wiedererwärmung komplett reversibel war. Dieses konnte auf eine verstärkte Aktivierung des thrombozytären Fibrinogenrezeptors während der Hypothermie zurückgeführt werden. Die Ergebnisse dieser Studie unterstreichen die Bedeutung normothermer Temperaturen in der Chirurgie, sowohl nach traumatischen Ereignissen, als auch im Rahmen elektiver Operationen. Sie zeigen zusätzlich, dass eine verstärkte Thrombogenität auch reversibel und somit einfach beeinflussbar sein kann, wenn die ablaufenden pathophysiologischen Mechanismen bekannt sind.

Die zusätzliche Induktion einer Endotoxinämie bei hypothermen Tieren zeigte in einer weiteren Untersuchung, dass die Kombination aus Hypothermie und Endotoxinämie einen

pro-thrombogenen Einfluss über eine spezifische Hochregulation von PAI-1 auf dem Endothel bzw. eine vermehrte Sekretion von sPAI-Ag ausübt. Dahingegen war eine Endotoxinämie ohne Hypothermie generell mit einer vermehrten unspezifischen endothelialen Aktivierung vergesellschaftet. Somit konnte erstmalig gezeigt werden, dass eine zusätzliche Hypothermie während einer bestehenden Endotoxinämie die mikrovaskuläre Thrombusbildung verstärkt und daher ein unabhängiger Faktor für die Verschlechterung der Prognose septischer Patienten sein könnte. Daher sollten prinzipiell normotherme Temperaturen bei septischen Patienten zur Vermeidung mikrovaskulärer Perfusionsstörungen angestrebt werden.

In einer weiteren Studie konnte gezeigt werden, dass protektive anti-thrombotische Mechanismen auch durch die Hochregulation endogener Enzymsysteme verstärkt werden können. So konnte durch die Applikation eines Hämoxygenase-1 Induktors eine verminderte mikrovaskuläre Thrombogenität erzielt werden. Diese war vor allem auf die vermehrte Produktion von anti-oxidativem Bilirubin zurückzuführen, was eine verminderte P-Selektin Expression auf dem Endothel bedingte. Die lokale Induktion der Hämoxygenase-1 könnte durch vektorbasierte Therapie in der Klinik nutzbar gemacht werden und von präventivem und therapeutischem Wert für Krankheitsbilder mit einem erhöhten thrombotischen Risiko sein.

Im Folgenden stellte sich die Frage, in wieweit die mikrovaskulären Thrombusbildung durch die Applikation körpereigener und synthetischer Substanzen beeinflusst werden könnte. Zunächst erfolgte die Untersuchung des Effektes von Ebselen unter besonderer Berücksichtigung der Thrombozytenfunktion. Es konnte gezeigt werden, dass Ebselen dosisabhängig die Thrombozytenaktivierbarkeit hemmte, was mit einer verminderten mikrovaskulären Thrombusbildung einherging. Ebselen stellt somit eine potentiell wirksame Substanz zur Vorbeugung mikrovaskulärer Thrombosen dar.

Besonders häufig treten mikrovaskuläre Komplikationen bei diabetischen Patienten auf. C-Peptid wird bei der Insulinbiosynthese abgespalten und wurde lange als inaktives Nebenprodukt angesehen. Nachdem mehrere neuere experimentelle und klinische Studien positive Effekte des C-Peptids in diabetischen Individuen zeigten, lag die Vermutung nahe, dass eventuell auch die diabetische Mikrothrombogenität durch C-Peptid positiv beeinflusst werden könnte. Es fand sich eine signifikant verlangsamte Thrombusbildung bei hochdosierter Gabe von C-Peptid, ein Effekt, welcher jedoch nach Gabe von Insulin aufgehoben werden konnte. Als ursächlich wurde eine verminderte Expression des pro-thrombogenen PAI-1 auf dem Endothel identifiziert. Eine klinische Anwendbarkeit erscheint in diesem Fall durch die Antagonisierung der positiven C-Peptid Effekte durch Insulin allerdings unwahrscheinlich.

Erythropoietin und seine langlebigeren Derivate, wie Darbepoetin-alpha, werden in

der Klinik zur Steigerung der Hämatopoese bei niereninsuffizienten Patienten verwendet, gleichzeitig aber auch zunehmend im Leistungssport missbraucht. Obwohl allgemein angenommen, war bisher nicht klar, inwiefern tatsächlich die Therapie mit diesen Substanzen zu vermehrten Thrombosen führt. Es konnte in einer weiteren Studie erstmalig gezeigt werden, dass die exogene Applikation von Darbepoetin-alpha zu einer signifikanten Hochregulation der anti-thrombogen wirksamen eNOS führt, und dass dieser Mechanismus entscheidend zur Vermeidung thromboembolischer Komplikationen beiträgt. Das Wissen um diese Zusammenhänge ist in der Klinik von großer Bedeutung, da Patienten mit defizienter Synthese von NO einem hohen prothrombogenen Risiko ausgesetzt sind. Dieses könnte auch erklären, warum Darbepoetin-alpha bei Tumorpatienten, welche potentiell eine gestörte endotheliale Funktion mit insgesamt prothrombogenem Status aufweisen, zu einer höheren Mortaliät führt und daher zur Behandlung der tumorassoziierten Anämie nicht mehr zugelassen ist. Auf der anderen Seite ist der Einsatz von NO-Donatoren bei diesen Patienten in Betracht zu ziehen und sollte in diesem Zusammenhang weiter untersucht werden.

Das Rauchen wird mit einer erhöhten Rate an thromboembolischen Ereignissen in Verbindung gebracht. Es ist jedoch nach wie vor nicht geklärt, ob das suchtverursachende Nikotin oder einer der vielen anderen Komponenten des Zigarettenrauchs dafür verantwortlich ist. Ebenso scheint das Thromboserisiko in Zusammenhang mit der Einnahme von weiblichen Geschlechtshormonen erhöht. Eine Untersuchung zur mikrovaskulären Thrombogenität an männlichen und weiblichen Tieren ergab keinen signifikanten Effekt chronischer Nikotinapplikation in Tieren beiden Geschlechts, jedoch führte die hochdosierte intravenöse Nikotingabe bei weiblichen Tieren zu einer signifikant schnelleren Thrombusbildung. Dieses ging einher mit einer erhöhten endothelialen Aktivierung. Aufgrund dieser Ergebnisse kann eine geschlechtsspezifische Wirkung der nikotinvermittelten Thrombogenität vermutet werden. Daher sollte in der Klinik der Einsatz der Nikotinsubstitution zur Raucherentwöhnung vor allem bei Frauen kritisch überdacht werden.

Die vorliegenden Untersuchungen zeigen, dass eine Beeinflussbarkeit der mikrovaskulären Thrombogenität in Kenntnis der zugrunde liegenden molekularen, zellulären und humoralen Vorgänge auf verschiedensten Ebenen möglich ist. Die Anwendung der in dieser Arbeit charakterisierten Beeinflussungsmöglichkeiten in klinischen Studien könnte zur Entwicklung neuer und viel versprechender Präventions- und Therapieoptionen in der Chirurgie beitragen.

5 Literaturverzeichnis

1. Furie B, Furie BC. Thrombus formation in vivo. J Clin Invest. 2005; 115: 3355-3362.
2. Furie B, Furie BC. The molecular basis of blood coagulation. Cell. 1988; 53: 505-518.
3. Spronk HM, Govers-Riemslag JW, ten Cate H. The blood coagulation system as a molecular machine. Bioessays. 2003; 25: 1220-1228.
4. Spronk HM, van der Voort D, Ten Cate H. Blood coagulation and the risk of atherothrombosis: a complex relationship. Thromb J. 2004; 2: 12.
5. Aird WC. Hemostasis and irreducible complexity. J Thromb Haemost. 2003; 1: 227-230.
6. ten Cate H, Aird WC. Molecular Mechanisms of disseminated intravascular coagulation. Landes Bioscience Publishers, Texas, 2003.
7. Becker BF, Heindl B, Kupatt C, Zahler S. Endothelial function and hemostasis. Z Kardiol. 2000; 89: 160-167.
8. Morrissey JH, Fakhrai H, Edgington TS. Molecular cloning of the cDNA for tissue factor, the cellular receptor for the initiation of the coagulation protease cascade. Cell. 1987; 50: 129-135.
9. Koolman J, Röhm KH. Hämostase. Taschenatlas der Biochemie. Georg Thieme Verlag, Stuttgart, 1994.
10. Alessi MC, Juhan-Vague I. Contribution of PAI-1 in cardiovascular pathology. Arch Mal Coeur Vaiss. 2004; 97: 673-678.
11. Monroe DM, Hoffman M. What does it take to make the perfect clot? Arterioscler Thromb Vasc Biol. 2006; 26: 41-48.
12. Monroe DM, Hoffman M, Roberts HR. Transmission of a procoagulant signal from tissue factor-bearing cell to platelets. Blood Coagul Fibrinolysis. 1996; 7: 459-464.
13. Briede JJ, Heemskerk JW, van't Veer C, Hemker HC, Lindhout T. Contribution of platelet-derived factor Va to thrombin generation on immobilized collagen- and fibrinogen-adherent platelets. Thromb Haemost. 2001; 85: 509-513.
14. Alberio L, Dale GL. Review article: platelet-collagen interactions: membrane receptors and intracellular signalling pathways. Eur J Clin Invest. 1999; 29: 1066-1076.
15. van Hinsbergh VW. The endothelium: vascular control of haemostasis. Eur J Obstet Gynecol Reprod Biol. 2001; 95: 198-201.
16. de Graaf JC, Banga JD, Moncada S, Palmer RM, de Groot PG, Sixma JJ. Nitric oxide functions as an inhibitor of platelet adhesion under flow conditions. Circulation. 1992; 85: 2284-2290.
17. Esmon CT. The protein C anticoagulant pathway. Arterioscler Thromb. 1992; 12: 135-145.

18. Michiels C. Endothelial cell functions. J Cell Physiol. 2003; 196: 430-443.
19. Stern DM, Esposito C, Gerlach H, Gerlach M, Ryan J, Handley D, Nawroth P. Endothelium and regulation of coagulation. Diabetes Care. 1991; 14: 160-166.
20. Sidelmann JJ, Gram J, Jespersen J, Kluft C. Fibrin clot formation and lysis: basic mechanisms. Semin Thromb Hemost. 2000; 26: 605-618.
21. Zimmerman GA, McIntyre TM, Mehra M, Prescott SM. Endothelial cell-associated platelet-activating factor: a novel mechanism for signaling intercellular adhesion. J Cell Biol. 1990; 110: 529-540.
22. van Mourik JA, Romani de Wit T, Voorberg J. Biogenesis and exocytosis of Weibel-Palade bodies. Histochem Cell Biol. 2002; 117: 113-122.
23. Ruggeri ZM. Structure and function of von Willebrand factor. Thromb Haemost. 1999; 82: 576-584.
24. Bogatcheva NV, Garcia JG, Verin AD. Molecular mechanisms of thrombin-induced endothelial cell permeability. Biochemistry (Mosc). 2002; 67: 75-84.
25. Wu KK, Thiagarajan P. Role of endothelium in thrombosis and hemostasis. Annu Rev Med. 1996; 47: 315-331.
26. Shebuski RJ, Kilgore KS. Role of inflammatory mediators in thrombogenesis. J Pharmacol Exp Ther. 2002; 300: 729-735.
27. Furie B, Furie BC, Flaumenhaft R. A journey with platelet P-Selectin: the molecular basis of granule secretin, signalling and cell adhesion. Throm Haemost. 2001; 86: 214-221.
28. Principe DD, Menichelli A, De Matteir W, Di Giulio S, Giodani M, Savini I, Finazzi Agro A. Hydrogen peroxide is an intermediate in the platelet activation cascade triggered by collagen, but not thrombin. Throm Res. 1991; 62: 365-375.
29. Merten M, Thiagarajan P. P-selectin expression on platelets determines the size and stability of platelet aggregates. Circulation. 2000; 102: 1931-1936.
30. Giesen PL, Rauch U, Bohrmann B, Kling D, Roque M, Fallon JT, Badimon JJ, Himber J, Riederer MA, Nemerson Y. Blood-borne tissue factor: another view of thrombosis. Proc Natl Acad Sci U S A. 1999; 96: 2311-2315.
31. Becker BF, Zahler S, Seligmann C, Kupatt C, Habazettl H. Interaction of adenosine with leukocytes and thrombocytes. Z Kardiol. 1996; 85 Suppl 6: 161-170.
32. Henn V, Slupsky JR, Grafe M, Anagnostopoulos I, Forster R, Muller-Berghaus G, Kroczek RA. CD40 ligand on activated platelets triggers an inflammatory reaction of endothelial cells. Nature. 1998; 391: 591-594.
33. Szmitko PE, Wang CH, Weisel RD, de Almeida JR, Anderson TJ, Verma S. New markers of inflammation and endothelial cell activation: Part I. Circulation. 2003; 108: 1917-1923.

34. Kaplanski G, Marin V, Fabrigoule M, Boulay V, Benoliel AM, Bongrand P, Kaplanski S, Farnarier C. Thrombin-activated human endothelial cells support monocyte adhesion in vitro following expression of intercellular adhesion molecule-1 (ICAM-1; CD54) and vascular cell adhesion molecule-1 (VCAM-1; CD106). Blood. 1998; 92: 1259-1267.
35. Ruggeri ZM. Platelets in atherothrombosis. Nat Med. 2002; 8: 1227-1234.
36. Clemetson KJ, Clemetson JM. Platelet collagen receptors. Thromb Haemost. 2001; 86: 189-197.
37. Savage B., Cattaneo M, Ruggeri ZM. Mechanisms of platelet aggregation. Curr Opin Hematol. 2001; 8: 270-276.
38. Beumer S, IJsseldijk MJ, de Groot PG, Sixma JJ. Platelet adhesion to fibronectin in flow: dependence on surface concentration and shear rate, role of platelet membrane glycoproteins GP IIb/IIIa and VLA-5, and inhibition by heparin. Blood. 1994; 84: 3724-3733.
39. Coughlin SR. Thrombin signalling and protease-activated receptors. Nature. 2000; 407: 258-264.
40. Woodside DG, Liu S, Ginsberg MH. Integrin activation. Thromb Haemost. 2001; 86: 316-323.
41. Falati S, Gross P, Merrill-Skoloff G, Furie BC, Furie B. Real-time in vivo imaging of platelets, tissue factor and fibrin during arterial thrombus formation in the mouse. Nat Med. 2002; 8: 1175-1181.
42. Baez S. An open cremaster muscle preparation for the study of blood vessels by in vivo microscopy. Microvasc Res. 1973; 5: 384-394.
43. Vollmar B, Schmitz R, Kunz D, Menger MD. Lack of in vivo function of CD31 in vascular thrombosis. Thromb Haemost. 2001; 85: 160-164.
44. Pierangeli SS, Colden-Stanfield M, Liu X, Barker JH, Anderson GL, Harris EN. Antiphospholipid antibodies from antiphospholipid syndrome patients activate endothelial cells in vitro and in vivo. Circulation. 1999; 99: 1997-2002.
45. Thorlacius H, Vollmar B, Seyfert UT, Vestweber D, Menger MD. The polysaccharide fucoidan inhibits microvascular thrombus formation independently from P- and L-selectin function in vivo. Eur J Clin Invest. 2000; 30: 804-810.
46. Endrich B, Asaishi K, Gotz A, Messmer K. Technical report--a new chamber technique for microvascular studies in unanesthetized hamsters. Res Exp Med (Berl). 1980; 177: 125-134.
47. Lehr HA, Kress E, Menger MD, Friedl HP, Hubner C, Arfors KE, Messmer K. Cigarette smoke elicits leukocyte adhesion to endothelium in hamsters: inhibition by CuZn-SOD. Free Radic Biol Med. 1993; 14: 573-581.

48. Roesken F, Ruecker M, Vollmar B, Boeckel N, Morgenstern E, Menger MD. A new model for quantitative in vivo microscopic analysis of thrombus formation and vascular recanalisation: the ear of the hairless (hr/hr) mouse. Thromb Haemost. 1997; 78: 1408-1414.
49. Denis C, Methia N, Frenette PS, Rayburn H, Ullman-Cullere M, Hynes RO, Wagner DD. A mouse model of severe von Willebrand disease: defects in hemostasis and thrombosis.Proc Natl Acad Sci U S A. 1998; 95: 9524-9529.
50. Raffael A, Nebe CT, Valet G. Grundlagen der Durchflußzytometrie. Durchflußzytometrie in der klinischen Zelldiagnostik. Schattauer, Stuttgart, 1994.
51. Shapiro HM. Practical flow cytometry. 3rd ed. Wiley-Liss, New York, 1995.
52. Schmitz G, Rothe G, Ruf A, Barlage S, Tschope D, Clemetson KJ, Goodall AH, Michelson AD, Nurden AT, Shankey TV.European Working Group on Clinical Cell Analysis: Consensus protocol for the flow cytometric characterisation of platelet function. Thromb Haemost. 1998; 79: 885-896.
53. Thorniley MS, Carver N, Jones DP. Free flap monitoring in plastic and reconstructive surgery. Adv Exp Med Biol. 2003; 530: 717-724.
54. Rucker M, Schafer T, Stamm A, Saueressig K, Vollmar B, Spitzer WJ, Menger MD. New model for in vivo quantification of microvascular embolization, thrombus formation, and recanalization in composite flaps. J Surg Res. 2002; 108: 129-137.
55. Chapman JR, Robertson P, Allen RD. Why do pancreas transplants thrombose? Transplantation. 2001; 72: 182-183.
56. Robson M, Cote I, Abbs I, Koffman G, Goldsmith D. Thrombotic micro-angiopathy with sirolimus-based immunosuppression: potentiation of calcineurin-inhibitor-induced endothelial damage? Am J Transplant. 2003; 3: 324-327.
57. Rendell MS, Milliken BK, Finnegan MF, Finney DA, Healy JC. The skin blood flow response in wound healing. Microvasc Res. 1997; 53: 222-234.
58. Reynolds JC, Agodoa LY, Yuan CM, Abbott KC. Thrombotic microangiopathy after renal transplantation in the United States. Am J Kidney Dis 2003; 42: 1058-1068.
59. Peter FW, Buttemeyer R, Vogt PM, Hussmann J, Steinau HU. Thrombosis and tissue protection in microvascular surgery- an overview. Zentralbl Chir. 1997; 122: 844-851.
60. Atchabahian A, Masquelet AC. Experimental prevention of free flap thrombosis. II: Normovolemic hemodilution for thrombosis prevention. Microsurgery. 1996; 17: 714-716.
61. Juttner B, Kuse ER, Elsner HA, Heine J, Jaeger K, Piepenbrock S, Scheinichen D. Differential platelet receptor expression following hydroxyethyl starch infusion in thrombocytopaenic orthotopic liver transplantation recipients. Eur J Anaesthesiol. 2004; 21: 309-313.

62. Levy, PS, Kim SJ, Eckel PK, Chavez R, Ismail EF, Gould SA, Ramez Salem M, and Crystal GJ. Limit to cardiac compensation during acute isovolemic hemodilution: influence of coronary stenosis. Am J Physiol Heart Circ Physiol 1993; 265: H340-H349.
63. Hyodo, A, Heros RC, Tu YK, Ogilvy C, Graichen R, Lagree K, and Korosue K. Acute effects of isovolemic hemodilution with crystalloids in a canine model of focal cerebral ischemia. Stroke 1989; 20: 534-540.
64. Klar E, Herfarth C, Messmer K. Therapeutic effect of isovolemic hemodilution with dextran 60 on the impairment of pancreatic microcirculation in acute biliary pancreatitis. Ann Surg. 1990; 211: 346-353.
65. Erni, D, Sakai H, Tsai AG, Banic A, Sigurdsson GH, and Intaglietta M. Haemodynamics and oxygen tension in the microcirculation of ischaemic skin flaps after neural blockade and haemodilution. Br J Plast Surg 1999; 52: 565-572.
66. Schramm, S, Wettstein R, Wessendorf R, Jakob SM, Banic A, and Erni D. Acute normovolemic hemodilution improves oxygenation in ischemic flap tissue. Anesthesiology 2002; 96: 1478-1484.
67. Chang TM. Oxygen carriers. Curr Opin Investig Drugs. 2002; 3: 1187-1190.
68. Erni D, Wettstein R, Schramm S, Contaldo C, Sakai H, Takeoka S, Tsuchida E, Leunig M, Banic A. Normovolemic hemodilution with Hb vesicle solution attenuates hypoxia in ischemic hamster flap tissue. Am J Physiol Heart Circ Physiol. 2003; 284: H1702-1709.
69. Rinker BD, Stewart DH, Pu LL, Vasconez HC. Role of recombinant tissue plasminogen activator in free flap salvage. J Reconstr Microsurg. 2007; 23: 69-73.
70. Peter FW, Franken RJ, Wang WZ, Anderson GL, Schuschke DA, O'Shaughnessy MM, Banis JC, Steinau HU, Barker JH. Effect of low dose aspirin on thrombus formation at arterial and venous microanastomoses and on the tissue microcirculation. Plast Reconstr Surg. 1997; 99: 1112-1121.
71. Chien W, Varvares MA, Hadlock T, Cheney M, Deschler DG. Effects of aspirin and low-dose heparin in head and neck reconstruction using microvascular free flaps. Laryngoscope. 2005; 115: 973-976.
72. Ritter EF, Cronan JC, Rudner AM, Serafin D, Klitzman B. Improved microsurgical anastomotic patency with low molecular weight heparin. J Reconstr Microsurg. 1998; 14: 331-336.
73. Murthy P, Riesberg MV, Hart S, Bustillo A, Duque CS, Said S, Civantos FJ. Efficacy of perioperative thromboprophylactic agents in the maintenance of anastamotic patency and survival of rat microvascular free groin flaps. Otolaryngol Head Neck Surg. 2003; 129: 176-182.
74. Renaud F, Succo E, Alessi MC, Legre R, Juhan-Vague I. Iloprost and salvage of a free flap. Br J Plast Surg. 1996; 49: 245-248.

75. Partecke BD, Fischer C, Buck-Gramcko D. Antithrombin III--an important factor in long-lasting microvascular operations. Handchir Mikrochir Plast Chir. 1985 ;17: 81-85.
76. Farina JA Jr, Piccinato CE, Campos AD, Rossi MA. Comparative study of isovolemic hemodilution with 3% albumin, dextran-40, and prophylactic enoxaparin (LMWH) on thrombus formation at venous microanastomosis in rats. Microsurgery. 2006; 26: 456-464.
77. Jokuszies A, Jansen V, Lahoda LU, Steinau HU, Vogt PM. Plasma concentration of endothelin-1 after myocutaneous latissimus dorsi-transplantation -- role in reperfusion injury. Handchir Mikrochir Plast Chir. 2005; 37: 193-201.
78. Eldwood PC, Beswick A, O'Brien JR, Renaud S, Fifield R, Limb ES, et al. Temperature and risk factors for ischaemic heart disease in the Caerphilly prospective study. Br Heart J. 1993; 70: 520-523.
79. Pell JP, Cobbe SM. Seasonal variations in coronary heart disease. QJM. 1999; 92: 689-696.
80. Peng RY, Bongard FS. Hypothermia in trauma patients. J Am Coll Surg. 1999; 188: 685-696.
81. Rohrer M, Natale A. Effect of hypothermia on the coagulation cascade. Crit Care Med. 1992; 20: 1402-1405.
82. Maurer-Spurej E, Pfeiler G, Maurer N, Lindner H, Glatter O, Devine DV. Room temperature activates human blood platelets. Lab Invest. 2001; 81: 581-592.
83. White JG, Krivit W. An ultrastructural basis for the shape changes induced in platelets by chilling. Blood. 1967; 30: 625-635.
84. Furie B, Furie BC, Flaumenhaft R. A journey with platelet P-selectin: the molecular basis of granule secretion, signalling and cell adhesion. Thromb Haemost. 2001; 86: 214-221.
85. Remick DG, Xioa H: Hypothermia and sepsis. Front Biosci. 2006; 11: 1006-1013.
86. Zeerleder S, Hack CE, Wuillemin WA: Disseminated intravascular coagulation in sepsis. Chest. 2005; 128: 2864-2875.
87. Vincent JL: Microvascular endothelial dysfunction: a renewed appreciation of sepsis pathophysiology. Crit Care. 2001; 5: S1-5.
88. Philippe J, Offner F, Declerck PJ, Leroux-Roels G, Vogelaers D, Baele G, Collen D: Fibrinolysis and coagulation in patients with infectious disease and sepsis. Thromb Haemost. 1991; 65: 291-295.
89. Levi M, de Jonge E, van der Poll T: Rationale for restoration of physiological anticoagulant pathways in patients with sepsis and disseminated intravascular coagulation. Crit Care Med. 2001; 29 Suppl 7: 90-94.

90. Levi M, de Jonge E, van der Poll T, ten Cate H: Novel approaches to the management of disseminated intravascular coagulation. Crit Care Med. 2000; 28 Suppl 9: 20-24.
91. Cines DB, Pollak ES, Buck CA, Loscalzo J, Zimmerman GA, McEver RP, Pober JS, Wick TM, Konkle BA, Schwartz BS, Barnathan ES, McCrae KR, Hug BA, Schmidt AM, Stern DM: Endothelial cells in physiology and in the pathophysiology of vascular disorders. Blood. 1998; 91: 3527-3561.
92. Prescott SM, McIntyre TM, Zimmerman GA, Stafforini DM: Sol Sherry lecture in thrombosis: molecular events in acute inflammation. Arterioscler Thromb Vasc Biol. 2002; 22: 727-733.
93. Willis D, Moore AR, Frederick R, Willoughby DA. Heme oxygenase: a novel target for the modulation of the inflammatory response. Nat Med. 1996; 2: 87-90.
94. Lee PJ, Alam J, Wiegand GW, Choi AM. Overexpression of heme oxygenase-1 in human pulmonary epithelial cells results in cell growth arrest and increased resistance to hyperoxia. Proc Natl Acad Sci USA. 1996; 93: 10393-10398.
95. Maines MD, Trakshel GM, Kutty RK. Characterization of two constitutive forms of rat liver microsomal heme oxygenase. Only one molecular species of the enzyme is inducible. J Biol Chem. 1986; 261: 411-419.
96. Maines MD. The heme oxygenase system: a regulator of second messenger gases. Annu Rev Pharmacol Toxicol. 1997; 37: 517-554.
97. Vachharajani TJ, Work J, Issekutz AC, Granger DN. Heme oxygenase modulates selectin expression in different regional vascular beds. Am J Physiol Heart Circ Physiol. 2000; 278: H1613-H1617.
98. Stocker R, Yamamoto Y, McDonagh AF, Glazer AN, Ames BN. Bilirubin is an antioxidant of possible physiological importance. Science. 1987; 235: 1043-1046.
99. Hayashi S, Takamiya R, Yamaguchi T, Matsumoto K, Tojo SJ, Tamatani T, Kitajima M, Makino N, Ishimura Y, Suematsu M. Induction of heme oxygenase-1 suppresses venular leukocyte adhesion elicited by oxidative stress: role of bilirubin generated by the enzyme. Circ Res. 1999; 85: 663-671.
100. Fujita T, Toda K, Karimova A, Yan SF, Naka Y, Yet SF, Pinsky DJ. Paradoxical rescue from ischemic lung injury by inhaled carbon monoxide driven by derepression of fibrinolysis. Nat Med. 2001; 7: 598-604.
101. Salonen JT, Alfthan G, Huttunen JK, Pikkarainen J, Puska P. Association between cardiovascular death and myocardial infarction and serum selenium in a matched-paired longitudinal study. Lancet. 1982; 2: 175-179.
102. Moore JA, Noiva R, Wells IC. Selenium concentrations in plasma of patients with arteriographicallly defined coronary atherosclerosis. Clin Chem. 1984; 30: 1171-1173.

103. Perona G, Guidi GC, Piga A, Cellerino R, Menna R, Zatti M. In vivo and in vitro variations of human erythrocyte glutathione peroxidase activity as result of cells aging, selenium availability and peroxide activation. Br J Haematol. 1978; 39: 399-408.
104. Palabrica T, Lobb R, Furie BC, Aronovitz M, Benjamin C, Hsu YM, Sajer SA Furie B. Leukocyte accumulation promoting fibrin deposition is mediated in vivo by P-selectin on adherent platelets. Nature. 1992; 359: 848-851.
105. Subramaniam M, Frenette PS, Saffaripour S, Johnson RC, Hynes RO, Wagner DD. Defects in hemostasis in P-selectin-deficient mice. Blood 1996; 87: 1238-1242.
106. De Vriese AS, Verbeuren TJ, Van de Voorde J, Lameire NH, Vanhoutte PM. Endothelial dysfunction in diabetes. Br J Pharmacol. 2000; 130: 963-974.
107. Luft FC. Proinflammatory effects of angiotensin II and endothelin: targets for progression of cardiovascular and renal diseases. Curr Opin Nephrol Hypertens. 2002; 11: 59-66.
108. Auwerx J, Bouillon R, Collen D, Geboers J. Tissue-type plasminogen activator antigen and plasminogen activator inhibitor in diabetes mellitus. Arteriosclerosis. 1988; 8: 68-72.
109. Vericel E, Januel C, Carreras M, Moulin P, Lagarde M. Diabetic patients without vascular complication display enhanced basal platelet activation and decreased antioxidant status. Diabetes. 2004; 53:1046-1051.
110. Ceriello A, Giacomello R, Stel G, Motz E, Taboga C, Tonutti L, Pirisi M, Falleti E, Bartoli E. Hyperglycemia-induced thrombin formation in diabetes. The possible role of oxidative stress. Diabetes. 1995; 44: 924-928.
111. Hafer-Macko CE, Ivey FM, Gyure KA, Sorkin JD, Macko RF. Thrombomodulin deficiency in human diabetic nerve microvasculature. Diabetes 2002; 51: 1957-1963.
112. Wahren J, Jornvall H. C-peptide makes a comeback. Diabetes Metab Res Rev. 2003; 19: 345-347.
113. Kunt T, Forst T, Coss E, Wallerath U, Förstermann R, Lehmann R, Pfützner A, Harzer O, Engelback M, Beyer J. Activation of endothelial nitric oxide synthetase (eNOS) by C-peptide (Abstract). Diabetologia 1998; 41: A176.
114. Scalia R, Coyle KM, Levine BJ, Booth G, Lefer AM. C-peptide inhibits leukocyte-endothelium interaction in the microcirculation during acute endothelial dysfunction FASEB J. 2000; 14: 2357-2364.
115. Johansson BL, Linde B, Wahren J. Effects of C-peptide on blood flow, capillary diffusion capacity and glucose utilization in the exercising forearm of type 1 (insulin-dependent) diabetic patients. Diabetologia. 1992; 35: 1151-1158.

116. Johansson BL, Pernow J.C-peptide potentiates the vasoconstrictor effect of neuropeptide Y in insulin-dependent diabetic patients. Acta Physiol Scand. 1999; 165: 39-44.
117. Johansson BL, Sjoberg S, Wahren J. The influence of human C-peptide on renal function and glucose utilization in type 1 (insulin-dependent) diabetic patients Diabetologia. 1992; 35: 121-128.
118. Johansson BL, Kernell A, Sjoberg S, Wahren J. Influence of combined C-peptide and insulin administration on renal function and metabolic control in diabetes type 1. J Clin Endocrinol Metab. 1993; 77: 976-981.
119. Johansson BL, Borg K, Fernqvist-Forbes E, Kernell A, Odergren T, Wahren J. Beneficial effects of C-peptide on incipient nephropathy and neuropathy in patients with Type 1 diabetes mellitus. Diabet Med. 2000; 17: 181-189.
120. Alessi MC, Juhan-Vague I. Contribution of PAI-1 in cardiovascular pathology. Arch Mal Coeur Vaiss. 2004; 97: 673-678.
121. Schafer K, Muller K, Hecke A, Mounier E, Goebel J, Loskutoff DJ, Konstantinides S. Enhanced thrombosis in atherosclerosis-prone mice is associated with increased arterial expression of plasminogen activator inhibitor-1. Arterioscler Thromb Vasc Biol. 2003; 23: 2097-2103.
122. Nordt TK, Sawa H, Fujii S, Sobel BE. Induction of plasminogen activator inhibitor type-1 (PAI-1) by proinsulin and insulin in vivo. Circulation 1995; 91: 764-770.
123. Trovati M, Anfossi G. Influence of insulin and of insulin resistance on platelet and vascular smooth muscle cell function. J Diabetes Complications. 2002; 16: 35-40.
124. Johansson BL, Borg K, Fernqvist-Forbes E, Odergren T, Remahl S, Wahren J.C-peptide improves autonomic nerve function in IDDM patients. Diabetologia. 1996; 39: 687-695.
125. Rigler R, Pramanik A, Jonasson P, Kratz G, Jansson OT, Nygren P, Stahl S, Ekberg K, Johansson B, Uhlen S, Uhlen M, Jornvall H, Wahren J. Specific binding of proinsulin C-peptide to human cell membranes. Proc Natl Acad Sci USA. 1999; 96: 13318-13323.
126. Jelkmann W. Molecular biology of erythropoietin. Intern Med. 2004; 43: 649-659.
127. Fisher JW. Erythropoietin: Physiology and pharmacology update. Exp Biol Med. 2003; 228: 1-14.
128. Fuste B, Serradell M, Escolar G, Cases A, Mazzara R, Castillo R, Ordinas A, Diaz-Ricart M. Erythropoietin triggers a signaling pathway in endothelial cells and increases the thrombogenicity of their extracellular matrices in vitro. Thromb Haemost. 2002; 88: 678-685.

129. Borawski J, Mysliwiec M. Effects of recombinant erythropoietin therapy on circulating endothelial markers in hemodialysis patients. Clin Appl Thromb Hemost. 2002; 8: 77-84.
130. Wolf RF, Peng J, Friese P, Gilmore LS, Burstein SA, Dale GL. Erythropoietin administration increases production and reactivity of platelets in dogs. Thromb Haemost. 1997; 78: 1505-1509.
131. Vogel J, Kiessling I, Heinicke K, Stallmach T, Ossent P, Vogel O, Aulmann M, Frietsch T, Schmid-Schonbein H, Kuschinsky W, Gassmann M.. Transgenic mice overexpressing erythropoietin adapt to excessive erythrocytosis by regulating blood viscosity. Blood. 2003; 102: 2278-2284.
132. Shibata J, Hasegawa J, Siemens HJ, Wolber E, Dibbelt L, Li D, Katschinski DM, Fandrey J, Jelkmann W, Gassmann M, Wenger RH, Wagner KF. Hemostasis and coagulation at a hematocrit level of 0.85: functional consequences of erythrocytosis. Blood. 2003; 101: 4416-4422.
133. Cadroy Y, Hanson SR. Effects of red blood cell concentration on hemostasis and thrombus formation in a primate model. Blood. 1990; 75: 2185-2193.
134. Ruschitzka FT, Wenger RH, Stallmach T, Quaschning T, de Wit C, Wagner K, Labugger R, Kelm M, Noll G, Rulicke. T, Shaw S, Lindberg RL, Rodenwaldt B, Lutz H, Bauer C, Luscher TF, Gassmann M. Nitric oxide prevents cardiovascular disease and determines survival in polyglobulic mice overexpressing erythropoietin. Proc Natl Acad Sci U S A. 2000; 97: 11609-11613.
135. US Department of Health and Human Services. The Health Benefits of Smoking Cessation. US Department of Health and Human Services, Public Health Service, Centers for Disease Control, Center for Chronic Disease Prevention and Health Promotion, Office on Smoking and Health, Washington, DC. DHHS Publication No. (CDC) 1990; 90-8416.
136. Helmerhorst FM, Bloemenkamp KW, Rosendaal FR, Vanderbroucke JP. Oral contraceptives and thrombotic disease: risk of venous thromboembolism. Thromb Haemost. 1997; 78: 327-333.
137. Benowitz NL. Pharmacology of nicotine: addiction and therapeutics. Annu Rev Pharmacol Toxicol. 1996; 36: 597-613.
138. Benowitz NL. Systemic absorption an d effects of nicotine from smokeless tobacco. Adv Dent Res. 1997; 11: 336-341.
139. Chalon S, Moreno H Jr, Benowitz NL, Hoffman BB, Blaschke TF. Nicotine impairs endothelium-dependent dilatation in human veins in vivo. Clin Pharmacol Ther. 2000; 67: 391-397.

140. Zidovetzki R, Chen P, Fisher M, Hofman FM, Faraci FM. Nicotine increases plasminogen activator inhibitor-1 production by human brain endothelial cells via protein kinase C-associated pathway. Stroke. 1999; 30: 651-655.
141. Ludviksdottir D, Blondal T, Franzon M, Gudmundsson TV, Sawe U.J. Effects of nicotine nasal spray on atherogenic and thrombogenic factors during smoking cessation. Intern Med. 1999; 246: 61-66.

6 Danksagung

Mein außerordentlicher Dank gilt Frau Prof. Dr. med. B. Vollmar, die mich jederzeit uneingeschränkt gefördert und bei der Durchführung der wissenschaftlichen Projekte angeleitet hat. Mein ganz besonderer Dank gilt auch Herrn Prof. Dr. med. E. Klar, der mich stets in allen meinen Vorhaben unterstützt hat, und es mir ermöglichte, neben der klinischen Tätigkeit meinem wissenschaftlichen Interesse intensiv nachzugehen. Weiterhin gilt mein besonderer Dank Herrn Prof. Dr. med. M.D. Menger, der mir stets mit gutem Rat zur Seite stand und mehrere Studien im Rahmen von Hospitationen an seinem Institut gefördert hat. Ich möchte mich desweiteren sehr bei Herrn Prof. Dr. med. W. Schareck dafür bedanken, dass er das Interesse an der experimentellen Forschung in mir geweckt und dadurch die Grundsteine zu dieser Arbeit gelegt hat. Ein sehr herzlicher Dank gilt auch Herrn Dr. med. L. Belusa, der mich allzeit uneingeschränkt unterstützt hat.

Mein Dank gilt auch den Doktoranden Heiko Sorg, Birte Braun und Uwe Platz, ohne die diese Arbeit nicht möglich gewesen wäre, für Ihre tatkräftige Unterstützung. Weiterhin gilt mein großer Dank der Tierpflegerin Kathrin Sievert, die mir bei den tierexperimentellen Studien stets hilfreich zur Seite stand. Herzlich bedanken möchte ich mich auch bei den Medizinisch Technischen Assistentinnen Berit Blendow, Doris Butzlaff, Dorothea Frenz, Maren Nerowski und Claudia Vergien für Ihre engagierte Hilfe bei der Durchführung der durchflußzytometrischen, immunhistochemischen und molekularbiologischen Untersuchungen.

Ebenso danke ich allen Mitarbeitern des Instituts für Experimentelle Chirurgie und der zentralen Tierhaltung für ihre Unterstützung bei der Betreuung der Tiere und ihre unkomplizierte Hilfe bei den organisatorischen Aufgaben.

7 Eidesstattliche Erklärung

gemäß der Habilitationsordnung der Medizinischen Fakultät der Universität Rostock

Hiermit erkläre ich, dass

- keine staatsanwaltschaftlichen Ermittlungsverfahren gegen mich anhängig sind
- an keiner anderen Fakultät ein Habilitationsverfahren eingeleitet wurde
- ich die vorgelegte Habilitationsschrift selbstständig abgefasst habe und dabei keine fremden, nicht erwähnten Hilfen verwendet wurden
- mir die geltende Habilitationsordnung bekannt ist

Rostock, 19.06.2007 Dr. med. Nicole Lindenblatt